

Fiscal Year 2016: First Quarter

Progress Report  
**Advanced Battery Materials  
Research (BMR) Program**

Released April 2016  
for the period of October – December 2015

*Approved by*

Tien Q. Duong, Advanced Battery Materials Research Program Manager  
Vehicle Technologies Office, Energy Efficiency and Renewable Energy

---

## TABLE OF CONTENTS

<b>A Message from the Advanced Battery Materials Research Program Manager.....</b>	<b>1</b>
<b>Task 1 – Advanced Electrode Architectures .....</b>	<b>3</b>
Task 1.1 – Higher Energy Density via Inactive Components and Processing Conditions (Vincent Battaglia, Lawrence Berkeley National Laboratory) .....	4
Task 1.2 – Electrode Architecture-Assembly of Battery Materials and Electrodes (Karim Zaghib, HydroQuebec).....	6
Task 1.3 – Design and Scalable Assembly of High-Density, Low-Tortuosity Electrodes (Yet-Ming Chiang, Massachusetts Institute of Technology) .....	8
Task 1.4 – Hierarchical Assembly of Inorganic/Organic Hybrid Si Negative Electrodes (Gao Liu, Lawrence Berkeley National Laboratory) .....	10
<b>Task 2 – Silicon Anode Research.....</b>	<b>13</b>
Task 2.1 – Development of Silicon-Based High- Capacity Anodes (Ji-Guang Zhang and Jun Liu, PNNL; Prashant Kumta, University of Pittsburgh; Jim Zheng, PSU) .....	14
Task 2.2 – Pre-Lithiation of Silicon Anode for High-Energy Li Ion Batteries (Yi Cui, Stanford University) .....	17
<b>Task 3 – High-Energy Density Cathodes for Advanced Lithium-ion Batteries.....</b>	<b>20</b>
Task 3.1 – Studies of High-Capacity Cathodes for Advanced Lithium-ion Systems (Jagjit Nanda, Oak Ridge National Laboratory) .....	21
Task 3.2 – High-Energy Density Lithium Battery (Stanley Whittingham, SUNY Binghamton) .....	24
Task 3.3 – Development of High-Energy Cathode Materials (Ji-Guang Zhang and Jie Xiao, Pacific Northwest National Laboratory) .....	27
Task 3.4 – <i>In situ</i> Solvothermal Synthesis of Novel High-Capacity Cathodes (Feng Wang and Jianming Bai, Brookhaven National Laboratory) .....	29
Task 3.5 – Novel Cathode Materials and Processing Methods (Michael M. Thackeray and Jason R. Croy, Argonne National Laboratory) .....	32
Task 3.6 – High-capacity, High-voltage Cathode Materials for Lithium-ion Batteries (Arumugam Manthiram, University of Texas, Austin) .....	35
Task 3.7 – Lithium-bearing Mixed Polyanion (LBMP) Glasses as Cathode Materials (Jim Kiggans and Andrew Kercher, Oak Ridge National Laboratory) .....	38
Task 3.8 – Materials for High-Energy Lithium Ion Batteries (Marca Doeff, Lawrence Berkeley National Laboratory) .....	40
Task 3.9 – Lithium Batteries with Higher Capacity and Voltage (John B. Goodenough, UT-Austin).....	43
Task 3.10 – Exploiting Co and Ni Spinel in Structurally Integrated Composite Electrodes (Michael M. Thackeray and Jason R. Croy, Argonne National Laboratory).....	45
Task 3.11 – Discovery of High-energy Li ion Battery Materials (Wei Tong, Lawrence Berkeley National Laboratory) .....	48

**Task 4 – Electrolytes for High-Voltage, High-Energy Lithium-Ion Batteries.....51**

*Note:* This task is now closed, with some extension work being completed this first quarter.  
The BMR will issue a call in this area later this fiscal year.

**Task 5 – Diagnostics .....52**

Task 5.1 – Design and Synthesis of Advanced High-Energy Cathode Materials (Guoying Chen, Lawrence Berkeley National Laboratory) ..... 53

Task 5.2 – Interfacial Processes – Diagnostics (Robert Kostecki, Lawrence Berkeley National Laboratory).....56

Task 5.3 – Advanced *in situ* Diagnostic Techniques for Battery Materials (Xiao-Qing Yang and Xiqian Yu, Brookhaven National Laboratory) ..... 60

Task 5.4 – NMR and Pulse Field Gradient Studies of SEI and Electrode Structure (Clare Grey, Cambridge University) .....63

Task 5.5 – Optimization of Ion Transport in High-Energy Composite Cathodes (Shirley Meng, UC San Diego) .....66

Task 5.6 – Analysis of Film Formation Chemistry on Silicon Anodes by Advanced *In situ* and *Operando* Vibrational Spectroscopy (Gabor Somorjai, UC Berkeley, and Phil Ross, Lawrence Berkeley National Laboratory) .....69

Task 5.7 – Microscopy Investigation on the Fading Mechanism of Electrode Materials (Chongmin Wang, Pacific Northwest National Laboratory).....71

Task 5.8 – Characterization and Computational Modeling of Structurally Integrated Electrodes (Michael M. Thackeray and Jason R. Croy, Argonne National Laboratory) .....74

**Task 6 – Modeling Advanced Electrode Materials .....77**

Task 6.1 – Electrode Materials Design and Failure Prediction (Venkat Srinivasan, Lawrence Berkeley National Laboratory) .....78

Task 6.2 – Predicting and Understanding Novel Electrode Materials from First-Principles (Kristin Persson, Lawrence Berkeley National Laboratory).....81

Task 6.3 – First Principles Calculations of Existing and Novel Electrode Materials (Gerbrand Ceder, MIT).....83

Task 6.4 – First Principles Modeling of SEI Formation on Bare and Surface/Additive Modified Silicon Anode (Perla Balbuena, Texas A&M University) .....85

Task 6.5 – A Combined Experimental and Modeling Approach for the Design of High-Current Efficiency Si Electrodes (Xingcheng Xiao, General Motors, and Yue Qi, Michigan State University) ..... 88

Task 6.6 – Predicting Microstructure and Performance for Optimal Cell Fabrication (Dean Wheeler and Brian Mazzeo, Brigham Young University) .....91

<b>Task 7 – Metallic Lithium and Solid Electrolytes .....</b>	<b>94</b>
Task 7.1 – Mechanical Properties at the Protected Lithium Interface (Nancy Dudney, ORNL; Erik Herbert, UTK; and Jeff Sakamoto, UM) .....	95
Task 7.2 – Solid Electrolytes for Solid-State and Lithium-Sulfur Batteries (Jeff Sakamoto, University of Michigan) .....	98
Task 7.3 – Composite Electrolytes to Stabilize Metallic Lithium Anodes (Nancy Dudney and Sergiy Kalnaus, Oak Ridge National Laboratory) .....	101
Task 7.4 – Overcoming Interfacial Impedance in Solid-State Batteries (Eric Wachsman, University of Maryland, College Park) .....	104
Task 7.5 – Nanoscale Interfacial Engineering for Stable Lithium Metal Anodes (Yi Cui, Stanford University) .....	107
Task 7.6 – Lithium Dendrite Suppression for Lithium-Ion Batteries (Wu Xu and Ji-Guang Zhang, Pacific Northwest National Laboratory) .....	110
<b>Task 8 – Lithium Sulfur Batteries .....</b>	<b>113</b>
Task 8.1 – New Lamination and Doping Concepts for Enhanced Li – S Battery Performance (Prashant N. Kumta, University of Pittsburgh) .....	115
Task 8.2 – Simulations and X-ray Spectroscopy of Li-S Chemistry (Nitash Balsara, Lawrence Berkeley National Laboratory) .....	117
Task 8.3 – Novel Chemistry: Lithium Sulfur and Sulfur Sulfur Couple (Khalil Amine, Argonne National Laboratory) .....	119
Task 8.4 – Multi-Functional Cathode Additives (MFCA) for Li-S Battery Technology (Hong Gan, Brookhaven National Laboratory, and Co-PI Esther Takeuchi, Brookhaven National Laboratory and Stony Brook University) .....	121
Task 8.5 – Development of High-Energy Lithium-Sulfur Batteries (Jie Xiao and Jun Liu, Pacific Northwest National Laboratory) .....	124
Task 8.6 – Nanostructured Design of Sulfur Cathodes for High-Energy Lithium-Sulfur Batteries (Yi Cui, Stanford University) .....	126
Task 8.7 – Addressing Internal “Shuttle” Effect: Electrolyte Design and Cathode Morphology Evolution in Li-S Batteries (Perla Balbuena, Texas A&M University) .....	128
Task 8.8 – Mechanistic Investigation for the Rechargeable Li S Batteries (Deyang Qu, U Wisconsin - Milwaukee; Xiao-Qing Yang, BNL) .....	131
Task 8.9 – Statically and Dynamically Stable Lithium Sulfur Batteries (Arumugam Manthiram, U Texas - Austin) .....	134
<b>Task 9 – Li-Air Batteries .....</b>	<b>137</b>
Task 9.1 – Rechargeable Lithium-Air Batteries (Ji-Guang Zhang and Wu Xu, PNNL) .....	138
Task 9.2 – Efficient Rechargeable Li/O <sub>2</sub> Batteries Utilizing Stable Inorganic Molten Salt Electrolytes (Vincent Giordani, Liox) .....	141
Task 9.3 – Li-Air Batteries (Khalil Amine, ANL) .....	143
<b>Task 10 – Na-ion Batteries .....</b>	<b>146</b>
Task 10.1 – Exploratory Studies of Novel Sodium-Ion Battery Systems (Xiao-Qing Yang and Xiqian Yu, Brookhaven National Laboratory) .....	147

## LIST OF FIGURES

Figure 1. Plot of the 10-s pulse resistance versus depth of discharge data for laminates ranging in loadings from 1.875 to 4.887 mAh/cm <sup>2</sup> . This data indicates a maximum in the resistance for electrodes cast at 2.655 mAh/cm <sup>2</sup> .	5
Figure 2. (a) Design concept for nano-Si/NCM large format cell (deliverable FY15). (b) Charge-discharge voltage profile of the large format cell charged to 4.4 V and discharged to 2.5 V. (c) Optical image of nano-Si anode after cycling.	7
Figure 3. 3D-optical microscope images of the nano-Si anode electrode; (a) fresh, (b) 10 cycles, and (c) 50 cycles.	7
Figure 4. Scanning electron microscopy images of nano-Si anode; (a) top view of electrode after 1st cycle, and (b) cross section view of electrode after 50th cycle. (c) Comparison of local chemical analysis; fresh (blue), 1st (orange), 10th (red), and 50th cycle (cyan).	7
Figure 5. USABC dynamic stress test profile (left) has discharge pulses of 8, 12, 24, 28, 32, and 36 sec and is net discharge. It was looped repeatedly, as illustrated on the right for area capacity ranges of 0-1, 5-6 and 9-10 mAh/cm <sup>2</sup> , to discharge a low tortuosity NCA cathode of 12.7 mAh/cm <sup>2</sup> theoretical capacity to 2.5 V vs Li/Li <sup>+</sup> , yielding 11.5 mAh/cm <sup>2</sup> discharge capacity.	9
Figure 6. Magnetic emulsion droplets chain in an applied field, producing sacrificial pore formers that are then removed by evaporation, leaving highly oriented low tortuosity pores threading through a sintered LiCoO <sub>2</sub> cathode.	9
Figure 7. (a) Chemical structure of PPyMAA [poly(1-pyrenemethyl methacrylate- co- methacrylic acid)] conductive polymer binder. (b) Wide angle X-ray scattering of PPy and PPyMAA polymers. (c) Carbon K-edge soft X-ray absorption spectroscopy of PPy and PPyMAA shows that the lowest unoccupied molecular orbital (LUMO) energy is intact in PPyMAA, although nonconductive methacrylic acid groups are introduced. Transmission electron microscopy morphology of (d) high-tap-density nano-Si and (e) regular nano-Si produced by chemical vapor deposition (right). (f) Cycling performance of PPyMAA/high-tap-density nano-Si.	11
Figure 8. (a) Schematic illustration of the synthesis of the HC-nSi/G. (b / c) Scanning electron microscopy images. (d) C/Si energy dispersive X-ray elemental maps. (e) X-ray diffraction patterns.	15
Figure 9. Rate capability testing of (a) Si nanoflakes and (b) Si nanorods at different current rates in Li/Li <sup>+</sup> system.	15
Figure 10. Fabrication and electrochemical characteristics of the N-Co/N-Li <sub>2</sub> O composite. (a) Schematic of the fabrication process of the N-M/N-Li <sub>2</sub> O composites. MOs are used as the starting materials and <i>in situ</i> converted into N-M/N-Li <sub>2</sub> O composites via the chemical reaction with molten Li. (b) The initial charge potential profiles of the electrodes made with various Co/Li <sub>2</sub> O nanocomposites: Micrometer-sized Co/nanometer-sized Li <sub>2</sub> O (M-Co/N-Li <sub>2</sub> O), submicrometer-sized Co/nanometer-sized Li <sub>2</sub> O (SM-Co/N-Li <sub>2</sub> O) and N-Co/N-Li <sub>2</sub> O composites. (c) The charge/discharge potential profiles of the N-Co/N-Li <sub>2</sub> O electrode after the first charge process. (d) The initial charge potential profiles of the LiFePO <sub>4</sub> electrodes with different amounts of the N-Co/N-Li <sub>2</sub> O additive in half cell configurations. (e and f) The initial charge/discharge potential profiles (e) and cycling performance (f) of LiFePO <sub>4</sub> /graphite full cells with and without the N-Co/N-Li <sub>2</sub> O additive. The specific capacities of the cathodes are evaluated based the weight of LiFePO <sub>4</sub> and the N-Co/N-Li <sub>2</sub> O additive.	18

Figure 11. X-ray diffraction patterns from different chemical routes towards partial fluorination of $\text{Li}_2\text{CuO}_2$ cathodes (see text for details) .....	22
Figure 12. Cycling capacity of a $\text{LiVOPO}_4$ electrode as a function of degree of ball-milling in hours and rate of charge/discharge: (left) C/50, (right) C/20 .....	25
Figure 13. (a) Initial voltage profiles vs. specific capacity. (b) Energy density. (c) Cycling performance of a variety of NMC cathode materials cycled in the voltage range of 2.7 ~ 4.5 V. (1C = 200 mAh g <sup>-1</sup> , loading: ca. 4 mg cm <sup>-2</sup> ).....	28
Figure 14. Synthetic control of the structural ordering and performance of Ni-rich layered oxides. (a) Thermogravimetric curves of the precursors for synthesizing $\text{LiNiO}_2$ in $\text{O}_2$ flow (black line), $\text{LiNi}_{0.8}\text{Co}_{0.2}\text{O}_2$ in $\text{O}_2$ flow (red), and $\text{LiNi}_{0.8}\text{Co}_{0.2}\text{O}_2$ in the air (blue). (b) X-ray diffraction patterns of $\text{LiNi}_{0.8}\text{Co}_{0.2}\text{O}_2$ prepared at different sintering temperatures in $\text{O}_2$ flow. (c) Electrochemical performance of $\text{LiNi}_{0.8}\text{Co}_{0.2}\text{O}_2$ synthesized in $\text{O}_2$ (red), compared to that of $\text{LiNiO}_2$ synthesized in $\text{O}_2$ (black), and $\text{LiNi}_{0.8}\text{Co}_{0.2}\text{O}_2$ synthesized in the air (blue).....	30
Figure 15. (a) X-ray diffraction patterns of targeted layered-layered-spinel (LLS) compositions. (b) Electrochemical properties of a $0.25\text{Li}_2\text{MnO}_3 \bullet 0.75\text{LiMn}_{0.375}\text{Ni}_{0.375}\text{Co}_{0.25}\text{O}_2$ cathode with a 7.5% targeted spinel content (activation: 4.6-2.0 V, subsequent cycles: 4.45-2.5 V). (c) Scanning electron microscopy image of LLS powders from a ~0.5 kg scaled batch of metal hydroxide precursors (scale bar=25 $\mu\text{m}$ ).....	33
Figure 16. Bond valence sum maps showing the potential positions for the additional lithium in $\alpha\text{-LiVOPO}_4$ . ....	36
Figure 17. Rietveld refinement fits of $\alpha\text{-Li}_2\text{VOPO}_4$ with the combined diffraction data. (a) POWGEN time-of-flight neutron powder diffraction data from Bank 2. (b) POWGEN Bank 4 data. (c) Transmission film X-ray diffraction (XRD) data. The region from $2\theta = 41.2^\circ$ to $44.7^\circ$ is excluded in the XRD data due to a contribution from the film holder to the pattern.....	36
Figure 18. Combined vanadate/borate substitution improved the electrochemical performance of silver-bearing phosphate glass.....	39
Figure 19. Galvanostatic cycling results on NMC-622 materials prepared by spray pyrolysis (a and b) and co-precipitation (c and d).....	41
Figure 20. Soft X-ray absorption spectroscopy of Ni L-edge in the total electron yield mode for NMC-622: P (pristine powder), PE (pristine electrode), and PES (pristine electrode soaked in electrolyte). ....	41
Figure 21. (left) Polymer membrane immersion test in the $\text{LiNO}_3\text{-KNO}_3$ nitrate electrolyte at $124^\circ\text{C}$ . (right) Photographs of the polymer membranes after the electrolyte soaking tests. ....	44
Figure 22. X-ray diffraction patterns of $x\text{Li}_2\text{MnO}_3 \bullet (1-x)\text{LiCo}_{1-y}\text{Ni}_y\text{O}_2$ samples made at $600^\circ\text{C}$ with (a) $x=0.1$ ; $y=0.1$ , (b) $x=0.1$ ; $y=0.2$ , (c) $x=0.2$ ; $y=0.1$ , (d) $x=0.2$ ; $y=0.2$ , and (e) $x=0.2$ ; $y=0.25$ . ....	46
Figure 23. (a) Initial voltage profiles. (b) Relative capacity retentions. (c) Cycle performances of $x\text{Li}_2\text{MnO}_3 \bullet (1-x)\text{LiCo}_{1-y}\text{Ni}_y\text{O}_2$ composite materials ( $0 \leq x \leq 0.2$ ; $0 \leq y \leq 0.25$ ) synthesized at $600^\circ\text{C}$ . Li half-cells were cycled between 2.5 – 4.2 V vs. Li at the current rate of 15 mA/g. ....	46
Figure 24. Synchrotron X-ray diffraction patterns and refinement for three $\text{LiNiO}_2$ samples (Solution_2exLi, solution_10exLi, and solid_10exLi).....	49
Figure 25. SEM images for $\text{LiNiO}_2$ samples (solution_2exLi, solution_10exLi, and solid_10exLi). ....	49

Figure 26. (a) The first-cycle voltage profiles. (b) The $dq/dV$ plot of $\text{LiNiO}_2$ samples (solution_2exLi, solution_10exLi, and solid_10exLi).....	49
Figure 27. X-ray diffraction patterns of the crystals.....	54
Figure 28. Galvanostatic charge-discharge profiles of the crystal electrodes: (a) $3^\circ\text{C}/3^\circ\text{C}$ . (b) $3^\circ\text{C}/15^\circ\text{C}$ . (c) $3^\circ\text{C}/\text{Q}$ . (d) $15^\circ\text{C}/3^\circ\text{C}$ . (e) Discharge capacities. (f) Capacity retention of the cells. (g) Soft X-ray absorption spectroscopy total electron yield spectra of Mn and Co $L_3$ -edges before and after 45 cycles. ....	54
Figure 29. Electrodes were cycled in EC:DEC 1:2, 1M $\text{LiPF}_6$ electrolyte up to 4.2 V. Fluorescence response of aged and binder-free NMC cycled 2 times (a). Metal species within the SEI of a NMC/graphite cell cycled 850 times (b-d).....	58
Figure 30. Fluorescence response obtained during the investigation of carbon- and binder-free NMC electrodes in the EC:DEC 1:2, 1M $\text{LiPF}_6$ electrolyte .....	58
Figure 31. Effect of Fe substitution on the structural evolution and oxygen release during heating the charged samples of $\text{LiNi}_{0.5-x}\text{Mn}_{1.5-x}\text{Fe}_{2x}\text{O}_4$ ( $2x=0, 0.2, 0.33$ ). The left panel is the <i>in situ</i> mass spectroscopy data for oxygen, and the right three panels are the <i>in situ</i> X-ray diffraction data for $\text{LiNi}_{0.5-x}\text{Mn}_{1.5-x}\text{Fe}_{2x}\text{O}_4$ ( $2x=0, 0.2, 0.33$ ). ....	61
Figure 32. Coin cells cycled using (a) $^{13}\text{C}_3$ EC, (b) $^{13}\text{C}_1$ EC, and (c) $^{13}\text{C}_3$ dimethyl carbonate (DMC) labeled electrolytes. $^{13}\text{C}$ spectra were acquired with (i) a Hahn echo (HEcho), (ii) $^1\text{H}$ - $^{13}\text{C}$ CP, and (iii) $^7\text{Li}$ - $^{13}\text{C}$ CP. ....	64
Figure 33. (a) Oxygen position from the refinement results. (b) Density functional theory results from the evolution of the lattice parameters. (c) Oxygen position in materials with and without oxygen vacancies. ....	67
Figure 34. Electrochemistry performance comparison of 1 nm molecular layer deposition (MLD) coated Si: (a) first cycle voltage profile; and (b) capacity comparison using a voltage range of 1-0.05 V at C/20.....	67
Figure 35. The reduction peaks of an electrolyte solution (1.0 M $\text{LiPF}_6$ in EC : DEC, 1:2 v/v) on amorphous silicon anode are presented in this cyclic-voltammogram. Scan range was 3.0 V to -0.1 V and the rate was 1mV/sec. ....	70
Figure 36. The evolution of sum frequency generation (SFG) signal under reaction conditions of amorphous silicon with $\text{SiO}_2$ terminated anode. The SFG spectra were taken at open circuit potential and after 10 (black), 15 (red) cyclic-voltammograms (CVs) and 20 (green) at 3.0 V $\leftrightarrow$ -0.1 V. All CVs were repeated for 10 cycles at a scan rate of 1mV/sec. ....	70
Figure 37. Correlation of scanning transmission electron microscopy imaging of structure, energy dispersive spectroscopy mapping of chemical composition, and electrochemical property measurement help to identify the effect of $\text{Al}_2\text{O}_3$ coating effect for improved battery performance. ....	72
Figure 38. High-resolution X-ray diffraction patterns of $\text{Li}_{1.2}\text{Ti}_{0.4}\text{Cr}_{0.4}\text{O}_2$ . ....	75
Figure 39. <i>In situ</i> Cr and Ti K-edge X-ray absorption near-edge structure data. These insets (a-b) show magnified views of respective pre-edge regions. ....	75
Figure 40. Comparison of results for a 3C discharge using original porous electrode model, modified model with porosity gradient, and tortuosity extracted from microtomography data and conductivity simulations, microscale model, and experimental data. ....	79
Figure 41. (a) Illustrations of the $\text{Li}_2\text{MnO}_3$ Li-excess compound. (b,c) Illustration of the four symmetry-distinguishable migration paths (i), (ii), (iii) and (iv) as indicated by their local cation environment. ....	82

Figure 42. Internal energy of $\text{LiCrO}_2$ (solid orange line) and $\text{LiNiO}_2$ (dashed blue line) during heat-up simulations of their layered ground state configurations from 100 K to 3000 K. The vertical dashed lines indicate the temperatures of their respective order-disorder phase transitions. The zero-point of the y axis corresponds to the energy of a fully random cation arrangement. ....	84
Figure 43. Correlation of the temperature of the order-disorder transition of different $\text{LiMO}_2$ (M = Sc, V, Cr, Mn, Fe, Ni, Cu) with the energy difference of the random cation arrangement ( $E_{\text{SQS}}$ ) and the ordered ground state ( $E_{\text{GS}}$ ). ....	84
Figure 44. Surface pattern as the SEI thickness grows. ....	86
Figure 45. (left) <i>In situ</i> atomic force microscopy images during cycling of patterned Si electrode ( $15\ \mu\text{m} \times 15\ \mu\text{m} \times 225\ \text{nm}$ ) showing failure of SEI in shear lag zone. (right) The evolution of section height with cycling (also showing how the crack is evolving).....	89
Figure 46. Schematic of the finite element model. (b) Snapshots of the finite element results upon 1st cycle and 4th cycle, respectively. ....	89
Figure 47. Final configurations of lithiated $\text{SiO}_2$ layer on Si electrode (a) and lithiated LiF layer on Si electrode (b) (Si:yellow, O:red, F:green, Li: blue). ....	89
Figure 48. Stress-strain data for Toda 523 cathode film, compressed in the out-of-plane direction to imitate the effect of calendaring. Both experimental and dynamic particle-packing model results are indicated. Experiments were performed on four different films by sequentially increasing the stress. ....	92
Figure 49. Thin film lithium on glass.....	96
Figure 50. Indenter and microscope installed in glove box. ....	96
Figure 51. Indent of Li film showing pile up.....	96
Figure 52. Modulus determined for four indentation tests using different strain rates and penetration. ....	96
Figure 53. Phase angle for the tests of Figure 52 revealing the strain rate dependence for plasticity and creep.....	96
Figure 54. (a) Hardness and (b) fracture toughness as a function of relative density.....	99
Figure 55. The Vickers indentation crack propagation path for (a) 92% and (b) 98% LLZO sample. Arrows point to the crack propagation path. ....	99
Figure 56. Data points shown in blue are spray coatings containing tetraglyme (TEGDME), after pressing and heating. ....	102
Figure 57. Electrochemical impedance spectroscopy of spray composite coatings pressed and sealed in a coin cell. ....	102
Figure 58. Electrochemical impedance spectroscopy of the samples shown in Figure 57 after heating and cooling from $90^\circ\text{C}$ . ....	102
Figure 59. (a) Electrochemical impedance spectroscopy (EIS) plot of cathode/garnet/cathode half cell without gel electrolyte. (b) EIS of cathode/gel/garnet/gel/cathode half cell. (c) EIS of Li/gel/garnet/gel/Li half cell. ....	105
Figure 60. 3D surface modification of garnet extends the surface area.....	105



Figure 61. Scanning electron microscopy images and schematics showing the well-confined stripping/plating behavior of the Li-coated polyimide matrix. (a) Exposed top fibers after stripping away 5 mAh cm <sup>-2</sup> Li. (b) Exposed top fibers partially filled with Li when plating 3 mAh cm <sup>-2</sup> Li back. (c) Completely filled matrix after plating an additional 2 mAh cm <sup>-2</sup> Li back. The top-right schematic illustrates the alternative undesirable Li stripping/plating where after stripping, Li nucleates on the top surface, leading to volume change and dendrites shooting out of the matrix. ....	108
Figure 62. Discharge capacity of various Li metal anode- LTO cathode full cells for the first 100 galvanostatic cycles in EC/DEC with 1 vol% vinylene carbonate. Rate was set at 0.2 C for the first 2 cycles and 0.5 C for later cycles (1 C = 170 mA g <sup>-1</sup> ). ....	108
Figure 63. Optical images of Al foils after anodic polarization test at 4.5 V and 60°C for one week in the electrolytes of (a) LiTFSI-LiBOB and (b) LiPF <sub>6</sub> with EC-EMC solvent mixture. ....	111
Figure 64. RT cycling performance of Li  NCA cells using LiTFSI-LiBOB and LiPF <sub>6</sub> electrolytes in the voltage range of 3.0 V and 4.3 V. The cells were cycled at 1C (that is, 1.5 mA/cm <sub>2</sub> ) after two formation cycles at C/10 rate. ....	111
Figure 65. (a) Cycling stability of Li  NMC cells using LiPF <sub>6</sub> electrolyte at different discharge rates. (b-c) Evolution of charge/discharge voltage profiles at C/10 (b) and 1C (c) discharge. (d) Discharge capacities at C/10 after 150 cycles from (a). For all cells, the formation cycles were conducted at C/10 rate, and all other charge processes were performed at C/3 rate. ....	111
Figure 66. X-ray diffraction spectrum of Li <sub>4</sub> SiO <sub>4</sub> doped with (a) dopant D1 and (b) dopant D2. ....	116
Figure 67. Electrochemical impedance spectroscopy plots of lithium-ion conductor for different doping concentration of (a) dopant D1 and (b) dopant D2. (c) Ionic conductivity versus concentration of Li vacancies for dopants D1 and D2. ....	116
Figure 68. Energy of formation for radical polysulfide anions in dimethylformamide (DMF) and diglyme (DGM). ....	118
Figure 69. <i>In situ</i> X-ray absorption spectroscopy of an Li-S cell stopped mid-discharge at 2.25 V. Spectra taken thereafter represent the subsequent disproportionation process. ....	118
Figure 70. PDF profiles of S <sub>x</sub> Se <sub>y</sub> showing the dependence of the bond length on the composition of the materials. ....	120
Figure 71. Charge/discharge capacity of S <sub>5</sub> Se <sub>2</sub> /Li cells using different electrolytes, showing that the fluorinated ether significantly suppresses the shuttle mechanism and has a high Coulombic efficiency. Note that open symbols are for charge capacities, and solid symbols are for discharge capacity. ....	120
Figure 72. Synthesized FeS <sub>2</sub> in hybrid cathode. ....	122
Figure 73. Ti Mapping by EDS. ....	122
Figure 74. TiS <sub>2</sub> particle size effect on S:TiS <sub>2</sub> hybrid electrode cell cycling at 2C discharge rate. ....	122
Figure 75. High-power TiS <sub>2</sub> cell without carbon. ....	122
Figure 76. AFM topographic images of an HOPG electrode immersed in 5M LiTFSI-DOL electrolyte with and without electrode polarization. (a) Before polarization (at open circuit potential). Polarized at: (b) 1.0 V, (c) 0.5 V, (d) 0.2 V, (e) 0.1 V. Time after removal of polarization: (f) 10.4 min, (g) 17.2 min, (h) 20.5 min. Time after addition of free DOL in (h): (i) 24.2 min. (j) Schematic diagram of electrode-concentrated electrolyte interface with and without electrode polarization. ....	125

Figure 77. Lithium diffusion mechanism on the surface of various metal oxides. (a-e) Minimum energy path for lithium ion diffusion on $\text{Al}_2\text{O}_3(110)$ , $\text{CeO}_2(111)$ , $\text{La}_2\text{O}_3(001)$ , $\text{MgO}(100)$ and $\text{CaO}(100)$ surfaces, respectively. (f) Potential energy profiles for $\text{Li}^+$ diffusion along different adsorption sites on the oxide surface. ....	127
Figure 78. Performance of cathode-coated materials with graphene-sulfur and Al-W coatings. Left: Effect of Al-W thickness in comparison with graphene-sulfur. Right: Comparative performance of the 1.5 nm Al-W 1.5 nm coating with graphene-S system at 50 mAh/g. ....	129
Figure 79. (left) The calibration curve and chromatograms of different elemental sulfur standards. (middle) The chromatograms of different simulated electrolytes and blank S/DME solution. The inset shows the change of S concentration with the amount of $\text{Na}_2\text{S}$ added. (right) The chromatogram of electrolyte from discharged Li-S battery and the discharged profile of Li-S battery. ....	132
Figure 80. Physical/chemical characteristics of various carbon materials: (a) pore-size distributions and (b) isotherms. ....	135
Figure 81. Cell performance of the cell employing the CNF-coated separator. ....	135
Figure 82. Morphology and crystal structure characterizations of NCO/carbon fabric (CF). (a) Scanning electron microscopy image of NCO nanowires (NW) grown on carbon fabric, where the inset is high-resolution image of NCO NWs. (b) Transmission electron microscopy image of single NCO NW. (c) Selected area electron diffraction pattern of NCO from its single NW. (d) X-ray diffraction pattern of the resulting NCO/CF composite. ....	139
Figure 83. Characterization of lithiated NCO nanowire (NW). (a) Schematic illustration of NCO NW under lithiation. (b) Transmission electron microscopy and (c) high-resolution transmission electron microscopy images of selected lithiation area of NCO NW. Inset: Selected area electron diffraction pattern of lithiated NCO. ....	139
Figure 84. (a) Voltage-capacity profile for molten nitrate $\text{Li}/\text{O}_2$ cells using different nanopowder cathodes. $E^\circ$ : thermodynamic potential for $2\text{Li} + \text{O}_{2(\text{g})} \rightleftharpoons \text{Li}_2\text{O}_2$ cell reaction. (b) <i>In situ</i> pressure analysis for the cell containing the Ni cathode cycled at 100 $\mu\text{A}$ constant current (5 mA/g). ....	142
Figure 85. Scanning electron microscopy image of 3c-Pd/2c-ZnO/C sample; c refers to number of ALD cycles. ....	144
Figure 86. Voltage profile for 13c-Pd/2c-ZnO/C sample; c refers to number of ALD cycles. ....	144
Figure 87. Structure evolution upon Na extraction/insertion. (a) <i>In situ</i> X-ray diffraction patterns collected during the first discharge/charge of the $\text{Na}/\text{Na}_{0.44}[\text{Mn}_{0.44}\text{Ti}_{0.56}]\text{O}_2$ cell under a current rate of C/10 at a voltage range between 1.5 V and 3.9 V. (b) Evolutions of the lattice parameters during charge/discharge process. ....	148

## LIST OF TABLES

Table 1. Solubility of elemental S in pure solvents and in corresponding electrolytes with different LiTFSi concentrations obtained through HPLC/UV method. ....	132
Table 2. Materials Chemistry Database. ....	135

## **A MESSAGE FROM THE ADVANCED BATTERY MATERIALS RESEARCH PROGRAM MANAGER**

The Advanced Battery Materials Research (BMR) Program brings together leading experts from top academic, commercial, government, and national laboratories to address the fundamental issues of electrode chemical and mechanical instabilities that have slowed the development of affordable, high performance, automotive batteries. The aim is to identify electrode/electrolyte materials that lead to enhanced battery performance and greater acceptance of electric vehicles. Novel diagnostics and modeling methods are employed to gain a better understanding of key factors that limit cell and material performance and to provide guidance in designing next-generation materials. The BMR Program not only supports research that leads to improvements to existing materials, but also investigations into high-risk technologies that might have a tremendous impact in the marketplace.

This document summarizes the investigator's activities performed during the period from October 1, 2015, through December 31, 2015. Selected highlights from the BMR tasks are summarized below:

- **Brookhaven National Laboratory and Stony Brook University** (Gan and Takeuchi) demonstrated that the use of  $\text{TiS}_2$  as a substitute for conductive carbon in Li-S cells improved high power cycling performance with both higher capacity and better capacity retention.
- **Lawrence Berkeley National Laboratory** (Doeff) successfully synthesized a Ni-rich NMC (NMC-622) composition using spray pyrolysis. Initial cycling results of this high-voltage cathode material (up to 4.7 V) showed superior performance compared to NMC-622 synthesized by a co-precipitation method.
- **Texas A&M University** (Balbuena and Mukherjee) showed that the chemical structure and concentration of the salt and oxidant additives (such as  $\text{LiNO}_3$ ) as well as their interactions determine the nature of the solid-electrolyte interphase (SEI) layer products and may affect the rate of polysulfide decomposition reactions on Li anodes. Guidelines for selection of potential materials incorporated to the C/S cathode for physical and chemical retention of polysulfide species were obtained both theoretically (Balbuena and Mukherjee) and experimentally in collaboration with Purdue University (Pol).
- **Brookhaven National Laboratory** (Yang and Yu) demonstrated that Fe substitution in  $\text{LiNi}_{0.5}\text{Mn}_{1.5}\text{O}_4$  spinel improves thermal stability of the charged cathode by suppressing oxygen release and maintaining the crystal structure.
- **Argonne National Laboratory** (Amine) prepared an atomic layer deposition (ALD)-coated, Pd/ZnO/C cathode for a rechargeable Li- $\text{O}_2$  battery that showed a highly active catalytic effect toward the oxygen evolution reaction. The group is exploring methods to improve cycle life.

The next BMR quarterly report will cover the progress made during January through March 2016 and will be available June 2016. For additional information regarding these efforts, please join us at our Annual Merit Review and Peer Evaluation meeting that will take place on 6 – 10 June 2016 at the Washington Marriott Wardman Park hotel. Details about this event will be posted on the DOE website.

Finally, this past quarter saw the completion of Task 4: Electrolytes for High-Voltage, High-Energy Lithium-ion Batteries. The task lead for this effort was Dr. Zhengcheng Zhang of Argonne National Laboratories. I wish to thank Dr. Zhang as well as the other members of the team (Drs. Ron Hendershot and Joe Sunstrom from Daikin America, and Dr. Dee Strand from Wildcat Discovery Technologies) for their hard work in addressing the many technological challenges confronting electrolyte development. As many in the field know, stable, high-voltage electrolytes will be essential to achieving DOE battery performance, cost and safety goals. Their efforts brought us one step closer.

Sincerely,

*Tien Q. Duong*

Manager, Advanced Battery Materials Research (BMR) Program

Energy Storage R&D

Vehicle Technologies Office

Energy Efficiency and Renewable Energy

U.S. Department of Energy

## TASK 1 – ADVANCED ELECTRODE ARCHITECTURES

### Summary and Highlights

Energy density is a critical characterization parameter for batteries for electric vehicles as there is only so much room for the battery and the vehicle needs to travel over 200 miles. The DOE targets are 500 Wh/L on a system basis and 750 Wh/L on a cell basis. Not only do the batteries have to have high energy density, they need to do so and still deliver 1000 Wh/L for 30 seconds on the system level. To meet these requirements not only entails finding new, high energy density electrochemical couples, but also highly efficient electrode structures that minimize inactive material content, allow for expansion and contraction from one to several thousand cycles, and allow full access to the active materials by the electrolyte during pulse discharges. In that vein, the DOE Vehicle Technology Office (VTO) supports four projects in the BMR Program under Advanced Electrode Architectures: (1) Higher Energy Density via Inactive Components and Processing Conditions, LBNL, (2) Assembly of Battery Materials and Electrodes, HydroQuebec (HQ), (3) Design and Scalable Assembly of High-Density, Low-Tortuosity Electrodes, Massachusetts Institute of Technology (MIT), and (4) Hierarchical Assembly of Inorganic/Organic Hybrid Si Negative Electrodes, LBNL.

The four subtasks take two general engineering approaches to improving the energy density. Subtasks 1 and 3 attempt to increase energy density by making thicker electrodes and reducing the overall amount of inactive components per cell. Subtasks 2 and 4 attempt to increase the energy density of Li-ion cells by replacing graphitic anodes with Si-based active materials. All four attempts are based on determining a suitable binder and a proper methodology for assembling the active material.

The problem being addressed with the first approach is that the salt in the electrolyte must travel a further distance to meet the current throughout the entire discharge. If the salt cannot reach the back of the electrode at the discharge rates required of batteries for automobiles, the battery is said to be running at its limiting current. If the diffusional path through the electrode is tortuous or the volume for electrolyte is too low, the limiting current is reduced. Another problem with thicker electrodes is that they tend to not cycle as well as thinner electrodes and thus reach the end-of-life condition sooner, delivering fewer cycles.

The problem of the second approach is that silicon suffers from two major problems, both associated with the 300% volume change the material experiences as it goes from a fully delithiated state to a fully lithiated one: (1) the change results in freshly exposed surface area to electrolyte during cycling that consumes electrolyte and results in a lithium imbalance between the two electrodes, and (2) the volume change causes the particles to become electrically disconnected, which is further enhanced if particle fracturing also occurs, during cycling.

The highlight for this quarter is that Yet-Ming Chiang's Group (MIT) has demonstrated that a sintered electrode of 12.7 mAh/cm<sup>2</sup> theoretical capacity can achieve 11.5 mAh/cm<sup>2</sup> available capacity under USABC dynamic stress test (DST) cycling conditions.

## Task 1.1 – Higher Energy Density via Inactive Components and Processing Conditions (Vincent Battaglia, Lawrence Berkeley National Laboratory)

**Project Objective.** Thicker electrodes with small levels of inactive components that can still deliver most of their energy at C-rates of C/3 should result in batteries of higher energy density. Higher energy density should translate to more miles per charge or smaller, less expensive batteries. Unfortunately, the limit to making thicker electrodes is not based on power capability but on mechanical capability; for example, thicker electrodes delaminate from the current collector during calendaring and slicing. The objective of this research is to produce a high energy density electrode with typical Li-ion components that does not easily delaminate and still meets the electric vehicle (EV) power requirements through changes to the polymer binder and concomitant changes to the processing conditions.

**Project Impact.** Today's batteries cost too much on a per kWh basis and have too low of an energy density to allow cars to be driven over 300 miles on a single charge. This research targets both of these problems simultaneously. By developing thicker, higher energy-density electrodes, the fraction of cost relegated to inactive components is reduced, and the amount of energy that can be introduced to a small volume can be increased. Macroscopic modeling suggests that this could have as much as a 20% impact on both numbers.

**Out-Year Goals.** In the first year, the project will change its binder supplier to a U.S. supplier willing to provide binders of differing molecular weights. The project will then establish the workability of the new binders, establish a baseline binder and processing conditions, and determine how thick an electrode can be made from the project's standard processes for making moderately thick electrodes.

In the outgoing years, changes will be made to the binder molecular weight and electrode processing conditions to whatever degree is necessary to increase the energy density while maintaining power capability. Changes in the processing conditions can include the time of mixing, rate of casting, temperature of the slurry during casting, drying conditions, and hot calendaring. Chemical modifications may include multiple binder molecular weights and changes in the conductive additive.

**Collaborations.** This project has collaborations with Zaghbi's Group (HQ) for materials and cell testing; Wheeler's Group (Brigham Young University, BYU) for modeling analysis; Liu's group on polymer properties; Arkema for binders; and a commercial cathode material supplier.

### Milestones

1. Fabricate laminates of NCM cast to different thicknesses using standard materials and various processing conditions to determine how thick one can cast an electrode that does not display cracking or delamination. (Q1 – Complete)
2. Fabricate laminates of NCM cast to different thicknesses using higher molecular weight binders and various processing conditions to determine how thick one can cast an electrode that does not show cracking or delamination. (Q2)
3. Fabricate laminates of NCM cast to different thicknesses using standard materials and various processing conditions on current collectors with a thin layer of binder and conductive additive pre-coated on the current collector to determine how thick one can cast an electrode that does not show cracking or delamination. (Q3)
4. *Go/No-Go.* Determine if a higher molecular weight binder is worth pursuing to achieve thicker electrodes based on ease of processing and level of performance. If no, pursue a path of polymer-coated current collectors. (Q4)

## Progress Report

Last month, the results of casting films using the project's standard materials and processes but at varying doctor blade heights were reported. Laminates were drawn with the doctor blade set as high as 750 microns. The laminates set to about one third of the doctor blade height after drying. It was found that laminates cast at doctor blade heights greater than 500 microns easily delaminated from the current collector.

This quarter, laminates were cast using a powder binder of PVDF provided by Arkema (761 – considered a standard binder for Li-ion cells and has a molecular weight of 400,000). The first discovery in switching to this new binder is that when added to NMP, the solution is clear. The standard binder used up to then, which is available in powder and solution form (dissolved in NMP), has a yellow to brown tinge to it. It is believed that this is probably some impurity that, for now, does not warrant further investigation but is notable. The second discovery to switching to the Arkema binder is that the processing with this binder is simpler: slurries mixed faster and more uniformly with the Arkema binder, despite the fact that the Arkema binder has a higher molecular weight than the old baseline binder (molecular weight ca. 250,000).

Until now, this group has been responsible for making electrodes for Focus Groups and evaluating new materials for their capacity and cyclability under galvanostatic conditions—typical conditions familiar to the scientific community. For this project, testing is shifting to be more consistent with the EV Battery Test Procedures Manual published by the DOE and USABC. Possessing less familiarity with this manual, the

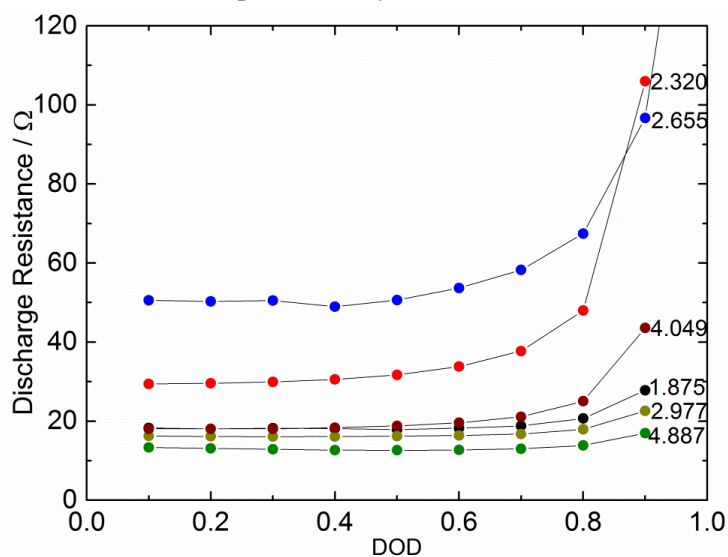


Figure 1. Plot of the 10-s pulse resistance versus depth of discharge data for laminates ranging in loadings from 1.875 to 4.887 mAh/cm<sup>2</sup>. This data indicates a maximum in the resistance for electrodes cast at 2.655 mAh/cm<sup>2</sup>.

Hybrid Pulse Power Characterization (HPPC) test was conducted, but was done so with the profile consistent for evaluating hybrid electric vehicles (HEVs), not EVs, and therefore, the test did not include a 30-second pulse. (The electrodes are presently under test with the proper load curve.) Figure 1 shows a plot of the 10-s pulse resistance versus depth of discharge data for laminates ranging in loadings from 1.875 to 4.887 mAh/cm<sup>2</sup>. One sees in this plot that there is a maximum in the resistance for electrodes cast at 2.655 mAh/cm<sup>2</sup>. This is somewhat of a surprise. It has long been believed that the resistance should start high for thin electrodes, drop down as the electrodes get thicker, and start to rise again as the electrodes get thicker still. The reason for this is that for thin electrodes, the Ohmic resistance is low, but all of the ionic current in the electrolyte has to cross through a small total surface area of active material in the transition to electronic current. This small surface area results in large superficial-area based resistance. Why the resistance drops down for the thinnest electrodes is still under debate. Next quarter a plot of max power density versus energy density for the new baseline polymer will be provided.



## Task 1.2 – Electrode Architecture-Assembly of Battery Materials and Electrodes (Karim Zaghib, HydroQuebec)

**Project Objective.** The project goal is to develop an electrode architecture based on nano-silicon materials and design a full cell having high energy density and long cycle life. To achieve the objective, this project investigates the structure of nano-Si materials that provide acceptable volume change to achieve long cycle life, while still maintaining the high-capacity performance of Si. The project scope includes the control of the particle size distribution of nano-Si materials, crystallinity, Si composition, and surface chemistry of the nano-Si materials. The focus is to develop electrode formulations and electrode architectures based on nano-Si materials that require optimized nano-Si/C composites and functional binders, as well as a controlled pore distribution in the electrode and the related process conditions to fabricate the electrode.

**Project Impact.** Silicon is a promising alternative anode material with a capacity of ~4200 mAh/g, which is about an order of magnitude higher than that of graphite. However, many challenges inhibiting the commercialization of Si remain unresolved. The primary culprit is viewed as the large volume variations of Si during charge/discharge cycles that result in pulverization of the particle and poor cycling stability. Success in developing highly reversible Si electrodes with acceptable cost will lead to higher energy density and lower cost batteries that are in high demand, especially for expanding the market penetration for EVs.

**Out-Year Goals.** This project investigates several steps to prepare an optimized composition and electrode structure of Si-based anode. HydroQuebec will use its advanced *in situ* analysis facilities to identify the limitations of the developed Si-based anode materials. *In situ* scanning electron microscopy (SEM) will be used to monitor crack formations in the particles along with delamination at the binder/particle and current collector/particle interfaces to improve the electrode architecture and cycle life.

Previously, serious gas evolution was observed during the mixing and coating steps of Si-based electrodes. To overcome these technical issues, surface treatment of the nano-Si powder will be considered to utilize the water-based binders. A physical or chemical surface coating to protect the nano-Si powders will be explored. The project will also explore approaches to optimize the particle size distribution (PSD) to achieve better performance.

To achieve high gravimetric energy density (Wh/kg), the electrode loading ( $\text{mg}/\text{cm}^2$ ) is a critical parameter in the electrode design. By increasing the anode loading to  $2 \text{ mg}/\text{cm}^2$ , a higher energy density of more than 300 Wh/kg can be achieved. By utilizing an improved electrode architecture, higher energy cells will be designed with high loading electrodes of  $> 3 \text{ mAh}/\text{cm}^2$ . The energy density of these cells will be verified in the format of pouch-type full cells ( $< 2 \text{ Ah}$ ); large format cells ( $> 40 \text{ Ah}$ ) will be estimated accordingly.

**Collaborations.** This project collaborates with BMR members: V. Battaglia and G. Liu from LBNL, C. Wong and Z. Jiguang from PNNL, and J. Goodenough from the University of Texas.

### Milestones

1. Failure mode analysis of large-format cells manufactured in 2015. (12/31/15 – Complete)
2. Finalize the structure of nano-Si composite. (3/31/16 – Ongoing)
3. Finalize the architecture of nano-Si composite electrode. *Go/No-Go*:  $> 300$  cycles (80% retention) with loading level of  $> 3 \text{ mAh}/\text{cm}^2$  ( $3 \text{ mg}/\text{cm}^2$  with 1000 mAh/g). (6/30/16 – Ongoing)
4. Verification of performance in pouch-type full cell ( $< 2 \text{ Ah}$ ). (9/30/16 – Ongoing)



## Progress Report

This quarter, HydroQuebec focused on characterization of the large-scale batteries (Figure 2) delivered in late September 2015. The cells reached a capacity of 46.7 Ah capacity and a specific energy of 193 Wh/kg.

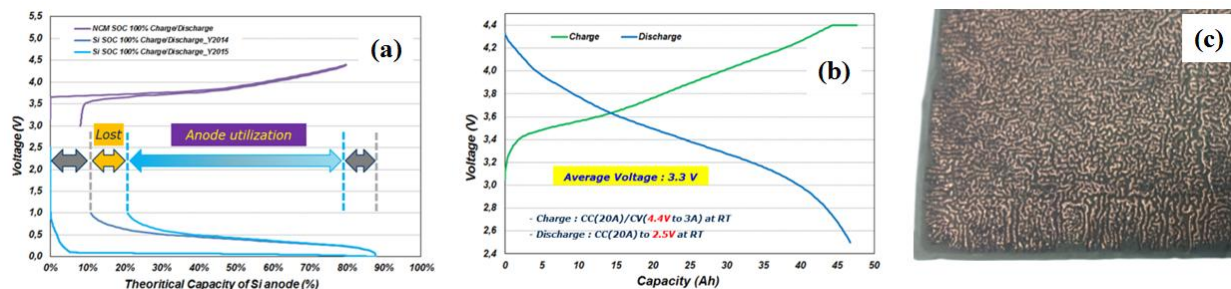


Figure 2. (a) Design concept for *nano-Si*/NCM large format cell (deliverable FY15). (b) Charge-discharge voltage profile of the large format cell charged to 4.4 V and discharged to 2.5 V. (c) Optical image of *nano-Si* anode after cycling.

The design capacity and specific energy are 49Ah and 220Wh/kg, respectively. The measured values are lower than designed because of the low Coulombic efficiency (CE) of the polyimide binder, which was utilized to prevent gas generation. The anode was damaged after just a few cycles. The electrode was severely delaminated: the current collector was curved on both sides and resembled a fingerprint (Figure 2c).

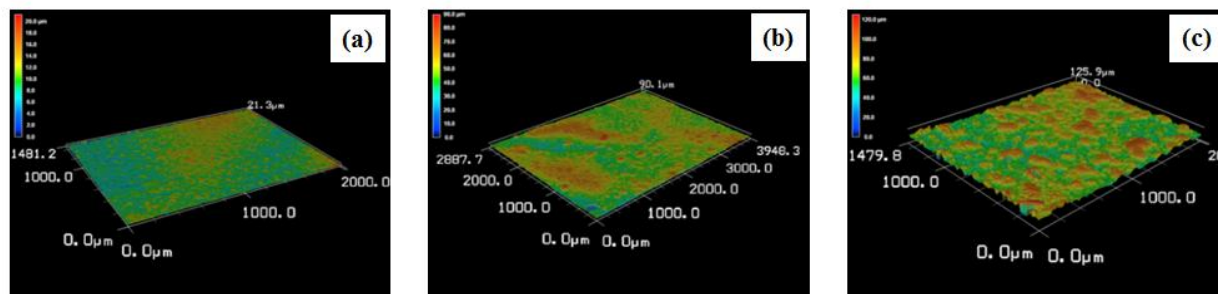


Figure 3. 3D-optical microscope images of the *nano-Si* anode electrode; (a) fresh, (b) 10 cycles, and (c) 50 cycles.

For better understanding, 12 cm<sup>2</sup> full cells were fabricated from the same electrodes and cycled under differing conditions to compare the propensity for electrode damage. The electrodes swelled markedly after cycling and the roughness index, Ra, increased from 1.3 μm for the fresh electrode to 5.6 μm after 10 cycles, and 8.4 μm after 50 cycles (Figure 3).

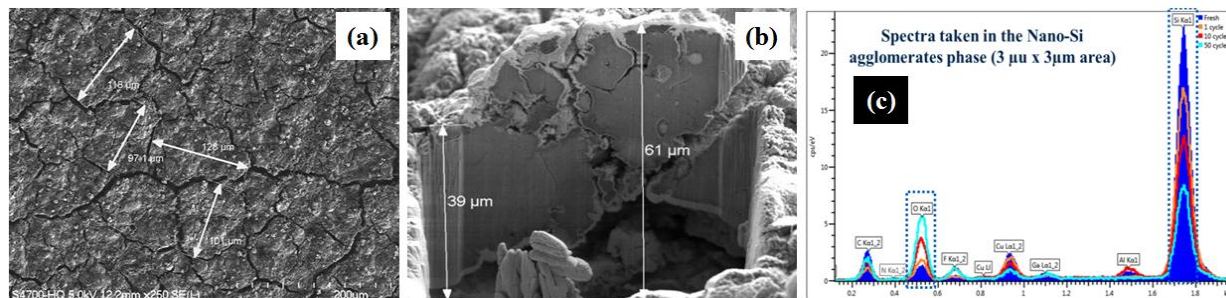


Figure 4. Scanning electron microscopy images of *nano-Si* anode; (a) top view of electrode after 1<sup>st</sup> cycle, and (b) cross section view of electrode after 50<sup>th</sup> cycle. (c) Comparison of local chemical analysis; fresh (blue), 1<sup>st</sup> (orange), 10<sup>th</sup> (red), and 50<sup>th</sup> cycle (cyan).

The electrode surface appears to have “mud cracked,” even after the first cycle (Figure 4a). The electrode layer also delaminated from the current collector (Figure 4b). According to the local chemical analysis in Figure 4c, the intensity of the Si peak decreases with cycling while the O peak increases. This change in electrode composition is believed to result from continuous electrolyte decomposition with cycling.

## Task 1.3 – Design and Scalable Assembly of High-Density, Low-Tortuosity Electrodes (Yet- Ming Chiang, Massachusetts Institute of Technology)

**Project Objective.** The project objective is to develop scalable, high-density, low-tortuosity electrode designs and fabrication processes enabling increased cell-level energy density compared to conventional Li-ion technology, and to characterize and optimize the electronic and ionic transport properties of controlled porosity and tortuosity cathodes as well as densely sintered reference samples. Success is measured by the area capacity ( $\text{mAh}/\text{cm}^2$ ) that is realized at defined C-rates or current densities.

**Project Impact.** The high cost (\$/kWh) and low energy density of current automotive lithium-ion technology is in part due to the need for thin electrodes and associated high inactive materials content. If successful, this project will enable use of electrodes based on known families of cathode and anode actives, but with at least three times the areal capacity ( $\text{mAh}/\text{cm}^2$ ) of current technology while satisfying the duty cycles of vehicle applications. This will be accomplished via new electrode architectures fabricated by scalable methods with higher active materials density and reduced inactive content; this will in turn enable higher energy density and lower-cost EV cells and packs.

**Approach.** Two techniques are used to fabricate thick, high-density electrodes with low tortuosity porosity oriented normal to the electrode plane: (1) directional freezing of aqueous suspensions; and (2) magnetic alignment. Characterization includes measurement of single-phase material electronic and ionic transport using blocking and non-blocking electrodes with ac and dc techniques, electrokinetic measurements, and drive-cycle tests of electrodes using appropriate battery scaling factors for EVs.

**Out-Year Goals.** The out-year goals are as follows:

- Identify anodes and fabrication approaches that enable full cells in which both electrodes have high area capacity under EV operating conditions. Anode approach will include identifying compounds amenable to the same fabrication approach as cathode, or use of very high-capacity anodes, such as stabilized lithium or Si-alloys that in conventional form can capacity-match the cathodes.
- Use data from best performing electrochemical couple in techno-economic modeling of EV cell and pack performance parameters.

**Collaborations.** Within BMR, this project collaborates with Antoni P. Tomsia (LBNL) in fabrication of low-tortuosity, high-density electrodes by directional freeze-casting, and with Gao Liu (LBNL) in evaluating Si anodes. Outside of BMR, the project collaborates with Randall Erb (Northeastern University) on magnetic alignment fabrication methods for low-tortuosity electrodes.

### Milestones

1. Obtain 2-, 10- and 30- sec pulse discharge data for an electrode of at least  $10 \text{ mAh}/\text{cm}^2$  area capacity. (12/31/15 – Revised and complete)
2. Test at least one cathode and one anode each having at least  $10 \text{ mAh}/\text{cm}^2$  area capacity under an accepted EV drive cycle. (3/31/16)
3. *Go/No-Go:* Demonstrate a cathode or anode having at least  $10 \text{ mAh}/\text{cm}^2$  area capacity that passes an accepted EV drive cycle. (6/30/16)
4. Construct and obtain test data for full cell in which area capacity of both electrodes is at least  $10 \text{ mAh}/\text{cm}^2$ . (9/30/16)

## Progress Report

**Milestone. Obtain 2-, 10-, and 30- sec pulse discharge data for an electrode of at least 10 mAh/cm<sup>2</sup> area capacity. (Complete)** Since the milestone was originally written, it became clear that model EV drive cycles do not include pulse discharge durations as short as 2 sec. For example, the USABC Dynamic Stress Test (DST), which has been adopted for most of the testing under this project, has a shortest duration of 8 sec (Figure 5). Accordingly, testing to meet this quarter's milestone was revised to correspond to the DST test, with discharge pulse durations of 8-, 12-, 24-, 28-, 32- and 36- sec duration, and maximum C-rate of 2C, as shown in Figure 5. The revised milestone was met by iteratively running the DST profile to discharge a directionally frozen and sintered NCA cathode in half-cell configuration.

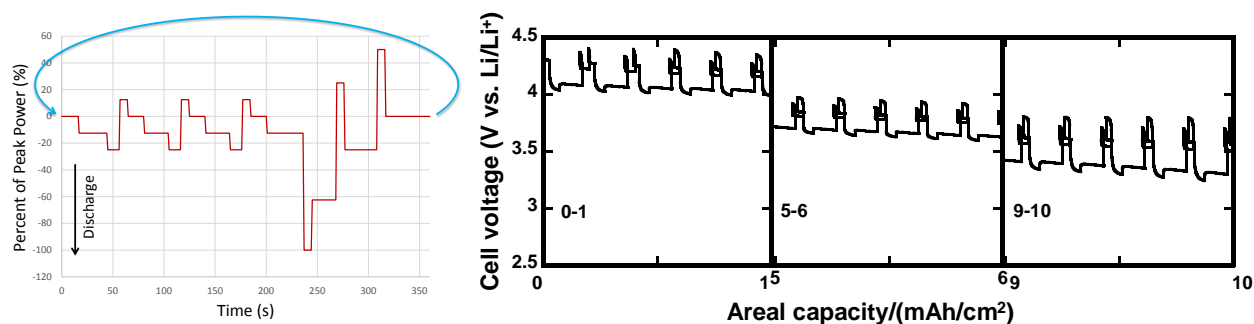


**Figure 5.** USABC dynamic stress test profile (left) has discharge pulses of 8, 12, 24, 28, 32, and 36 sec and is net discharge. It was looped repeatedly, as illustrated on the right for area capacity ranges of 0-1, 5-6 and 9-10 mAh/cm<sup>2</sup>, to discharge a low tortuosity NCA cathode of 12.7 mAh/cm<sup>2</sup> theoretical capacity to 2.5 V vs Li/Li<sup>+</sup>, yielding 11.5 mAh/cm<sup>2</sup> discharge capacity.

Additionally, a new magnetic alignment approach for producing low-tortuosity porosity was demonstrated, in which emulsion droplets of magnetic fluid form chains under an applied magnetic field. These chained droplets are subsequently removed by evaporation, leaving aligned pore arrays that thread completely through the electrode thickness (Figure 6). Upon sintering, the resulting cathode has low-tortuosity, continuous pores oriented in the desired direction normal to the electrode plane. Electrochemical tests in half-cells show that, in 310 micron thick electrodes of ca. 40% porosity, capacity utilization at 1C rate is about twice that in identical electrodes that have not been magnetically aligned. A variant of this process that does not require sintering is being developed.

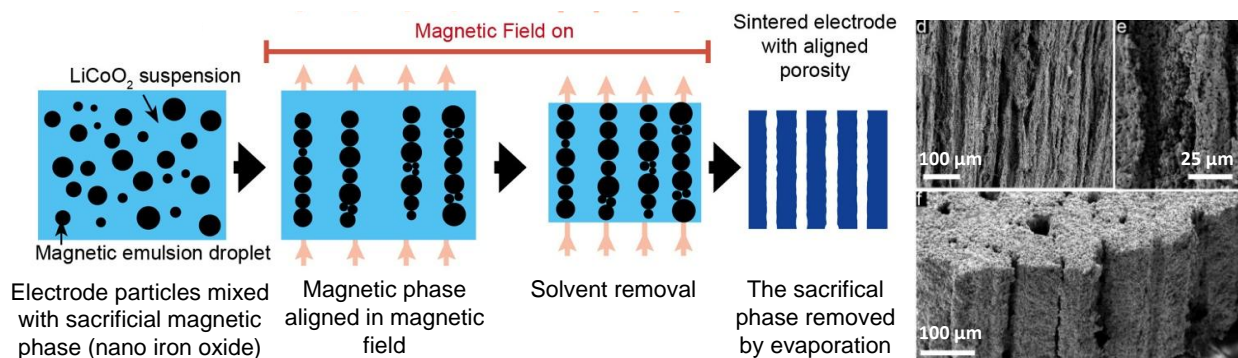


**Figure 6.** Magnetic emulsion droplets chain in an applied field, producing sacrificial pore formers that are then removed by evaporation, leaving highly oriented low tortuosity pores threading through a sintered LiCoO<sub>2</sub> cathode.

## Task 1.4 – Hierarchical Assembly of Inorganic/Organic Hybrid Si Negative Electrodes (Gao Liu, Lawrence Berkeley National Laboratory)

**Project Objective.** This work aims to enable silicon as a high-capacity and long cycle-life material for negative electrode to address two of the barriers of lithium-ion chemistry for EV and plug-in hybrid electric vehicle (PHEV) application: insufficient energy density and poor cycle life performance. The proposed work will combine material synthesis and composite particle formation with electrode design and engineering to develop high-capacity, long-life, and low-cost hierarchical Si-based electrode. State of the art Li-ion negative electrodes employ graphitic active materials with theoretical capacities of 372 mAh/g. Silicon, a naturally abundant material, possesses the highest capacity of all Li-ion anode materials. It has a theoretical capacity of 4200 mAh/g for full lithiation to the  $\text{Li}_{22}\text{Si}_5$  phase. However, Si volume change disrupts the integrity of electrode and induces excessive side reactions, leading to fast capacity fade.

**Project Impact.** This work addresses the adverse effects of Si volume change and minimizes the side reactions to significantly improve capacity and lifetime to develop negative electrode with Li-ion storage capacity over 2000 mAh/g (electrode level capacity) and significantly improve the CE to over 99.9%. The research and development activity will provide an in-depth understanding of the challenges associated with assembling large volume change materials into electrodes and will develop a practical hierarchical assembly approach to enable Si materials as negative electrodes in Li-ion batteries.

**Out-Year Goals.** The three main aspects of this proposed work (that is, bulk assembly, surface stabilization, and Li enrichment) are formulated into 10 tasks in a four-year period.

- Develop hierarchical electrode structure to maintain electrode mechanical stability and electrical conductivity. (bulk assembly)
- Form *in situ* compliant coating on Si and electrode surface to minimize Si surface reaction. (surface stabilization)
- Use prelithiation to compensate first cycle loss of the Si electrode. (Li enrichment)

The goal is to achieve a Si-based electrode at higher mass loading of Si that can be extensively cycled with minimum capacity loss at high CE to qualify for vehicle application.

**Collaborations.** This project collaborates with the following: Vince Battaglia and Venkat Srinivasan of LBNL; Xingcheng Xiao of GM; Jason Zhang and Chongmin Wang of PNNL; Yi Cui of Stanford University; and the Si Anode Focus Group.

### Milestones

1. Investigate the impact of different side chain conducting moieties to the electric conductivity of the functional conductive binders. (December 2015 – Complete)
2. Quantify the adhesion group impact to the electrode materials and current collector. (March 2016 – On schedule)
3. Fabricate higher loading electrode ( $> 3 \text{ mAh/cm}^2$ ) based on the Si electrode materials and select binder; test cycling stability. (June 2016 – On schedule)
4. Fabricate NMC/Si full cell and quantify the performance. (September 2016)



## Progress Report

High-tap-density silicon nanomaterials are highly desirable as anodes for lithium-ion batteries due to small surface area and minimum first-cycle loss. However, this material poses formidable challenges to polymeric binder design. Binders adhere to the small surface area to sustain the drastic volume changes during cycling; also, low porosities and small pore size resulting from this material are detrimental to Li-ion transport.

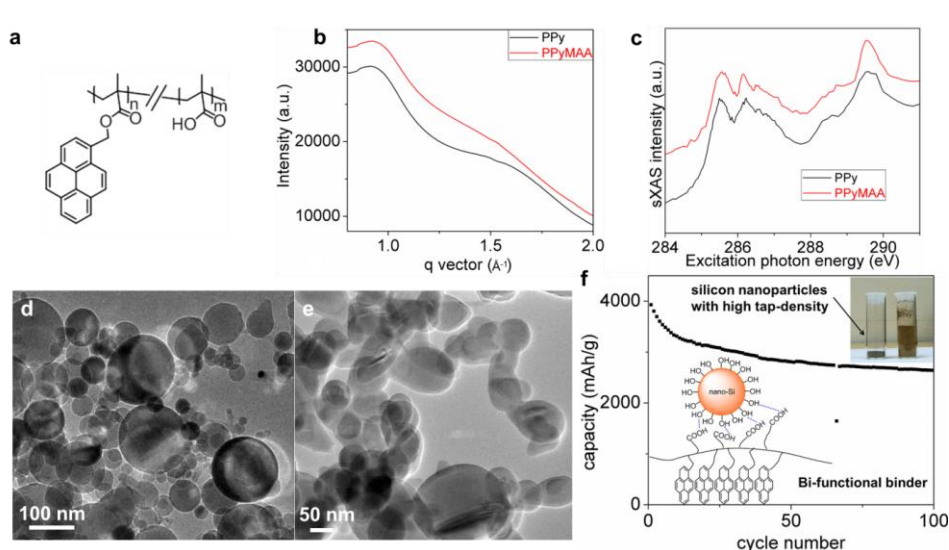


**Figure 7.** (a) Chemical structure of PPyMAA [poly(1-pyrenemethyl methacrylate-co-methacrylic acid)] conductive polymer binder. (b) Wide angle X-ray scattering of PPy and PPyMAA polymers. (c) Carbon K-edge soft X-ray absorption spectroscopy of PPy and PPyMAA shows that the lowest unoccupied molecular orbital (LUMO) energy is intact in PPyMAA, although nonconductive methacrylic acid groups are introduced. Transmission electron microscopy morphology of (d) high-tap-density nano-Si and (e) regular nano-Si produced by chemical vapor deposition (right). (f) Cycling performance of PPyMAA/high-tap-density nano-Si.

This study introduces a new binder, poly(1-pyrenemethyl methacrylate-co-methacrylic acid) (PPyMAA), for a high-tap-density nano-silicon electrode cycled in a stable manner with a first-cycle efficiency of 82%—a value that is further improved to 87% when combined with graphite material. The content of MAA is limited to 30 mol% to enhance the adhesion of the binder while not disturbing the conjugation of the PPy unit. Wide angle X-ray scattering (WAXS) of the PPy and PPyMAA polymers exhibit a very similar pattern (Figure 7b), indicating that the ordered phase characteristic of the pyrene is still maintained in the synthesized PPyMAA copolymer. Figure 7c shows the soft X-ray absorption spectroscopy (sXAS) spectra of PPy and PPyMAA. The splitting peaks around 285–286 eV correspond to the  $\pi^*_{C=C}$  bonds with conjugation, and the features around 288 eV are from  $\pi^*_{C=O}$ . It is obvious that incorporating the MAA group does not change the lowest-energy features in sXAS, indicating the lowest unoccupied molecular orbital (LUMO) of the PPy polymer is intact in PPyMAA. The consistency of the overall lineshape also implies that the electron states close to the Fermi level are dominated by the pyrene-based PPy states.

The regular nano-Si shown here was synthesized using a chemical vapor deposition (CVD) process, which has an average particle size of 50 to 70 nm and a tap density of 0.1 g/cm<sup>3</sup>. Most of the particles are fused together in the regular nano-Si (Figure 7e); the fused particles form a “network”-like structure that is maintained even after laminate fabrication. Thus, the high surface area of the pristine CVD nano-Si translates into a high porosity of the electrode laminate, which has a calculated pore value of 86%. SEM indicates that the high-tap-density nano-Si has a regular round shape with a median size of 200 nm (Figure 7d). Although this Si particle is in nano-size, Brunauer-Emmett-Teller (BET) analysis indicates a surface area of only 12 m<sup>2</sup>/g, with a tap-density of 0.51 g/cm<sup>3</sup>. The cycling performance of high-tap-density nano-Si with PPyMAA is shown in Figure 7f, which indicates a long-term stable electrochemical performance with a high specific capacity above 2500 mAh/g and a high first-cycle CE (87%). The high-tap-density nano-Si-based high-capacity anodes enabled by the PPyMAA binder shows great promise toward a commercial product.

## Patents/Publications/Presentations

### Publications

- Ai, Guo, and Zhihui Wang, Hui Zhao, Wenfeng Mao, Yanbao Fu, Vincent Battaglia, Sergey Lopatin, and Gao Liu. “Scalable Process for Application of Stabilized Lithium Metal Powder in Li-Ion Batteries.” *Journal of Power Sources*. Minor revision.
- Zhao, Hui, and Wei Yang, Ruimin Qiao, Chenhui Zhu, Ziyang Zheng, Min Ling, Zhe Jia, Ying Bai, Yanbao Fu, Jinglei Lei, Xiangyun Song, Vincent Battaglia, Wanli Yang, Phillip Messersmith, and Gao Liu. “Conductive Polymer Binder for High-Tap-Density Nano-Silicon Material for Lithium Ion Battery Negative Electrode Application.” *Nano Letters* 15 (2015): 7927-7932.

## Task 2 – Silicone Anode Research

### Summary and Highlights

Most Li-ion batteries used in the state-of-the-art EVs contain graphite as their anode material. Limited capacity of graphite ( $\text{LiC}_6$ , 372 mAh/g) is one of the barriers that prevent the long range operation of EVs required by the EV Everywhere Grand Challenge proposed by the DOE/EERE. In this regard, silicon is one of the most promising candidates as an alternative anode for Li-ion battery applications. Si is environmentally benign and ubiquitous. The theoretical specific capacity of silicon is 4212 mAh/g ( $\text{Li}_{21}\text{Si}_5$ ), which is 10 times greater than the specific capacity of graphite. However, the high specific capacity of silicon is associated with large volume changes (more than 300 percent) when alloyed with lithium. These extreme volume changes can cause severe cracking and disintegration of the electrode and can lead to significant capacity loss.

Significant scientific research has been conducted to circumvent the deterioration of silicon-based anode materials during cycling. Various strategies, such as reduction of particle size, generation of active/inactive composites, fabrication of silicon-based thin films, use of alternative binders, and the synthesis of one-dimensional silicon nanostructures have been implemented by a number of research groups. Fundamental mechanistic research also has been performed to better understand the electrochemical lithiation and delithiation processes during cycling in terms of crystal structure, phase transitions, morphological changes, and reaction kinetics. Although significant progress has been made on developing silicon-based anodes, many obstacles still prevent their practical application. Long-term cycling stability remains the foremost challenge for Si-based anode, especially for the high loading electrode ( $> 3\text{mAh/cm}^2$ ) required for many practical applications. The cyclability of full cells using silicon-based anodes is also complicated by multiple factors, such as diffusion-induced stress and fracture, loss of electrical contact among silicon particles and between silicon and current collector, and the breakdown of solid-electrolyte interphase (SEI) layers during volume expansion/contraction processes. The design and engineering of a full cell with a silicon-based anode still needs to be optimized. Critical research remaining in this area includes, but is not limited to, the following:

- Low-cost manufacturing processes have to be found to produce nano-structured silicon with the desired properties.
- The effects of SEI formation and stability on the cyclability of silicon-based anodes need to be further investigated. Electrolytes and additives that can produce a stable SEI layer need to be developed.
- A better binder and a conductive matrix need to be developed. They should provide flexible but stable electrical contacts among silicon particles and between particles and the current collector under repeated volume changes during charge/ discharge processes.
- The performances of full cells using silicon-based anode need to be investigated and optimized.

The main goal of this project is to have a fundamental understanding on the failure mechanism on Si based anode and improve its long term stability, especially for thick electrode operated at full cell conditions. Success of this project will enable Li-ion batteries with a specific energy of  $>350\text{ Wh/kg}$  (in cell level), 1000 deep-discharge cycles, 15-year calendar life, and less than 20% capacity fade over a 10-year to meet the goal of EV everywhere.

## Task 2.1 – Development of Silicon-Based High Capacity Anodes

(Ji-Guang Zhang/Jun Liu, PNNL; Prashant Kumta, Univ. of Pittsburgh; Jim Zheng, PSU)

**Project Objective.** The project objective is to develop high-capacity and low-cost silicon-based anodes with good cycle stability and rate capability to replace graphite in lithium-ion batteries. In one approach, the low cost Si-graphite-carbon (SGC) composite will be developed to improve the long-term cycling performance while maintaining a reasonably high capacity. Si-based secondary particles with a nano-Si content of ~10 to 15 wt% will be embedded in the matrix of active graphite and inactive conductive carbon materials. Controlled void space will be pre-created to accommodate the volume change of Si. A layer of highly graphitized carbon coating at the outside will be developed to minimize the contact between Si and electrolyte, and hence minimize the electrolyte decomposition. New electrolyte additives will be investigated to improve the stability of SEI layer. In another approach, nanoscale silicon and Li-ion conducting lithium oxide composites will be prepared by *in situ* chemical reduction methods. The stability of Si-based anode will be improved by generating the desired nanocomposites containing nanostructured amorphous or nanocrystalline Si as well as amorphous or crystalline lithium oxide (Si+Li<sub>2</sub>O) by the direct chemical reduction of a mixture and variety of Si sub oxides (SiO and SiO<sub>x</sub>) and/or dioxides. Different synthesis approaches comprising direct chemical reduction using solution, solid-state and liquid-vapor phase methods will be utilized to generate the Si+Li<sub>2</sub>O nanocomposites. The electrode structures will be modified to enable high utilization of thick electrode.

**Project Impact.** Si-based anodes have much larger specific capacities compared with conventional graphite anodes. However, the cyclability of Si-based anodes is limited because of the large volume expansion characteristic of these anodes. This work will develop a low-cost approach to extend the cycle life of high-capacity, Si-based anodes. The success of this work will further increase the energy density of Li-ion batteries and accelerate market acceptance of EVs, especially for the PHEVs required by the EV Everywhere Grand Challenge proposed by the DOE/EERE.

**Out-Year Goals.** The main goal of the proposed work is to enable Li-ion batteries with a specific energy of >200 Wh/kg (in cell level for PHEVs), 5000 deep-discharge cycles, 15-year calendar life, improved abuse tolerance, and less than 20% capacity fade over a 10-year period.

### Milestones

1. Identify and synthesize the active-inactive Si-based nanocomposite with low-cost approach and a specific capacity ~800 mAh/g. (12/31/2015 – Complete)
2. Achieve 80% capacity retention over 200 cycles for graphite supported nano Si-carbon shell composite. (3/31/2016 – Ongoing)
3. Synthesize the suitable active-inactive nanocomposite with Li<sub>2</sub>O as matrix (Si+Li<sub>2</sub>O) or intermetallic matrix (Si+ MnBm) of specific capacity ~1000-1200mAh/g. (March 2016 – Ongoing)
4. Optimize the cost-effective, scalable high-energy mechanical milling (HEMM) and solid state synthesis techniques for generation of active-inactive composite with capacities ~1000-1200 mAh/g. (June 2016 – Ongoing)
5. Develop interface control agents and surface electron conducting additives to reduce the first cycle irreversible loss and improve the CE of Si-based anode. (6/30/2016 – Ongoing)
6. Achieve > 80% capacity retention over 300 cycles for thick electrodes (> 2 mAh cm<sup>-2</sup>) through optimization of the Si electrode structure and binder. (9/30/2016 – Ongoing)



## Progress Report

This quarter, a cost-effective hydrothermal-carbonization approach has been developed to synthesis the hard carbon coated nano-Si/graphite (HC-nSi/G) composite as a high-performance anode for Li-ion batteries. In this hierarchical structured composite, the hard carbon coating layer not only provides an efficient pathway for electron transfer, but also alleviates the volume variation of silicon during charge/discharge processes. Figure 8 shows the schematic illustration of the synthesis process of HC-nSi/G composite; Figure 8b-e shows SEM images, C/Si energy dispersive X-ray (EDX) elemental maps and X-ray spectra of HC-nSi/G composite. It demonstrated excellent electrochemical performances including a high specific capacity of  $878.6 \text{ mAh g}^{-1}$  based on the total weight of composite and good rate performance ( $680 \text{ mAh g}^{-1}$  at 2C), which is promising for practical applications.

Si nanoflakes and nanorods prepared by low-pressure chemical vapor deposition (LPCVD) using a low-cost water soluble template derived by optimized milling time were tested for rate capability at different current rates (Figure 9). The Si nanoflakes show stable performance and higher capacities ( $\sim 780 \text{ mAh/g}$  at 2A/g) even at high cycling rates of 2A/g compared to Si nanorods ( $\sim 470 \text{ mAh/g}$  at 2A/g). Si nanorods show stable performance up to current rates of 0.5A/g. The Si nanoflakes show a high capacity of  $\sim 1260 \text{ mAh/g}$ , while the nanorods show  $\sim 900 \text{ mAh/g}$  capacity at 1A/g. The normalized capacity of nanorods declines at higher current rates of 1A/g and 2A/g, while the nanoflakes show a better rate capability. The amorphous state of the Si nanoflakes likely contributes to the stable cycling performance, and the lower  $\text{Li}^+$  diffusion distances possibly contribute to the better rate capability observed in the nanoflakes.

The effect of stabilized lithium metal powder (SLMP) on the CE of pre-lithiated anode was further investigated. The silicon nanoparticles (SiNPs)-CNTs composite paper anodes were lithiated with different amount of SLMP and tested in a voltage range of 1-0.005 V versus  $\text{Li/Li}^+$  under a constant current of 1 mA. The CE after first discharge-charge cycle as a function of applied SLMP to SiNPs-CNTs anode mass ratio was measured. As the SLMP/anode mass ratio increases from 0 to 0.21, the first-cycle CE increases from 65 to 90%. When the SLMP/anode mass ratio equals 0.26, the first-cycle CE is 98%. Further increase of SLMP/anode ratio will lead to decrease of the first cycle discharge capacity and is detrimental for long-term cycling of SiNPs-CNTs composite anode. Therefore, a well balanced SLMP/anode ratio is required for the stable operation of pre-lithiated Si based anode.

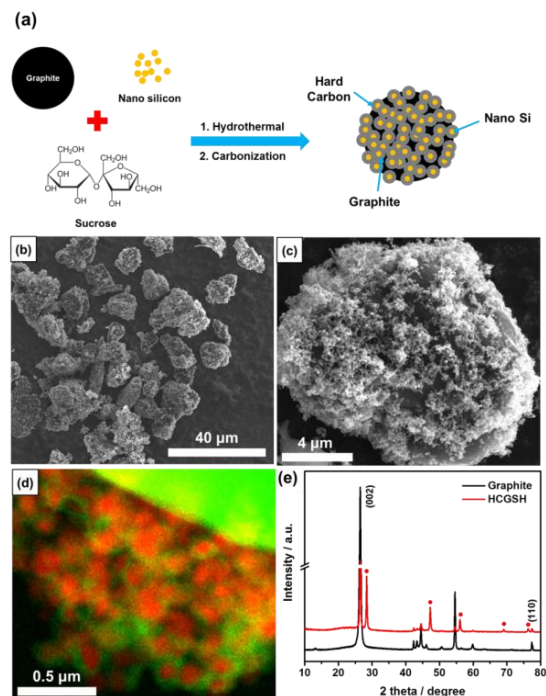


Figure 8. (a) Schematic illustration of the synthesis of the HC-nSi/G. (b/c) Scanning electron microscopy images. (d) C/Si energy dispersive X-ray elemental maps. (e) X-ray diffraction patterns.

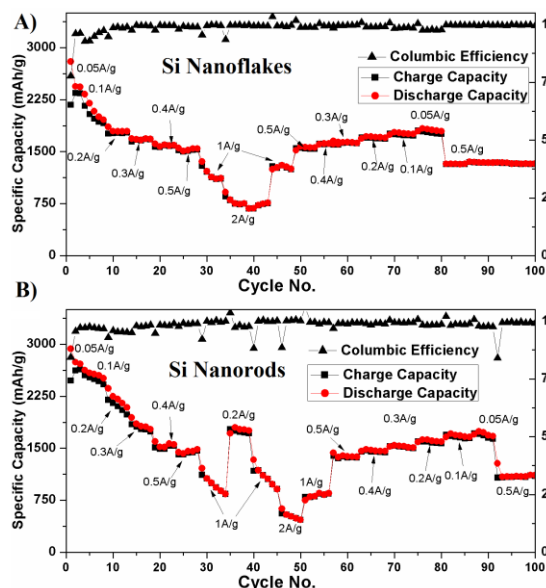


Figure 9. Rate capability testing of (a) Si nanoflakes and (b) Si nanorods at different current rates in  $\text{Li/Li}^+$  system.

## Patents/Publications/Presentations

### Publications

- Epur, Rigved, and Madhumati Ramanathan, Moni K. Datta, Dae Ho Hong, Prashanth H. Jampani, Bharat Gattu, and Prashant N. Kumta. “Scribable Multi-Walled Carbon Nanotube-Silicon Nanocomposites: A Viable Lithium-Ion Battery System.” *Nanoscale* 7 (2015): 3504-3510.
- Epur, Rigved, and Prashanth H. Jampani, Moni K. Datta, Dae Ho Hong, Bharat Gattu, and Prashant N. Kumta. “A Simple and Scalable Approach to Hollow Silicon Nanotube (h-SiNT) Anode Architectures of Superior Electrochemical Stability and Reversible Capacity.” *J. Mater. Chem. A* 3 (2015): 11117-11129.
- Jeong, Sookyung, and Xiaolin Li, Jianming Zheng, Pengfei Yan, Ruiguo Cao, Hee Joon Jung, Chongmin Wang, Jun Liu, and Ji-Guang Zhang. “Hard Carbon Coated Nano-Si/graphite Composite as a High Performance Anode for Li-Ion Batteries.” Submitted for publication.

### Presentations

- 228<sup>th</sup> ECS Meeting, Phoenix (October 2015): “Nano Silicon (Si<sub>NP</sub>) Based Carbon Composite: Flexible Anode System in Lithium Ion Batteries”; B. Gattu, P. P. Patel, P. Jampani, M. K. Datta, and P. N. Kumta.
- 227<sup>th</sup> ECS Meeting, Chicago (May 2015): “High Performing Hollow Silicon Nanotube Anodes for Lithium Ion Batteries”; B. Gattu, P. Jampani, P. P. Patel, M. K. Datta, and P. N. Kumta.

## Task 2.2 – Pre-Lithiation of Silicon Anode for High Energy Li Ion Batteries (Yi Cui, Stanford University)

**Project Objective.** Prelithiation of high-capacity electrode materials such as silicon is an important means to enable those materials in high-energy batteries. This study pursues two main directions: (1) developing facile and practical methods to increase first-cycle CE of Si anodes, and (2) synthesizing fully lithiated Si to pair with high-capacity lithium-free cathode materials.

**Project Impact.** The lithium loss for first cycle in existing Li-ion batteries will be compensated by using these cathode prelithiation materials. The cathode prelithiation materials have good compatibility with ambient air, regular solvent, binder and the thermal processes used in current Li-ion battery manufacturing. This project's success will improve the energy density of existing Li-ion batteries and help to achieve high-energy-density Li-ion batteries for electric vehicles.

**Out-Year Goals.** Compounds containing a large quantity of Li will be synthesized for pre-storing Li ions inside batteries. First-cycle CE will be improved and optimized (over 95%) by prelithiating anode materials with the synthesized Li-rich compounds.

**Collaborations.** The Project works with the following collaborators: (1) BMR program principal investigators (PIs), and (2) SLAC: *in situ* X-ray, Dr. Michael Toney.

### Milestones

1. Prelithiate conversion oxides by the reaction between molten Li metal and oxide. (December 31, 2015 – Complete)
2. Synthesize LiF/metal nanocomposite for cathode prelithiation with high capacity and good air stability (> 500 mAh/g). (March 31, 2016 – Ongoing)
3. Synthesize Li<sub>2</sub>S/metal nanocomposite for cathode prelithiation with high capacity. (June 31, 2016 – Ongoing)

## Progress Report

The cathode prelithiation additives based on nanoscale mixtures of transition metal (M) and lithium oxide ( $\text{Li}_2\text{O}$ ) have been developed. These additives are the reaction products of transition metal oxide ( $\text{M}_x\text{O}_y$ ) and Li metal via a well known conversion reaction mechanism (Figure 10a). The composites of nanometer-sized M/nanometer-sized  $\text{Li}_2\text{O}$  (N-M/N- $\text{Li}_2\text{O}$ ) afford a high prelithiation capacity [for example,  $619 \text{ mAh g}^{-1}$  for the nanometer-sized Co/ nanometer-sized  $\text{Li}_2\text{O}$  (N-Co/N- $\text{Li}_2\text{O}$ ; molar ratio, 3/4) composite, Figure 10b] when converted back to  $\text{M}_x\text{O}_y$  and Li ions during cathode charge. The N-Co/N- $\text{Li}_2\text{O}$  electrode lost nearly all the capacity after the first cycle, suggesting that after providing Li ion during the first charge, these nanocomposites did not contribute to the active electrochemical process in the cathode (Figure 10c). The response of the additive at different potential ranges is clearly shown by a  $\text{LiFePO}_4$  electrode containing different amounts of such additive (Figure 10d). In a full cell configuration, the  $\text{LiFePO}_4$  electrode with a 4.8% Co/ $\text{Li}_2\text{O}$  additive shows 11% higher overall capacity than that of the pristine  $\text{LiFePO}_4$  electrode (Figure 10e-f).

To show the generality of using N-M/N- $\text{Li}_2\text{O}$  composites as high-capacity cathode additives, the project also prepared N-Ni/N- $\text{Li}_2\text{O}$  and N-Fe/N- $\text{Li}_2\text{O}$  composites using the same synthesis procedure. Similar to the N-Co/N- $\text{Li}_2\text{O}$  composite, the N-Ni/N- $\text{Li}_2\text{O}$  and N-Fe/N- $\text{Li}_2\text{O}$  electrodes possess high initial high open circuit voltage (OCV, higher than 1.5 V) and deliver high charge capacities of 506 and  $631 \text{ mAh g}^{-1}$ , respectively, and very low discharge capacity of 11 and  $19 \text{ mAh g}^{-1}$ , respectively. The  $\text{LiFePO}_4$  electrodes with the two additives were both subject to cycling. As expected, their first-cycle charge capacities are improved significantly. The initial charge capacities are  $180 \text{ mAh g}^{-1}$  for the electrode with a 4.8% N-Ni/N- $\text{Li}_2\text{O}$  additive and  $178 \text{ mAh g}^{-1}$  for that with a 4.8% N-Fe/N- $\text{Li}_2\text{O}$  composites, respectively. These capacities are ~10% higher than that of  $\text{LiFePO}_4$  electrodes without any prelithiation additive. Moreover, these electrodes also show very good cycling stability.

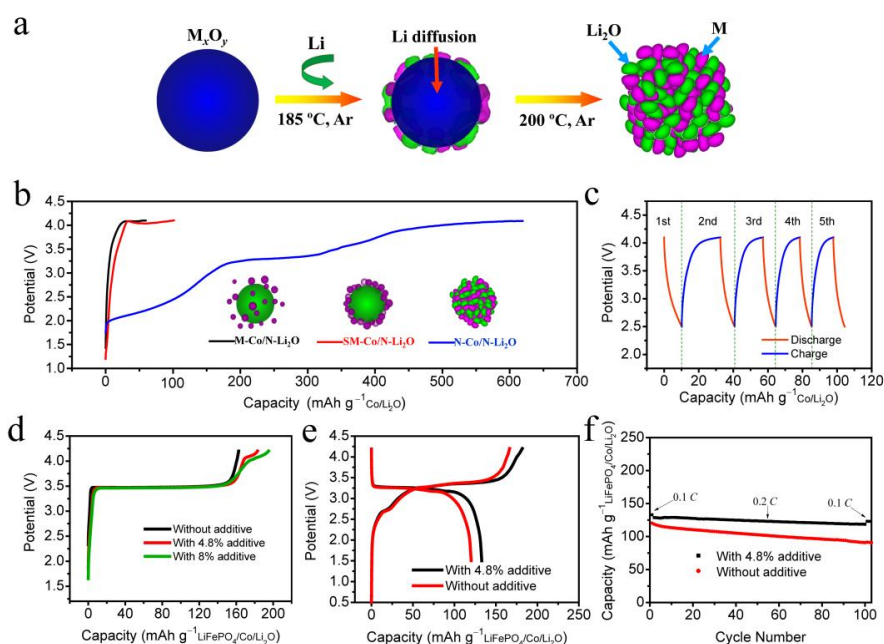


**Figure 10. Fabrication and electrochemical characteristics of the N-Co/N- $\text{Li}_2\text{O}$  composite.** (a) Schematic of the fabrication process of the N-M/N- $\text{Li}_2\text{O}$  composites. MOs are used as the starting materials and *in situ* converted into N-M/N- $\text{Li}_2\text{O}$  composites via the chemical reaction with molten Li. (b) The initial charge potential profiles of the electrodes made with various Co/ $\text{Li}_2\text{O}$  nanocomposites: Micrometer-sized Co/nanometer-sized  $\text{Li}_2\text{O}$  (M-Co/N- $\text{Li}_2\text{O}$ ), submicrometer-sized Co/nanometer-sized  $\text{Li}_2\text{O}$  (SM-Co/N- $\text{Li}_2\text{O}$ ) and N-Co/N- $\text{Li}_2\text{O}$  composites. (c) The charge/discharge potential profiles of the N-Co/N- $\text{Li}_2\text{O}$  electrode after the first charge process. (d) The initial charge potential profiles of the  $\text{LiFePO}_4$  electrodes with different amounts of the N-Co/N- $\text{Li}_2\text{O}$  additive in half cell configurations. (e and f) The initial charge/discharge potential profiles (e) and cycling performance (f) of  $\text{LiFePO}_4$ /graphite full cells with and without the N-Co/N- $\text{Li}_2\text{O}$  additive. The specific capacities of the cathodes are evaluated based on the weight of  $\text{LiFePO}_4$  and the N-Co/N- $\text{Li}_2\text{O}$  additive.

## Patents/Publications/Presentations

### Patent

- *High-Capacity Conversion Reaction-Based Cathode Additives for Lithium-Ion Batteries.* WebDisclosure197169.

### Publication

- Sun, Y. M., and H.-W. Lee, Z. W. Seh, N. Liu, J. Sun, Y. Z. Li, and Y. Cui\*. “High-Capacity Battery Cathode Prelithiation to Offset Initial Lithium Loss.” *Nature Energy* 1 (2016): 15008.

## TASK 3 – HIGH-ENERGY DENSITY CATHODES FOR ADVANCED LITHIUM-ION BATTERIES

### Summary and Highlights

Developing high energy density, low-cost, thermally stable, and environmentally safe electrode materials is a key enabler for advanced batteries for transportation. High energy density is synonymous with reducing cost per unit weight or volume. Currently, one major technical barrier toward developing high energy density lithium-ion batteries (LiBs) is the lack of robust, high-capacity cathodes. As an example, the most commonly used anode material for LiBs is graphitic carbon, which has a specific capacity of 372 mAh/g, while even the most advanced cathodes like lithium nickel manganese cobalt oxide (NMC) have a maximum capacity of ~180 mAh/g. This indicates an immediate need to develop high-capacity (and voltage) intercalation type cathodes that have stable reversible capacities of 250 mAh/g and beyond. High volumetric density is also critical for transportation applications. Alternative high-capacity cathode chemistries such as those based on conversion mechanisms, Li-S, or metal air chemistries still have fundamental issues that must be addressed before integration into cells for automotive use. Successful demonstration of practical high energy cathodes will enable high energy cells that meet or exceed the DOE cell level targets of 400 Wh/kg and 600 Wh/L with a system level cost target of \$125/kWh.

During the last decade, many high-voltage cathode chemistries have been developed under the BATT (now BMR) program, including Li-rich NMC and Ni-Mn spinels. Current efforts are directed towards new syntheses and modifications to improve their stability under high-voltage cycling condition ( $> 4.4$  V) for Ni-rich NMC and LMR-NMC [Zhang/Jie, PNNL; Thackeray/Croy, ANL; Looney/Wang, BNL, Doeff and Tong, LBNL]. Three other subtasks are directed towards synthesis and structural stabilization of high-capacity polyanionic cathodes that can have  $> 1$  lithium per transition metal (TM) and can be in crystalline or amorphous phases [Nanda, ORNL; Manthiram, University of Texas (UT) at Austin; Whittingham, State University of New York (SUNY) at Binghamton; and Kercher/Kiggans, ORNL]. Approaches also include aliovalent or isovalent doping to stabilize cathode structures during delithiation as well as stabilizing oxygen. John Goodenough's group at UT-Austin is developing membranes to stabilize lithium metal anodes and eventually enable high-capacity cathodes in full cell configuration.

The highlights for this quarter are as follows:

- **Task 3.1.** Fluorination method for  $\text{Li}_2\text{CuO}_2$  cathodes to improve stability at voltages  $> 3.9$  V.
- **Task 3.2.** Synthesis optimization of  $\text{LiVOPO}_4$  with capacities  $\sim 200$  mAh/g for 40 cycles.
- **Task 3.3.** Evaluation of  $\text{LiNi}_x\text{Mn}_y\text{Co}_y\text{O}_2$  (NMC) with different Ni content at high charge cutoff voltage of 4.5 V.
- **Task 3.4.** Synthesis and stabilization of  $\text{LiNiO}_2$  and solid solutions  $\text{LiNi}_{1-x}\text{M}_x\text{O}_2$  ( $\text{M}=\text{Co}, \text{Mn}$ ).
- **Task 3.5.** Performance of a model layered-layered-spinel (LLS) compound derived from a base LL composition;  $0.25\text{Li}_2\text{MnO}_3 \cdot 0.75\text{LiMn}_{0.375}\text{Ni}_{0.375}\text{Co}_{0.25}\text{O}_2$  demonstrated capacity of  $\sim 200$  mAh/g.
- **Task 3.6.** Synthesis method for  $\alpha_1\text{-Li}_2\text{VOPO}_4$  nanoparticles and identification of crystal structure.
- **Task 3.7.** Combination of vanadate/borate substitution to improve the electrochemical performance of silver-bearing phosphate glass.
- **Task 3.8.** Synthesis and characterization of NMCs with higher Ni content (for example, NMC-532 and NMC-622) using co-precipitation and spray pyrolysis method.
- **Task 3.9.** Fabrication and testing of solid electrolyte membranes comprising a low melting point  $\text{Li}^+$  electrolyte glass in a thiol-ene based polymer.
- **Task 3.10.** Synthesis and structural characterization of LT-  $\text{Li}[\text{Mn}_{1.5}\text{Ni}_{0.5-2x}\text{Co}_{2x}]\text{O}_4$ ;  $x = 0, 0.125$  to stabilize spinel in layered TM oxides.
- **Task 3.11.** Solid-state synthesis of  $\text{LiNiO}_2$  compositions to optimize electrochemical performance.



## Task 3.1 – Studies of High Capacity Cathodes for Advanced Lithium-ion Systems (Jagjit Nanda, Oak Ridge National Laboratory)

**Project Objective.** The overall project goal is to develop high energy density lithium-ion electrodes for EV and PHEV applications that meet and/or exceed the DOE energy density and life cycle targets from the USDRIVE/USABC roadmap. Specifically, this project aims to mitigate the technical barriers associated with high-voltage cathode compositions such as lithium-manganese rich NMC (LMR-NMC), and  $\text{Li}_2\text{M}_x^{\text{I}}\text{M}_{1-x}^{\text{II}}\text{O}_2$ , where  $\text{M}^{\text{I}}$  and  $\text{M}^{\text{II}}$  are transition metals that do not include Mn or Co. Major emphasis is placed on developing new materials modifications (including synthetic approaches) for high-voltage cathodes that will address issues such as: (i) voltage fade associated with LMR-NMC composition that leads to loss of energy over the cycle life; (ii) transition metal dissolution that leads to capacity and power fade; (iii) thermal and structural stability under the operating SOC range; and (iv) voltage hysteresis associated with multivalent transition metal compositions. Another enabling feature of the project is utilizing (and developing) various advanced characterization and diagnostic methods at the electrode and/or cell level for studying cell and/or electrode degradation under abuse conditions. The techniques include electrochemical impedance spectroscopy (EIS), micro-Raman spectroscopy; aberration corrected electron microscopy combined with electron energy loss spectroscopy (EELS), X-ray photoelectron spectroscopy, inductively coupled plasma – atomic emission spectroscopy (ICP-AES), fluorescence, and X-ray and neutron diffraction.

**Project Impact.** The project has short- and long- term deliverables directed toward VTO Energy Storage 2015 and 2022 goals. Specifically, work focuses on advanced electrode couples that have cell level energy density targets of 400 Wh/kg and 600 Wh/l for 5000 cycles. Increasing energy density per unit mass or volume reduces the cost of battery packs consistent with the DOE 2022 EV everywhere goal of \$125/kWh.

**Out-Year Goals.** The project is directed toward developing high-capacity cathodes for advanced lithium-ion batteries. The goal is to develop new cathode materials that have high capacity, are based on low-cost materials, and meet the DOE road map in terms of safety and cycle life. Two kinds of high energy cathode materials are being studied. Over the last few years, the PI has worked on improving cycle life and mitigating energy losses of high-voltage, Li-rich composite cathodes (referred to as LMR-NMC) in collaboration with the voltage fade team at ANL. Since last year, the PI has developed a high-capacity, two-lithium, copper-nickel system ( $\text{Li}_2\text{Cu}_x\text{Ni}_{1-x}\text{O}_2$ ) and similar systems. The plan includes improving the oxygen stability by using anionic substitution. Approaches include fluorination and changing to suitable polyanionic species. The tasks also include working in collaboration with researchers at Stanford Synchrotron Research Laboratory (SSRL) and Advanced Light Source (LBNL) to understand local changes in morphology, microstructure, and chemical composition under *in situ* and *ex situ* conditions.

**Collaborations.** This project collaborates with Johanna Nelson, SSRL, Stanford Linear Accelerator Center (SLAC): X-ray imaging and X-ray absorption near edge structure (XANES); Guoying Chen, LBNL: *in situ* XAS and X-ray diffraction (XRD); Feng Wang, Brookhaven National Lab: X-ray synchrotron spectroscopy and microscopy; and Bryant Polzin, Argonne Research Laboratory: CAMP Facility for electrode fabrication.

### Milestones

1. Synthesize three compositions of  $\text{Li}_2\text{Cu}_x\text{Ni}_{1-x}\text{O}_2$  cathodes with  $x$  between 0.4-0.6 and improve their anionic stability by fluorination. Subtask-1.1: Fluorination of  $\text{Li}_2\text{CuO}_2$ . (Q1 – In progress)
2. Fluorination of  $\text{Li}_2\text{Cu}_x\text{Ni}_{1-x}\text{O}_2$  with  $x \sim 0.4-0.6$ . (Q2 – In progress)
3. Identify roles of Ni and F in obtaining reversible redox capacity at higher voltage, and stabilize Ni-rich compositions. XANES, microscopy, and X-ray photoelectron spectroscopy (XPS) studies. (Q3)
4. Identify roles of Ni and F in obtaining reversible redox capacity at higher voltage, and stabilize Ni-rich compositions. Gas evolution and electrochemistry. (Q4 – Smart Milestone)

## Progress Report

This quarter, the project carried out chemical fluorination of as synthesized  $\text{Li}_2\text{CuO}_2$  powders to increase their electrochemical stability when charged to voltages  $> 3.9$  V. The goal is to partially fluorinate the oxide with approximately 5% substitution of fluorine for oxygen. This can potentially increase the ionicity of the compound as well as reduce oxygen participation in the redox chemistry. Figure 11 summarizes several different fluorination approaches.

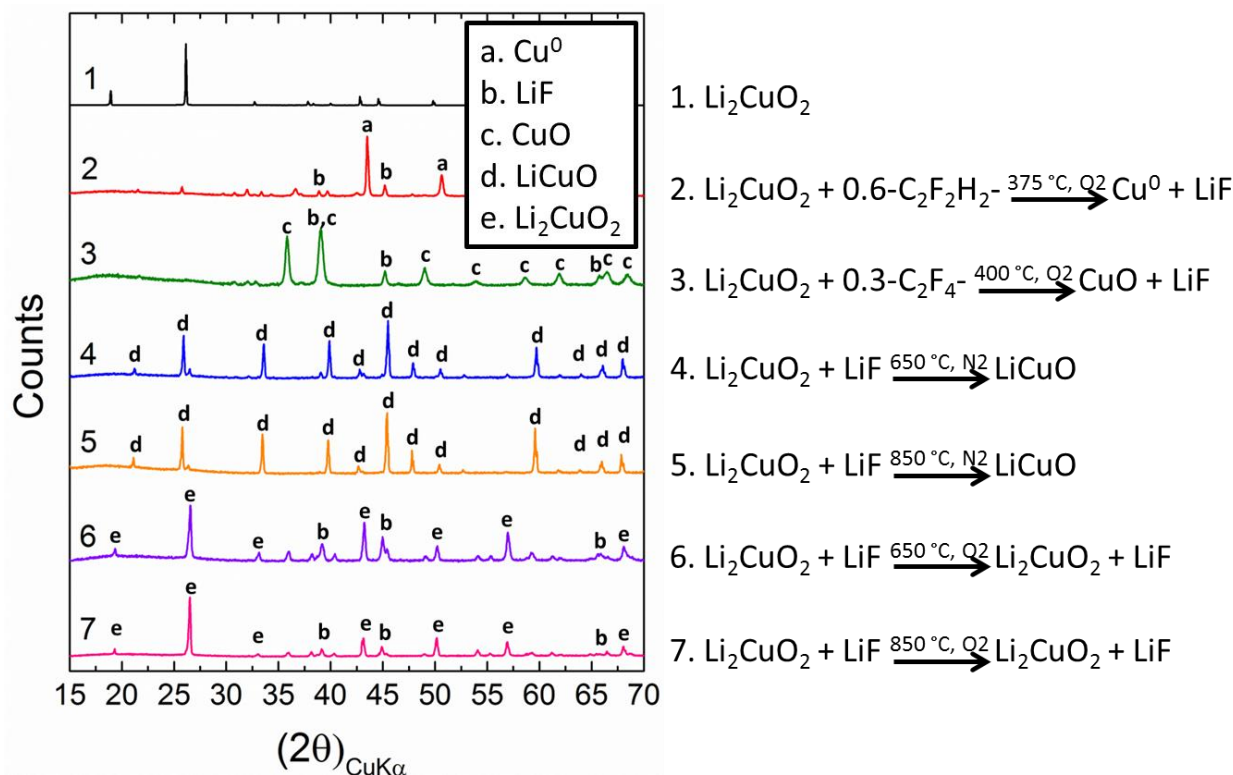


Figure 11. X-ray diffraction patterns from different chemical routes towards partial fluorination of  $\text{Li}_2\text{CuO}_2$  cathodes (see text for details).

The project first attempted to use fluorinated polymers (PVDF and teflon) as fluorinating agents (Figure 11, reactions 2 and 3). These polymers are safe and easy to handle, and have been used by others to fluorinate copper oxide based superconductors. Reaction with PVDF, even under oxygen, was found to produce significant amounts of fully reduced copper metal and  $\text{LiF}$ . The products from reaction with teflon were mainly  $\text{CuO}$  and  $\text{LiF}$ . The project also attempted to use  $\text{LiF}$  as a fluorinating agent, again motivated by its relative safety and ease of use (Figure 11, reactions 4-7).  $\text{Li}_2\text{CuO}_2$  is reduced under nitrogen atmosphere to  $\text{LiCuO}$ . Under oxygen, no reaction occurs. Based on experience with partial fluorination of lithium transition metal phosphates, the project suspects that the lithium fluoride may react at high temperature, but phase segregate as the material cools. Thus, the next efforts will focus on using *in situ* XRD to characterize the high-temperature phases. Based on these results, it may be possible to quench the material to capture a metastable fluorinated phase. The project also plans to use  $\text{CuF}_2$  and  $\text{NH}_4\text{F}$  as possible fluorine sources in future syntheses.



## Patents/Publications/Presentations

### Presentation

- MRS Fall Meeting, Boston (29 November to 3 December 2015): “Synthesis, Structure, and Electrochemical Performance of High-Capacity  $\text{Li}_2\text{Cu}_{0.5}\text{Ni}_{0.5}\text{O}_2$  Cathodes”; R. Ruther, et al.

### Publication

- Yang, J., and M. Naguib, Michael Ghidui, L. Pan, Jian Gu, J. Nanda, Joseph Halim, Yury Gogotsi, and Michel W. Barsoum. “Two-Dimensional Nb-Based  $\text{M}_4\text{C}_3$  Solid Solutions (MXenes).” *J. Am. Ceram. Soc.* 99, no. 2 (2016): 660.

## Task 3.2 – High Energy Density Lithium Battery (Stanley Whittingham, SUNY Binghamton)

**Project Objective.** The project objective is to develop the anode and cathode materials for high energy density cells for use in PHEVs and EVs that offer substantially enhanced performance over current batteries used in PHEVs and with reduced cost. Specifically, the primary objectives are to:

- Increase the volumetric capacity of the anode by a factor of 1.5 over today's carbons
  - Using a SnFeC composite conversion reaction anode
- Increase the capacity of the cathode
  - Using a high-capacity conversion reaction cathode,  $\text{CuF}_2$ , and/or
  - Using a high-capacity 2 Li intercalation reaction cathode,  $\text{VOPO}_4$
- Enable cells with an energy density exceeding 1 kWh/liter

**Project Impact.** The volumetric energy density of today's lithium-ion batteries is limited primarily by the low volumetric capacity of the carbon anode. If the volume of the anode could be cut in half, and the capacity of the cathode to over 200 Ah/kg, then the cell energy density can be increased by over 50% to approach 1 kWh/liter (actual cell). This will increase the driving range of vehicles.

Moreover, smaller cells using lower cost manufacturing will lower the cost of tomorrow's batteries.

**Out-Year Goals.** The long-term stretch goal of this project is to enable cells with an energy density of 1 kWh/liter. This will be accomplished by replacing both the present carbon used in Li-ion batteries with anodes that approach double the volumetric capacity of carbon, and the present intercalation cathodes with materials that significantly exceed 200 Ah/kg. By the end of this project, it is anticipated that cells will be available that can exceed the volumetric energy density of today's Li-ion batteries by 50%.

**Collaborations.** The Advanced Photon Source at ANL and, when available, the National Synchrotron Light Source II at BNL will be used to determine the phases formed in both *ex situ* and *operando* electrochemical cells. University of Colorado, Boulder, will provide some of the electrolytes to be used.

### Milestones

1. Determine the optimum composition  $\text{Li}_x\text{VOPO}_4$ . (December 2015 – Complete)
2. Demonstrate  $\text{VOPO}_4$  rate capability. (March 2016)
3. Demonstrate  $\text{Sn}_2\text{Fe}$  rate capability. (June 2016)
4. Demonstrate  $\text{CuF}_2$  rate capability. (September 2016)
5. *Go/No-Go*: Demonstrate lithiation method. *Criteria*: A cycling cell containing lithium in one of the intercalation or conversion electrodes must be achieved. (September 2016)

## Progress Report

The project goal is to synthesize tin-based anodes that have 1.5 times the volumetric capacity of the present carbons, and conversion and intercalation cathodes with capacities over 200 Ah/kg.

The major effort in this first quarter of year two was to determine the optimum composition of the initial cathode material,  $\text{Li}_x\text{VOPO}_4$ , and perform initial cycling studies of it versus a lithium anode.

**Milestone (4).** “Determine the optimum composition  $\text{Li}_x\text{VOPO}_4$ .” This milestone has been completed. The project has determined that the optimum composition of the starting cathode is  $\Sigma\text{-LiVOPO}_4$ , that is, a material containing some lithium rather than the Li-free  $\Sigma\text{-VOPO}_4$ . The best synthetic approach is a solid state reaction at  $750^\circ\text{C}$ . Hydrothermal synthesis results in the incorporation of protonic species into the lattice, and that approach will not be considered further. The material made, however, has particles in the range of 2-5  $\mu\text{m}$  in size, so must be ground down to sub-micron to ensure effective reaction with lithium. This was accomplished by high energy ball-milling. The extended cyclability of such  $\text{LiVOPO}_4$  materials is shown in Figure 12 under ambient conditions for two rates, C/20 and C/50. Through the first 20 cycles the C/50 materials show minimal capacity loss, and the highest capacity is seen for a ball-milling time of 0.5 hours. After this time the particles are around 200 nm in size. The cells are still cycling. At the higher rate, the capacities are slightly lower and 40 cycles have been achieved at over 200 mAh/g. The researchers are optimistic that the initial goal of over 50 cycles will be attained within the next quarter.

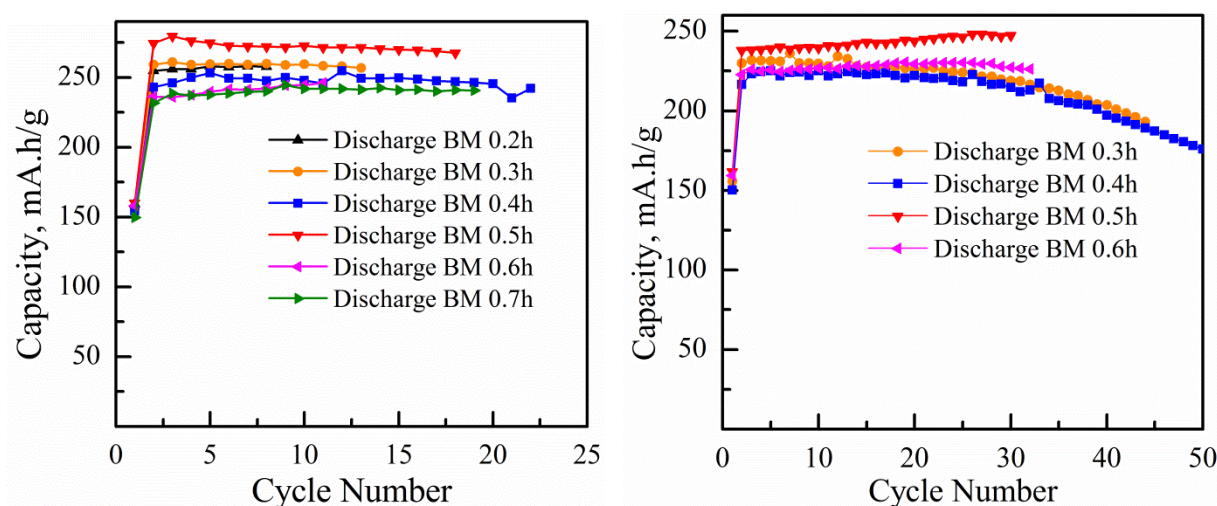


Figure 12. Cycling capacity of a  $\text{LiVOPO}_4$  electrode as a function of degree of ball-milling in hours and rate of charge/discharge: (left) C/50, (right) C/20

## Patents/Publications/Presentations

### Presentation

- DOE-EERE-NETL visit, Binghamton, New York (24 September 2015): “High-Energy Density Lithium Battery – an update”; Fredrick Omenya and M. Stanley Whittingham.

### Publication

- Dong, Zhixin, and R. Zhang, D. Ji, N. A. Chernova, K. Karki, S. Sallis, L. Piper, and M. S. Whittingham. “The Anode Challenge for Lithium-Ion Batteries: A Mechanochemically Synthesized Sn-Fe-C Composite Anode Surpasses Graphitic Carbon.” *Advanced Science* 3 (2011, in press).

### Task 3.3 – Development of High-Energy Cathode Materials (Ji-Guang Zhang and Jie Xiao, Pacific Northwest National Laboratory)

**Project Objective.** The project objective is to develop high-energy-density, low-cost, cathode materials with long cycle life. The previous investigation demonstrates that synthesis condition, synthesis approach, and surface modification have significant effects on the performances of high-voltage spinel and LMR-NCM cathodes. These valuable understandings will be used to guide the development of high energy-density, enhanced long-term cycling stability of Ni-rich  $\text{LiNi}_x\text{Mn}_y\text{Co}_z\text{O}_2$  (NMC) cathode materials that can deliver a high discharge capacity with long-term cycling stability.

**Project Impact.** Although state-of-the-art layered structure cathode materials such as  $\text{LiNi}_x\text{Mn}_y\text{Co}_z\text{O}_2$  (NMC) have relatively good cycling stability when charge to 4.3 V, their energy densities need to be further improved to meet the requirements of EVs. This work focuses on the two closely integrated parts: (1) Develop the high energy-density NMC layered cathode materials for Li-ion batteries (LIBs); and (2) characterize the structural properties of the NMC materials by a variety of diagnostic techniques including scanning transmission electron microscopy (STEM)/EELS, EDX mapping and secondary ion mass spectrometry (SIMS), and correlate with part (1). The success of this work will increase the energy density of LIBs and accelerate market acceptance of EVs, especially for PHEVs required by the EV Everywhere Grand Challenge proposed by DOE/EERE.

**Out-Year Goals.** The long-term goal of the proposed work is to enable LIBs with a specific energy of  $> 96 \text{ Wh kg}^{-1}$  (for PHEVs), 5000 deep-discharge cycles, 15-year calendar life, improved abuse tolerance, and less than 20% capacity fade over a 10-year period.

**Collaborations.** This project engages with the following collaborators:

- Dr. Bryant Polzin (ANL) – NMC electrode supply
- Dr. X.Q. Yang (BNL) – *in situ* XRD characterization during cycling
- Dr. Kang Xu (U.S. Army Research Laboratory) – new electrolyte

#### Milestones

1. Identify NMC candidates that can deliver  $190 \text{ mAh g}^{-1}$  at high voltages. (12/31/15 – Complete)
2. Complete multi-scale quantitative atomic level mapping to identify the behavior of Co, Ni, and Mn in NMC during battery charge/discharge, correlation with battery fading characteristics. (3/31/16 – Ongoing)
3. Identify structural/chemical evolution of modified-composition NMC cathode during cycling. (6/30/2016 – Ongoing)
4. Optimize compositions of NMC materials to achieve improved electrochemical performance (90% capacity retention in 100 cycles). (9/30/2016 – Ongoing)

## Progress Report

This quarter's milestone is complete. The electrochemical performances of  $\text{LiNi}_x\text{Mn}_y\text{Co}_z\text{O}_2$  (NMC) cathode materials with different Ni contents were systematically investigated at a high charge cutoff voltage of 4.5 V. Four NMC cathode candidates that can deliver  $190 \text{ mAh g}^{-1}$  were identified.

The initial charge/discharge voltage profiles demonstrated that much higher charge and discharge capacities were achieved with the increase of Ni content in these NMC cathode materials (Figure 13a). This is because Ni could operate between  $\text{Ni}^{2+/3+}$  and  $\text{Ni}^{3+/4+}$ , which offers higher discharge capacity without severe variation in discharge voltage profiles. The discharge capacity of traditional  $\text{LiNi}_{1/3}\text{Mn}_{1/3}\text{Co}_{1/3}\text{O}_2$  (NMC-333) was only about  $185 \text{ mAh g}^{-1}$ . In comparison, ca.  $200 \text{ mAh g}^{-1}$  and ca.  $215 \text{ mAh g}^{-1}$  were delivered by NMC materials with 0.5~0.62 Ni content and 0.76~0.80 Ni content, respectively. By calculating the energy density based on the discharge voltage profiles in half-cells, it was found that Ni-rich NMC cathode materials (0.76~0.80 Ni) delivered the highest discharge energy density of  $830\sim 840 \text{ Wh kg}^{-1}$  (Figure 13b), which was about 15% higher than the value of traditional NMC-333 ( $\sim 730 \text{ Wh kg}^{-1}$ ).

The long-term cycling performances of these NMC cathode materials were shown in Figure 13c. Even though the Ni-rich NMC cathodes delivered much higher discharge capacity and energy density in the beginning, they experienced faster capacity degradation during cycling, especially those with 0.76~0.80 Ni content, which could be ascribed to the parasitic reactions between  $\text{Ni}^{4+}$  and the electrolyte, as well as the large volume variation during charge/discharge processes. The NMC materials with medium Ni content showed a good balance between high discharge capacity and long-term cycling stability. In particular, the material with 0.62 Ni delivered a high discharge capacity of  $200 \text{ mAh g}^{-1}$  and showed a very decent cyclability comparable to traditional NMC-333. Based on these results, the future work will be focused on investigating the behavior of Co, Ni, and Mn in NMC during charge/discharge processes, and further improving the cycle life of Ni-rich cathode materials at elevated cutoff voltages.

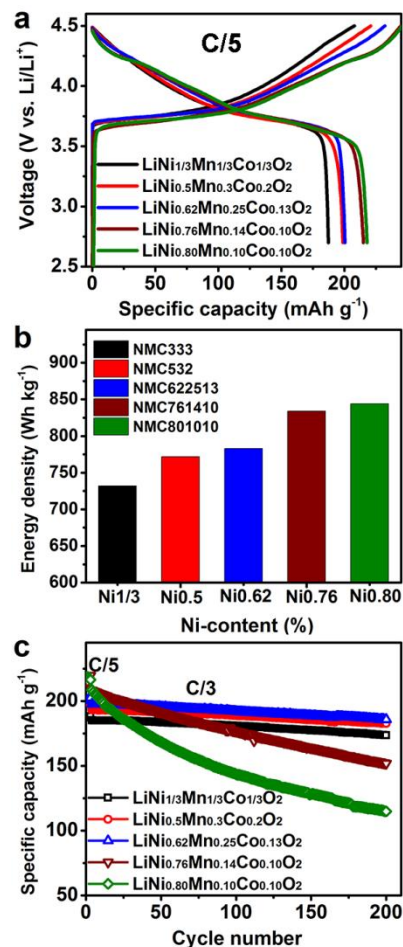


Figure 13. (a) Initial voltage profiles vs. specific capacity. (b) Energy density. (c) Cycling performance of a variety of NMC cathode materials cycled in the voltage range of 2.7 ~ 4.5 V. (1C =  $200 \text{ mAh g}^{-1}$ , loading: ca.  $4 \text{ mg cm}^{-2}$ )

## Patents/Publications/Presentations

Yan, Pengfei, and Jianming Zheng, Sarvanan Kuppen, Qiuyan Li, Dongping Lu, Jie Xiao, Guoying Chen, Ji-Guang Zhang, and Chong-Min Wang. "Phosphorus Enrichment as a New Composition in the Solid Electrolyte Interphase of High-Voltage Cathodes and Its Effects on Battery Cycling." *Chemistry of Materials* 27, no. 21 (2015): 7447-7451.



## Task 3.4 – *In situ* Solvothermal Synthesis of Novel High Capacity Cathodes (Feng Wang and Jianming Bai, Brookhaven National Laboratory)

**Project Objective.** The goal is to develop novel high-capacity cathodes with precise control of the phase, stoichiometry and morphology. Despite considerable interest in developing low-cost, high energy cathodes for Li-ion batteries, designing and synthesizing new cathode materials with the desired phases and properties has proven difficult, due to the complexity of the reactions involved in chemical synthesis. Building on established *in situ* capabilities/techniques for synthesizing and characterizing electrode materials, this project will undertake *in situ* studies of synthesis reactions under real conditions to identify the intermediates and to quantify the thermodynamic and kinetic parameters governing the reaction pathways. The results of such studies will enable strategies to “dial in” desired phases and properties, opening up a new avenue for synthetic control of the phase, stoichiometry, and morphology during preparing novel high-capacity cathodes.

**Project Impact.** Present-day Li-ion batteries are incapable of meeting the targeted miles of all-electric-range within the weight and volume constraints, as defined by the DOE in the EV Everywhere Grand Challenge. New cathodes with higher energy density are needed for Li-ion batteries so that they can be widely commercialized for plug-in electric vehicle (PEV) applications. The effort will focus on increasing energy density (while maintaining the other performance characteristics of current cathodes) using synthesis methods that have the potential to lower cost. The primary deliverable for this project is a reversible cathode with an energy density of 660 Wh/kg or higher.

**Out-Year Goals.** In FY16, the project will continue developing *in situ* techniques and capabilities, for *real time* probing synthesis reactions in preparing novel high-capacity cathodes, with a focus on Ni-rich layered oxides. Specifically, it will develop synthesis procedures for making  $\text{LiNiO}_2$  and a series of Co/Mn substituted solid solutions,  $\text{LiNi}_{1-x}\text{M}_x\text{O}_2$  ( $\text{M}=\text{Co}, \text{Mn}$ ); through *in situ* studies, it will make systemic investigation of the impact of synthesis conditions on the reaction pathways and cationic ordering processes toward the final layered phases. The structural and electrochemical properties of the synthesized materials will be characterized using synchrotron X-ray, neutron scattering, TEM, EELS, and various electrochemical techniques. By the end of this year, the project expects to have identified synthetic approaches for stabilizing the structure of Ni-rich layered oxides.

**Collaborations.** This project engages with the following collaborators: Lijun Wu and Yimei Zhu at BNL; Khalil Amine, Zonghai Chen, and Yang Ren at ANL; Jagjit Nanda and Ashfia Huq at ORNL; Nitash Balsara, Wei Tong, and Gerbrand Ceder at LBNL; Arumugam Manthiram at UT-Austin; Scott Misture at Alfred University; Peter Khalifha at SUNY; Kirsuk Kang at Seoul National University; Brett Lucht at University of Rhode Island; and Jason Graetz at HRL Laboratories.

### Milestones

1. Develop synthesis procedures for preparing Ni-Mn-Co layered oxides. (12/01/15 – Complete)
2. Identify the impact of synthesis conditions on the reaction kinetics and pathways toward forming layered Ni-Mn-Co oxides via *in situ* studies. (03/01/16)
3. Develop new capabilities for monitoring synthesis parameters ( $P$ ,  $T$ ,  $PH$  values) in real time during solvothermal synthesis of cathode materials. (06/01/16)
4. Identify synthetic approaches for stabilizing the layered structure of Ni-Mn-Co cathodes. (09/01/16)

## Progress Report

For the application of Li-ion batteries in electric vehicles, NMC-based cathodes (Li-Ni-Mn-Co-O) have proven to be the most promising. Among them, Ni-rich layered ones are particularly interesting for their high capacity (~200 mAh/g) and low cost; however, it is difficult to synthesize highly ordered layered oxides due to cation mixing, one critical issue (among many others) leading to reduced capacity and poor cycling performance of the electrodes. This quarter, synthesis procedures were developed for preparing  $\text{LiNiO}_2$  and solid-solution phases,  $\text{LiNi}_{1-x}\text{M}_x\text{O}_2$  ( $\text{M}=\text{Co}, \text{Mn}$ ). In Ni-rich oxides, such as  $\text{LiNi}_{0.8}\text{Co}_{0.2}\text{O}_2$ , structure stabilization against thermally induced oxygen loss during high-temperature synthesis was achieved by Co substitution. The electrodes made from highly ordered  $\text{LiNi}_{0.8}\text{Co}_{0.2}\text{O}_2$  exhibited an initial capacity about 180 mAh/g, and 85% retention after 50 cycles.

Synthesis procedures, based on a sol-gel process followed by high-temperature calcination, were developed to make  $\text{LiNiO}_2$  and solid solutions  $\text{LiNi}_{1-x}\text{M}_x\text{O}_2$  ( $\text{M}=\text{Co}, \text{Mn}$ ) from lithium acetate and transition-metal acetate hydrates (with certain nominal molar ratios). The synthesis process, and impact of synthesis conditions on the structural and electrochemical properties of the final phases were explored, using a combination of thermogravimetric (TG), X-ray/neutron diffraction and electrochemical measurements; some of these results were provided in Figure 14. The TG analysis revealed a series of phase transformations in the precursors and intermediates, indicating that  $\text{O}_2$  is needed to reduce cation mixing in Ni-rich layered oxides, while Co substitution is crucial to stabilizing the layered phase against oxygen loss at high temperatures (Figure 14a). Synthesis conditions were optimized to obtain Co-substituted layered oxides with lowest possible cation mixing. In those Ni-rich ones, such as  $\text{LiNi}_{0.8}\text{Co}_{0.2}\text{O}_2$ , only 1.5%  $\text{Ni}^{2+}$  on  $\text{Li}^+$  sites was identified by neutron diffraction measurements; correspondingly, the electrodes made from the material exhibited an initial capacity of ~180 mAh/g and 85% retention after 50 cycles under a moderate cycling condition (0.1 C rate; 2.7-4.3 V window), in contrast to poor cycling stability in  $\text{LiNiO}_2$  and low capacity in  $\text{LiNi}_{0.8}\text{Co}_{0.2}\text{O}_2$  synthesized in the air (Figure 14c).

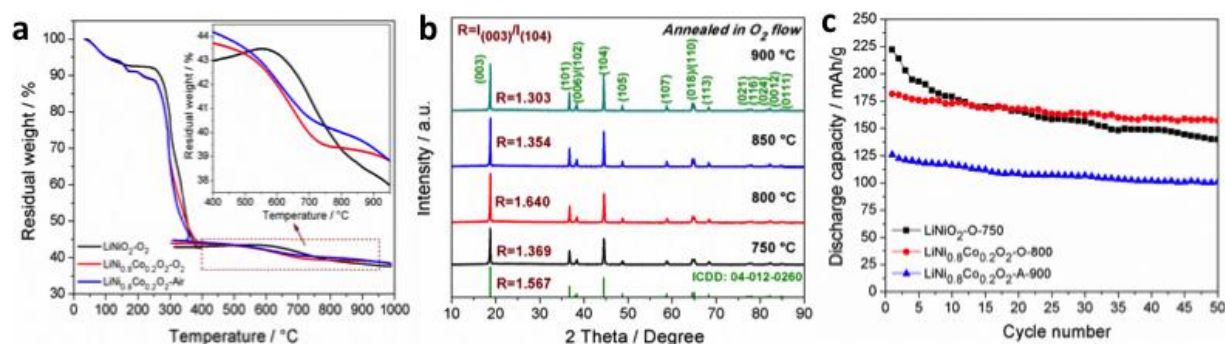


**Figure 14. Synthetic control of the structural ordering and performance of Ni-rich layered oxides.** (a) Thermogravimetric curves of the precursors for synthesizing  $\text{LiNiO}_2$  in  $\text{O}_2$  flow (black line),  $\text{LiNi}_{0.8}\text{Co}_{0.2}\text{O}_2$  in  $\text{O}_2$  flow (red), and  $\text{LiNi}_{0.8}\text{Co}_{0.2}\text{O}_2$  in the air (blue). (b) X-ray diffraction patterns of  $\text{LiNi}_{0.8}\text{Co}_{0.2}\text{O}_2$  prepared at different sintering temperatures in  $\text{O}_2$  flow. (c) Electrochemical performance of  $\text{LiNi}_{0.8}\text{Co}_{0.2}\text{O}_2$  synthesized in  $\text{O}_2$  (red), compared to that of  $\text{LiNiO}_2$  synthesized in  $\text{O}_2$  (black), and  $\text{LiNi}_{0.8}\text{Co}_{0.2}\text{O}_2$  synthesized in the air (blue).

The results from this study demonstrated the strong dependence of electrode performance on the synthesis conditions; further mechanistic studies via *in situ*, real-time probing synthesis reactions are needed for synthetic control of the reaction pathway and cationic ordering, particularly for preparing quaternary NMC cathodes, wherein the incorporation of Mn makes structural control even more challenging. This work has begun.



## Patents/Publications/Presentations

### Presentations

- Boston (29 November to 4 December 2015): “Structure Stabilization of Ni-Rich Layered Oxides as High-Energy Cathodes for Lithium-Ion Batteries”; Jianqing Zhao, Jianming Bai, and Feng Wang.
- Boston (29 November to 4 December 2015): “*In Situ* Solvothermal Synthesis of High-Energy Cathodes for Li-Ion Batteries”; Jianming Bai, Liping Wang, Young-Uk Park, Wei Zhang, J. Patrick Looney, and Feng Wang.

## Task 3.5 – Novel Cathode Materials and Processing Methods (Michael M. Thackeray and Jason R. Croy, Argonne National Laboratory)

**Project Objective.** The project goal is to develop low-cost, high-energy, and high-power Mn-oxide-based cathodes for lithium-ion batteries that will meet the performance requirements of PHEVs and EVs. Improving the design, composition, and performance of advanced electrodes with stable architectures and surfaces, facilitated by an atomic-scale understanding of electrochemical and degradation processes, is a key objective.

**Project Impact.** Standard lithium-ion battery technologies are unable to meet the demands of the next-generation electric and plug-in hybrid electric vehicles. Battery developers and scientists will take advantage of the knowledge generated from this project, both applied and fundamental, to advance the field. In particular, this knowledge should enable progress toward meeting DOE goals for 40-mile, all-electric range PHEVs.

**Approach.** This project will exploit the concept and optimize the electrochemical properties of structurally integrated “composite” electrode structures with a prime focus on “layered-layered-spinel” (LLS) materials. Processing routes will be investigated, particularly for scaling up materials for testing by industry; ANL’s comprehensive characterization facilities will be used to explore novel surface and bulk structures by both *in situ* and *ex situ* techniques in pursuit of advancing the electrochemical performance of state-of-the-art cathode materials. A theoretical component will complement the experimental work of this project.

**Out-Year Goals.** The out-year goals are as follows:

- Identify high-capacity (‘layered-layered’ and ‘layered-spinel’) composite electrode structures and compositions that are stable to electrochemical cycling at high potentials (~4.5 V).
- Identify and characterize surface chemistries and architectures that allow fast Li-ion transport and mitigate or eliminate transition-metal dissolution.
- Scale-up, evaluate, and verify promising cathode materials in conjunction with ANL’s scale-up and cell fabrication facilities.

**Collaborators.** This project engages with the following collaborators: Joong Sun Park, Bryan Yonemoto, and Eungie Lee (CSE, ANL), along with collaborators of the Spinel, Characterization and Computer Modeling Tasks that complement this project.

### Milestones

1. Optimize the composition, capacity, and cycling stability of structurally integrated cathode materials with a low (~10 – 20%)  $\text{Li}_2\text{MnO}_3$  content. Target capacity = 200 mAh/g or higher (baseline electrode). (Q1 – In progress; see text)
2. Scale up the most promising materials to batch sizes required for evaluation by industry (10g-100g-1kg). (Q2 – In progress; see text)
3. Synthesize and determine the electrochemical properties of unique surface architectures that enable > 200 mAh/g at a > 1C rate. (Q3/Q4 – In progress)

## Progress Report

Lithium- and manganese-rich  $y[x\text{Li}_2\text{MnO}_3 \cdot (1-x)\text{LiMO}_2] \cdot (1-y)\text{LiM}_2\text{O}_4$  ( $\text{M}=\text{Mn}, \text{Ni}, \text{Co}$ ) LLS materials have demonstrated improved electrochemical properties relative to their LL counterparts. It is believed that embedded  $\text{LiM}_2\text{O}_4$  spinel-like configurations with TM in the lithium layers, act as stabilizing pillars at high states of charge and mitigate the migration of TM ions into the lithium layer during electrochemical cycling (that is, the ‘voltage fade’ phenomenon). This approach has been used to assess the electrochemical performance of a series of model LLS compounds derived from a base LL composition,  $0.25\text{Li}_2\text{MnO}_3 \cdot 0.75\text{LiMn}_{0.375}\text{Ni}_{0.375}\text{Co}_{0.25}\text{O}_2$ . Precursor materials were synthesized by transition metal oxalate co-precipitation methods using the requisite proportions of Mn, Ni, and Co; a targeted spinel content, ranging between 0 and 25%, was introduced into the structure of the final electrode product during the firing process by systematically decreasing the Li:TM ratio of the lithium source ( $\text{Li}_2\text{CO}_3$ ) and the TM oxalate precursor. Cathode compositions were determined and confirmed using inductively coupled plasma optical emission spectroscopy (ICP-OES). Electrodes were cycled electrochemically in lithium half-cells (coin cells) at  $30^\circ\text{C}$ . Figure 15a shows XRD patterns of the electrode series labeled according to the targeted spinel content,  $x$ . Peaks corresponding to a cubic phase, that are likely associated with TM ions in the lithium layer, evolve as the Li:TM ratio decreases. Plots of discharge capacities and first-cycle CE of the LLS electrodes as a function of the targeted spinel content (not shown) indicate that the discharge capacity increases with  $x$  to reach a maximum at  $x=7.5\%$  with a first-cycle CE value close to 90%. Figure 15b shows the variation of the charge/discharge capacity of the targeted  $x=7.5\%$  electrode when subjected to an initial activation charge/discharge cycle between 4.6–2.0 V and, thereafter, to cycling between 4.45–2.5 V (15 mA/g,  $30^\circ\text{C}$ ); the electrode delivers  $\sim 200$  mAh/g during the early cycles. Characterization of this electrode system, which includes combined XRD, neutron diffraction, nuclear magnetic resonance (NMR), and TEM studies, is in progress. These studies, which are expected to provide detailed information about atomic configurations in these complex structures, and how the structures relate to synthesis parameters and electrochemical properties, will be discussed in a future report.

Parallel to the above efforts, studies are being conducted to understand the factors that control the large-scale synthesis of high-tap-density LLS powders using stirred tank reactors. A metal hydroxide precursor composition was selected to match the TM ratio in the base  $0.25\text{Li}_2\text{MnO}_3 \cdot 0.75\text{LiMn}_{0.375}\text{Ni}_{0.375}\text{Co}_{0.25}\text{O}_2$  composition discussed above. Figure 15c shows a SEM image of LLS particles from a  $\sim 0.5$  kg production batch with a 15% targeted spinel content; they have an attractive tap density of 2.25 g/cc. The XRD patterns of scaled LLS products (not shown) provide evidence, like their oxalate-based counterparts, that a cubic phase is present with clear evidence of a (220) diffraction peak, characteristic of a spinel component for samples with the higher target spinel values.

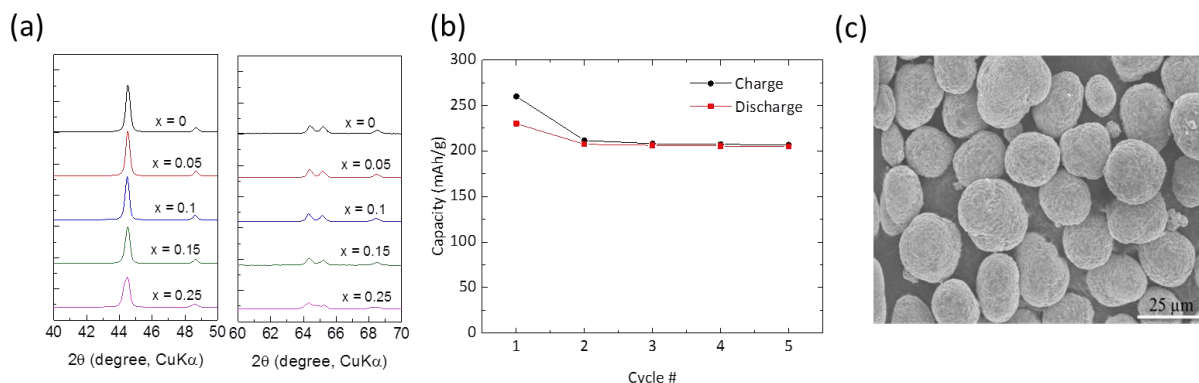


**Figure 15. (a) X-ray diffraction patterns of targeted layered-layered-spinel (LLS) compositions. (b) Electrochemical properties of a  $0.25\text{Li}_2\text{MnO}_3 \cdot 0.75\text{LiMn}_{0.375}\text{Ni}_{0.375}\text{Co}_{0.25}\text{O}_2$  cathode with a 7.5% targeted spinel content (activation: 4.6–2.0 V, subsequent cycles: 4.45–2.5 V). (c) Scanning electron microscopy image of LLS powders from a  $\sim 0.5$  kg scaled batch of metal hydroxide precursors (scale bar=25  $\mu\text{m}$ ).**

## Patents/Publications/Presentations

### Patent

- Thackeray, M. M., and S.-H. Kang and C. S. Johnson. *Surface Stabilized Electrodes for Lithium Batteries*. U.S. Patent 9,130,226 (8 September 2015).

### Presentation

- 228<sup>th</sup> ECS Meeting, Phoenix (October 2015): “Composite ‘Layered-Layered-Spinel’ Electrodes for High-Energy Lithium-Ion Batteries”; J. S. Park, J. R. Croy, B. R. Long, E. Lee, and M. M. Thackeray.

## Task 3.6 – High-capacity, High voltage Cathode Materials for Lithium-ion Batteries (Arumugam Manthiram, University of Texas, Austin)

**Project Objective.** A significant increase in capacity and/or operating voltage is needed to make the lithium-ion technology viable for vehicle applications. This project addresses this issue by focusing on the design and development of cathode materials based on polyanions that have the possibility for reversibly inserting/extracting more than one lithium ion per transition-metal ion and/or operating above 4.3 V. Specifically, high-capacity and/or high-voltage lithium transition-metal phosphate, silicate, and carbonophosphate cathodes are investigated. The major issue with the phosphate and silicate cathodes is the poor electronic and ionic transport, which limits the practical capacity, energy density, and power density. To overcome these difficulties, novel microwave-assisted solvothermal, microwave-assisted hydrothermal, and template-assisted synthesis approaches are pursued to realize controlled morphology with smaller particle size and to integrate conductive additives like graphene in a single synthesis step.

**Project Impact.** The critical requirements for the widespread adoption of lithium-ion batteries for vehicle applications are high-energy, high-power, long cycle life, low cost, and acceptable safety. The currently available cathode materials do not adequately fulfill these requirements. The polyanion cathodes with the novel synthesis approaches pursued in this project have the potential to significantly increase the energy and power. More importantly, the covalently bonded polyanion groups can offer excellent thermal stability and enhanced safety. The microwave-assisted synthesis approaches pursued also lower the manufacturing cost of the cathodes through a significant reduction in reaction time and temperature.

**Out-Year Goals.** The overall goal is to enhance the electrochemical performances of high-capacity, high-voltage polyanion cathode systems and to develop a fundamental understanding of their structure-composition-performance relationships. Specifically, the project is focused on enhancing the electrochemical performance of systems such as  $\text{LiMPO}_4$ ,  $\text{Li}_2\text{MP}_2\text{O}_7$ ,  $\text{LiYMSiO}_4$ ,  $\text{Li}_3\text{V}_2(\text{PO}_4)_3$ ,  $\text{Li}_9\text{V}_3(\text{P}_2\text{O}_7)_3(\text{PO}_4)_2$ ,  $\text{Li}_3\text{M}(\text{CO}_3)(\text{PO}_4)$ , and their solid solutions with  $\text{M} = \text{Mn, Fe, Co, Ni, and VO}$ . Advanced structural, chemical, surface, and electrochemical characterizations of the materials synthesized by novel approaches are anticipated to provide in-depth understanding of the factors that control the electrochemical properties of the polyanion cathodes. For example, the possible segregation of certain cations to the surface in solid solution cathodes consisting of multiple transition-metal ions as well as the role of conductive graphene integrated into the polyanion cathodes can help design better performing cathodes.

**Collaborations.** This project collaborates with Craig Bridges (ORNL) on structural characterizations of polyanion cathodes.

### Milestones

1. Demonstrate the synthesis of  $\alpha\text{-Li}_2\text{VOPO}_4$  nanoparticles and identification of its crystal structure. (December 2015 – Complete)

## Progress Report

Previously, it was demonstrated that the layered  $\alpha_1$ -LiVOPO<sub>4</sub> (tetragonal) could be electrochemically lithiated to form  $\alpha_1$ -Li<sub>1+x</sub>VOPO<sub>4</sub>. This quarter, chemical lithiation of  $\alpha_1$ -LiVOPO<sub>4</sub> was studied to obtain  $\alpha_1$ -Li<sub>2</sub>VOPO<sub>4</sub>. The tetragonal  $\alpha_1$ -LiVOPO<sub>4</sub> was first prepared by a microwave-assisted solvothermal method, and then lithiated with n-butyllithium in pre-dried acetonitrile. Bond-valence sum map calculations were performed to obtain insights on possible Li sites in the  $\alpha_1$ -LiVOPO<sub>4</sub> lattice by identifying sites that have sufficient space for Li<sup>+</sup> ions with a bond valence close to 1. As shown in Figure 16, all the potential positions are adjacent to the original Li sites between two adjacent VOPO<sub>4</sub> planes. In the previous structural analysis of  $\alpha_1$ -LiVOPO<sub>4</sub>, lithium ions were determined to occupy a quarter of the 8j Wyckoff positions (octahedral). Thus, it is reasonable that the additional lithium ions take the empty 8j sites in  $\alpha_1$ -Li<sub>2</sub>VOPO<sub>4</sub>, as indicated by the bond valence sum maps.

To confirm the structure of  $\alpha_1$ -Li<sub>2</sub>VOPO<sub>4</sub> and obtain more detailed structural information, powder neutron diffraction data were collected on the POWGEN beamline at the Spallation Neutron Source (SNS) at ORNL (Figure 17). The final refinements were conducted with a combined POWGEN and transmission XRD data. Le Bail refinements were used to examine several lower symmetry space groups, such as *P4* and *P2/m*, and compared against *P4/nmm*; there was no evidence from these tests that a lower symmetry space group is required to describe the data. The cell parameters of  $\alpha_1$ -Li<sub>2</sub>VOPO<sub>4</sub> from the refinement are *a* = 6.4793(2) Å, *b* = 6.4793(2) Å, and *c* = 4.2130(2) Å. The insertion of additional lithium into the  $\alpha_1$ -LiVOPO<sub>4</sub> framework may cause Li<sup>+</sup>-O<sup>2-</sup> electrostatic attraction and Li<sup>+</sup>-Li<sup>+</sup> electrostatic repulsion, exerting a greater influence on the lattice. In the case of vanadium, reduction to V<sup>3+</sup> results in weaker V-O bonding along the *c* axis, resulting in a trend towards a more symmetric VO<sub>6</sub> octahedron with increasing lithiation. A symmetric VO<sub>6</sub> octahedron is expected for the 3+ oxidation state, but some distortion remains, suggesting that vanadium may not be fully reduced. This is supported by the refined composition of Li<sub>1.74(2)</sub>V<sub>0.9</sub>PO<sub>4</sub>, which leads to an oxidation state of V<sup>3.63+</sup> due to a combination of partial lithiation and a vanadium-site occupancy of 0.9. Overall, the combined refinement of neutron diffraction and XRD demonstrates successful chemical lithiation of  $\alpha_1$ -LiVOPO<sub>4</sub> through a low-temperature soft chemistry method to form a defective lithium vanadium phosphate with a somewhat disordered geometry around the vanadium sites as a consequence of the mixed oxidation state.

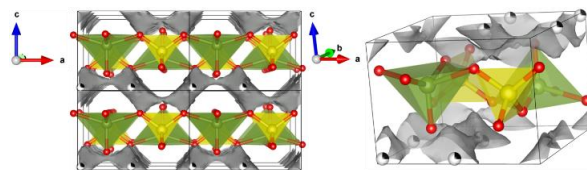


Figure 16. Bond valence sum maps showing the potential positions for the additional lithium in  $\alpha_1$ -LiVOPO<sub>4</sub>.

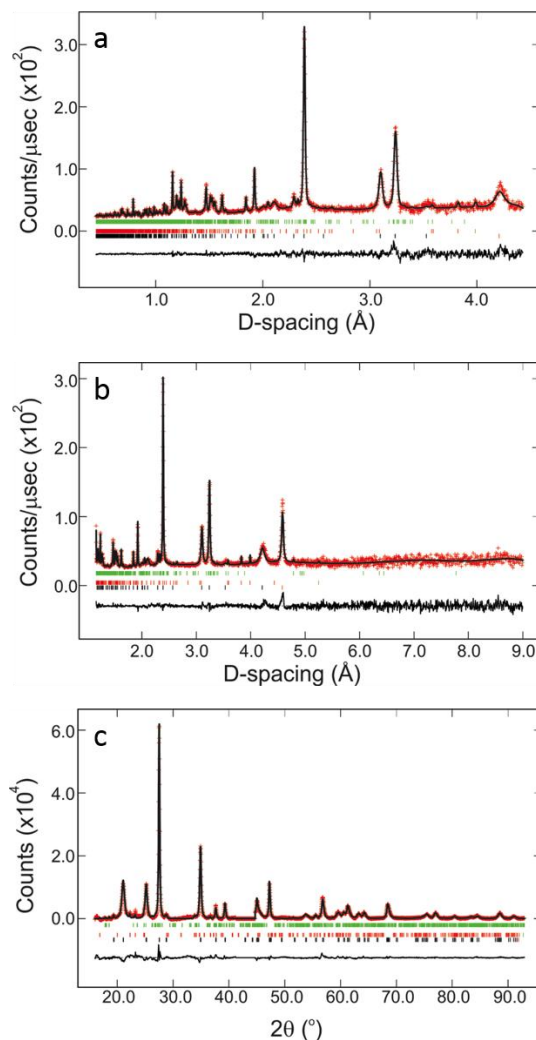


Figure 17. Rietveld refinement fits of  $\alpha_1$ -Li<sub>2</sub>VOPO<sub>4</sub> with the combined diffraction data. (a) POWGEN time-of-flight neutron powder diffraction data from Bank 2. (b) POWGEN Bank 4 data. (c) Transmission film X-ray diffraction (XRD) data. The region from  $2\theta = 41.2^\circ$  to  $44.7^\circ$  is excluded in the XRD data due to a contribution from the film holder to the pattern.

## Patents/Publications/Presentations

### Publications

- He, G., and C. A. Bridges and A. Manthiram. “Crystal Chemistry of Electrochemically and Chemically Lithiated Layered  $\alpha_1$ -LiVOPO<sub>4</sub>.” *Chemistry of Materials* 27 (2015): 6699-6707.
- Knight, J. C., and A. Manthiram. “Effect of Nickel Oxidation State on the Structural and Electrochemical Characteristics of Lithium-Rich Layered Oxide Cathodes.” *Journal of Materials Chemistry A* 3 (2015): 22199-22207.
- Assat, G., and A. Manthiram. “Rapid Microwave-Assisted Solvothermal Synthesis of Non-Olivine *Cmcm* Polymorphs of LiMPO<sub>4</sub> (M = Mn, Fe, Co, and Ni) at Low Temperature and Pressure.” *Inorganic Chemistry* 54 (2015): 10015-10022.
- He, G., and W. H. Kan and A. Manthiram. “A 3.4 V Layered VOPO<sub>4</sub> Cathode for Na-Ion Batteries.” *Chemistry of Materials* (2015). doi: 10.1021/acs.chemmater.5b04605.
- He, G., and A. Huq, W. H. Kan, and A. Manthiram. “ $\beta$ -NaVOPO<sub>4</sub> Obtained by a Low-Temperature Synthesis Process: A New 3.3 V Cathode for Sodium-ion Batteries.” *Chemistry of Materials* (submitted).
- Kreder III, K. J., and G. Assat and A. Manthiram. “Aliovalent Substitution of V<sup>3+</sup> for Co<sup>2+</sup> in LiCoPO<sub>4</sub> by a Low-Temperature Microwave-Assisted Solvothermal Process.” *Chemistry of Materials* (submitted).

### Presentations

- International Symposium on Clusters and Nanomaterials, Richmond, Virginia (26 – 29 October 2015): “Nanomaterials for Electrical Energy Storage”; A. Manthiram. Invited.
- International Conference on Innovative Electrochemical Energy Materials and Technologies (EEMT2015), Nanning, China (8 – 11 November 2015): “Electrical Energy Storage: Next Generation Battery Chemistries”; A. Manthiram. Invited plenary talk.
- Symposium X: Frontiers of Materials Research, Fall Meeting of the Materials Research Society, Boston (29 November – 4 December 2015): “Electrical Energy Storage: Materials Challenges and Prospects”; A. Manthiram. Invited.



## Task 3.7 – Lithium-bearing Mixed Polyanion (LBMP) Glasses as Cathode Materials (Jim Kiggans and Andrew Kercher, Oak Ridge National Laboratory)

**Project Objective.** Develop mixed polyanion (MP) glasses as potential cathode materials for lithium-ion batteries with superior performance to lithium iron phosphate for use in EV applications. Modify MP glass compositions to provide higher electrical conductivities, specific capacities, and specific energies than similar crystalline polyanionic materials. Test MP glasses in coin cells for electrochemical performance and cyclability. The final goal is to develop MP glass compositions for cathodes with specific energies up to near 1,000 Wh/kg.

**Project Impact.** The projected performance of MP glass cathode materials addresses the VTO Multi-Year Program Plan goals of higher energy densities, excellent cycle life, and low cost. MP glasses offer the potential of exceptional cathode energy density up to 1000 Wh/kg, excellent cycle life from a rigid polyanionic framework, and low-cost, conventional glass processing.

**Out-Year Goals.** MP glass development will focus on compositions with expected multivalent intercalation reactions within a desirable voltage window and/or expected high-energy glass-state conversion reactions.

Polyanion substitution will be further adjusted to improve glass properties to potentially enable multi-valent intercalation reactions and to improve the discharge voltage and cyclability of glass-state conversion reactions. Cathode processing of the most promising mixed polyanion glasses will be refined to obtain desired cycling and rate performance. These optimized glasses will be disseminated to BMR collaborators for further electrochemical testing and validation.

**Collaborations.** No collaborations this quarter.

### Milestones

1. Produce glass compositions for high-energy cathodes giving maximally oxidized transition metals upon first charge. (March 2016)
2. Produce unconventional glass cathodes using alternative glass formers or partial crystallinity. (June 2016)

## Progress Report

Previously, a polyanion mixture of phosphate, borate, and vanadate (PBV) in a copper-bearing glass was found to improve first-cycle reversibility, reduce voltage hysteresis, and promote limited intercalation capacity. The addition of borate was believed to increase the free volume of the glass and to allow for better ionic diffusion. The same PBV mixture was tested in a silver-bearing glass. In Figure 18, a silver phosphate-vanadate glass is compared to a lithium silver PBV glass. Similar to what was observed in copper glasses, the lithium silver PBV glass had improved first-cycle reversibility in comparison to a silver phosphate vanadate glass. First cycle irreversible loss was a key shortcoming of glasses studied earlier in the program. Since the effect was observed in both Ag and Cu bearing glasses, the improved first-cycle reversibility may be observed in PBV other glasses as well.

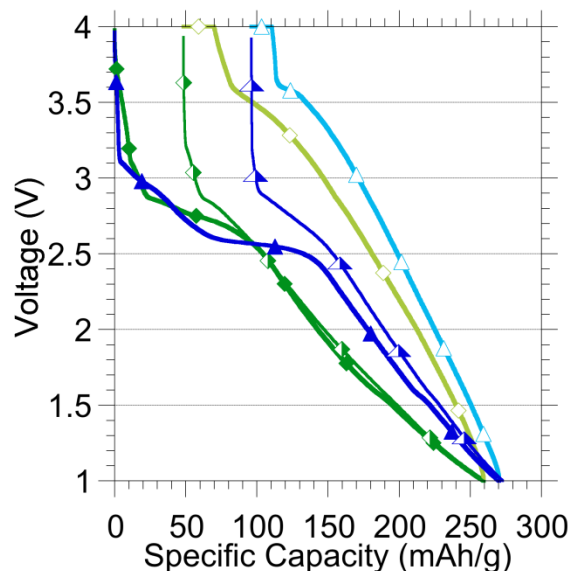


Figure 18. Combined vanadate/borate substitution improved the electrochemical performance of silver-bearing phosphate glass.

Despite its theoretical capability for multivalent intercalation in a reasonable voltage window, previous work on manganese borate glasses with vanadate substitution showed no electrochemical activity involving the Mn cation for an intercalation or conversion reaction. Antimony is also theoretically capable of a multivalent intercalation reaction in a reasonable voltage window, so lithium antimony borate glass was produced and tested as a cathode. The lithium antimony borate glass demonstrated a high-capacity conversion reaction (>200 mAh/g) at ~1.5V, but no intercalation reaction. However, with vanadate substitution, the electrical conductivity and electrochemical performance would be expected to improve. A lithium antimony borate vanadate glass has been produced and will be electrochemically tested in the near future.

## Patents/Publications/Presentations

### Presentation

- Fall MRS Meeting, Boston (2015): “Mixed Polyanion Glasses as Li-Ion Battery Materials”; A. K. Kercher, J. Kolopus, J. Ramey, K. Carroll, R. R. Unocic, S. Stooksbury, J. Kiggans, L. A. Boatner, and N. J. Dudney.

### Publication

- Kercher, A. K., and J. A. Kolopus, K. J. Carroll, R. R. Unocic, S. Kirklin, C. Wolverton, S. L. Stooksbury, L. A. Boatner, and N. J. Dudney. “Mixed Polyanion Glass Cathodes: Glass-State Conversion Reactions.” *Journal of the Electrochemical Society* 163, no. 2, (2016): A131-A137.

## Task 3.8 – Materials for High Energy Lithium Ion Batteries (Marca Doeff, Lawrence Berkeley National Laboratory)

**Project Objective.** Microscopy and synchrotron X-ray absorption and photoemission techniques will be used to study the phenomenon of surface reconstruction to rock salt on NMC particle surfaces as a function of composition, synthesis method, surface chemistry, and electrochemical history. Because the surface reconstruction is implicated in capacity fading and impedance rise during high-voltage cycling, a thorough understanding of this phenomenon is expected to lead to principles that can be used to design robust, high-capacity NMC materials for Li-ion cells. The emphasis will be on stoichiometric NMCs with high Ni contents such as 622 and 523 compositions.

**Project Impact.** To increase the energy density of Li-ion batteries, cathode materials with higher voltages and/or higher capacities are required, but safety and cycle life cannot be compromised. Nickel rich NMCs can provide higher capacities and lower cost in comparison with low nickel content NMCs, but surface reactivity is an issue. A systematic evaluation of the effects of synthesis method, composition, and cell history on the surface reconstruction phenomenon will lead to higher capacity, robust and structurally stable positive electrode materials that result in higher energy density Li-ion cells than currently available.

**Out-Year Goals.** The information generated by the in-depth characterization will be used to design robust NMC materials that can withstand cycling to high potentials and deliver >200 mAh/g.

**Collaborations.** Transmission X-ray microscopy (TXM) has been used this quarter to characterize NMC materials, with work done in collaboration with Yijin Liu (SSRL). Synchrotron and computational efforts continued in collaboration with Professor M. Asta (University of California at Berkeley); and Dr. Dennis Nordlund, Dr. Yijin Liu and Dr. Dimosthenis Sokaras (SSRL). The TEM effort is in collaboration with Dr. Huolin Xin (BNL).

### Milestones

1. Synthesize baseline NMC-523 and NMC-622 and Ti-substituted variants by spray pyrolysis and co-precipitation. (12/31/15 – Completed)
2. Complete surface characterization of pristine materials by XAS and XPS. (3/31/16 – On track).
3. Complete soft XAS experiments on electrodes cycled to high potentials. (6/30/16 – On track)
4. *Go/No-Go*: Core-shell composites made by infiltration and re-firing of spray-pyrolyzed hollow spherical particles. (9/30/16)

## Progress Report

Previous results on NMC-442 materials prepared by spray pyrolysis show that they exhibit better performance than those made by co-precipitation. The in-depth characterization reveals a compositional gradient, where the secondary particles are Ni-poor on the surface in the spray pyrolyzed samples, leading to reduced surface reconstruction. With the attempt to further increase discharge capacity and reduce cost, NMCs with higher Ni content (for example, NMC-532 and NMC-622) were synthesized this quarter by co-precipitation and spray pyrolysis methods. To optimize the synthetic conditions of spray pyrolysis, parameters including carrier gas, flow rate, precursor solution injection rate, precursor solution concentrations, spray temperature and

annealing temperature were systematically investigated using NMC-622 as the model material. Evidence showed that the annealing temperature and precursor concentration play vital roles in achieving higher discharge capacity and better cycling stability. The representative cycling performance between various voltage cutoff windows of NMC-622 prepared with spray pyrolysis is presented in Figure 19a-b. The cell outperforms the co-precipitated NMC-622 materials (Figure 19c-d) in terms of the first cycle discharge capacity. The cycling stability of spray pyrolyzed materials is being investigated. Optimization of NMC-532 and NMC-811 compositions will be carried out soon.

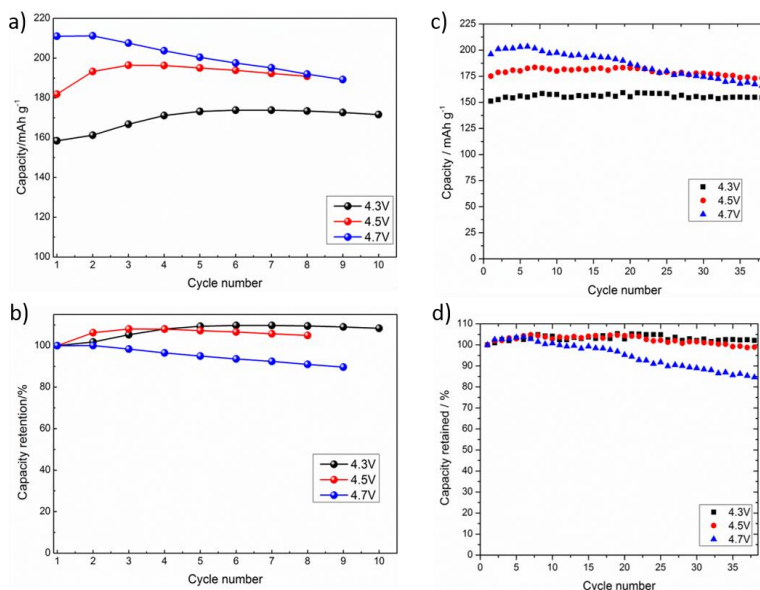


**Figure 19.** Galvanostatic cycling results on NMC-622 materials prepared by spray pyrolysis (a and b) and co-precipitation (c and d).

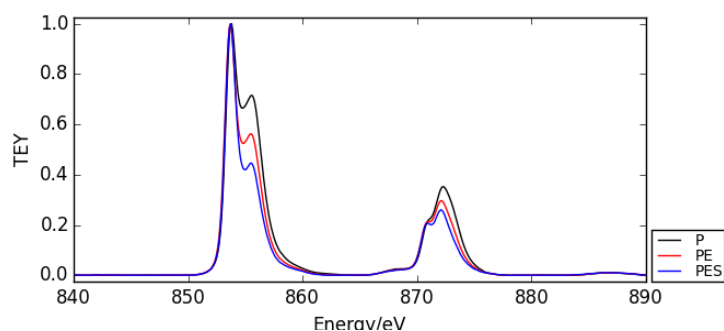


**Figure 20.** Soft X-ray absorption spectroscopy of Ni L-edge in the total electron yield mode for NMC-622: P (pristine powder), PE (pristine electrode), and PES (pristine electrode soaked in electrolyte).

Nickel ions have a higher average oxidation state in NMC-622 than those in NMC-442 or NMC-333, and are expected to have higher reactivity. Soft XAS results (Figure 20) shows that the surface nickel of NMC-622 is reduced during electrode preparation and more significantly reduced after being soaked in electrolyte. This behavior is different from what was observed in NMC-442, where the nickel oxidation state remained intact during electrode fabrication and electrolyte soaking. Further soft XAS characterization is planned for the next quarter on cycled electrodes.

## Patents/Publications/Presentations

### Publications

- Rettenwander, D., and A. Welzl, L. Cheng, J. Fleig, M. Musso, E. Suard, M. M. Doeff, G. J. Redhammer, and G. Amthauer. “Synthesis, Crystal Chemistry, and Electrochemical Properties of  $\text{Li}_{7-2x}\text{La}_3\text{Zr}_{2-x}\text{Mo}_x\text{O}_{12}$  ( $x=0.1-0.4$ ): Stabilization of the Cubic Garnet Polymorph via Substitution of  $\text{Zr}^{4+}$  by  $\text{Mo}^{6+}$ .” *Inorg. Chem.* (2015). doi:10.1021/acs.inorgchem.5b01895.
- Hou, H., and L. Cheng, T. Richardson, G. Chen, M. Doeff, R. Zheng, R. Russo, and V. Zorba. “Three-Dimensional Elemental Imaging of Li-Ion Solid-State Electrolytes Using fs-Laser Induced Breakdown Spectroscopy (LIBS).” *J. Anal. Atomic Spectroscopy* 30 (2015): 2295.

### Presentations

- 2015 Lithium Battery Power, Baltimore, Maryland (17-19 November 2015): “High Potential NMC Cathode Materials – A Route to High Energy Density Li-Ion Batteries”; Marca M. Doeff and Feng Lin. Invited.
- Energy Storage and Conversion Symposium, Northern California Chapter of American Vacuum Society, San Jose, California (13 November 2015): “The Future of Energy Storage”; Marca M. Doeff and Venkat Srinivasan. Invited.
- 62<sup>nd</sup> American Vacuum Society International Symposium, San Jose, California (19- 23 October 2015): Abstract #261, “Behavior of Layered Cathode Materials: A Route to Higher Energy Density for Lithium Ion Batteries”; Marca M. Doeff, Feng Lin, and Isaac Markus. Invited.
- 2<sup>nd</sup> International Conference on Sodium Batteries, Phoenix (7-9 October 2015): “Advances in Sodium Ion Battery Chemistry”; Marca M. Doeff, Mona Shirpour, and Xiaowen Zhan. Invited.

### Task 3.9 – Lithium Batteries with Higher Capacity and Voltage (John B. Goodenough, UT – Austin)

**Project Objective.** The project objective is to develop an electrochemically stable alkali-metal anode that can avoid the SEI layer formation and the alkali-metal dendrites during charge/discharge. To achieve the goal, a thin and elastic solid electrolyte membrane with a Fermi energy above that of metallic Li and an ionic conductivity  $\sigma > 10^{-4} \text{ S cm}^{-1}$  (1) will be tested in contact with alkali-metal surface. (2) The interface between the alkali-metal and the electrolyte membrane should be free from liquid electrolyte, (3) have a low impedance for alkali-metal transport and plating, and (4) keep good mechanical contact during electrochemical reactions.

**Project Impact.** An alkali-metal anode (Li or Na) would increase the energy density for a given cathode by providing a higher cell voltage. However, lithium is not used as the anode in today's commercial lithium-ion batteries because electrochemical dendrite formation can induce a cell short-circuit and critical safety hazards. This project is to find a way to avoid the formation of alkali-metal dendrites and to develop an electrochemical cell with dendrite-free alkali-metal anode. Therefore, once realized, the project will have a significant impact by an energy-density increase and battery safety; it will enable a commercial lithium-metal rechargeable battery of increased cycle life.

The key approach is to introduce a solid-solid contact between an alkali metal and a solid electrolyte membrane. Where SEI formation occurs, the creation of new anode surface at dendrites with each cycle causes capacity fade and a shortened cycle life. To avoid the SEI formation, a thin and elastic solid electrolyte membrane will be introduced, and liquid electrolyte will be eliminated from the anode surface.

**Out-Year Goals.** The out-year goals are to increase cell energy density for a given cathode and to allow low-cost, high-capacity rechargeable batteries with cathodes other than insertion compounds.

**Collaborations.** This project collaborates with A. Manthiram at UT Austin and with Karim Zaghib at Hydro Quebec.

#### Milestones

1. Test incorporating a low-melting-point Li<sup>+</sup>-electrolyte glass in the thiol-ene polymer for a solid electrolyte membrane. (31 December 2015 – Ongoing)
2. Identify a Li<sup>+</sup> solid electrolyte for contacting an alkali-ion anode to eliminate SEI formation. (31 March 2016)
3. Testing a cell having an alkali-metal anode not contacting a liquid electrolyte. (30 June 2016)
4. Optimizing the electrochemical performance of a cell having no SEI formation on an alkali-metal anode. (31 September 2016)



## Progress Report

Test incorporating a low-melting-point  $\text{Li}^+$ -electrolyte glass in the thiol-ene polymer for a solid electrolyte membrane has been performed with molten nitrate electrolytes. Molten nitrate electrolytes show low melting points, especially at the eutectic points. For the test,  $\text{LiNO}_3$  was mixed with  $\text{NaNO}_3$  or  $\text{KNO}_3$ . The eutectic temperatures for  $\text{LiNO}_3$ - $\text{KNO}_3$  (42-58 mol%) and  $\text{LiNO}_3$ - $\text{NaNO}_3$  (56-44 mol%) are  $124^\circ\text{C}$  and  $187^\circ\text{C}$ , respectively. The molten nitrate electrolytes offer a high ionic conductivity and a chemical stability over a wide temperature range. Moreover, it has a low viscosity, so it is a good candidate for the incorporation test.

For the thiol-ene polymer membranes, the project fabricated (1) a tetrathiol-cross-linked ester (*divinyl adipate*) and (2) a di- and tetra-thiol(50-50 mol%)-cross-linked polyethylene oxide (*Poly(ethylene glycol) diacrylate*,  $M_n \sim 700$ ) membranes. The second crosslinked poly(ethylene oxide) (PEO) membrane was developed to enlarge the pore volume of the membrane and thereby increase the chance of nitrate solution uptake: the mixed di- and tetra-thiol crosslinker can decrease the crosslinking density less than that of the 100% tetrathiol crosslinker, and the PEO chain is longer in length than the ester monomer that was used in this study.

The two membranes were immersed in the nitrate eutectic solutions in an Ar-filled glove box, as shown in Figure 21. Immersion in the  $\text{LiNO}_3$ - $\text{NaNO}_3$  nitrate electrolyte at  $187^\circ\text{C}$  resulted in a rapid degradation of both of the membranes. Even after 10 minutes of storage, the membranes turned from transparent to black. The  $\text{LiNO}_3$ - $\text{NaNO}_3$  mixture also turned brown, which indicates a chemical reaction with the membranes. In the  $\text{LiNO}_3$ - $\text{KNO}_3$  nitrate electrolyte at  $124^\circ\text{C}$ , the membranes were much more stable, probably owing to the lower eutectic temperature. After 1 hour of storage, no color changes were noticed, but both of the membranes did not absorb the nitrate electrolyte. However, after prolonged storage for 10 hours, those membranes turn brown and were oxidized. After cooling down the electrolyte, the membranes were still transparent, and the electrolyte uptake did not occur in the experiment. From the experiment, it is obvious that the thiol-ene polymer membrane is not stable in a nitrate eutectic electrolyte at high temperature.

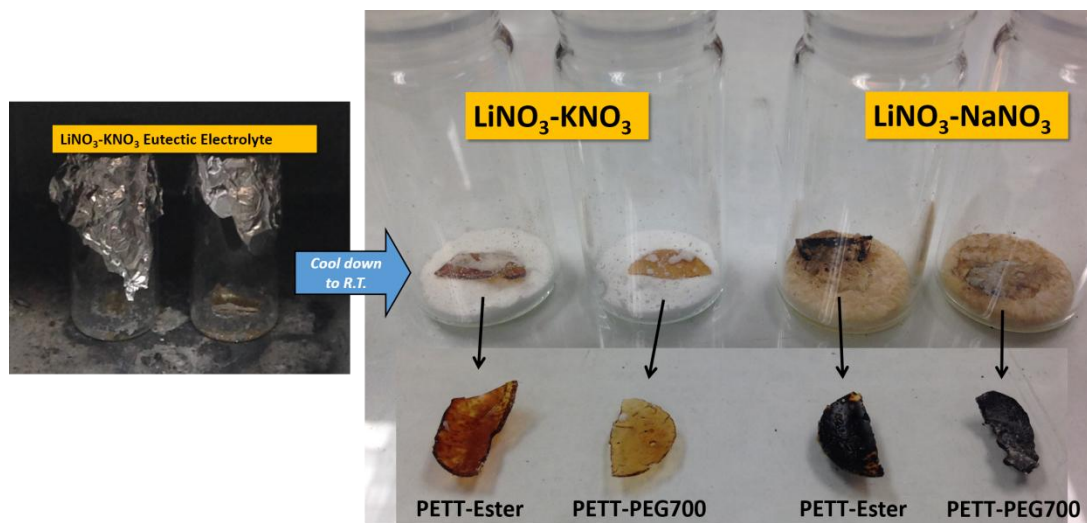


Figure 21. (left) Polymer membrane immersion test in the  $\text{LiNO}_3$ - $\text{KNO}_3$  nitrate electrolyte at  $124^\circ\text{C}$ . (right) Photographs of the polymer membranes after the electrolyte soaking tests.

## Task 3.10 – Exploiting Co and Ni Spinel in Structurally Integrated Composite Electrodes (Michael M. Thackeray and Jason R. Croy, Argonne National Laboratory)

**Project Objective.** The project goal is to stabilize high-capacity, composite ‘layered-layered’ electrode structures with lithium-cobalt-oxide and lithium-nickel-oxide spinel components (referred to as LCO-S and LNO-S, respectively), or solid solutions thereof (LCNO-S), which can accommodate lithium at approximately 3.5 V vs. metallic lithium. This approach and the motivation to use LCO-S and LNO-S spinel components, about which relatively little is known, is novel.

**Project Impact.** State-of-the-art lithium-ion batteries are unable to satisfy the performance goals for PHEVs and all-electric EVs. If successful, this project will impact the advance of energy storage for electrified transportation as well as other applications, such as portable electronic devices and the electrical grid.

**Approach.** This work will focus on the design and synthesis of new spinel compositions and structures that operate above 3 V and below 4 V and to determine their structural and electrochemical properties through advanced characterization. This information will subsequently be used to select the most promising spinel materials for integration as stabilizers into high-capacity composite electrode structures.

**Out-Year Goals.** The electrochemical capacity of most high-potential lithium-metal oxide insertion electrodes is generally severely compromised by their structural instability and surface reactivity with the electrolyte at low lithium loadings (that is, at highly charged states). Although some progress has been made by cation substitution and structural modification, the practical capacity of these electrodes is still restricted to approximately 160-170 mAh/g. This project proposes a new structural and compositional approach with the goal of producing electrode materials that can provide 200-220 mAh/g without significant structural or voltage decay for 500 cycles. If successful, the materials processing technology will be transferred to the Argonne Materials Engineering and Research Facility (MERF) for scale up and further evaluation.

**Collaborations.** This project collaborates with Eungje Lee, Joong Sun Park (Chemical Sciences & Engineering, ANL), Mali Balasubramanian (APS, ANL), and V. Dravid and C. Wolverton (Northwestern University).

### Milestones

1. Synthesize and optimize spinel compositions and structures with a focus on Co-based systems for use in structurally integrated layered-spinel electrodes. (Q1 – In progress; see text)
2. Determine electrochemical properties of Co-based spinel materials, and when structurally integrated in composite layered-spinel electrodes. (Q2 – In progress; see text)
3. Evaluate the electrochemical migration of transition metal ions in Co-based layered-spinel electrodes. (Q3/Q4)

## Progress Report

Previous reports have described the synthesis and electrochemistry of  $\text{Li}[\text{Co}_{1-x-y}\text{Ni}_x\text{Mn}_y]\text{O}_2$  spinel materials prepared at low temperature (LT). Of the various LT-spinel materials tested,  $\text{Li}[\text{Co}_{1-y}\text{Ni}_y]\text{O}_2$  compositions have shown the most promising electrochemical properties. To explore the possible integration of LT-spinels with a layered component, a series of initial experiments was undertaken on targeted  $x\text{Li}_2\text{MnO}_3 \cdot (1-x)\text{Li}[\text{Co}_{1-y}\text{Ni}_y]\text{O}_2$  ( $0 \leq x \leq 0.2$ ;  $0 \leq y \leq 0.25$ ) cathode compositions.

Cathode powders were prepared by solid-state synthesis by thoroughly mixing metal carbonate- and metal nitrate precursors followed by calcination between 400–600°C. The synthesis conditions were determined from previous studies that showed the temperature-dependent evolution of  $\text{Li}[\text{Co}_{1-y}\text{Ni}_y]\text{O}_2$  products from a lithiated-spinel structure to a layered configuration between 400–700°C; it is also significant that layered  $\text{Li}_2\text{MnO}_3$  can form in air at temperatures between 400°C and 850°C.

Figure 22 shows the XRD patterns of  $x\text{Li}_2\text{MnO}_3 \cdot (1-x)\text{Li}[\text{Co}_{1-y}\text{Ni}_y]\text{O}_2$  samples fired at 600°C in air for 3 days. All samples clearly exhibit merged (018)/(110) peaks at  $\sim 65^\circ$   $2\theta$ , suggesting the presence of a cubic, lithiated-spinel structure. The low-intensity diffraction peaks at  $\sim 22^\circ$   $2\theta$ , due to Li/Mn ordering, are broad as a result of the LT synthesis. However, first-cycle voltage profiles (not shown) reveal an irreversible plateau at  $\sim 4.5$  V consistent with Li/Mn ordered regions within the electrode structures. Figure 23 shows the electrochemical data of lithium half cells, when cycled between 2.5 and 4.2 V. After the initial charge, the voltage profiles in Figure 23a show two electrochemical events during discharge, one at  $\sim 3.9$  V and the second at  $\sim 3.5$  V. These plateaus are tentatively assigned to lithium insertion into localized layered regions ( $\sim 3.9$  V) and into spinel regions (3.6 V). (Note that the presence of local layered domains in LT- $\text{Li}_2[\text{Co}_{1-y}\text{Ni}_y]\text{O}_4$  lithiated-spinel samples was suggested in previous reports.) With increasing  $\text{Li}_2\text{MnO}_3$  content,  $x$ , the specific capacity decreases (Figure 23c), while the capacity retention improves (Figure 23b). In addition, comparisons between the samples having the same  $\text{Li}_2\text{MnO}_3$  content show an enhancement of cycling stability as nickel is substituted for cobalt (Figure 23c). The results highlight (i) the competing forces at play during the construction of ‘layered-spinel’ composite electrode structures and (ii) the dependence of the structural and electrochemical stability of LT- $\text{Li}[\text{Co}_{1-y}\text{Ni}_y]\text{O}_2$  electrodes on the Ni:Co ratio.

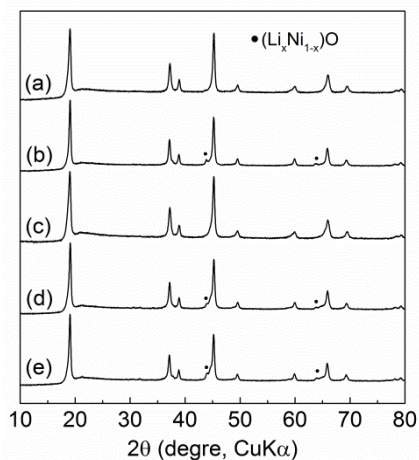


Figure 22. X-ray diffraction patterns of  $x\text{Li}_2\text{MnO}_3 \cdot (1-x)\text{LiCo}_{1-y}\text{Ni}_y\text{O}_2$  samples made at 600°C with (a)  $x=0.1$ ;  $y=0.1$ , (b)  $x=0.1$ ;  $y=0.2$ , (c)  $x=0.2$ ;  $y=0.1$ , (d)  $x=0.2$ ;  $y=0.2$ , and (e)  $x=0.2$ ;  $y=0.25$ .

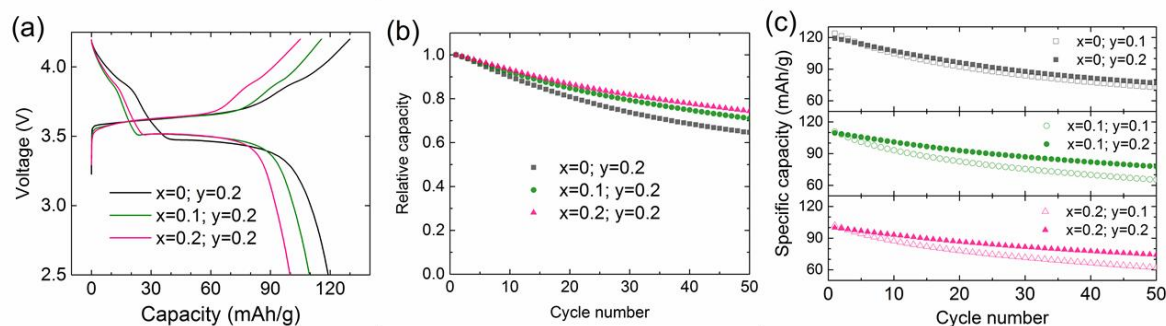


Figure 23. (a) Initial voltage profiles. (b) Relative capacity retentions. (c) Cycle performances of  $x\text{Li}_2\text{MnO}_3 \cdot (1-x)\text{LiCo}_{1-y}\text{Ni}_y\text{O}_2$  composite materials ( $0 \leq x \leq 0.2$ ;  $0 \leq y \leq 0.25$ ) synthesized at 600°C. Li half-cells were cycled between 2.5 – 4.2 V vs. Li at the current rate of 15 mA/g.

## Patents/Publications/Presentations

### Patent Application

- Thackeray, M. M., and J. R. Croy, B. R. Long, J. S. Park, and E. Lee. *Layered-Spinel Electrodes for Lithium Batteries*. U.S. Pat. Application. Filed 29 December 2015.

### Presentation

- Victor Pretorius Memorial Lecture, University of Pretoria, South Africa (6 October 2015): “Energy Storage: Challenges and Opportunities in an Evolving Lithium Economy.” M. M. Thackeray. Invited.

## Task 3.11 – Discovery of High energy Li ion Battery Materials (Wei Tong, Lawrence Berkeley National Laboratory)

**Project Objective.** This project aims to develop a cathode that can cycle  $> 200$  mAh/g while exhibiting minimal capacity and voltage fade. The emphasis will be on oxides with high nickel contents. This task focuses on the compositions in the Li-Ni-O phase space, which will be explored using a combinatorial materials approach to search for new high-capacity cathodes. The specific objectives of this project are to: (1) investigate and understand the correlation between the synthesis and electrochemical performance of Ni-based compounds, (2) design, synthesize, and evaluate the potential new high-capacity cathodes within Li-Ni-O composition space using the percolation theory as a guideline.

**Project Impact.** In the commercial Li-ion batteries, the well ordered, close-packed oxides, particularly, layered lithium transition metal oxides ( $\text{LiTmO}_2$ , Tm is transition metal) are widely used. However, the energy density needs to be at least doubled to meet the performance requirements of EVs (300 to 400 miles). Although capacities approaching 300 mAh/g have been reported in Li, Mn-rich layered oxide compounds, capacity decay and voltage fading in the long-term cycling are always observed. Therefore, new materials are urgently needed to make the breakthrough in Li-ion battery technology.

**Approach.** The recent discovery of high-capacity materials with lithium excess provides new insights into design principles for potential high-capacity cathode materials. According to the percolation theory, lithium excess is required to access 1 lithium exchange capacity in  $\text{LiTmO}_2$  compounds. This seems to be independent of transition metal species; therefore, it could open up a composition space for the search of new materials with high capacity. The interesting  $\text{Ni}^{2+}/\text{Ni}^{4+}$  redox is selected as the electrochemically active component and combinatorial materials design concept will be used to discover the potential cathode material candidates in the Li-Ni-O phase space.

**Out-Year Goals.** The long-term goal of this project is to search new high-energy cathodes that can potentially meet the performance requirements of EVs with a 300- to 400-mile range in terms of cost, energy density, and performance. Work will progress from the understanding of the known compounds,  $\text{LiNiO}_2$  and  $\text{Li}_2\text{NiO}_2$ , toward development of new Ni-based, high-energy cathode oxides.

**Collaborations.** The PI closely collaborates with M. Doeff (LBNL) on soft XAS, C. Ban (NREL) on atomic layer deposition (ALD) coating, B. McCloskey (LBNL) for differential electrochemical mass spectrometry, and R. Kostecki (LBNL) for Raman spectroscopy. In addition, collaboration with other BMR PIs (X.-Q. Yang and F. Wang, BNL; and K. Persson, LBNL) for crystal structure evolution upon cycling and material computation, is ongoing.

### Milestones

1. Determine synthetic approach and identify the key synthetic parameters for  $\text{Ni}^{3+}$ -containing compounds, for example,  $\text{LiNiO}_2$ . (Q1 – Complete)
2. Complete the structural and electrochemical characterization of  $\text{LiNiO}_2$ . (Q2 – Ongoing)
3. Determine synthetic approach and identify the key synthetic parameters for  $\text{Ni}^{2+}$ -containing compounds, for example,  $\text{Li}_2\text{NiO}_2$ . (Q3)
4. Complete the structural, and electrochemical characterization of  $\text{Li}_2\text{NiO}_2$  and down select the synthetic approach for the phase screening within Li-Ni-O chemical space. (Q4)



## Progress Report

LiNiO<sub>2</sub> samples were prepared by a solid state method using both commercial and precipitated Ni(OH)<sub>2</sub> precursors. 2% and 10% excess LiOH precursors were used; the as-prepared samples are denoted as “solution\_2exLi” and “solution\_10exLi,” respectively. The third sample was simply synthesized following a general solid state reaction protocol by milling Li<sub>2</sub>CO<sub>3</sub> and Ni(OH)<sub>2</sub> precursors with 10% excess Li, henceforth referred to as “solid\_10exLi.” Figure 24 shows the synchrotron X-ray diffraction (SXRD) patterns of the as-synthesized LiNiO<sub>2</sub> powders. The high intensity ratios between (003)/(104) and clear peak splits between (108) and (110) suggest good phase crystallinity and cation ordering, which was further confirmed by the Rietveld refinement results. Overall, the occupancies of 3a sites by Ni ions are less than 2% for all three samples.

Scanning electron microscopy (SEM) images (Figure 25) illustrate that the secondary particle size of the as-synthesized powders averages about a few microns and a relatively uniform particle size distribution was observed for the solid\_10exLi sample.

The materials were then cycled between 4.3 and 2.7 V at C/10 for the electrochemical tests. The first cycle voltage profiles are shown in Figure 26a. Solution\_2exLi delivered a capacity of 223 mAh/g in the first charge, and 190 mAh/g in the first discharge. The first cycle electrochemical behaviors of LiNiO<sub>2</sub> prepared with 10% excess Li (solution\_10exLi and solid\_10exLi) were quite similar, suggesting negligible effect of Ni(OH)<sub>2</sub> precursor. These two samples delivered a charge capacity of 240 mAh/g (corresponding to 0.85 Li deintercalation) and a discharge capacity of 206 mAh/g (corresponding to 0.73 Li re-intercalation). Based on the dq/dV plot in Figure 25b, the materials synthesized by 10% excess Li also demonstrated smaller polarization. These differences among the samples were repeatable and beyond what would be expected from cell-to-cell variation (< 5 mAh/g) within the project's

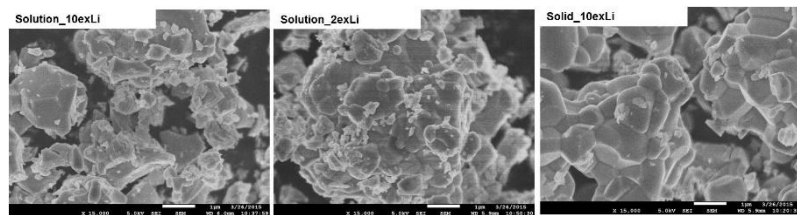
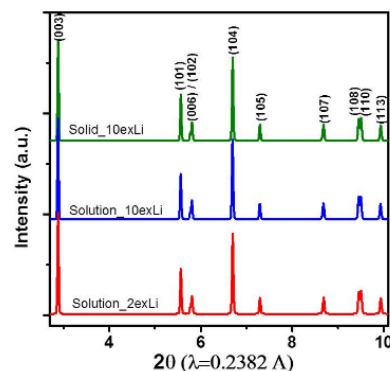


Figure 25. SEM images for LiNiO<sub>2</sub> samples (solution\_2exLi, solution\_10exLi, and solid\_10exLi).



Sample	Lattice Parameter (Å)	Ni on 3a site (%)	R value (%)
Solid_10exLi	a = 2.875(7) c = 14.197(2)	1.44(3)	3.02(5)
Solution_10exLi	a = 2.874(0) c = 14.190(1)	1.03(6)	3.09(1)
Solution_2exLi	a = 2.874(1) c = 14.188(5)	1.08(4)	3.12(9)

Figure 24. Synchrotron X-ray diffraction patterns and refinement for three LiNiO<sub>2</sub> samples (Solution\_2exLi, solution\_10exLi, and solid\_10exLi).

experiments, and thus can be considered to result from changing the active material. The higher capacity and lower polarization for these two samples compared to those of solution\_2exLi indicated that the amount of excess Li in the synthesis had a larger effect on the electrochemical properties than the source of the Ni precursor.

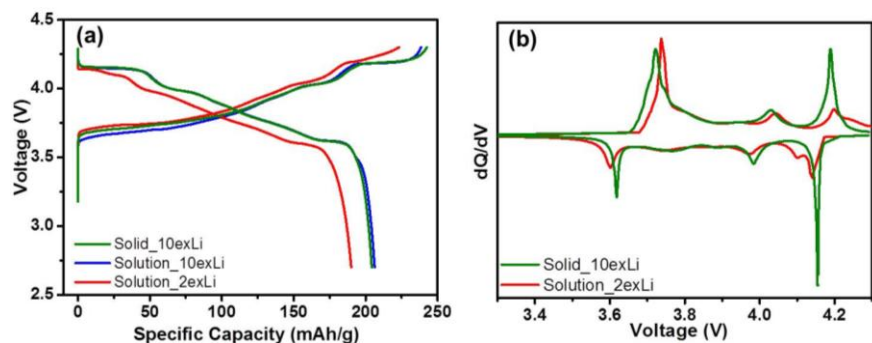


Figure 26. (a) The first cycle voltage profiles. (b) The dq/dV plot of LiNiO<sub>2</sub> samples (solution\_2exLi, solution\_10exLi, and solid\_10exLi).



## Patents/Publications/Presentations

### Publication

- Villaluenga, Irune, and Kevin H. Wujcik, Wei Tong, Didier Devaux, Dominica H. C. Wong, Joseph M. DeSimone, and Nitash P. Balsara. “Compliant Glass-Polymer Hybrid Single Ion-Conducting Electrolytes for Lithium Batteries.” *PNAS* 113 (2015): 52-57.

### Presentation

- 228<sup>th</sup> Electrochemical Society Meeting, Phoenix (11 – 15 October 2015): “Investigating Synthetic Effects on Ni-Based Oxide as a Cathode Material for Li-Ion Batteries.” J. Xu and W. Tong.

## TASK 4 – ELECTROLYTES FOR HIGH-VOLTAGE, HIGH-ENERGY LITHIUM-ION BATTERIES

**NOTE:** This task is now closed, with limited extension work being completed this quarter. The BMR will issue a Call in this area later this fiscal year.

### Summary

The current lithium-ion electrolyte technology is based on  $\text{LiPF}_6$  solutions in organic carbonate mixtures with one or more functional additives. Lithium-ion battery chemistries with energy density of 175~250 Wh/Kg are the most promising choice. To further increase the energy density, the most efficient way is to raise either the voltage and/or the capacity of the positive materials. Several high-energy materials including high-capacity composite cathode  $x\text{Li}_2\text{MnO}_3 \cdot (1-x)\text{LiMO}_2$  and high-voltage cathode materials such as  $\text{LiNi}_{0.5}\text{Mn}_{1.5}\text{O}_4$  (4.8 V) and  $\text{LiCoPO}_4$  (5.1 V) have been developed. However, their increased operating voltage during activation and charging poses great challenges to the conventional electrolytes, whose organic carbonate-based components tend to oxidatively decompose at the threshold beyond 4.5 V vs  $\text{Li}^+/\text{Li}$ .

Other candidate positive materials for PHEV application that have potential of providing high capacity are the layered Ni-rich NCM materials. When charged to a voltage higher than 4.5 V, they can deliver a much higher capacity. For example,  $\text{LiNi}_{0.8}\text{Co}_{0.1}\text{Mn}_{0.1}\text{O}_2$  (NCM 811) only utilizes 50% of its theoretical capacity of 275 mAh/g when operating in a voltage window of 4.2 V – 3.0 V. Operating voltage higher than 4.4 V would significantly increase the capacity to 220 mAh/g; however, the cell cycle life becomes significantly shortened mainly due to the interfacial reactivity of the charged cathode with the conventional electrolyte. The oxidative voltage instability of the conventional electrolyte essentially prevents the practicality to access the extra capacities of these materials.

To address the above challenges, new electrolytes that have substantial high-voltage tolerance at high temperature with improved safety are needed urgently. Organic compounds with low HOMO (highest occupied molecular orbital) energy level are suitable candidates for high-voltage application. An alternative approach to address the electrolyte challenges is to mitigate the surface reactivity of high-voltage cathodes by developing cathode passivating additives. Like the indispensable role of SEI on the carbonaceous anodes, cathode electrolyte interphase (CEI) formation additives could kinetically suppress the thermodynamic reaction of the delithiated cathode and electrolyte, thus significantly improving the cycle life and calendar life of the high energy density lithium-ion battery.

An ideal electrolyte for high-voltage, high-energy cathodes also requires high compatibility with anode materials (graphite or silicon). New anode SEI formation additives tailored for the new high-voltage electrolyte are equally critical for the high-energy lithium-ion battery system. Such an electrolyte should have the following properties: high stability against 4.5 – 5.0 V charging state, particularly with cathodes exhibiting high surface oxygen activity; high compatibility with a strongly reducing anode under high-voltage charging; high Li salt solubility ( $> 1.0 \text{ M}$ ) and ionic conductivity ( $> 6 \times 10^{-3} \text{ S/cm}$  @ room temperature); and non-flammability (no flash point) for improved safety and excellent low-temperature performance ( $-30^\circ\text{C}$ ).

## TASK 5 – DIAGNOSTICS

### Summary and Highlights

To meet the goals of VTO Multi Year Program Plan and develop lower-cost, abuse-tolerant batteries with higher energy density, higher power, better low-temperature operation and longer lifetimes suitable for the next-generation of HEVs, PHEVs and EVs, there is a strong need to identify and understand structure-property-electrochemical performance relationships in materials, life-limiting and performance-limiting processes, and various failure modes to guide battery development activities and scale-up efforts. In the pursuit of batteries with high energy density, high cell operating voltages and demanding cycling requirements lead to unprecedented chemical and mechanical instabilities in cell components. Successful implementation of newer materials such as Si anode and high-voltage cathodes also requires better understanding of fundamental processes, especially those at the solid/electrolyte interface of both anode and cathode.

The BMR Task 5 takes on these challenges by combining model system, *ex situ*, *in situ*, and *operando* approaches with an array of the start-of-the-art analytical and computational tools. Four subtasks are tackling the chemical processes and reactions at the electrode/electrolyte interface. Researchers at LBNL use *in situ* and *ex situ* vibrational spectroscopy, far- and near-field scanning probe spectroscopy and laser-induced breakdown spectroscopy (LIBS) to understand the composition, structure, and formation/degradation mechanisms of the solid electrolyte interface at Si anode and high-voltage cathodes. The University of California at San Diego (UCSD) subtask combines STEM/EELS, XPS, and *ab initio* computation for surface and interface characterization and identification of instability causes at both electrodes. At Cambridge, NMR is being used to identify major SEI components, their spatial proximity, and how they change with cycling. Subtasks at BNL and PNNL focus on the understanding of fading mechanisms in electrode materials, with the help of synchrotron based X-ray techniques (diffraction and hard/soft X-ray absorption) at BNL and HRTEM and spectroscopy techniques at PNNL. At LBNL, model systems of electrode materials with well defined physical attributes are being developed and used for advanced diagnostic and mechanistic studies at both bulk and single-crystal levels. These controlled studies remove the ambiguity in correlating material's physical properties and reaction mechanisms to its performance and stability, which is critical for further optimization. The final subtask takes advantage of the user facilities at ANL that bring together X-ray and neutron diffraction, X-ray absorption, emission and scattering, HRTEM, Raman spectroscopy and theory to look into the structural, electrochemical, and chemical mechanisms in the complex electrode/electrolyte systems. The diagnostics team not only produces a wealth of knowledge that is key to developing next-generation batteries, it also advances analytical techniques and instrumentation that have a far-reaching effect on material and device development in a range of fields.

The highlights for this quarter are as follows:

- Cambridge University (Grey's Group) employed multinuclear  $^1\text{H}$ ,  $^7\text{Li}$ ,  $^{19}\text{F}$ , and  $^{13}\text{C}$  NMR solid state NMR spectroscopy for comprehensive analysis of the SEI passivating layer that grows on silicon nanoparticles.
- Brookhaven National Laboratory (Yang and Yu Team) demonstrated that Fe substitution in  $\text{LiNi}_{0.5}\text{Mn}_{1.5}\text{O}_4$  spinel improves thermal stability of the charged cathode by suppressing oxygen release and maintaining the crystal structure.

## Task 5.1 – Design and Synthesis of Advanced High-Energy Cathode Materials (Guoying Chen, Lawrence Berkeley National Laboratory)

**Project Objective.** The successful development of next-generation electrode materials requires particle-level knowledge of the relationships between materials' specific physical properties and reaction mechanisms to their performance and stability. This single-crystal-based project was developed specifically for this purpose, and it has the following objectives: (1) obtain new insights into electrode materials by utilizing state-of-the-art analytical techniques that are mostly inapplicable on conventional, aggregated secondary particles, (2) gain fundamental understanding on structural, chemical, and morphological instabilities during Li extraction/insertion and prolonged cycling, (3) establish and control the interfacial chemistry between the cathode and electrolyte at high operating voltages, (4) determine transport limitations at both particle and electrode levels, and (5) develop next-generation electrode materials based on rational design as opposed to more conventional empirical approaches.

**Project Impact.** This project will reveal performance-limiting physical properties, phase-transition mechanisms, parasitic reactions, and transport processes based on the advanced diagnostic studies on well formed single crystals. The findings will establish rational, non-empirical design methods that will improve the commercial viability of next-generation  $\text{Li}_{1+x}\text{M}_{1-x}\text{O}_2$  (M=Mn, Ni and Co) and spinel  $\text{LiNi}_x\text{Mn}_{2-x}\text{O}_4$  cathode materials.

**Approach.** This project scope will encompass the following: (1) Prepare crystal samples of Li-rich layered oxides and high-voltage Ni/Mn spinels with well defined physical attributes, (2) Perform advanced diagnostic and mechanistic studies at both bulk and single-crystal levels, and (3) Establish global properties and performance of the samples from the bulk analyses, while, for the single-crystal based studies, utilizing time- and spatial-resolved analytical techniques to probe material's redox transformation and failure mechanisms.

**Out-Year Goals.** This project aims to determine performance and stability limiting fundamental properties and processes in high-energy cathode materials and to outline mitigating approaches. Improved electrode materials will be designed and synthesized.

**Collaborations.** This project collaborates with Drs. E. Crumlin and P. Ross (LBNL), Drs. Y. Liu and D. Nordlund (SSRL), Prof. C. Grey (Cambridge), Dr. C. Wang (PNNL), and Dr. J. Nanda (ORNL).

### Milestones

1. Establish synthesis-structure-electrochemical property relationship in high-voltage Li-TM-oxides. (12/31/15 – Complete)
2. *Go/No-Go*: Downselect alternative high-energy cathode materials for further investigation, if the material delivers > 200mAh/g capacity in the voltage window of 2 – 4.5 V. (3/31/16 – On schedule)
3. Determine Li concentration and cycling dependent transition-metal movement in and out of oxide particles. Examine the mechanism. (6/30/16 – On schedule)
4. Identify key surface properties and features hindering stable high-voltage cycling of Li-TM-oxides. (9/30/16 – On schedule)

## Progress Report

Previous studies revealed that contrary to the common notion of a layered-layered composite structure in LMR-NMCs, crystals synthesized by the molten-salt method adopt a single-phase monoclinic structure (C2/m) with random domains of [100], [110] and [1-10] variants. In an effort to better understand the relationship between synthesis, composition, morphology, transition metal ordering/crystal structure, and electrochemical behavior of these complex oxides, a systematic study on the effect of heating and cooling conditions was performed. Four samples, labeled as 3°C/3°C, 3°C/15°C, 3°C/Q, and 15°C/3°C to indicate the heating and cooling rates used in each case (Q refers to quenching), were synthesized in a composition of  $\text{Li}_{1.2}\text{Ni}_{0.13}\text{Mn}_{0.54}\text{Co}_{0.13}\text{O}_2$  at 900°C. Figure 27 shows the XRD patterns of the samples, which support good crystallinity and phase purity. The intensity of the diffraction peaks from 20° to 23° (2 $\theta$ ) is noticeably higher in the 3°C/3°C sample, suggesting larger domain size. SEM studies showed that all samples were discrete crystals exhibiting a plate shape with an average size of 1  $\mu\text{m}$ . The thickness of the 3°C/3°C and 3°C/15°C plates are similar at about 200 nm, whereas the 3°C/Q and 15°C/3°C crystals are much thicker at about 300 and 350 nm, respectively. This corresponds to an increase in surface contribution from facets other than the large (001) planes in the latter two samples. The voltage profiles from half-cell cycling of the crystal composite electrodes are shown in Figure 28a-d. At a current density of 20 mA/g, similar first charge profiles were obtained, including a sloping region and a plateau region. The discharge capacity gradually decreased during the first 100 cycles, but the 3°C/3°C sample had the best performance in both capacity and capacity retention, which was closely followed by the 3°C/15°C sample. Inferior performance was observed on the 3°C/Q and 15°C/3°C samples (Figure 28 e-f). Figure 28g shows the Mn and Co soft XAS total electron yield (TEY) spectra collected before and after 45 cycles. At pristine, Mn and Ni remain at 4+ and 2+ on all samples. The intensity of the low-energy shoulder peak at the Co L<sub>3</sub> edge, closely associated with the reduced Co<sup>2+</sup> content in the sample, increases following the order of 3°C/3°C < 3°C/15°C < 3°C/Q < 15°C/3°C. This is consistent with the increase in sample thickness, suggesting that thicker plates have more reactive surface. After 45 cycles, the intensity of both lower-energy shoulder peaks at the Mn and Co L<sub>3</sub> edges increased drastically, corresponding to extensive Mn and Co reductions during cycling. The reduction progressed from the surface towards the bulk, as evidenced by depth-profiling soft XAS. Samples with more cycling-induced Mn and Co reductions were found to have worse electrochemical performance. The study clearly shows that synthesis conditions impact particle surface terminations and transition-metal reduction, which subsequently impact chemical and cycling stabilities of the LMR-NMC cathodes.

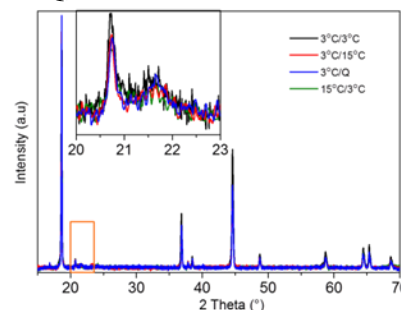


Figure 27. X-ray diffraction patterns of the crystals.

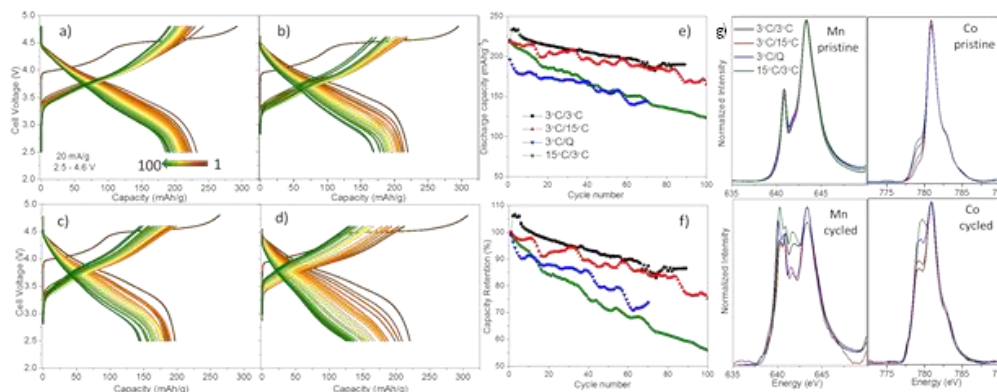


Figure 28. Galvanostatic charge-discharge profiles of the crystal electrodes: (a) 3°C/3°C. (b) 3°C/15°C. (c) 3°C/Q. (d) 15°C/3°C. (e) Discharge capacities. (f) Capacity retention of the cells. (g) Soft X-ray absorption spectroscopy total electron yield spectra of Mn and Co L<sub>3</sub>-edges before and after 45 cycles.

## Patents/Publications/Presentations

### Publications

- Yan, P., and Jianming Zheng, Jiaxin Zheng, Z. Wang, G. Teng, S. Kuppan, J. Xiao, G. Chen, F. Pan, J.-G. Zhang, and C.-M. Wang. “Ni and Co Segregations on Selective Surface Facets and Their Composition Dependence in Layered Lithium Transition-Metal Oxide Cathodes.” *Advanced Energy Materials*, accepted (2016).
- Shukla, K., and Q. Ramasse, C. Ophus, H. Duncan, and G. Chen. “Unraveling Structural Ambiguities in Li and Mn Rich Transition Metal Oxides.” *Nature Communications*. doi: 10.1038/ncomms9711 (2015).
- Yan, P., and J. Zheng, S. Kuppan, Q. Li, D. Lu, J. Xiao, G. Chen, J.-G. Zhang, and C.-M. Wang. “Phosphorus Enrichment in Solid Electrolyte Interphase Layer on High-Voltage Cathodes for Lithium Ion Battery.” *Chemistry of Materials* 27, no. 21 (2015): 7447.
- Ruther, R., and H. Zhou, C. Dhital, S. Kuppan, A. Kercher, G. Chen, A. Huq, F. Delnick, and J. Nanda. “Synthesis, Structure, and Electrochemical Performance of High-Capacity  $\text{Li}_2\text{Cu}_{0.5}\text{Ni}_{0.5}\text{O}_2$  Cathodes.” *Chemistry of Materials* 27, no. 19 (2015): 6746.



## Task 5.2 – Interfacial Processes – Diagnostics (Robert Kostecki, Lawrence Berkeley National Laboratory)

**Project Objective.** The main task objective is to obtain detailed insight into the dynamic behavior of molecules, atoms, and electrons at electrode/electrolyte interfaces of high-voltage  $\text{Li}[\text{Ni}_x\text{Mn}_y\text{Co}_z]\text{O}_2$  materials at a spatial resolution that corresponds to the size of basic chemical or structural and chemical building blocks. This project focuses on high Ni content NMC compositions such as 523 and 622, which are expected to achieve high discharge capacities even within conservative electrode potential limits. The aim of these studies is to unveil the structure and reactivity at hidden or buried interfaces and interphases that determine material, composite electrode and battery cell performance and failure modes. To accomplish these goals novel far- and near-field optical multifunctional probes must be developed and deployed *in situ*. This work constitutes an integral part of the concerted effort within the BMR Program, and it attempts to establish clear connections between diagnostics, theory/modelling, materials synthesis, and cell development efforts.

**Project Impact.** This project provides better understanding of the underlying principles that govern the function and operation of battery materials, interfaces, and interphases, which is inextricably linked with successful implementation of high-energy density materials such as  $\text{Li}[\text{Ni}_x\text{Mn}_y\text{Co}_z]\text{O}_2$  compounds (NMCs) that can cycle stably to high potentials and deliver  $> 200 \text{ mAh/g}$  at CE close to 100%. This task also involves development and application of novel innovative experimental methodologies to study and understand the basic function and mechanism of operation of materials, composite electrodes, and high-energy Li-ion battery systems for PHEV and EV applications.

**Approach.** The *in situ/ex situ* investigations of surface reconstruction into rock salt on NMC samples of different morphology and composition will be linked with investigations of interfacial reactivity toward organic electrolytes. Pristine and cycled NMC powders and electrodes will be probed using surface- and bulk-sensitive techniques, including Fourier transform infrared (FTIR), attenuated total reflectance (ATR)-FTIR, near-field IR, and Raman spectroscopy and microscopy and scanning probe microscopy to identify and characterize changes in structure and composition. The effect of electrolyte composition, additives, and protective coatings will be explored to determine the mechanism and kinetics of surface phenomena and implications for long-term electrochemical performance of NMC cathodes in high-energy Li-ion systems.

**Out-Year Goals.** The requirements for long-term stability of Li-ion batteries are extremely stringent and necessitate control of the chemistry at a wide variety of temporal and structural length scales. Progress toward identifying the most efficient mechanisms for electrical energy storage and the ideal material depends on a fundamental understanding of how battery materials function and what structural/electronic properties limit their performance. This project provides better understanding of the underlying principles that govern the function and operation of battery materials, interfaces, and interphases, which is inextricably linked with successful implementation of high energy density materials in Li-ion cells for PHEVs and EVs.

**Collaborations.** This project collaborates with Marca Doeff, Vincent Battaglia, Vassilia Zorba, Bryan D. McCloskey (LBNL), and Chunmei Ban (NREL).

### Milestones

1. Build and test binder- and carbon-free model NMC electrodes. (12/31/15 – Complete)
2. Complete preliminary characterization of interfacial activity of the baseline NMC material in organic carbonate electrolytes. (3/31/16 – On schedule)
3. Determine relationship between surface reconstruction and surface layer formation during cycling in NMC electrodes. (6/30/16 – On schedule)
4. *Go/No-Go*: Demonstrate feasibility of *in situ* near-field FTIR microscopy and spectroscopy to study interfacial phenomena at Li-battery electrodes. *Criteria*: Stop development of near-field and LIBS techniques, if the experiments fail to deliver adequate sensitivity. (9/30/16 – On schedule).

## Progress Report

This quarter, the project evaluated interfacial phenomena at NMC using fluorescence spectroscopy. Previous work demonstrated that surface reactivity of LMNO Li-ion positive electrode materials toward the electrolyte strongly depends on the surface crystalline orientation and local defects. This results in electrochemical oxidation of di-ethyl carbonate (DEC) and ethylene carbonate (EC) at the electrode at potentials  $> 4.2$  V, leading to the formation of fluorescent  $\text{Ni}^{\text{II}}$  and  $\text{Mn}^{\text{II/III}}$  complexes with  $\beta$ -diketonate ligands, which have detrimental impact on the on  $\text{Li}^+$  transport.

This project demonstrated the universality of this mechanism by using the same systematic approach on high energy density materials such as NMCs. *Ex situ* fluorescence signal of aged binder- and carbon-free baseline NMC (111) electrodes cycled in coin cells confirmed the deposition of metal complexes with  $\beta$ -keto esters ligands at the NMC surface (Figure 29a). The presence of Co(II), Mn(II), and Ni(II) complexes within the SEI of a NMC (111)/graphite cell was also confirmed by XANES experiments (Figure 29a-c).

The binder- and carbon-free baseline NMC (111) electrodes were prepared using a standard procedure. However, it was observed that contrary to  $\text{LiNi}_{0.5}\text{Mn}_{1.5}\text{O}_4$  electrodes, NMC model electrodes exhibit a very low CE, in particular in the *in situ* spectro-electrochemical cell (Figure 30). A plausible explanation for this difference is the loss of NMC active material, most likely involving a delamination of the layered NMC powder due to the lack of pressure and binder. Variation of powder composition, synthesis procedure, morphology, active mass, or pressure did not resolve this issue. To unveil the relationship between NMC surface structure, interfacial properties, and battery failure modes, there must be rigorous control of the surface property and a perfect reproducibility. From these attempts, the project concluded that thin films rather than powder pressed into aluminum are necessary for this investigation. This completes efforts toward Milestone 1.

Further investigations regarding NMC thin film preparation and interaction between NMC and organic electrolyte are underway (Milestone 2).

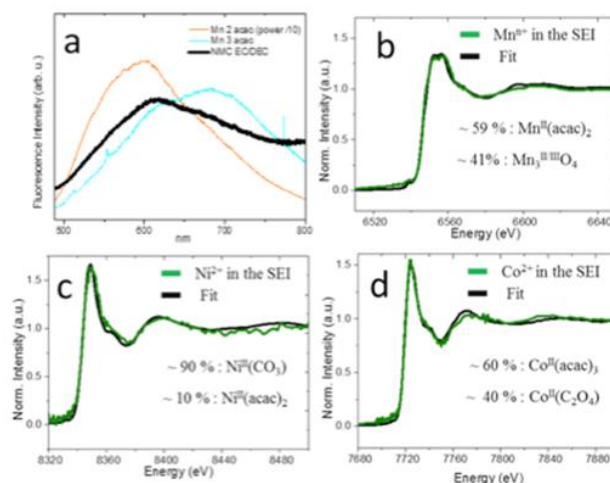


Figure 29. Electrodes were cycled in EC:DEC 1:2, 1M  $\text{LiPF}_6$  electrolyte up to 4.2 V. Fluorescence response of aged and binder-free NMC cycled 2 times (a). Metal species within the SEI of a NMC/graphite cell cycled 850 times (b-d).

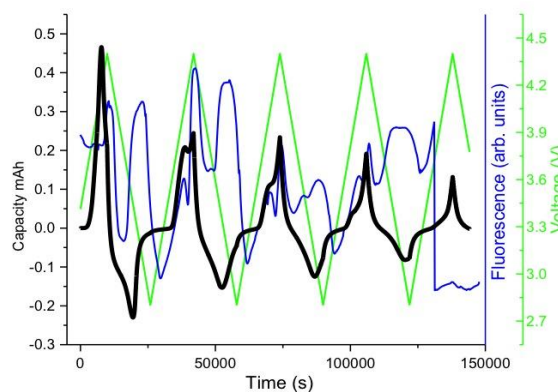


Figure 30. Fluorescence response obtained during the investigation of carbon- and binder-free NMC electrodes in the EC:DEC 1:2, 1M  $\text{LiPF}_6$  electrolyte.

## Patents/Publications/Presentations

### Presentations

- 8th International Workshop for Infrared Microscopy and Spectroscopy using Accelerator Based Sources – WIRMS, Riverhead, New York (11 – 15 October 2015): “Characterization of the Solid Electrolyte Interphase on Silicon by Synchrotron Infrared Nanospectroscopy”; M. Ayache, A. Jarry, H. A. Bechtel, M. C. Martin, and R. Kostecki.
- 228th ECS Meeting, Phoenix (11 – 15 October 2015): “Origins of the DC-Resistance Increase in HCMR<sup>TM</sup> Cathodes”; V. Battaglia, G. Chen, W. Chen, G. Liu, D. Membreno, K. Persson, A. Shukla, L. Terborg, T. Yi, and R. Kostecki.
- 66th Annual Meeting of the International Society of Electrochemistry, Taipei, Taiwan (4 – 9 October 2015): “Near-Field Optical Spectroscopy and Imaging of the SEI Layer on Sn, Si, and Graphite Li-Ion Anodes”; Robert Kostecki, Maurice Ayache, Simon Lux, and Ivan Lucas.

## Task 5.3 – Advanced *in situ* Diagnostic Techniques for Battery Materials (Xiao-Qing Yang and Xiqian Yu, Brookhaven National Laboratory)

**Project Objective.** The primary project objective is to develop new advanced *in situ* material characterization techniques and to apply these techniques to support development of new cathode and anode materials for the next generation of lithium-ion batteries (LIBs) for PHEVs. To meet the challenges of powering the PHEV, LIBs with high energy and power density, low cost, good abuse tolerance, and long calendar and cycle life must be developed.

**Project Impact.** The VTO Multi Year Program Plan describes the goals for battery: “Specifically, lower-cost, abuse-tolerant batteries with higher energy density, higher power, better low-temperature operation, and longer lifetimes are needed for the development of the next-generation of HEVs, PHEVs, and EVs.” The knowledge gained from diagnostic studies through this project will help U.S. industries develop new materials and processes for new generation LIBs in the effort to reach these VTO goals.

**Approach.** This project will use the combined synchrotron based *in situ* X-ray techniques (XRD, and hard and soft X-ray absorption) with other imaging and spectroscopic tools such as HRTEM and mass spectroscopy (MS) to study the mechanisms governing the performance of electrode materials and provide guidance for new material and new technology development regarding Li-ion battery systems.

**Out-Year Goals.** Complete the first stage development of diagnostic technique to study kinetic property of advanced Li-ion electrode materials using time resolved XRD (TR-XRD) and X-ray absorption (TR-XAS) combined with STEM imaging and transmission X-ray microscopy (TXM). Apply this technique to study the structural changes of new cathode materials including various NCM and high-voltage spinel materials during high rate cycling.

**Collaborations.** The BNL team will work closely with material synthesis groups at ANL (Drs. Thackeray and Amine) for the high-energy composite; and at PNNL for the Si-based anode materials. Such interaction between the diagnostic team at BNL and synthesis groups of these other BMR members will catalyze innovative design and synthesis of advanced cathode and anode materials. The project will also collaborate with industrial partners at General Motors and Johnson Controls, as well as with international collaborators.

### Milestones

1. Complete the thermal stability studies of Fe substituted high-voltage spinel cathode materials  $\text{LiNi}_{1/3}\text{Mn}_{4/3}\text{Fe}_{1/3}\text{O}_4$  in comparison with un-substituted  $\text{LiNi}_{0.5}\text{Mn}_{1.5}\text{O}_4$  using *in situ* TR-XRD and MS techniques. (12/31/15 – Complete)
2. Complete the energy resolved TXM investigation on new concentration gradient NCM cathode sample particles in a noninvasive manner with 3D reconstructed by images through tomography scans to study the 3D Ni, Co, and Mn elemental distribution from surface to the bulk. (3/31/16 – In progress)
3. Complete the *in situ* TR-XRD studies of the structural changes of  $\text{Li}_{1-x}\text{Ni}_{1/3}\text{Co}_{1/3}\text{Mn}_{1/3}\text{O}_2$  from  $x=0$  to  $x=0.7$  during high rate charge process at different C rates at 10C, 30C, and 60C. (6/30/16 – In progress)
4. Complete the *in situ* TR- XAS of  $\text{Li}_{1-x}\text{Ni}_{1/3}\text{Co}_{1/3}\text{Mn}_{1/3}\text{O}_2$  cathode material at Ni, Co and Mn K-edge during 30C high rate charge. (9/30/16 – In progress)

## Progress Report

The first milestones for FY16 were completed this quarter. BNL has been focused on the studies of thermal stability studies of Fe-substituted high-voltage spinel cathode materials  $\text{LiNi}_{1/3}\text{Mn}_{4/3}\text{Fe}_{1/3}\text{O}_4$  in comparison with unsubstituted  $\text{LiNi}_{0.5}\text{Mn}_{1.5}\text{O}_4$  using *in situ* TR-XRD and MS techniques.

To study the effect of Fe substitution on the structural evolution and oxygen release during heating the charged cathode, *in situ* XRD-MS experiments were carried out for the  $\text{LiNi}_{0.5-x}\text{Mn}_{1.5-x}\text{Fe}_{2x}\text{O}_4$  ( $2x = 0, 0.2, 0.33$ ) samples. It can be seen from Figure 31 that Fe substitution clearly improves thermal stability of charged cathode by suppressing the oxygen release and maintaining the structure. Charged  $\text{LiNi}_{0.5}\text{Mn}_{1.5}\text{O}_4$  releases oxygen at around 250°C, and this threshold is pushed to around 380°C for the  $2x=0.2$  sample. Further improvement is achieved in the  $2x=0.33$  sample, which showed no oxygen release up to 500°C. Correlating with suppressed oxygen release is the integrity of the structure, as seen in the right panel of Figure 31.

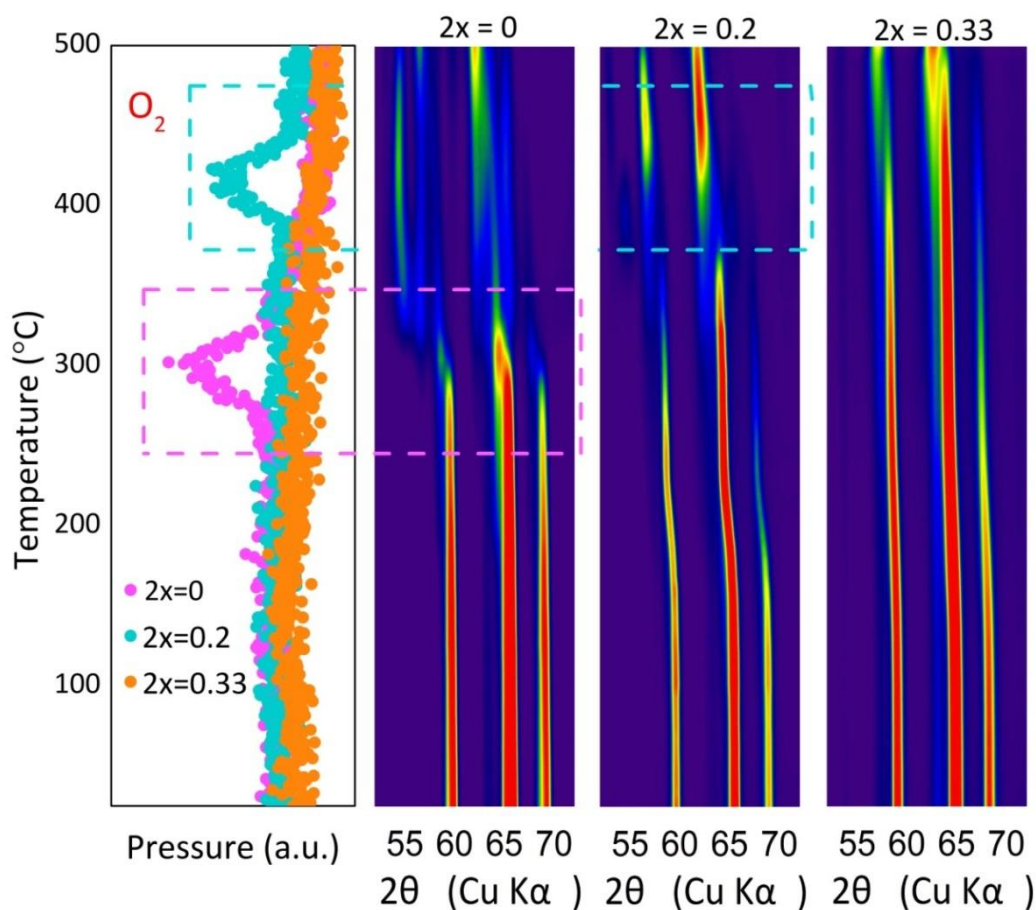


Figure 31. Effect of Fe substitution on the structural evolution and oxygen release during heating the charged samples of  $\text{LiNi}_{0.5-x}\text{Mn}_{1.5-x}\text{Fe}_{2x}\text{O}_4$  ( $2x=0, 0.2, 0.33$ ). The left panel is the *in situ* mass spectroscopy data for oxygen, and the right three panels are the *in situ* X-ray diffraction data for  $\text{LiNi}_{0.5-x}\text{Mn}_{1.5-x}\text{Fe}_{2x}\text{O}_4$  ( $2x=0, 0.2, 0.33$ ).



## Patents/Publications/Presentations

### Publications

- von Wald Cresce\*, Arthur, and Mallory Gobet, Oleg Borodin, Jing Peng, Selena M. Russell, Emily Wikner, Adele Fu, Libo Hu, Hung-Sui Lee, Zhengcheng Zhang, Xiao-Qing Yang, Steven Greenbaum, Khalil Amine, and Kang Xu. “Anion Solvation in Carbonate-Based Electrolytes.” *J. Phys. Chem. C* 119, no. 49 (November 2015): 27255–27264. doi: 10.1021/acs.jpcc.5b08895.
- Yu, X., and E. Hu, S. Bak, Y. Zhou, and X.-Q. Yang. “Structural Changes of Lithium Transition Metal Oxide Cathode Materials and their Effects on Thermal and Cycling Stability.” *Chin. Phys. B* 25, no. 1 (December 2015): 018205. doi: 10.1088/1674-1056/25/1/018205.
- Hu, Enyuan, and Seong-Min Bak, Yijin Liu, Jue Liu, Xiqian Yu, Yongning Zhou, Jigang Zhou, Peter Khalifah, Kingo Ariyoshi, Kung-Wan Nam, and Xiao-Qing Yang. “Utilizing Environmental Friendly Iron as a Substitution Element in Spinel Structured Cathode Materials for Safer High-Energy Lithium-Ion Batteries.” *Adv. Energy Mater.* (December 2015). doi: 10.1002/aenm.201501662.

## Task 5.4 – NMR and Pulse Field Gradient Studies of SEI and Electrode Structure (Clare Grey, Cambridge University)

**Project Objective.** The formation of a stable SEI is critical to the long-term performance of a battery, since the continued growth of the SEI on cycling/aging results in capacity fade (due to Li consumption) and reduced rate performance due to increased interfacial resistance. Although arguably a (largely) solved problem with graphitic anodes/lower voltage cathodes, this is not the case for newer, much higher capacity anodes such as silicon, which suffer from large volume expansions on lithiation, and for cathodes operating above 4.3 V. Thus it is essential to identify how to design a stable SEI. The objectives are to identify major SEI components, and their spatial proximity, and how they change with cycling. SEI formation on Si versus graphite and high-voltage cathodes will be contrasted. Li<sup>+</sup> diffusivity in particles and composite electrodes will be correlated with rate. The SEI study will be complemented by investigations of local structural changes of high-voltage/high-capacity electrodes on cycling.

**Project Impact.** The first impact of this project will be an improved, molecular based understanding of the surface passivation (SEI) layers that form on electrode materials, which are critical to the operation of the battery. Second, the project will provide direct evidence for how additives to the electrolyte modify the SEI. Third, it will provide insight to guide and optimize the design of more stable SEIs on electrodes beyond LiCoO<sub>2</sub>/graphite.

**Out-Year Goals.** The project goals are to identify the major components of the SEI as a function of state of charge and cycle number different forms of silicon. The project will determine how the surface oxide coating affects the SEI structure and will establish how the SEI on Si differs from that on graphite and high-voltage cathodes. The project will determine how the additives that have been shown to improve SEI stability affect the SEI structure and will explore the effect of different additives that react directly with exposed fresh silicon surfaces on SEI structure. Via this program, the project will develop new NMR-based methods for identifying different components in the SEI and their spatial proximities within the SEI, which will be broadly applicable to the study of SEI formation on a much wider range of electrodes. These studies will be complemented by studies of electrode bulk and surface structure to develop a fuller model with which to describe how these electrodes function.

**Collaborations.** This project collaborates with B. Lucht (Rhode Island); E. McCord and W. Holstein (DuPont); J. Cabana, (University of Illinois at Chicago); G. Chen and K. Persson (LBNL); S. Whittingham (SUNY Binghamton); P. Bruce (St. Andrews); R. Seshadri and A. Van der Ven (UCSB); S. Hoffman and A. Morris (University of Cambridge); N. Brandon (Imperial); and P. Shearing (University College London).

### Milestones

1. Identify the major carbon-containing break down products that form on graphene platelets. (12/31/15 – Ongoing. Decision made to complete Si studies from Q3 milestone first since student is graduating.)
2. *Go/No-Go:* Establish the difference between extrinsic and P-doped silicon nanowires. *Criteria:* If no difference in performance of P-doped wires established after the first cycle, terminate project. (3/31/16 – Ongoing)
3. Complete SEI study of silicon nanoparticles by NMR spectroscopy. Develop NMR methodology to examine cathode SEI. (6/30/16 – Complete; papers in preparation)
4. Produce first optimized coating for Si electrode. (9/30/16 – Ongoing)

## Progress Report

The project has completed a detailed investigation of the SEI passivating layer that grows on silicon nanoparticles, employing multinuclear  $^1\text{H}$ ,  $^7\text{Li}$ ,  $^{19}\text{F}$ , and  $^{13}\text{C}$  NMR solid state NMR spectroscopy (ssNMR). A binder-free Si electrode (with 50 nm particles) was used in the first study to remove the variable of common binders such as carboxymethylcellulose (CMC) often used in electrode formulation, which may also inhibit SEI growth, and to simplify the NMR analysis. Both the conductive carbon and mixed Si/C composite electrodes were studied separately. SEI growth was observed by  $^1\text{H}$  ssNMR as a function of voltage, with electrochemical experiments demonstrating SEI forming on both C and Si surfaces. One consequence of the long lithiation process on Si at approximately 150 mV versus Li is that substantial SEI is formed below this voltage. Using selective  $^{13}\text{C}$  labeling, the decomposition products of electrolyte solvents ethylene carbonate (EC) and dimethyl carbonate (DMC) were detected independently (Figure 32).  $^1\text{H} - ^{13}\text{C}$  and  $^7\text{Li} - ^{13}\text{C}$  cross-polarization (CP) experiments were performed to identify species close to protons and lithium ions, respectively. To aid assignments of the  $^{13}\text{C}$  spectra, chemical shifts of predicted SEI decomposition products were determined. The density functional theory (DFT) calculations of relevant small molecules provided useful trends regarding the chemical shifts, guiding the low sensitivity experiments and assignments.

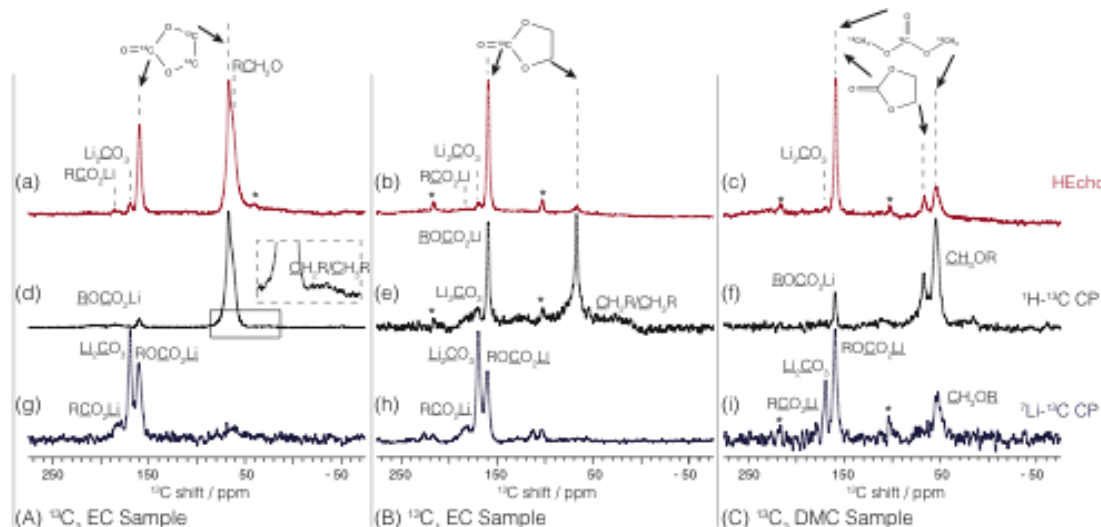


Figure 32. Coin cells cycled using (a)  $^{13}\text{C}_3$  EC, (b)  $^{13}\text{C}_1$  EC, and (c)  $^{13}\text{C}_2$  dimethyl carbonate (DMC) labeled electrolytes.  $^{13}\text{C}$  spectra were acquired with (i) a Hahn echo (HEcho), (ii)  $^1\text{H} - ^{13}\text{C}$  CP, and (iii)  $^7\text{Li} - ^{13}\text{C}$  CP.

EC decomposition products are present in higher concentrations and are dominated by polyethylene oxide (PEO)-type oligomer species. ssNMR applied to both rinsed and unrinsed electrodes showed that the organics are easily rinsed away, suggesting they are located on the outer layer of the SEI. A  $\text{CH}_3\text{R}$  or  $\text{R}'\text{CH}_2\text{R}$  environment was formed below 40 mV; while many oligomeric species cannot be ruled out, the experimental results are consistent with an assignment of these carbon functionalities to those present in the theoretically predicted SEI decomposition products lithium butylene dicarbonate (LBDC) and lithium ethyl carbonate (LEC).  $\text{RCO}_2\text{Li}$  species in low relative abundance were also detected, the majority being assigned to  $\text{HCO}_2\text{Li}$ .  $\text{ROCO}_2\text{Li}$  EC decomposition products were confirmed by correlation (two dimensional NMR) experiments, showing a chemical signature consistent with lithium ethylene dicarbonate (LEDC). Lithium methyl carbonate (LMC) was the dominant DMC decomposition product. The binder-free system resulted in a very dry electrode system and now  $\text{LiOH}$  was detected. Furthermore,  $\text{LiF}$  and  $\text{LiPF}_6$  were the only F-containing species. The results of this comprehensive NMR study have been used to analyze the NMR spectra of electrodes acquired after multiple cycles.

**Patents/Publications/Presentations**

## Publications

- Clement, R. J., and P. G. Bruce and C. P. Grey. “Review-Manganese-Based P2-Type Transition Metal Oxides as Sodium-Ion Battery Cathode Materials.” *J. Electrochem. Soc.* 162 (2015): A2589–A2604.
- Liu, T., and M. Leskes, W. J. Yu, A. J. Moore, L. N. Zhou, P. M. Bayley, G. Kim, and C. P. Grey. “Cycling Li-O<sub>2</sub> Batteries via LiOH Formation and Decomposition.” *Science* 350 (2015): 530–533.
- Chang, H. J., and A. J. Ilott, N. M Trease, M. Mohammadi, A. Jerschow, and C. P. Grey. “Correlating Microstructural Lithium Metal Growth with Electrolyte Salt Depletion in Lithium Batteries Using Li-7 MRI.” *J. Am. Chem. Soc.* 137 (2015): 15209–15216.
- Michan, A. L., and M. Leskes, and C. P. Grey. “Voltage Dependent Solid Electrolyte Interphase Formation in Silicon Electrodes: Monitoring the Formation of Organic Decomposition Products.” *Chem. Mater.* 28 (2016): 85–398.

## Task 5.5 – Optimization of Ion Transport in High-Energy Composite Cathodes (Shirley Meng, UC – San Diego)

**Project Objective.** This project aims to probe and control the atomic-level kinetic processes that govern the performance limitations (rate capability and voltage stability) in a class of high-energy composite electrodes. A systematic study with powerful suite of analytical tools [including atomic resolution scanning transmission electron microscopy (a-STEM) and EELS, neutron, XPS and first principles (FP) computation] will elucidate approaches to optimize ion transport. Ultimately, this will hone in on the optimum bulk compositions and surface characteristics to improve the mechanistic rate and cycling performance of high-energy composite electrodes. Moreover, it aims to develop the large-scale synthesis efforts in order to produce materials with consistent performance. The surface-sensitive characterization tools will be extended to diagnose various silicon anode types.

**Project Impact.** If successful, this research will provide a major breakthrough in commercial applications of the class of high energy density cathode material for lithium ion batteries. Additionally, it will provide in-depth understanding of the role of surface modifications and bulk substitution in the high-voltage composite materials. The diagnostic tools developed here can also be leveraged to study a wide variety of cathode and anode materials for rechargeable batteries.

**Approach.** This unique approach combines STEM/EELS, XPS, and *ab initio* computation as diagnostic tools for surface and interface characterization. This allows for rapid identification of surface interphases that provide surface instability or stability in various types of electrode materials including both high-voltage cathodes and low-voltage anodes. Neutron enables the characterization of bulk material properties to enhance and further optimize high-energy electrode materials.

**Out-Year Goals.** The goal is to control and optimize Li-ion transport, TM migration, and oxygen activity in the high-energy composite cathodes and to optimize electrode/electrolyte interface in silicon anodes so that their power performance and cycle life can be significantly improved.

**Collaborations.** This work funds collaborations on silicon thin film fabrication (Nancy Dudney, ORNL); molecular layer deposition (MLD) (Chunmei Ban, NREL); neutron diffraction (Ken An, ORNL); and XPS, TOF-SIMS characterization (Keith Stevenson, UT Austin). It supports collaborative work with Zhaoping Liu and Yonggao Xia at Ningbo Institute of Materials Technology and Engineering China.

### Milestones

1. Identify the mechanisms of ALD- and MLD- coated silicon anode for their improved chemical stability upon long cycling. (12/30/15 – Complete)
2. Obtain the optimum surface coating and substitution compositions in Li-rich layered oxides when charged up to 4.8 V (or 5.0 V). (12/30/15 – Complete)
3. Investigate the mechanism of improved performance in high-voltage, Li-rich, Mn-rich, layered oxides with LLTO (Li–La–Ti–O) coating. (03/31/16 – Ongoing)
4. Quantify the SEI characteristics of ALD and MLD coated silicon anode upon long cycling with a combination of STEM/EELS and XPS. (03/31/16 – On track)

## Progress Report

**Lattice Dynamics and Lattice Oxygen Evolution in Li-Rich Layered Oxide During Battery Charge and Discharge via *Operando* Neutron Diffraction.** Neutron diffraction was used to investigate the lattice dynamics and oxygen evolution of two distinct materials:  $\text{Li}[\text{Li}_{x/3}\text{Ni}_{(3/8-3x/8)}\text{Co}_{(1/4-x/4)}\text{Mn}_{(3/8+7x/24)}\text{O}_2$  ( $x=0.6$ , high lithium rich or HLR) and  $\text{Li}[\text{Li}_{x/3}\text{Ni}_{(1/3-x/3)}\text{Co}_{(1/3-x/3)}\text{Mn}_{(1/3+x/3)}\text{O}_2$  ( $x=0.24$ , low lithium rich or LLR), respectively. These Li-rich materials contain various degrees of oxygen activation at high voltage. The lattice parameter changes and oxygen position were measured by *operando* battery cycling, where the LLR exhibits larger oxygen movement and higher lattice contractions compared to the HLR. Figure 33a demonstrates that both HLR and LLR maintain relatively constant oxygen position during the high voltage plateau, until the end of charge. Furthermore, the DFT calculations show that in the presence of oxygen vacancy during the high voltage plateau, the changes in the lattice parameters and oxygen positions are consistent with the experimental observations.

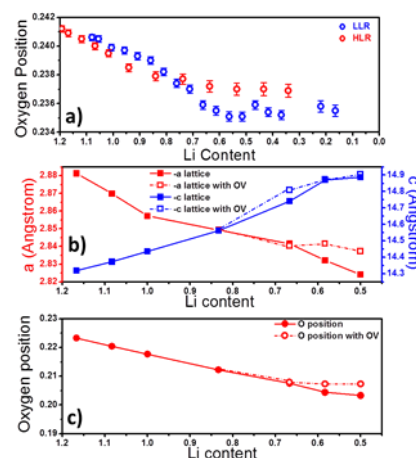


Figure 33. (a) Oxygen position from the refinement results. (b) Density functional theory results from the evolution of the lattice parameters. (c) Oxygen position in materials with and without oxygen vacancies.

**Enhancing the Electrochemical Performance of Li-Rich Layered Oxide via a Facile Nanoscale Surface Modification.** Herein, a facile surface modification using nanoscale equilibrium  $\text{Li}_3\text{PO}_4$ -based amorphous film (SAF) was applied to a Li-rich layered oxide cathode ( $\text{Li}_{1.13}\text{Ni}_{0.3}\text{Mn}_{0.57}\text{O}_2$ , LNMO). The project has compared the first-cycle voltage profiles of the uncoated LNMO and  $\text{Li}_3\text{PO}_4$  surface modified LMNO (LP600) at  $55^\circ\text{C}$ , cycled from 2–4.8 V, and using a  $250 \text{ mA g}^{-1}$  current. At  $55^\circ\text{C}$ , the LP600 material consistently gives a shorter slope and plateau, which leads to a lower charge capacity ( $332 \text{ mAh g}^{-1}$ ) than its counterpart ( $390 \text{ mAh g}^{-1}$ ). However, the discharge capacity significantly improved to more than  $270 \text{ mAh g}^{-1}$ , while the uncoated sample only gives  $240 \text{ mAh g}^{-1}$ . Finally, the SAF drastically demonstrated an increase in the initial CE from 63.1% to 81.6%. Overall, the SAF enhanced the long-term cycling performance.

### Alucone-coated Si nanoparticles

#### Using MLD. Si (50 nm) particles

were coated with 1-nm alucone using the MLD process. The coated Si nanoparticles were used to make a slurry using carboxymethyl cellulose (250,000 MW), super P carbon, and cycled using traditional electrolyte (1M  $\text{LiPF}_6$  in EC:DEC). Figure 34a displays the first-cycle voltage profile of the uncoated Si and MLD-coated Si, where the MLD-coated materials have a higher capacity.

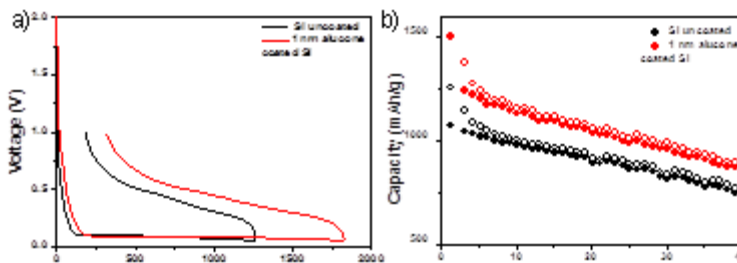


Figure 34. Electrochemistry performance comparison of 1 nm molecular layer deposition (MLD) coated Si: (a) first cycle voltage profile; and (b) capacity comparison using a voltage range of 1-0.05V at C/20.

After 40 cycles, the MLD-coated Si has a slightly better capacity retention (Figure 34b). However, the effect of the alucone coating is not as significant as demonstrated in the literature; therefore, further optimization is required. In addition, the first-cycle CE of the coated electrode was reduced from 85% to 82%. Given that the binder and conductive additive contribute to the irreversible side reactions, the MLD alucone coating will be applied to coat stable 50-nm amorphous Si thin films. This will enable a proper characterization platform to understand the effect of alucone coating on Si.



## Patents/Publications/Presentations

### Patent

- Zhang, M., and H. D. Liu and Y. S. Meng. *Lithium Excess Cathode Material and Co-Precipitation Formation Method*. Provisional U.S. Patent.

### Presentations

- Liu, H. D., and Y. Chen, S. Hy, K. An, S. Venkatachalam, D. Qian, M. Zhang, Y. S. Meng. “Operando Lithium Dynamics in the Li-Rich Layered Oxide Cathode Material via Neutron Diffraction.” *Advanced Energy Materials*, accepted.
- Qiu, B., and M. Zhang, L. Wu, J. Wang, Y. Xia, D. Qian, H. D. Liu, S. Hy, Y. Zhu, Y. S. Meng, Z. Liu. “Gas-Solid Interfacial Modification of Oxygen Activities in Li-Rich Layered Oxide Cathodes for Next-Generation Lithium-Ion Battery.” *Nature Communication*, under review.
- Liu, H. D., and J. Huang, D. Qian, S. Hy, C. Fang, J. Luo, and Y. S. Meng. “Enhancing the Electrochemical Performance of Lithium-Excess Layered Oxide  $\text{Li}_{1.13}\text{Ni}_{0.3}\text{Mn}_{0.57}\text{O}_2$  via a Facile Nanoscale Surface Modification.” Submitted.

## Task 5.6 – Analysis of Film Formation Chemistry on Silicon Anodes by Advanced *In situ* and *Operando* Vibrational Spectroscopy

(Gabor Somorjai, UC – Berkeley; Phil Ross, Lawrence Berkeley National Laboratory)

**Project Objective.** Understand the composition, structure, and formation/degradation mechanisms of the SEI on the surfaces of Si anodes during charge/discharge cycles by applying advanced *in situ* vibrational spectroscopies. Determine how the properties of the SEI contribute to failure of Si anodes in Li-ion batteries in vehicular applications. Use this understanding to develop electrolyte additives and/or surface modification methods to improve Si anode capacity loss and cycling behavior.

**Project Impact.** A high-capacity alternative to graphitic carbon anodes is Si, which stores 3.75 Li per Si versus 1 Li per 6 C yielding a theoretical capacity of 4008 mAh/g versus 372 mAh/g for C. But Si anodes suffer from large first-cycle irreversible capacity loss and continued parasitic capacity loss upon cycling leading to battery failure. Electrolyte additives and/or surface modification developed from new understanding of failure modes will be applied to reduce irreversible capacity loss, and to improve long-term stability and cyclability of Si anodes for vehicular applications.

**Approach.** Model Si anode materials including single crystals, e-beam deposited polycrystalline films, and nanostructures are studied using baseline electrolyte and promising electrolyte variations. A combination of *in situ* and *operando* Fourier Transform Infrared (FTIR), Sum Frequency Generation (SFG), and UV-Raman vibrational spectroscopies are used to directly monitor the composition and structure of electrolyte reduction compounds formed on the Si anodes. Pre-natal and post-mortem chemical composition is identified using XPS. The Si films and nanostructures are imaged using SEM.

**Out-Year Goals.** Extend study of interfacial processes with advanced vibrational spectroscopies to high-voltage oxide cathode materials. The particular oxide to study will be chosen based on materials of interest and availability of the material in a form suitable for these studies (for example, sufficiently large crystals or sufficiently smooth/reflective thin films). The effect of electrolyte composition, electrolyte additives, and surface coatings will be determined, and new strategies for improving cycle life developed.

**Collaborations.** None this quarter.

### Milestones

1. Modifying the SFG apparatus to obtain high-resolution SFG spectra further allowing particles, thin film, and microstructures of Si and the electrolyte interface research. (12/31/15 – Initiated)
2. Performing ps-SFG measurement under constant and dynamic potentials (-0.01 V, 0.5 V, and 1.0 V versus Li/Li<sup>+</sup>) of 1 M LiPF<sub>6</sub> in EC without DEC to probe the SEI formed on amorphous silicon anodes. (3/31/16 – Initiated)
3. *Go/No-Go*: Can this task distinguish between the various SEI products in the C-H stretch mode (2800 – 3200 cm<sup>-1</sup>)? If not, proceed to conventional C-O region (1700 – 1800 cm<sup>-1</sup>). (6/30/16)
4. Performing fs-SFG measurement in tandem with cyclic voltammetry (CV) (potential sweep) to find the ring opening kinetics of EC. Preforming fs-SFG measurement in tandem with cyclic voltammetry (potential sweep) to find the ring opening kinetics of EC. (9/30/16)

## Progress Report

In 2016, to emphasize that the specific chemical composition of the SEI is governed by the surface properties of the anode, this project has started working on a new anode model system of amorphous silicon (a-Si). The CV shown in Figure 35 is of a 200-nm thick a-Si that has native oxide termination. It is evident that in the first CV cycle (CV#11, black curve), there are three reduction peaks. These reduction peaks are consistent with values reported in the literature for the reduction of DEC, EC (consequently SEI formation) and the onset for lithiation, respectively. The delithiation peaks are smeared with an additional broad oxidation peak around 1 V. Figure 36, a-Si electrode, shows the resulting spectrum of dividing the SFG spectrum after CV by the SFG spectrum obtained at open current potential (OCP). Dividing the SFG spectra emphasizes the appearance or trend of vibrational peaks that are less clear in a regular SFG scan, since in most cases the SFG from the Si/SEI is interfered with the SFG generated from the Si substrate. It is assumed that in the course of the electrolyte reduction, an intermediate species, for example, ethoxy radical  $\cdot\text{OCH}_2\text{CH}_3$  (or anion,  $^-\text{OCH}_2\text{CH}_3$ ), exists. It is also assumed that the ethoxy radical is formed near the Si anode surface and that it reacts with Si-hydrogen terminated anode to produce a Si-OCH<sub>2</sub>CH<sub>3</sub> bond. This reaction cannot take place if a thick passivating oxide layer is present, although it can take place in silicon electrodes with thin native oxides, as shown in Figure 36. The researchers assigned the SFG peaks corresponding to Si-ethoxy bonds and various SEI components found in SiO<sub>x</sub> (oxide termination) anodes. The absence of other expected Si-ethoxy peaks (for example, 3040 cm<sup>-1</sup>) had led to the conclusion that the amorphous silicon anode has different domains. Whether they are intrinsic or form due to the expansion and contraction of the Si lattice associated with lithiation and de-lithiation, respectively, is still unclear. Further controlled experiments are needed.

In conclusion, the project observed that amorphous Si with a native oxide surface termination has a mixed SFG spectrum that has both SiO<sub>x</sub> and Si-hydrogen features. However, the Si-ethoxy (Si-OCH<sub>2</sub>CH<sub>3</sub>) features are not clear, as in the case of crystalline silicon (for example, Si(100)-H surfaces). Unlike crystalline Si(100) with hydrogen termination that shows these peaks at ~1.0 V. Future experiments, such as four-point probe, XPS, and conducting atomic force microscopy (AFM), will determine the origin of these peaks. Also, surface passivation combined with further SFG-VS experiments in the C=O carbonyl stretch range should determine the role of Si surface termination and crystalline order on the SEI formation structure and cycling properties.

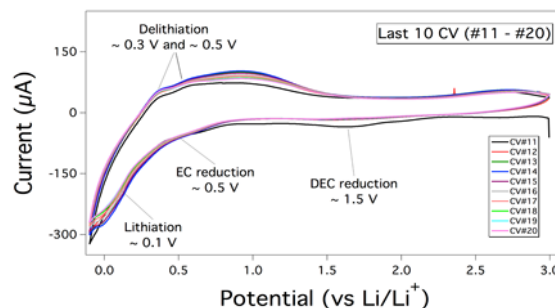


Figure 35. The reduction peaks of an electrolyte solution (1.0 M LiPF<sub>6</sub> in EC : DEC, 1:2 v/v) on amorphous silicon anode are presented in this cyclic-voltammogram. Scan range was 3.0 V to -0.1 V and the rate was 1mV/sec.

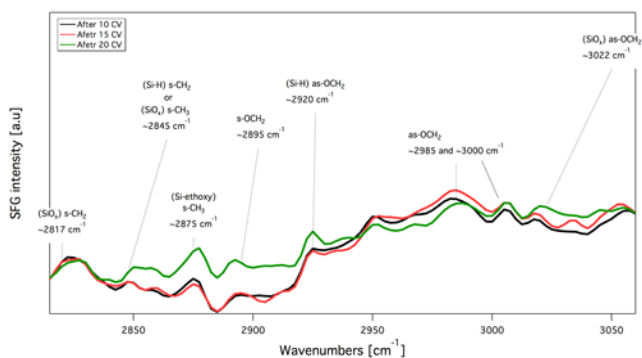


Figure 36. The evolution of sum frequency generation (SFG) signal under reaction conditions of amorphous silicon with SiO<sub>2</sub> terminated anode. The SFG spectra were taken at open circuit potential and after 10 (black), 15 (red) cyclic-voltammograms (CVs) and 20 (green) at 3.0 V ↔ -0.1 V. All CVs were repeated for 10 cycles at a scan rate of 1mV/sec.

## Task 5.7 – Microscopy Investigation on the Fading Mechanism of Electrode Materials (Chongmin Wang, Pacific Northwest National Laboratory)

**Project Objective.** The overall objective is to develop low-cost, high-energy cathode materials with long cycle life. This part is focused on microscopy investigation on the fading mechanism of the electrode materials. The focus will be on using *ex situ*, *in situ*, and *operando* HR-TEM and spectroscopy to probe the structural evolution of electrodes and interfaces between the electrode and electrolyte and correlate this structural and chemical evolution with battery performance.

**Project Impact.** Both *ex situ* and *in situ* TEM have been demonstrated to be critical for probing the structure and chemistry of electrode and SEI layer, which leads to a direct correlation of microstructure/chemistry and their evolution with battery properties. The proposed research will provide key insight for designing new electrode structure. Recently, the project developed new *operando* characterization tools to characterize SEI formation and electrode/electrolyte interaction using practical electrolyte that are critical for making new breakthroughs in the battery field. The success of this work will increase the energy density of Li-ion batteries and accelerate market acceptance of EVs, especially for PHEVs required by the EV Everywhere Grand Challenge proposed by the DOE/EERE.

**Approach.** Extend and enhance the unique *ex situ* and *in situ* TEM methods for probing the structure of Li-ion batteries, especially for developing a biasing liquid electrochemical cell that uses a real electrolyte in a nano-battery configuration. Use various microscopic techniques, including *ex situ*, *in situ*, and especially the *operando* TEM system, to study the fading mechanism of electrode materials in batteries. This project will be closely integrated with other research and development efforts on high-capacity cathode and anode projects in the BMR Program to (1) discover the origins of voltage and capacity fading in high-capacity layered cathodes and (2) provide guidance for overcoming barriers to long cycle stability of electrode materials.

**Out-Year Goals.** The out-year goals are as follows:

- Multi-scale (ranging from atomic scale to meso-scale) *ex situ/in situ* and *operando* TEM investigation of failure mechanisms for energy-storage materials and devices.
- Integration of the *in situ* TEM capability with other microscopy and spectroscopy methods to study energy-storage materials, such as *in situ* SEM, *in situ* SIMS, and *in situ* XRD.
- Atomic-level *in situ* TEM and STEM imaging to help develop a fundamental understanding of electrochemical energy-storage processes and kinetics of electrodes.
- Extension of the *in situ* TEM capability for energy storage technology beyond Li ions, such as Li-S, Li-air, Li-metal, sodium ions, and multi-valence ions.

**Collaborations.** The project is collaborating with the following principal investigators: Michael M. Thackeray (ANL); Guoying Chen (LBNL); Chunmei Ban (NREL); Khalil Amine (ANL); Donghai Wang (Pennsylvania State University); Arumugam Manthiram (UT-Austin); Gao Liu (LBNL); Yi Cui (Stanford University); Jason Zhang (PNNL); Jun Liu (PNNL); and Xingcheng Xiao (GM).

## Milestones

1. Complete multi-scale quantitative atomic level mapping to identify the behavior of Co, Ni, and Mn in NCM during battery charge/discharge. (3/31/2016 – Ongoing)
2. Complete quantitative measurement of structural/chemical evolution of modified-composition NCM cathode during cycling of battery. (6/31/2016)
3. Complete the correlation between structure stability and charge voltage of NCM for optimized charge voltage. (9/30/2016)

## Progress Report

Surface coating of cathode has been identified as an effective approach for enhancing the capacity retention of layered structure cathode. However, the underlying operating mechanism of such thin coating layer, in terms of surface chemical functionality and capacity retention, remains unclear.

Aberration corrected STEM and high efficient spectroscopy were used to probe the delicate functioning mechanism of  $\text{Al}_2\text{O}_3$  coating layer on  $\text{Li}_{1.2}\text{Ni}_{0.2}\text{Mn}_{0.6}\text{O}_2$  cathode. It is discovered that in terms of surface chemical function, the  $\text{Al}_2\text{O}_3$  coating suppresses the side reaction between cathode and the electrolyte upon the battery cycling. At the same time, the  $\text{Al}_2\text{O}_3$  coating layer also eliminates the chemical reduction of Mn from the cathode particle surface, therefore avoiding the dissolution of the reduced Mn into the electrolyte. In terms of structural stability, the  $\text{Al}_2\text{O}_3$  coating layer can mitigate the layer to spinel phase transformation, which otherwise will initiate from the particle surface and propagate towards the interior of the particle with the progression of the battery cycling (Figure 37). The atomic to nanoscale effects of the coating layer observed here provide insight for optimized design of coating layer on cathode to enhance the battery properties.

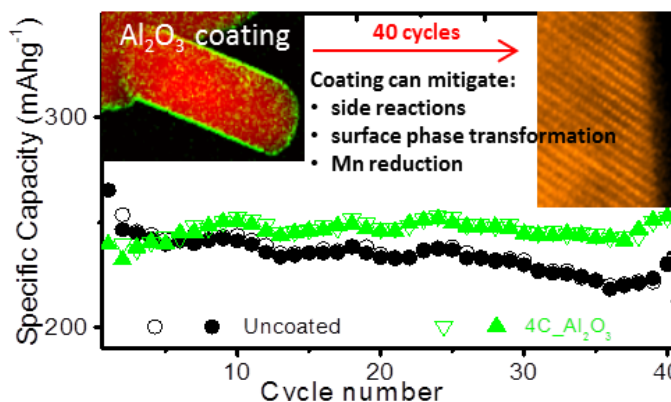


Figure 37. Correlation of scanning transmission electron microscopy imaging of structure, energy dispersive spectroscopy mapping of chemical composition, and electrochemical property measurement help to identify the effect of  $\text{Al}_2\text{O}_3$  coating effect for improved battery performance.

Battery cycling induced surface Mn reduction was also perceived as one of the most important causes of cathode material degradation. Moreover, the well known Jahn-Teller effect will occur and destabilize the structure when Mn average valence state is reduced to  $3^+$ . Therefore, the stability of LMR cathode is heavily dependent on Mn valence state. Thus, the Mn valence state and its spatial distribution on both uncoated and coated particle upon battery cycling were probed using STEM-EELS. The present studies indicate that distinctive difference can be seen on the spatial distribution of Mn valence between uncoated and  $\text{Al}_2\text{O}_3$  coated particles. For the uncoated particle, the  $\text{Mn}^{2+}$  is uniquely located at the outmost surface of particle followed by a thick  $\text{Mn}^{3+}$  layer. In contrast, for the  $\text{Al}_2\text{O}_3$  coated particle, Mn reduction only occurred in a very thin surface layer and their valence states are well above  $3^+$ . The spatial mapping of Mn valence distribution and its apparent correlation with the  $\text{Al}_2\text{O}_3$  coating layer clearly indicates the  $\text{Al}_2\text{O}_3$  coating suppresses the reduction of Mn at the cathode/electrolyte interface, therefore mitigating the dissolution of the Mn into the electrolyte.

ALD- $\text{Al}_2\text{O}_3$  coating has been demonstrated to significantly improve cycle stability of the  $\text{Li}_{1.2}\text{Ni}_{0.2}\text{Mn}_{0.6}\text{O}_2$  cathode. Systematic STEM atomic level imaging and nanoscale chemical composition analysis directly reveal that the ALD- $\text{Al}_2\text{O}_3$  coating layer plays an important role in terms of the following three aspects: mitigating side reactions between the cathode and electrolyte; eliminating the surface structure transformation; and suppressing the reduction of Mn at the particle surface. It has been shown that the advanced structural and chemical imaging techniques using TEM are able to diagnose cathode surface coating in atomic level and provide in-depth understanding of coating layer's protecting mechanism. The fundamental understanding on the structure and composition changes observed in ALD- $\text{Al}_2\text{O}_3$  coated samples clearly demonstrate the effect of this surface coating and may also guide the design of new cathode materials.

### Patents/Publications/Presentations

#### Publications

- Yan, Pengfei, and Jianming Zheng, Saravanan Kuppan, Qiuyan Li, Dongping Lu, Jie Xiao, Guoying Chen, Ji-Guang Zhang, and Chong-Min Wang. "Phosphorus Enrichment as a New Composition in the Solid Electrolyte Interphase of High-Voltage Cathodes and Its Effects on Battery Cycling." *Chem. Mater.* 27 (2015): 7447–7452.
- Xiao, Qiangfeng, and Meng Gu, Hui Yang, Bing Li, Cunman Zhang, Yang Liu, Fang Liu, Fang Dai, Li Yang, Zhongyi Liu, Xingcheng Xiao, Gao Liu, Peng Zhao, Sulin Zhang, Chongmin Wang, Yunfeng Lu, and Mei Cai. "Inward Lithium-Ion Breathing of Hierarchically Porous Silicon Anodes." *Nature Communications* 6 (2015): 8844.
- Zhu, Zihua, and Yufan Zhou, Pengfei Yan, Rama Sesha Vemuri, Wu Xu, Rui Zhao, Xuelin Wang, Suntharampillai Thevuthasan, Donald R. Baer, and Chong-Min Wang. "In Situ Mass Spectrometric Determination of Molecular Structural Evolution at the Solid Electrolyte Interphase in Lithium-Ion Batteries." *Nano Lett.* 15 (2015): 6170.



## Task 5.8 – Characterization and Computational Modeling of Structurally Integrated Electrode (Michael M. Thackeray and Jason R. Croy, Argonne National Laboratory)

**Project Objective.** The primary project objective is to explore the fundamental, atomic-scale processes that are most relevant to the challenges of next-generation, energy-storage technologies, in particular, high-capacity, structurally integrated electrode materials. A deeper understanding of these materials relies on novel and challenging experiments that are only possible through unique facilities and resources. The goal is to capitalize on a broad range of facilities to advance the field through cutting-edge science, collaborations, and multi-disciplinary efforts to characterize and model structurally integrated electrode systems, notably those with both layered and spinel character.

**Project Impact.** This project capitalizes on and exploits DOE user facilities and other accessible national and international facilities (including skilled and trained personnel) to produce knowledge to advance lithium-ion battery materials. Specifically, furthering the understanding of structure-electrochemical property relationships and degradation mechanisms will contribute significantly to meeting the near- to long- term goals of PHEV and EV battery technologies.

**Approach.** A wide array of characterization techniques including X-ray and neutron diffraction, X-ray absorption, emission and scattering, HR-TEM, Raman spectroscopy, and theory will be brought together to focus on challenging experimental problems. Combined, these resources promise an unparalleled look into the structural, electrochemical, and chemical mechanisms at play in novel, complex electrode/electrolyte systems being explored at ANL.

**Out-Year Goals.** The out-year goals are as follows:

- Gain new, fundamental insights into complex structures and degradation mechanisms of high-capacity composite cathode materials from novel, probing experiments carried out at user facilities and beyond.
- Investigate structure-property relationships that will provide insight into the design of improved cathode materials.
- Use knowledge and understanding gained from this project to develop and scale up advanced cathode materials in practical lithium-ion prototype cells.

**Collaborators.** This project engages in collaboration with Mahalingam Balasubramanian, Michael Murphy, and Yang Ren (APS); Roy Benedek (CSE, ANL); Soo Kim, Chris Wolverton, Vinayak Dravid, and Jinsong Wu (Northwestern University); Bill David (Rutherford Laboratory, UK); Debasish Mohanty (ORNL); and Chongmin Wang and Pengfei Yan (PNNL).

### Milestones

1. Characterize bulk and surface properties of structurally integrated electrode materials using DOE user facilities at Argonne (APS, Electron Microscopy Center, and Argonne Leadership Computing Facility) and facilities elsewhere, for example, Spallation Neutron Source (ORNL), Environmental Transmission Electron Microscope (PNNL), and Northwestern University Atomic and Nanoscale Characterization Experimental Center (NUANCE). (9/30/16 – In progress)
2. Use complementary theoretical approaches to further the understanding of the structural and electrochemical properties of layered-spinel electrodes and protective surface layers. (9/30/16 – In progress)

Analysis, interpretation, and dissemination of collected data for publication and presentation. (12/31/15 – 9/30/16; In progress)

## Progress Report

Structurally integrated  $y[x\text{Li}_2\text{M}'\text{O}_3 \cdot (1-x)\text{LiMO}_2] \cdot (1-y)\text{LiM}_2\text{O}_4$  ( $\text{M}' = \text{Mn, Ti, Zr} \dots \text{M} = \text{Mn, Ni, Co}$ ) layered-layered-spinel electrodes offer a unique opportunity for high-energy cathode design. These electrodes have shown promise for improving first-cycle efficiencies, rate capability, and possibly structural stability compared to their “layered-layered” counterparts. However, to achieve targeted capacities of  $> 200 \text{ mAh/g}$ , it is desirable to maximize the excess lithium content,  $x$ , in these materials while simultaneously stabilizing lithium-excess regions (for example,  $\text{Li}_2\text{M}'\text{O}_3$ -ordered structures). One such strategy is to incorporate a completely inactive  $\text{Li}_2\text{M}'\text{O}_3$  component where  $\text{M}'$  may consist of, for example,  $\text{Ti}^{4+}$ . Octahedral  $\text{Ti}^{4+}$  ( $d^0$ ) will not oxidize and is expected to be robust against oxygen loss. However, when incorporated into materials, at the nanoscale, unique behavior might be expected from lithiated compounds. For example, bulk  $\text{LiCrO}_2$  is not particularly active as a cathode material, but when synthesized as nanoparticles becomes highly active for Li de-intercalation/intercalation. Furthermore,  $\text{Cr}^{3+/6+}$  activity induces facile migration of Cr cations into tetrahedral sites of the lithium layers, disrupting the local structure around migrated cations. To study the behavior of this unique combination of materials,  $\text{Li}_{1.2}\text{Ti}_{0.4}\text{Cr}_{0.4}\text{O}_2/\text{Li}$  pouch-cells were studied by X-ray absorption spectroscopy [XANES and extended X-ray absorption fine structure (EXAFS)], *in situ*, during first-cycle delithiation to 4.8 V.

Figure 38 shows high-resolution synchrotron XRD (HR-XRD, 11BM, APS) of the synthesized powders showing the expected pattern and good phase purity. Also clearly observed are the signature peaks related to Li-Ti ordering (inset), similar to Li-Mn ordering found in  $\text{Li}_2\text{MnO}_3$ . EXAFS data (not shown) confirms that the local structure around Ti is very similar to that of a reference  $\text{Li}_2\text{TiO}_3$  sample (for example, Li-Ti ordering) while the Cr EXAFS shows that Cr is fully coordinated in the second shell (Cr-M coordination = 6). Therefore, the overall structure is similar to that of LL compositions such as  $\text{Li}_{1.2}\text{Mn}_{0.4}\text{Co}_{0.4}\text{O}_2$ , where  $4^+$  and  $3^+$  TM cations strongly charge order to create distinct local environments. Figure 39a shows the *in situ* development of the Cr K-edge XANES as a function of lithium content,  $x$ . As expected for active  $\text{Cr}^{3+}$  compounds,  $\text{Cr}^{3+}$  is immediately oxidized to  $\text{Cr}^{6+}$  and migrates easily to tetrahedral sites, as clearly indicated by the large increase in the pre-edge region (inset). Figure 39b shows the evolution of the Ti K-edge during delithiation. Interestingly, the main edge changes in a somewhat ambiguous way similar to the Mn edge of Mn-rich, LL materials. However, the pre-edge region shows a large increase in intensity and a shift to lower energies (inset). EXAFS analysis also shows that the Ti-O coordination decreases by  $\sim 10\%$  during the first-cycle charge. This shift in Ti pre-edge energies, along with increased intensities, is known to occur in Ti compounds as the Ti-O coordination goes from 6 to 4 and octahedral to tetrahedral. Although  $\text{Li}_2\text{TiO}_3$  is a completely inactive material for Li deintercalation/intercalation, this property does not preclude instabilities and Ti migration associated with the local domain structures that appear in complex, Li-rich materials. Further analysis is ongoing on these and other model compounds.

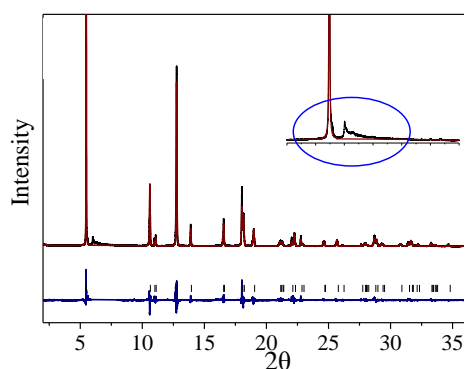


Figure 38. High-resolution X-ray diffraction patterns of  $\text{Li}_{1.2}\text{Ti}_{0.4}\text{Cr}_{0.4}\text{O}_2$ .

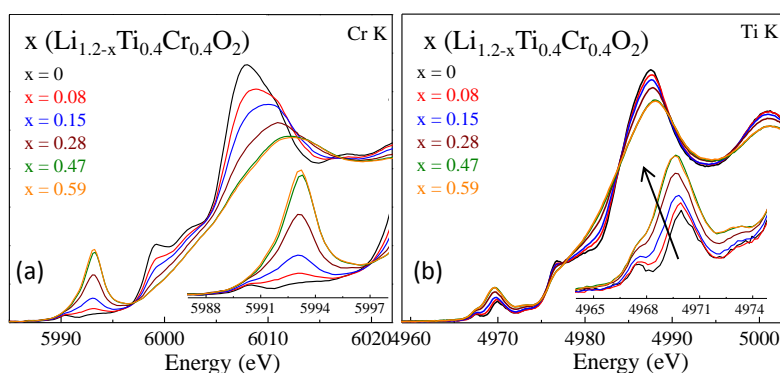


Figure 39. *In situ* Cr and Ti K-edge X-ray absorption near-edge structure data. These insets (a-b) show magnified views of respective pre-edge regions.

### Patents/Publications/Presentations

Presentation: Topics in Energy and Sustainability, University of Illinois, Chicago (24 November 2015): “The Next Generation of Li-Ion Batteries for Transportation Applications: Perception, Promises and Problems”; Croy, Jason R. Invited.

## TASK 6 – MODELING ADVANCED ELECTRODE MATERIALS

### Summary and Highlights

Achieving the performance, life, and cost targets outlined in the EV Everywhere Grand Challenge will require moving to next generation chemistries, such as higher capacity Li-ion intercalation cathodes, silicon and other alloy-based anodes, lithium metal anode, and sulfur cathodes. However, numerous problems plague the development of these systems, from material level challenges in ensuring reversibility to electrode level issues in accommodating volume changes, to cell-level challenges in preventing cross talk between the electrodes. In this task, a mathematical perspective is applied to these challenges to provide an understanding of the underlying phenomenon and to suggest solutions that can be implemented by the material synthesis and electrode architecture groups.

The effort spans multiple length scales from *ab initio* methods to continuum-scale techniques. Models are combined with experiments and extensive collaborations are established with experimental groups to ensure that the predictions match reality. Efforts are also focused on obtaining the parameters needed for the models either from lower length scale methods or from experiments. Projects also emphasize pushing the boundaries of the modeling techniques used to ensure that the task stays at the cutting edge.

In the area of intercalation cathodes, the effort is focused on understanding the working principles of the high Ni layered materials with an aim of understanding structural changes and the associated changes in transport properties. In addition, focus is paid to the assembling of porous electrodes with particles to predict the conduction behavior and developing tools to measure electronic conduction. This quarter, the lithium diffusion process in the excess-lithium material was studied. In the area of new disordered materials, the project is now making progress on predicting materials that are disordered as synthesized. Finally, to understand how cathodes are assembled the dynamic packing model (DPP) was compared to stress strain measurements on cathode samples. Results show the validity of the model.

In the area of silicon anodes, the effort is in trying to understand the interfacial instability and suggest ways to improve the cyclability of the system. In addition, effort is focused on designing artificial SEI layers that can accommodate the volume change, and in understanding the ideal properties for a binder to accommodate the volume change without delamination. Work on the SEI on these electrodes continues this quarter, and new chemistry was seen to occur at the alucone coating/Si interface. Simulations of the SEI suggest a plastic ratcheting effect whereby the SEI starts to wrinkle and delaminate.

In the area of sulfur cathodes, the focus is on developing better models for the chemistry with the aim of describing the precipitation reactions accurately. Efforts are focused on performing the necessary experiments to obtain a physical picture of the phase transformations in the system and in measuring the relevant thermodynamic, transport, and kinetic properties. In addition, changes in the morphology of the electrode are described and tested experimentally. Work continued this quarter to understand the impact of film resistance on performance.

Finally, microstructure models are an area of focus to ensure that the predictions move away from average techniques to more sophisticated descriptions of processes inside electrodes. Efforts are focused on understanding conduction within the electrode and also on simulating the full electrode that describe the intricate physics inside the battery electrode. These efforts are combined with tomography information as input into the models. Last quarter, progress was made in correcting macro-scale simulations using tomographic information. More is needed to ensure that accurate measurements are made in the microscale.

## Task 6.1 – Electrode Materials Design and Failure Prediction (Venkat Srinivasan, Lawrence Berkeley National Laboratory)

**Project Objective.** The project goal is to use continuum-level mathematical models along with controlled experiments on model cells to (i) understand the performance and failure models associated with next-generation battery materials, and (ii) design battery materials and electrodes to alleviate these challenges. The research will focus on the Li-S battery chemistry and on microscale modeling of electrodes. Initial work on the Li-S system will develop a mathematical model for the chemistry along with obtaining the necessary experimental data, using a single ion conductor (SIC) as a protective layer to prevent polysulfide migration to the Li anode. The initial work on microscale modeling will use the well understood  $\text{Li}(\text{NiMnCo})_{1/3}\text{O}_2$  (NMC) electrode to establish a baseline for modeling next-generation electrodes.

**Project Impact.** Li-S cells promise to increase the energy density and decrease the cost of batteries compared to the state of the art. If the performance and cycling challenges can be alleviated, these systems hold the promise for meeting the EV Everywhere targets.

**Out-Year Goals.** At the end of this project, a mathematical model will be developed that can address the power and cycling performance of next-generation battery systems. The present focus is on microscale modeling of electrodes and Li-S cells, although the project will adapt to newer systems, if appropriate. The models will serve as a guide for better design of materials, such as in the kinetics and solubility needed to decrease the morphological changes in sulfur cells and increase the power performance.

**Collaborations.** This project collaborates with Vincent Battaglia and Dula Parkinson of LBNL.

### Milestones

1. Replace parameters (porosity gradient and tortuosity) in macroscale NMC model with corresponding values or functions obtained from tomography data. (12/31/15 – Complete)
2. Measure the relationship of film growth to electrochemical response and develop a model to interpret the relationship. (3/31/16 – In progress)
3. Measure transport properties of polysulfide solutions using electrochemical methods. If unsuccessful at obtaining concentration-dependent diffusion coefficient, use fixed diffusion coefficient value in upcoming simulations. (6/30/16 – In progress)
4. Incorporate measured properties into porous-electrode model of a Li-S cell and compare to data (9/30/16 – In progress)

## Progress Report

### Replacement of porous electrode model parameters with information from microtomography.

The same electrode microtomography data sample used to complete the last milestone was used this quarter to obtain tortuosity and porosity gradient information.

Tortuosity was obtained by constructing a new simulation in which the same spatial domain was placed between two electrodes maintained at different potentials, with the phase previously representing active and conductive material now taken as an insulator, and the phase previously representing the pore space now taken as a conductor. Laplace's equation, describing electrical potential, was then solved over the combined domain. The average current density through a plane parallel to the electrodes was then used to determine the ratio of effective conductivity of the microporous structure to intrinsic conductivity of the pore "material." This ratio is equal to the ratio of porosity and tortuosity. A porosity of 0.43 was used last quarter for consistency with the macroscale model developed earlier in this group. The tortuosity value extracted from the conduction simulation results was then approximately 1.2, which is within the range of values measured by M. Ebner, D.-W. Chung, R. E. Garcia, and V. Wood in *Adv. Energy. Mater.* 2013 in NMC electrodes with larger NMC particles, but which is substantially different from the value of approximately 22 used with the original macroscale simulations, determined through a fitting procedure over a range of C-rates.

Custom programs were written and applied to the raw tomography data to determine the spatially averaged porosity of each voxel "slice" through the electrode parallel to the current collector and to then compute a least-squares straight-line fit to the results. This line provides a simple position-dependent description of porosity, with the slope describing an approximate porosity gradient. The average value of this function over

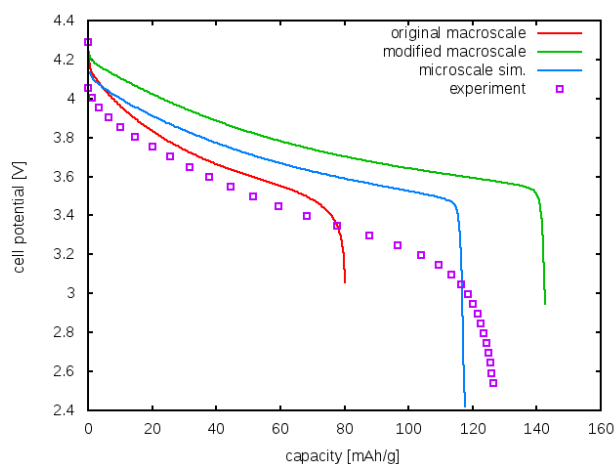


**Figure 40. Comparison of results for a 3C discharge using original porous electrode model, modified model with porosity gradient, and tortuosity extracted from microtomography data and conductivity simulations, microscale model, and experimental data.**

the electrode is approximately 0.48, somewhat larger than the porosity obtained from electrode composition. Some discrepancy was expected from these very different approaches. A modified porosity function was constructed, using the average porosity obtained from the composition and the derivative of the linear fit. This spatially varying description of porosity was then incorporated into the macroscale simulation, as was the newly determined tortuosity value. The resulting discharge curve is shown along with those from the original macroscale model and microscale model in Figure 40. Primarily as a consequence of using very different tortuosity values, the original and modified macroscale simulations show very different results; capacity in the former case is limited by solution-phase transport, and in the latter case, solid-phase transport. The introduction of microscale information into the porous electrode model moves the discharge curve in the direction of the microscale simulation results, but

to even higher capacities. This discrepancy might be the consequence of the small region (10  $\mu\text{m}$  by 10  $\mu\text{m}$  by 60  $\mu\text{m}$ ) examined in the microscale simulations last quarter, for which much of the solid surface is not available to the solution phase because it coincides with the boundaries of the simulation volume. Further work will consider larger domains involving greater computational cost.



## Patents/Publications/Presentations

### Publication

- Takahashi\*, K., and K. Higa\*, S. Mair, M. Chintapalli, N. Balsara, and V. Srinivasan. “Mechanical Degradation of Graphite/PVDF Composite Electrodes: A Model-Experimental Study.” *J. Electrochem. Soc.* 163, no. 3 (2016): A385-A395.

### Open source software release

- K. Higa and V. Srinivasan, PyGDH: The Python-Based Grid Discretization Helper, available from <https://sites.google.com/a/lbl.gov/pygdh/>.

## Task 6.2 – Predicting and Understanding Novel Electrode Materials from First-Principles (Kristin Persson, Lawrence Berkeley National Laboratory)

**Project Objective.** The project aim is to model and predict novel electrode materials from first-principles focusing on (1) understanding the atomistic interactions behind the behavior and performance of the high-capacity lithium excess and related composite cathode materials, and (2) predicting new materials using the recently developed Materials Project high throughput computational capabilities at LBNL. More materials and new capabilities will be added to the Materials Project Lithium Battery Explorer App ([www.materialsproject.org/apps/battery\\_explorer/](http://www.materialsproject.org/apps/battery_explorer/)).

**Project Impact.** The project will result in a profound understanding of the atomistic mechanisms underlying the behavior and performance of the Li-excess as well as related composite cathode materials. The models of the composite materials will result in prediction of voltage profiles and structural stability—the ultimate goal being to suggest improvements based on the fundamental understanding that will increase the life and safety of these materials. The Materials Project aspect of the work will result in improved data and electrode properties being calculated to aid predictions of new materials for target chemistries relevant for ongoing BMR experimental research.

**Out-Year Goals.** During years one and two, the bulk phase diagram will be established, including bulk defect phases in layered  $\text{Li}_2\text{MnO}_3$ , layered  $\text{LiMO}_2$  ( $\text{M} = \text{Co}, \text{Ni}, \text{and Mn}$ ) and  $\text{LiMn}_2\text{O}_4$  spinel to map out the stable defect intermediate phases as a function of possible transition metal rearrangements. Modeling of defect materials (mainly  $\text{Li}_2\text{MnO}_3$ ) under stress/strain will be undertaken to simulate effect of composite nano-domains. The composite voltage profiles as function of structural change and Li content will be obtained. In years two to four, the project will focus on obtaining Li activation barriers for the most favorable TM migration paths as a function of Li content, as well as electronic DOS as a function of Li content for the most stable defect structures identified in years one to two. Furthermore, stable crystal facets of the layered and spinel phases will be explored, as a function of  $\text{O}_2$  release from surface and oxygen chemical potential. Within the Materials Project, hundreds of novel Li intercalation materials will be calculated and made available.

**Collaborations.** This project engages in collaboration with Gerbrand Ceder (MIT), Clare Grey (Cambridge, UK), Mike Thackeray (ANL), and Guoying Chen (LBNL).

### Milestones

1. Mn mobilities as a function of Li content in layered  $\text{Li}_x\text{MnO}_3$  and related defect spinel and layered phases. (3/31/15 – Complete)
2. Surface facets calculated and validated for  $\text{Li}_2\text{MnO}_3$ . (3/31/16 – Delayed)
3. Calculate stable crystal facets. Determine whether facet stabilization is possible through morphology tuning. (3/31/16 – Delayed)
4. *Go/No-Go*: Stop this approach if facet stabilization cannot be achieved. (3/31/16 – Delayed)
5. Li mobilities as a function of Li content in layered  $\text{Li}_x\text{MnO}_3$  and related defect spinel and layered phases. (9/30/15 – Complete)

## Progress Report

This project has continued to elucidate the lithium (Li)-ion diffusion mechanisms of Li-excess layered materials using first-principles nudge-elastic band calculations. It has systematically investigated the diffusion paths to find four distinguishable migration patterns for intra-layer Li-migration. Here, the calculation shows that those paths have various activation energy barriers as a result of their local cation environments.

The lithium-excess model material  $\text{Li}_2\text{MnO}_3$  has two symmetrical octahedral sites in Li-layer, which are 4h and 2c (see Figure 41a). In addition, two distinguishable tetrahedral sites exist between those two octahedral sites; the tetrahedral sites can be distinguished by their face-sharing octahedral neighbors. The project defined two tetrahedral sites as  $\text{T}^{4g}_{\text{Li}}$  and  $\text{T}^{2b}_{\text{Li}}$ . Here, ‘T’ stands for the tetrahedral site, subscript ‘Li’ points out the type of layer, and superscript ‘4g’/‘2b’ indicate the facing octahedral site at the upper or lower layer. Therefore, the first neighboring Li-ion migration can be explained as a combination of ‘initial octahedral site’-‘saddle point tetrahedral site’-‘final octahedral site’; Figure 41b shows four distinct paths, which are (i)  $4\text{h}-\text{T}^{4g}_{\text{Li}}-4\text{h}$ , (ii)  $4\text{h}-\text{T}^{2b}_{\text{Li}}-4\text{h}$ , (iii)  $2\text{b}-\text{T}^{4g}_{\text{Li}}-4\text{h}$ , and (iv)  $2\text{c}-\text{T}^{2b}_{\text{Li}}-4\text{h}$ . The calculation shows that path (ii) is slightly lower than (i) or (iii), and (iv) exhibits the lowest energy barrier.

In detail, paths (i), (ii), and (iii) show the mobile Li-ion passing through the oxygen dumbbell (or equivalently the oxygen edge) path at the saddle point, but path (iv) exhibits the Li passing through the tetrahedral site (see Figure 41c). This phenomenon can be explained by the face-sharing ions at the top and bottom layer of the saddle point. More specifically, Mn-ions face-share at the top and bottom of the saddle point of the tetrahedral sites in paths (i) and (iii). Similarly, Li-ions face-share at the top and bottom for path (ii). Intuitively, the cation repulsion from the Li-contained octahedral site is weaker than the Mn-contained one. Indeed, the Li activation energy barrier difference can be rationalized by its local cation environment, as the calculated energy barrier of path (ii; 0.60 eV) is lower than (i; 0.78 eV) or (iii; 0.80 eV). On the other hand, in path (iv), the face-sharing ions at the top and bottom layer are different (for example, Li at one side and Mn at the other side), which results in the lowest barrier for Li mobility path (0.56 eV).

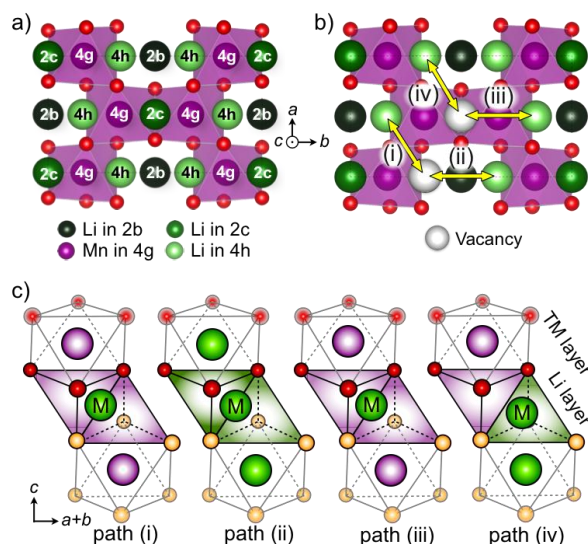


Figure 41. (a) Illustrations of the  $\text{Li}_2\text{MnO}_3$  Li-excess compound. (b, c) Illustration of the four symmetry-distinguishable migration paths (i), (ii), (iii) and (iv) as indicated by their local cation environment.

## Patents/Publications/Presentations

- Presentation. MRS Fall Meeting, Boston (1 December 2015): “Elucidating the Delithiation Mechanism of Lithium-Excess Materials”; Yongwoo Shin, Hong Ding, and Kristin A. Persson.

## Task 6.3 – First Principles Calculations of Existing and Novel Electrode Materials (Gerbrand Ceder, MIT)

**Project Objective.** Identify the structure of layered cathodes that leads to high capacity. Clarify the role of the initial structure as well as structural changes upon first charge and discharge. Give insight into the role of Li-excess and develop methods to predict ion migration in layered cathodes upon cycling and during overcharge. Develop predictive modeling of oxygen charge transfer and oxygen loss. Give insight into the factors that control the capacity and rate of Na-intercalation electrodes, as well as Na-vacancy ordering. Develop very high-capacity layered cathodes with high structural stability ( $> 250$  mAh/g).

**Project Impact.** The project will lead to insight in how Li excess materials work and ultimately to higher capacity cathode materials for Li-ion batteries. The project will help in the design of high-capacity cathode materials that are tolerant to transition metal migration.

**Out-Year Goals.** The out-year goals are as follows:

- Higher capacity Li-ion cathode materials
- Novel chemistries for higher energy density storage devices
- Guide field in search for higher energy density Li-ion materials

**Collaborations.** This project collaborates with K. Persson (LBNL) and C. Grey (Cambridge).

### Milestones

1. Model to predict compositions that will disorder as synthesized. (Q1 – Complete)
2. At least one Ti-based compound with high capacity. (Q2)
3. Predictive model for the voltage curve (slope) of cation-disordered materials. (Q3)
4. Modeling capability for materials with substantial oxygen redox capability. (Q4)

## Progress Report

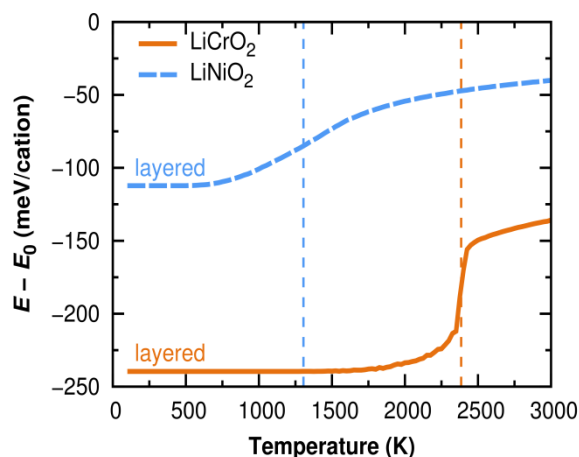


Figure 42. Internal energy of  $\text{LiCrO}_2$  (solid orange line) and  $\text{LiNiO}_2$  (dashed blue line) during heat-up simulations of their layered ground state configurations from 100 K to 3000 K. The vertical dashed lines indicate the temperatures of their respective order-disorder phase transitions. The zero-point of the  $y$  axis corresponds to the energy of a fully random cation arrangement.

order-disorder phase transition from first-principles calculations. As an example, Figure 42 shows the result of Monte-Carlo heat-up simulations of  $\text{LiCrO}_2$  and  $\text{LiNiO}_2$  using lattice-model Hamiltonians based on first-principles calculations, and the temperatures of the order-disorder transitions are indicated by vertical dashed lines. Note that the energies after the order-disorder transitions are still significantly lower than the energy of fully random cation arrangements ( $E - E_0 = 0$  in Figure 42), which is due to short-range interactions present in the cation-disordered phases. While these MC simulations did not consider melting or decomposition of the materials, they nevertheless allow the ranking of different compositions by likelihood to disorder. However, the construction of lattice models is time consuming, especially for compositions with multiple TM species.

Despite material-dependent short-range interactions, the project found that the temperature of the order-disorder transition correlates strongly with the energy difference between the completely random state and the ordered ground state (Figure 43). The energy of the random state can be well approximated based on *special quasi-random structures* (SQS), so that only two first-principles calculations, the ground state structure and the SQS, are required to estimate the likelihood of cation disorder in any given composition. This approach has also been confirmed for compositions with multiple TM species (not shown) and is, hence, suitable for an automated computational search for new cation-disordered cathode materials.

1. Lee, J., et al. *Science* 343 (2014): 519–522.
2. Urban, A., et al. *Adv. Energy Mater.* 4 (2014): 1400478.
3. Wang, R., et al. *Electrochem. Commun.* 60 (2015): 70–73.

Cathode materials based on cation-disordered Li transition-metal (TM) oxides have recently been demonstrated to deliver high capacities and sustain efficient Li transport, provided an excess of at least 10% of Li compared to the TM concentration [1, 2]. In addition, cation disorder has been credited with improved structural stability of  $\text{Li}_{1.211}\text{Mo}_{0.467}\text{Cr}_{0.3}\text{O}_2$ , which undergoes only negligible volume changes during cycling [1]. Similarly, cation-disordered  $\text{Li}_{1.25}\text{Nb}_{0.25}\text{Mn}_{0.5}\text{O}_2$  with a large capacity of 287 mAh/g from TM and  $\text{O}^{2-}/\text{O}^-$  redox activity has been reported without indications of material decay through oxygen release [3]. However, the discovery of novel cation-disordered cathode materials has so far either been by chance or through the modification of known disordered materials.

To aid the systematic design of new cation-disordered cathode materials, the project devised a methodology for the computational prediction of materials that will disorder as synthesized. The approach is based on estimating the temperature of the configurational

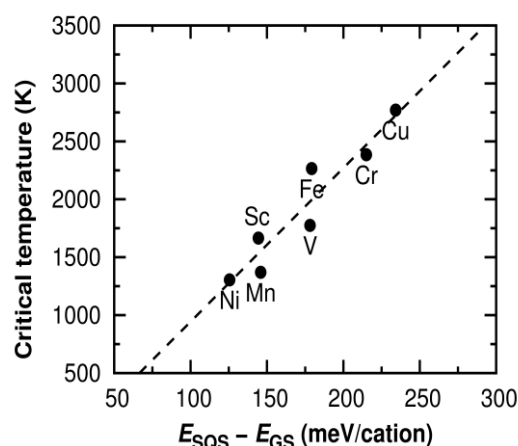


Figure 43. Correlation of the temperature of the order-disorder transition of different  $\text{LiMO}_2$  ( $M = \text{Sc}, \text{V}, \text{Cr}, \text{Mn}, \text{Fe}, \text{Ni}, \text{Cu}$ ) with the energy difference of the random cation arrangement ( $E_{\text{SQS}}$ ) and the ordered ground state ( $E_{\text{GS}}$ ).

## Task 6.4 – First Principles Modeling of SEI Formation on Bare and Surface/Additive Modified Silicon Anode (Perla Balbuena, Texas A&M University)

**Project Objective.** This project aims to develop fundamental understanding of the molecular processes that lead to the formation of a SEI layer due to electrolyte decomposition on Si anodes, and to use such new knowledge in a rational selection of additives and/or coatings. The focus is on SEI layer formation and evolution during cycling and subsequent effects on capacity fade through two concatenated problems: (1) SEI layers formed on lithiated Si surfaces, and (2) SEI layers formed on coated surfaces. Key issues being addressed include the dynamic evolution of the system and electron transfer through solid-liquid interfaces.

**Project Impact.** Finding the correspondence between electrolyte molecular properties and SEI formation mechanism, structure, and properties will allow the identification of new/improved additives. Studies of SEI layer formation on modified surfaces will allow the identification of effective coatings able to overcome the intrinsic deficiencies of SEI layers on bare surfaces.

**Approach.** Investigating the SEI layer formed on modified Si surfaces involves analysis of the interfacial structure and properties of specific coating(s) deposited over the Si anode surface, characterization of the corresponding surface properties before and after lithiation, especially how such modified surfaces may interact with electrolyte systems (solvent/salt/additive), and what SEI layer structure, composition, and properties may result from such interaction. This study will allow identification of effective additives and coatings able to overcome the intrinsic deficiencies of SEI layers on bare surfaces. Once the SEI layer is formed on bare or modified surfaces, it is exposed to cycling effects that influence its overall structure (including the anode), chemical, and mechanical stability.

**Out-Year Goals.** Elucidating SEI nucleation and electron transfer mechanisms leading to growth processes using a molecular level approach will help establish their relationship with capacity fading, which will lead to revisiting additive and/or coating design.

**Collaborations.** Work with Chunmei Ban (NREL) consists in modeling the deposition-reaction of alucon coating on Si surfaces and their reactivity. Work with B. Lucht (Rhode Island) relates to finding the best additives for optimum SEI formation on Si anodes. Reduction of solvents and additives on Si surfaces were studied in collaboration with K. Leung and S. Rempe (SNL). Collaborated with Prof. Jorge Seminario (Texas A&M University, TAMU) on electron transfer reactions, and Dr. Partha Mukherjee (TAMU) on development of a multi-scale model to describe SEI growth on Si anodes.

### Milestones

1. Identify SEI nucleation and growth on Si surfaces modified by deposition of alucone coatings as a function of degree of lithiation of the film. (Q1 – Complete)
2. Quantify chemical and electrochemical stability of various SEI components: competition among polymerization, aggregation, and dissolution reactions. Evaluate voltage effects on SEI products stability. (Q2)
3. Identify alternative candidate electrolyte and coating formulations. (Q3)
4. *Go/No-Go:* Test potential candidate electrolyte and coating formulations using coarse-grained model and experimentally via collaborations. (Q4)



## Progress Report

**Reactivity of alucone coating.** New chemistry was discovered that takes place at the alucone/lithiated Si anode and the alucone/electrolyte interfaces due to electrolyte decomposition. The  $\text{AlO}_3$  and OH groups in the film play a very important role in the SEI formation as revealed by *ab initio* molecular dynamics simulations. EC is able to migrate through the porous film and get reduced at the anode surface and sometimes at the alucone/electrolyte interface. Most of the EC decomposition products may be found bonded to  $\text{AlO}_3$ . H product of OH decomposition may act as a reduction agent. Thus, besides the usual  $\text{LiF}$ ,  $\text{Li}_2\text{CO}_3$ , and  $\text{Li}_2\text{O}$  products, the SEI film is predicted to have a mixed organic/inorganic nature due to the presence of numerous  $\text{AlO}_3$  groups participating of the SEI film. A manuscript is in preparation.

**SEI structure, growth, and stability of SEI components.** Electron transfer mechanisms via radicals that arise from organic product decomposition have been elucidated and proposed as the main mechanism for SEI growth after film thicknesses are larger than the electron tunneling length. Clear evidence for the decomposition of organic oligomers such as  $\text{Li}_2\text{EDC}$  and  $\text{Li}_2\text{VDC}$  were shown. The vinylene carbonate (VC) versus EC decomposition effects on SEI growth are analyzed and new rules for electrolyte selection are proposed in *Chem. Mater.* 27, no. 23 (2015): 7990-8000. In collaboration with Balbuena's group, Leung (SNL) refined calculations of  $\text{Li}_2\text{CO}_3$  decomposition on lithium-rich active material surfaces. With excess lithium at the Li (100)/ $\text{Li}_2\text{CO}_3$  interface, the C-O bond breaking barrier in  $\text{CO}_3^{2-}$  is predicted to be about 0.8 eV and is consistent with  $\sim 10$  second reaction time scale. Each excess Li atom at the interface only costs  $\sim 0.1$  eV; this is equivalent to a small 0.1 V overpotential. Thus, the  $\text{Li}_2\text{CO}_3$  is not just thermodynamically but also kinetically unstable. The root cause seems to be the +4 formal charge state on carbon at Li metal interface. This work has been submitted for publication in the *Journal of Physical Chemistry*.

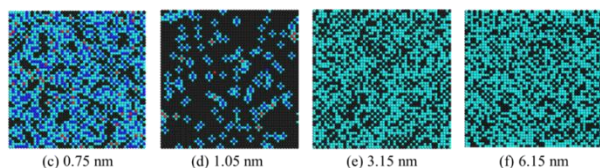


Figure 44. Surface pattern as the SEI thickness grows.

interactions dominate the stabilization of the porous block. In terms of association,  $\text{Li}_2\text{EDC}$  tends to associate with the bare and covered surface through O-Li-O bridges. However, the association mechanism depends on whether the surface is covered with a LiF layer. Decomposition of the oligomers on the  $\text{Li}_{13}\text{Si}_4$  (010) surface can also lead to  $\text{CO}_2$  evolution. Once a monolayer of  $\text{Li}_2\text{EDC}$  has been formed at the surface, it will decompose generating a  $\text{CO}_2$  molecule bonded to the Si surface and an  $\text{OC}_2\text{H}_4\text{CO}_3$  fragment. A coarse-grained kinetic Monte-Carlo (KMC) model was developed to study the growth of the  $\text{Li}_2\text{EDC}$  film. The model involves multiple-step reactions. It is found that the reduction of EC limits the film growth rate. A simple approach is used to incorporate the effect of the SEI thickness, which shows the reduction of the growth rate as the film thickness increases. The evolution of the surface pattern is detected as a function of SEI thickness (Figure 44). A manuscript has been submitted to *Physical Chemistry Chemical Physics*.

**Dynamics and free energy studies of electrolyte solvation.** Ion dissolution and diffusion in battery electrolytes are correlated with solvent dielectric response. Dielectric constants/relaxation times and molecular mobilities were computed by Rempe's group (SNL). Notably, the work showed that the dielectric relaxation times are remarkably long on conventional simulation times, even though these are small-molecule liquids. The values of the relaxation times, for example, 46 ps for PC and 31 ps for EC, compared to 7.5 ps for liquid water at 303 K, highlight the fact that these cyclic carbonate solvents are comparatively sluggish. Thus, very long simulations are required to obtain sound results for solvent kinetic properties. Comparison with the limited available experimental data on solvent dielectric properties, both for static dielectric constants and dielectric relaxation times, is favorable and suggests that the classical force field parameters (OPLS-AA) are reasonably accurate.

## Patents/Publications/Presentations

### Publications

- Perez-Beltrán, S., and G. E. Ramirez-Caballero and P. B. Balbuena. “First Principles Calculations of Lithiation of a Hydroxylated Surface of Amorphous Silicon Dioxide.” *J. Phys. Chem. C* 119 (2015): 16424–16431.
- Ma, Y., and J. M. Martinez de la Hoz, I. Angarita, J. M. Berrio-Sanchez, L. Benitez, J. M. Seminario, S.-B. Son, S.-H. Lee, S. M. George, C. M. Ban, and P. B. Balbuena. “Structure and Reactivity of Alucone-Coated Films on Si and  $\text{Li}_x\text{Si}_y$  Surfaces.” *ACS Appl. Mater. Inter.* 7 (2015): 11948–11955.
- Martinez de la Hoz, J. M., and F. A. Soto and P. B. Balbuena. “Effect of the Electrolyte Composition on SEI reactions at Si Anodes of Li-ion Batteries.” *J. Phys. Chem. C* 119 (2015): 7060-7068. doi: 10.1021/acs.jpcc.5b01228.
- Soto, F. A., and Y. Ma, J. M. Martinez de la Hoz, J. M. Seminario, and P. B. Balbuena. “Formation and Growth Mechanisms of Solid-Electrolyte Interphase Layers in Rechargeable Batteries.” *Chem. Mater.* 27, no. 23 (2015): 7990–8000.
- You, X., and M. I. Chaudhari, S. B. Rempe, and L. R. Pratt. “Dielectric Relaxation of Ethylene Carbonate and Propylene Carbonate from Molecular Dynamics Simulations.” *J. Phys. Chem. B*. doi: 10.1021/acs.jpcb.5b09561.
- Leung, K., and F. A. Soto, K. Hankins, P. B. Balbuena, and K. L. Harrison. “Stability of Solid Electrolyte Interphase Components on Reactive Anode Surfaces.” *J. Phys. Chem. C*. Under review.
- Soto, F. A., and Z. Liu, P. P. Mukherjee, and P. B. Balbuena. “Elucidating Oligomer-Surface Interactions and Organic Film Growth at a Lithiated Silicon Surface.” *Phys. Chem. Chem. Phys.* Under review.

## Task 6.5 – A Combined Experimental and Modeling Approach for the Design of High Current Efficiency Si Electrodes

(Xingcheng Xiao, General Motors; Yue Qi, Michigan State University)

**Project Objective.** The use of high-capacity, Si-based electrode has been hampered by its mechanical degradation due to large volume expansion/contraction during cycling. Nanostructured Si can effectively avoid Si cracking/fracture. Unfortunately, the high surface to volume ratio in nanostructures leads to an amount of SEI formation and growth, and thereby low current/CE and short life. Based on mechanics models, the project demonstrates that the artificial SEI coating can be mechanically stable despite the volume change in Si, if the material properties, thickness of SEI, and the size/shape of Si are optimized. Therefore, the project objective is to develop an integrated modeling and experimental approach to understand, design, and make coated Si anode structures with high current efficiency and stability.

**Project Impact.** The validated model will ultimately be used to guide the synthesis of surface coatings and the optimization of Si size/geometry that can mitigate SEI breakdown. The optimized structures will eventually enable a negative electrode with a 10x improvement in capacity (compared to graphite), while providing a > 99.99% CE; this could significantly improve the energy/power density of current lithium-ion batteries.

**Out-Year Goals.** The out-year goal is to develop a well validated mechanics model that directly imports material properties either measured from experiments or computed from atomic simulations. The predicted SEI induced stress evolution and other critical phenomena will be validated against *in situ* experiments in a simplified thin-film system. This comparison will also allow fundamental understanding of the mechanical and chemical stability of artificial SEI in electrochemical environments and the correlation between the CE and the dynamic process of SEI evolution. Thus, the size and geometry of coated Si nanostructures can be optimized to mitigate SEI breakdown, thus providing high current efficiency.

**Collaborations.** This project engages in collaboration with LBNL, PNNL, and NREL.

### Milestones

1. Identify critical mechanical and electrochemical properties of the SEI coating that can enable high current efficiency. (12/31/15 – Complete)
2. Design a practically useful Si electrode where degradation of the SEI layer is minimized during lithiation and delithiation. (3/31/16 – On going)
3. Construct an artificial SEI design map for Si electrodes, based on critical mechanical and transport properties of desirable SEI for a given Si architecture. (6/30/16)
4. Validated design guidance on how to combine the SEI coating with a variety of Si nano/microstructures. *Go/No-Go:* Decision based on whether the modeling guided electrode design can lead to high CE > 99.9%. (9/30/16 – Complete; identified the desirable SEI component)

## Progress Report

**Investigated the failure mechanisms of SEI.** *In situ* AFM experiments were conducted on patterned island samples to study failure mechanisms of SEI. It was clearly observed in Figure 45 that the patterned islands exhibit lateral expansion and contraction along with vertical. During lithiation, cracking of SEI was observed mainly at the edge of the island due to shear lag effect. However, during delithiation, these cracks get closed due to contraction of island. These results are in agreement with previous measurements of irreversible capacities and also TOF-SIMS study comparing SEI behavior in continuous film and patterned island.

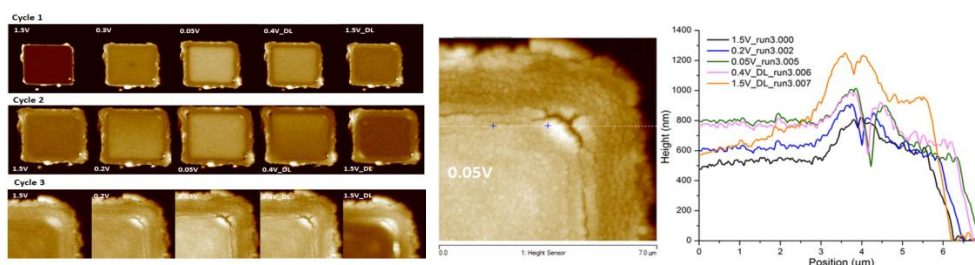


Figure 45. (left) *In situ* atomic force microscopy images during cycling of patterned Si electrode ( $15\ \mu\text{m} \times 15\ \mu\text{m} \times 225\ \text{nm}$ ) showing failure of SEI in shear lag zone. (right) The evolution of section height with cycling (also showing how the crack is evolving).

**Simulation discovered the potential SEI failure mode induced by plastic ratcheting in a-Si anode.** The finite element simulations have identified a potentially new and important failure mode of SEI layer as a result of plastic ratcheting in the a-Si electrode. In the model, SEI is modeled as a nanoscale thin layer that is attached on the a-Si anode. Cyclic Li flux is applied on the top surface to simulate the lithiation/delithiation cycles (Figure 46). Upon cycling, a ratcheting mechanism of accumulative plastic deformation in the a-Si has been observed, leading to the gradual wrinkling and eventual delamination of SEI.

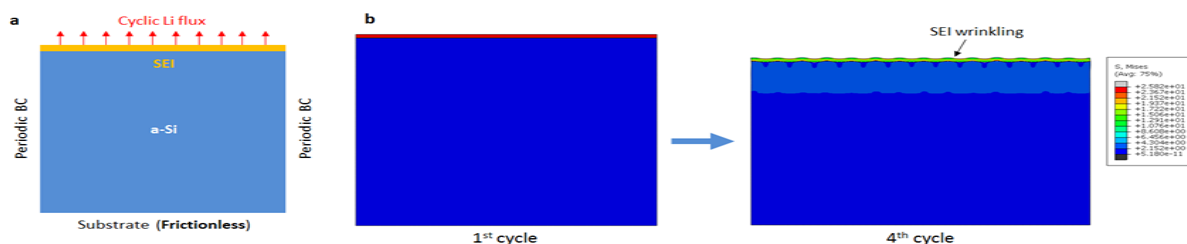


Figure 46. Schematic of the finite element model; (b) Snapshots of the finite element results upon 1<sup>st</sup> cycle and 4<sup>th</sup> cycle, respectively.

**Distinct Li diffusion behavior between  $\text{SiO}_2$  and LiF layers on Si electrode.** Finished developing ReaxFF for Li-Si-O-Al and Li-Si-O-F systems. Reactive molecular dynamics simulations were conducted to compare Li diffusion behavior of a- $\text{SiO}_2$  with a-LiF on a-Si thin film electrode. For  $\text{SiO}_2$  case, Li diffuses very fast to  $\text{SiO}_2$  layer leading to subsequent lithiation to Si electrode (Figure 47a). On the contrary, for LiF layer case, instead of passing through the LiF layer, Li plating occurs accompanied by the growth of the mixture of LiF and Li layer (Figure 47b). This further supports the previous conclusion that LiF is a Li transport barrier.

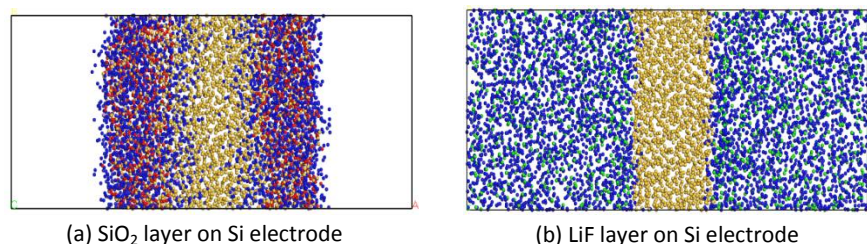


Figure 47. Final configurations of lithiated  $\text{SiO}_2$  layer on Si electrode (a) and lithiated LiF layer on Si electrode (b) (Si: yellow, O: red, F: green, Li: blue).

## Patents/Publications/Presentations

### Publications

- Kim, S., and A. Ostadhossein, A. van Duin, X. Xiao, H. Gao, and Y. Qi. Self-generated Concentration and Modulus Gradients Coating Design to Protect Si Nano-wire Electrodes During Lithiation.” *Phys. Chem. Chem. Phys.* (2016). doi: 10.1039/C5CP07219K.
- Feng, K., and W. Ahn, G. Lui, H. Park, A. Kashkooli, G. Jiang, X. Wang, X. Xiao, and Z. Chen. “Implementing an *In Situ* Carbon Network in Si/Reduced Graphene Oxide for High-Performance Lithium-Ion Battery Anodes.” *Nano Energy* 19 (2015):187–197.
- Li, J., and Q. Zhang, X. Xiao\*, Y. Cheng, C. Liang, and N. J. Dudney\*. “Unravelling the Impact of Reaction Paths on Mechanical Degradation of Intercalation Cathodes for Lithium-Ion Batteries.” *Journal of American Chemical Society* (2015). doi: 10.1021/jacs.5b06178.
- Hassan, F. M., and R. Batmaz, J. Li, X. Wang, X. Xiao\*, A. Yu, and Z. Chen\*. “Evidence of Covalent Synergy in Silicon-Sulfur-Graphene Yielding Highly Efficient and Long-Life Lithium-Ion Batteries.” *Nature Communication* (2015). doi: 10.1038/ncomms9597.

### Presentation

- MRS Fall Meeting, Boston (2 December 2015): “Towards High Cycle Efficiency of Si-Based Negative Electrodes for Next Generation Lithium Ion Batteries”; X. Xiao. Invited.

## Task 6.6 – Predicting Microstructure and Performance for Optimal Cell Fabrication (Dean Wheeler and Brian Mazzeo, Brigham Young University)

**Project Objective.** This work uses microstructural modeling coupled with extensive experimental validation and diagnostics to understand and optimize fabrication processes for composite particle-based electrodes. The first main outcome will be revolutionary methods to assess electronic and ionic conductivities of porous electrodes attached to current collectors, including heterogeneities and anisotropic effects. The second main outcome is a particle-dynamics model parameterized with fundamental physical properties that can predict electrode morphology and transport pathways resulting from particular fabrication steps. These two outcomes will enable the third, which is an understanding of the effects of processing conditions on microscopic and macroscopic properties of electrodes.

**Project Impact.** This work will result in new diagnostic tools for rapidly and conveniently interrogating electronic and ionic pathways in porous electrodes. A new mesoscale 3D microstructure prediction model, validated by experimental structures and electrode-performance metrics, will be developed. The model will enable virtual exploration of process improvements that currently can only be explored empirically.

**Out-Year Goals.** This project was initiated April 2013 and concludes March 2017. Goals by fiscal year are as follows.

- 2013: Fabricate first-generation micro-four-line probe, and complete associated computer model.
- 2014: Assess conductivity variability in electrodes; characterize microstructures of multiple electrodes.
- 2015: Fabricate first-gen ionic conductivity probe, N-line probe, and DPP model.
- 2016: Improve robustness of N-line probe and DPP model; assess structure correlation to conductivity.
- 2017: Using model and probe, evaluate effect of processing conditions.

**Collaborations.** Bryant Polzin (ANL) and Karim Zaghib (Hydro-Québec) provided battery materials. Transfer of technology to A123 to improve their electrode production process took place in FY15. There are ongoing collaborations with Simon Thiele (IMTEK, University of Freiburg) and Mårten Behm (KTH, Sweden).

### Milestones

1. Demonstrate that the DPP model can accurately imitate the mechanical calendering process for a representative electrode film. (December 2015 – Complete)
2. Develop a robust numerical routine for interpreting N-line conductivity measurements. (March 2016 – Ongoing)
3. *Go/No-Go*: Continue work on N-line probe and inversion routine if they can accurately determine anisotropic conductivity for test materials. (June 2016 – Ongoing)
4. *Go/No-Go*: Demonstrate correlations between DPP modeled conductivities and those determined by FIB/SEM and N-line probe. (September 2016 – Ongoing)



## Progress Report

### Milestone 1 (Complete)

The first FY16 milestone was to demonstrate that the dynamic particle-packing (DPP) model can accurately imitate the mechanical calendering process for a representative electrode film. Last fiscal year, it was demonstrated that the DPP model could reproduce experimental viscosities for the slurry, the shrinkage ratio during drying, the elasticity of the dried but uncalendered electrode film, and some additional microstructural properties. This success has led researchers at BYU to continue developing and improving the model. The primary test material continues to be Toda NCM-523 cathodes supplied by ANL. In addition, tests are done on a material developed at BYU to imitate the carbon black and binder domains of the electrode film.

Initially the DPP model showed correct qualitative agreement with experiment for the calendering process. In particular, the model showed plastic deformation during application of calendering pressure, including a reduction in the larger-size pores. However, the onset of plastic deformation took place at small pressures (around 3 bar). Small adjustments to the solid particle interaction parameters were made to improve agreement. The results of this effort are shown in Figure 48, which is a stress-strain curve for the DPP model and four redundant Toda 523 films. The agreement between model and experiment is quite satisfactory, at least at the moderate pressures tested. Additional tests at higher pressures are being performed and will be a part of future reports.

These results as well as those reported in FY15 show agreement between model and experiment for a broad range of properties. This suggests that the simulations reasonably reproduce the relevant physics of particle arrangement during fabrication. It is anticipated that it will become a powerful platform for predicting the effects of fabrications steps on the evolution of the particle microstructure and will accelerate efforts to optimize electrodes.

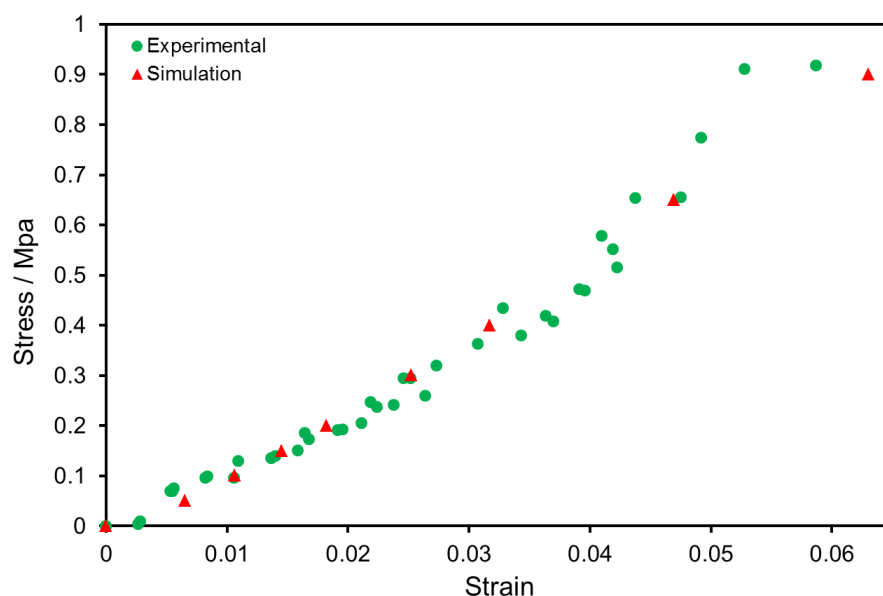


Figure 48. Stress-strain data for Toda 523 cathode film, compressed in the out-of-plane direction to imitate the effect of calendering. Both experimental and dynamic particle-packing model results are indicated. Experiments were performed on four different films by sequentially increasing the stress.

## Patents/Publications/Presentations

### Publication

- Nichols, J. W., and D. R. Wheeler. “Fourier Correlation Method for Simulating Mutual Diffusion Coefficients in Condensed Systems at Equilibrium.” *Indust. Eng. Chem. Res.* 54 (2015): 12156.

### Presentations

- Annual Meeting of AIChE, Salt Lake City (2015): “Measurement of Ionic Conductivity of Intact Battery Electrodes Using a Four-Line Probe”; F. Pouraghajan, R. L. Fitzhugh, M. Wray, B. A. Mazzeo, and D. R. Wheeler.
- Annual Meeting of AIChE, Salt Lake City (2015): “Predicting Transport, Mechanical, and Microstructural Properties of Porous Li-Ion Battery Electrodes by a Particle-Based Simulation”; M. M. Forouzan, C.-W. Chien, D. Bustamante, W. Lange, B. A. Mazzeo, and D. R. Wheeler.
- Annual Meeting of AIChE, Salt Lake City (2015): “Battery Modeling Using Porous Electrode Theory”; D. R. Wheeler.
- 228th Meeting of the Electrochemical Society, Phoenix (2015): “Non-Destructive High-Resolution Conductivity Mapping of Thin-Film Battery Electrodes”; A. Riet, J. Sedgewick, J. Vogel, D. Clement, A. Cutler, B. A. Mazzeo, and D. R. Wheeler.
- Workshop on Advanced Battery Research, University of Illinois at Chicago, Department of Mechanical and Industrial Engineering and the Joint Center for Energy Storage Research, Chicago (2015): “A Particle-Based Model to Optimize Electrode Microstructure and Manufacturing”; D. Wheeler.

## TASK 7 – METALLIC LITHIUM AND SOLID ELECTROLYTES

### Summary and Highlights

The use of a metallic lithium anode is required for advanced battery chemistries like Li-air and Li-S to realize dramatic improvements in energy density, vehicle range, cost economy, and safety. However, the use of metallic Li with liquid and polymer electrolytes has been so far limited due to parasitic SEI reactions and dendrite formation. Adding excess lithium to compensate for such losses effectively negates the high energy density for lithium in the first place. For a long lifetime and safe anode, it is essential that no lithium capacity is lost to physical isolation from roughening, to dendrites or delamination processes, or to chemical isolation from side reactions. The key risk and current limitation for this technology is the gradual loss of lithium over the cycle life of the battery.

To date there are no examples of battery materials and architectures that realize such highly efficient cycling of metallic lithium anodes for a lifetime of 1000 cycles due to degradation of the Li-electrolyte interface. A much deeper analysis of the degradation processes is needed, so that materials can be engineered to fulfill the target level of performance for EV, namely 1000 cycles and a 15-year lifetime, with adequate pulse power. Projecting the performance required in terms of just the Li anode, this requires a high rate of lithium deposition and stripping reactions, specifically about 40 $\mu$ m Li per cycle, with pulse rates up to 10 and 20 nm/s charge and discharge, respectively. This is a conservative estimate, yet daunting in the total mass and rate of material transport. While such cycling has been achieved for state-of-the-art batteries using *molten* Na in Na-S and zebra cells, solid Na and Li anodes are proving more difficult.

The efficient and safe use of metallic lithium for rechargeable batteries is then a great challenge, and one that has eluded research and development efforts for many years. The BMR Task 7 takes a broad look at this challenge for both solid state batteries and batteries continuing to use liquid electrolytes. Four of the projects are new endeavors; two are ongoing. For the liquid electrolyte batteries, PNNL researchers are examining the use of cesium salts and organic additives to the typical organic carbonate electrolytes to impede dendrite formation at both the lithium and graphite anodes. If successful, this is the simplest approach to implement. At Stanford, novel coatings of carbon and boron nitride with a 3D structure are applied to the lithium surface and appear to suppress roughening and lengthen cycle life. A relatively new family of solid electrolytes with a garnet crystal structure shows superionic conductivity and good electrochemical stability. Four programs chose this family of solid electrolytes for investigation. Aspects of the processing of this ceramic garnet electrolyte are addressed at the University of Maryland and at the University of Michigan (UM), with attention to effect of flaws and composition. Computational models will complement their experiments to better understand interfaces and reduce the electrode area specific resistance (ASR). At ORNL, composite electrolytes composed of ceramic and polymer phases are being investigated, anticipating that the mixed phase structures may provide additional means to adjust the mechanical and transport properties. The last project takes on the challenge to use nano-indentation methods to measure the mechanical properties of the solid electrolyte, the lithium metal anode, and the interface of an active electrode. Each of these projects involves a collaborative team of experts with the skills needed to address the challenging materials studies of this dynamic electrochemical system.

## Task 7.1 – Mechanical Properties at the Protected Lithium Interface (Nancy Dudney, ORNL; Erik Herbert, UT – Knoxville; Jeff Sakamoto UM)

**Project Objective.** This project will develop understanding of the Li metal SEI through state-of-the-art mechanical nano-indentation methods coupled with solid electrolyte fabrication and electrochemical cycling. The goal is to provide the critical information that will enable transformative insights into the complex coupling between the microstructure, its defects, and the mechanical behavior of Li metal anodes.

**Project Impact.** Instability and/or high resistance at the interface of lithium metal with various solid electrolytes limit the use of the metallic anode for batteries with high-energy density batteries, such as Li-air and Li-S. The critical impact of this endeavor will be a much deeper analysis of the degradation, so that materials can be engineered to fulfill the target level of performance for EV batteries, namely 1000 cycles and a 15-year lifetime, with adequate pulse power.

**Approach.** Mechanical properties studies through state-of-the-art nano-indentation techniques will be used to probe the surface properties of the solid electrolyte and the changes to the lithium that result from prolonged electrodeposition and dissolution at the interface. An understanding of the degradation processes will guide future electrolyte and anode designs for robust performance. In the first year, the team will address the two critical and poorly understood aspects of the protected Li metal anode assembly: (1) the mechanical properties of the solid electrolyte and (2) the morphology of the cycled Li metal.

**Out-Year Goals.** Work will progress toward study of the electrode assembly during electrochemical cycling of the anode. This project hopes to capture the formation and annealing of vacancies and other defects in the lithium and correlate this with the properties of the solid electrolyte and the interface.

**Collaborations.** This project funds work at ORNL, Michigan Technological University (MTU), and UM. Asma Sharafi (UM, Ph. D. student), Dr. Robert Schmidt (UM) also contribute to the project. Steve Visco (PolyPlus) will serve as a technical advisor.

### Milestones

1. Determine elastic properties of battery grade lithium from different sources and preparation, comparing to values from the reference literature. (9/30/2015 – Delayed due to relocation of indenter; now nearly complete)
2. Compare lithium properties, uncycled versus cycled, using thin film battery architecture. (6/30/2016)
3. View annealing of defects following a single stripping and plating half cycle, using thin film battery architecture. (9/30/2016)

## Progress Report

Dynamic nano-indentation was used to probe thin lithium metal films, typically about 5-micrometers thick (Figure 49). For initial test, the indenter [Nanomechanics Inc.] was installed in the same glove box used for the vacuum evaporation of the lithium onto substrates of glass, kapton, and bulk Li ribbon; fresh samples were immediately mounted for indentation. Since these initial tests, the nanoindenter has been relocated and installed in a dedicated glove box with vibration isolation and optical microscope and camera (Figure 50). First indents of lithium with this facility revealing significant pile up are shown in Figure 51.



Figure 49. Thin film lithium on glass.

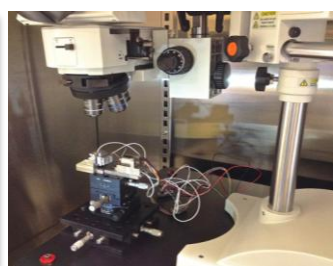


Figure 50. Indenter and microscope installed in glove box.

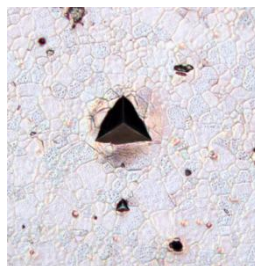


Figure 51. Indent of Li film showing pile up.

With the dynamic method, a 2-nm oscillation of the Berkovich indenter at 100 Hz provides a continuous measure of the stiffness and damping as a function of the probe depth [1]. For lithium, the large coefficient of thermal expansion and the plasticity present challenges in the study [2].

The indentation was done with constant ratio of the strain rate to displacement ( $dP/dt)/P$  which logarithmically scales data collection. An example of data collected for fast and slow strain rates and for different maximum depths (1250 and 2500 nm) is shown in Figures 52 and 53. The best measure of the modulus is obtained for a combination of the low strain rate ( $0.1 \text{ s}^{-1}$ ) and shallow indentation, 300 to 500 nm, where the effect of the plasticity of the lithium is lowest. The hardness and modulus of the lithium film were found to be  $\sim 0.018$  and  $\sim 6$  GPa, respectively, which is slightly higher than published results for single-crystal, body-centered cubic (BCC) lithium. Further analysis will correct for the pile up of material around the indenter which changes the contact area.

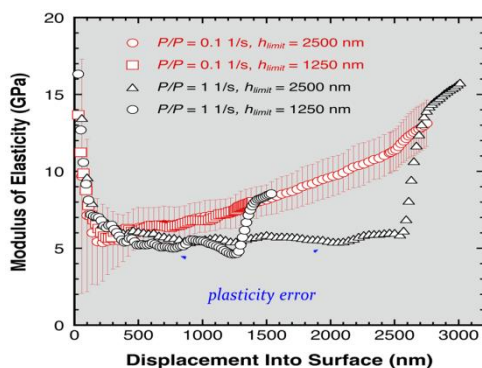


Figure 52. Modulus determined for four indentation tests using different strain rates and penetration.

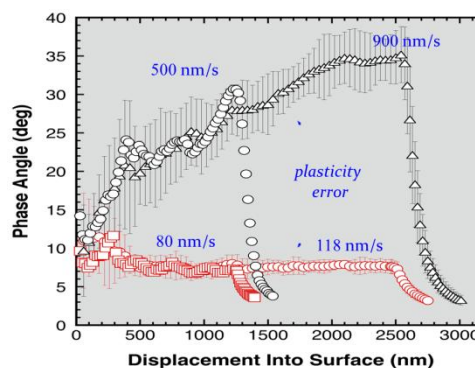


Figure 53. Phase angle for the tests of Figure 52 revealing the strain rate dependence for plasticity and creep.

Work presented at the MRS meeting compared acoustic pulse tests of Al-doped LLZO pellets of slightly different densities, 5.023 and 4.957  $\text{g/cm}^3$ . The higher density pellet, which was optically transparent, reached twice the current density before showing evidence of electrical shorts compared to the pellet with slightly lower density. The denser sample also had a higher observed Young's modulus. The decrease in stiffness that accompanied the onset of the electrical short was found to be consistent with established theory for a microcracked solid.

1. Oliver, W. C. *J. Mater. Res.* 19 (2004): 3–20.

2. Herbert, E. G., et al. *Cur. Opin. Sol. St. Mat. Sci.* 19 (2015): 334.

## Patents/Publications/Presentations

### Presentations

- Fifth International Indentation Workshop, Austin, Texas (November 2015): “The Hardness and Elastic Modulus of Lithium and Solid Electrolytes for Next Generation Battery Applications”; E. G. Herbert, P. S. Phani, N. J. Dudney, G. M. Pharr, R. Schmidt, A. Sharafi, T. Thompson, and J. Sakamoto. Invited.
- MRS Presentation, Boston (December 2015): “Acoustic Monitoring of Solid State Electrolytes to Enable Next Generation Li-ion Battery Development”; Robert D. Schmidt, Jeffrey S. Sakamoto, Travis R. Thompson, Asma Sharafi, and Nancy J. Dudney.



## Task 7.2 – Solid Electrolytes for Solid-State and Lithium-Sulfur Batteries (Jeff Sakamoto, University of Michigan)

**Project Objectives.** *Enable advanced Li-ion solid-state and lithium-sulfur EV batteries using LLZO solid-electrolyte membrane technology.* Owing to its combination of fast ion conductivity, stability, and high elastic modulus, LLZO exhibits promise as an advanced solid-state electrolyte. To demonstrate relevance in EV battery technology, several objectives must be met. First, LLZO membranes must withstand current densities approaching  $\sim 1 \text{ mA/cm}^2$  (commensurate with EV battery charging and discharging rates). Second, low ASR between Li and LLZO must be achieved to achieve cell impedance comparable to conventional Li-ion technology ( $\sim 10 \text{ Ohms/cm}^2$ ). Third, low ASR and stability between LLZO and sulfur cathodes must be demonstrated.

**Project Impact.** The expected outcomes will: (i) enable Li metal protection, (ii) augment DOE access to fast ion conductors and/or hybrid electrolytes, (iii) mitigate Li-polysulfide dissolution and deleterious passivation of Li metal anodes, and (iv) prevent dendrite formation. Demonstrating these aspects could enable Li-S batteries with unprecedented end-of-life, cell-level performance:  $> 500 \text{ Wh/kg}$ ,  $> 1080 \text{ Wh/l}$ ,  $> 1000$  cycles, lasting  $> 15$  years.

**Approach.** This effort will focus on the promising new electrolyte known as LLZO ( $\text{Li}_7\text{La}_3\text{Zr}_2\text{O}_{12}$ ). LLZO is the first bulk-scale ceramic electrolyte to simultaneously exhibit the favorable combination of high conductivity ( $\sim 1 \text{ mS/cm}$  at 298K), high shear modulus (61 GPa) to suppress Li dendrite penetration, and apparent electrochemical stability (0-6V vs  $\text{Li/Li}^+$ ). While these attributes are encouraging, additional research and development is needed to demonstrate that LLZO can tolerate current densities in excess of  $1 \text{ mA/cm}^2$ , thereby establishing its relevance for PHEV/EV applications. This project hypothesizes that defects and the polycrystalline nature of realistic LLZO membranes can limit the critical current density. However, the relative importance of the many possible defect types (porosity, grain boundaries, interfaces, surface and bulk impurities), and the mechanisms by which they impact current density, have not been identified. Using experience with the synthesis and processing of LLZO (Sakamoto and Wolfenstine), combined with sophisticated materials characterization (Nanda), this project will precisely control atomic and microstructural defects and correlate their concentration with the critical current density. These data will inform multi-scale computation models (Siegel and Monroe), which will isolate and quantify the role(s) that each defect plays in controlling the current density. By bridging the knowledge gap between composition, structure, and performance, this project will determine if LLZO can achieve the current densities required for vehicle applications.

**Collaborations.** This project collaborates with Don Siegel (UM atomistic modeling), Chuck Monroe (UM, continuum scale modeling), Jagjit Nanda (ORNL, sulfur chemical and electrochemical spectroscopy), and Jeff Wolfenstine (ARL, atomic force microscopy of Li-LLZO interfaces).

### Milestones

1. Complete critical current density versus porosity measurements. (12/31/2015 – Complete)

## Progress Report

This project successfully evaluated the effect of porosity on the critical current density (CCD). The volume fraction of porosity was controlled by varying the temperature during densification at fixed pressure and time. The effect of relative density on the ionic conductivity and mechanical integrity of polycrystalline LLZO was characterized. The resistance was determined using EIS at room temperature from 1 Hz to 7 MHz. The total ionic conductivity was calculated using ( $\sigma = \frac{L}{R \times A}$ ), where  $\sigma$  is the total ionic conductivity,  $L$  is the thickness,  $R$  is the resistance, and  $A$  is the area of the hot-pressed LLZO pellets. Measurements for Vickers' hardness ( $H_v = \frac{1.854 P}{d^2}$ ) and fracture toughness ( $K_{IC} = \alpha \sqrt{\frac{E}{H_v} \frac{P}{C^3}}$ ) were calculated using indentation (Mitutoyo Hardness Tester), where  $H_v$  is the hardness,  $P$  is the applied load,  $d$  is the length of the diagonal of the Vickers indentation impression,  $K_{IC}$  is the fracture toughness,  $\alpha$  is a material-independent constant (0.016),  $E$  is the Young's modulus, and  $C$  is the crack length.

The total ionic conductivity was increased by increasing the relative density from 85 to 98%, which is comparable to previous work [1, 2]. Figure 54 shows, the Vickers hardness increased with increasing relative density from 80 to 98%, while an inverse correlation between fracture toughness and relative density was observed. Figure 55 shows representative SEM images of the crack propagation path for the indented 95% and 98% relative density LLZO samples. Using these data, a correlation between ionic conductivity and mechanical integrity was determined.

To correlate the effect of porosity on the CCD, dc cycling of Li/LLZO/Li symmetric cells was conducted. Several observations were made. First, a relative density of at least 85% is required to enable cycling of LLZO at reasonable current densities ( $\geq 0.1$  mA/cm<sup>2</sup>). Second, pellets with relative densities between 85-90% showed lower CCD compared to pellets with relative densities  $\geq 92\%$ . The project believes that increasing the relative density to values higher than 92% significantly increases the CCD of polycrystalline LLZO. Lastly, the highest CCD of 0.3 mA.cm<sup>-2</sup> was achieved for LLZO with 98±1%.

1. David, Isabel N., et al. "Microstructure and Li-ion Conductivity of Hot-pressed Cubic Li<sub>7</sub>La<sub>3</sub>Zr<sub>2</sub>O<sub>12</sub>" *J. Am. Ceram. Soc.* (2015).
2. Kim, Yunsung, et al. "The Effect of Relative Density on the Mechanical Properties of Hot-Pressed Cubic Li<sub>7</sub>La<sub>3</sub>Zr<sub>2</sub>O<sub>12</sub>." *J. Am. Ceram. Soc.* (2016).

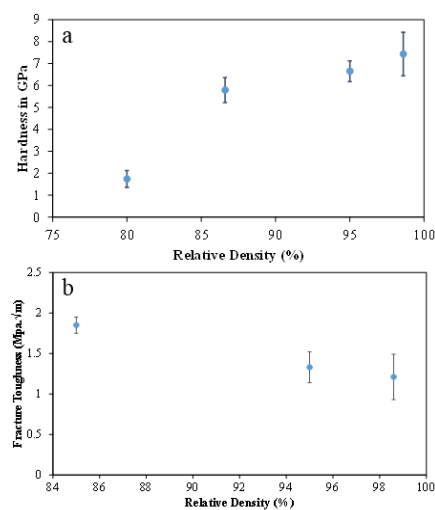


Figure 54. (a) Hardness and (b) fracture toughness as a function of relative density

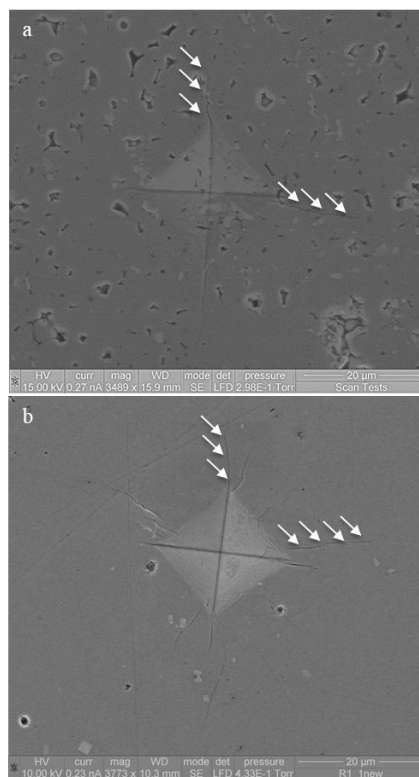


Figure 55. The Vickers indentation crack propagation path for (a) 92% and (b) 98% LLZO sample. Arrows point to the crack propagation path.

## Patents/Publications/Presentations

### Publication

- Sharafi, A., and H. Mayer, J. Nanda, J. Wolfenstine, J. Sakamoto. “Characterizing the Li-Li<sub>7</sub>La<sub>3</sub>Zr<sub>2</sub>O<sub>12</sub> Interface Stability and Kinetics as a Function of Temperature and Current Density.” *J. Power Resources* (2016).

### Presentations

- Material Research Society (2015): “The Stability of Garnet Based Li<sub>7</sub>La<sub>3</sub>Zr<sub>2</sub>O<sub>12</sub> and Li Anode Interface as a Function of Current Density”; A. Sharafi.
- PlugVolt (2015): “Recent Progress with Ceramic Solid Electrolytes for Advanced Battery Concepts”; A. Sharafi.
- Material Research Society (2015): “Garnet Ceramic Electrolyte Enabling Li Metal Anodes and Solid-State Batteries”; J. Sakamoto.
- Material Research Society (2015): “Room and Elevated Temperature Mechanical Behavior of Li<sub>7</sub>La<sub>3</sub>Zr<sub>2</sub>O<sub>12</sub>”; J. Wolfenstine.

## Task 7.3 – Composite Electrolytes to Stabilize Metallic Lithium Anodes (Nancy Dudney and Frank Delnick, Oak Ridge National Laboratory)

**Project Objective.** Prepare composites of representative polymer and ceramic electrolyte materials to achieve thin membranes that have the unique combination of electrochemical and mechanical properties required to stabilize the metallic lithium anode while providing for good power performance and long cycle life. Understand the lithium-ion transport at the interface between polymer and ceramic solid electrolytes, which is critical to the effective conductivity of the composite membrane. Identify key features of the composite composition, architecture, and fabrication that optimize the performance. Fabricate thin electrolyte membranes to use with a thin metallic lithium anode to provide good power performance and long cycle life.

**Project Impact.** A stable lithium anode is critical to achieve high energy density with excellent safety, lifetime, and cycling efficiency. This study will identify the key design strategies that should be used to prepare composite electrolytes to meet the challenging combination of physical, chemical, and manufacturing requirements to protect and stabilize the lithium metal anode for advanced batteries. By utilizing well characterized and controlled component phases, the design rules developed for the composite structures will be generally applicable toward the substitution of alternative and improved solid electrolyte component phases as they become available. Success in this program will enable these specific DOE technical targets: 500-700 Wh/kg, 3000-5000 deep discharge cycles, and robust operation.

**Approach.** This project seeks to develop practical solid electrolytes that will provide stable and long-lived protection for the lithium metal anode. Current electrolytes all have serious challenges when used alone: oxide ceramics are brittle, sulfide ceramics are air sensitive, polymers are too resistive and soft, and many electrolytes react with lithium. Composites provide a clear route to address these issues. This project does not seek discovery of new electrolytes; rather, the goal is to study combinations of current well known electrolytes. The project emphasizes the investigation of polymer-ceramic interfaces formed as bilayers and as simple composite mixtures where the effects of the interface properties can be readily isolated. In general, the ceramic phase is several orders of magnitude more conductive than the polymer electrolyte, and interfaces can contribute an additional source of resistance. Using finite element simulations as a guide, composites with promising compositions and architectures are fabricated and evaluated for lithium transport properties using ac impedance and dc cycling with lithium in symmetric or half cells. General design rules will be determined that can be widely applied to other combinations of solid electrolytes.

**Out-Year Goal.** Use advanced manufacturing processes where the architecture of the composite membrane can be developed and tailored to maximize performance and cost-effective manufacturing.

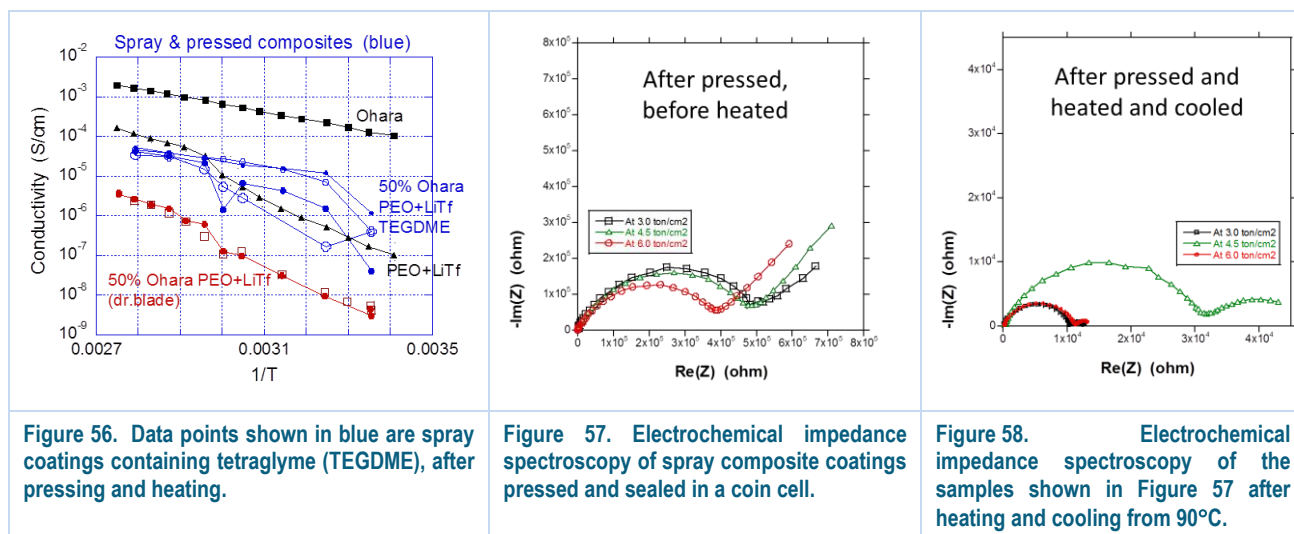
**Collaborations.** Electrolytes under investigation include a garnet electrolyte from Jeff Sakamoto (UM) and ceramic powder from Ohara. Staff at Corning Corporation will serve as the industrial consultant. Student intern, Cara Herwig, from Virginia Technological University assisted this quarter.

### Milestones

1. Measure the removal of solvent molecules introduced via solution synthesis or gas absorption from ceramic-polymer composite sheets under vacuum and heating conditions. (3/30/2016 – Ongoing)
2. Prepare ceramic-polymer electrolyte sheets with a coating and map the uniformity with nano-indentation and by profiling the Li plating. (9/30/2016 – On schedule)

## Progress Report

Composites of 50 vol% Ohara ceramic + PEO + LiTf were spray coated onto Al, Cu, and carbon coated Al foils. The slurry composition was modified to include tetraglyme (TEGDME), which improved the wetting and adhesion of the slurry to the foils and reduced the tendency of the coatings to crack upon drying. Because of the low vapor pressure, the TEGDME remains in the coating when the water is removed by drying overnight at 80°C. The project also anticipates that this plasticizer will passivate the Li contact. While the as-sprayed and dried coating was quite resistive (last quarterly report), after cold pressing and heating in a sealed coin cell, the conductivity of the coatings increased by at least an order of magnitude. Results are illustrated in Figures 56 to 58. Typically two coatings were pressed together to increase the thickness of the composite membrane and minimize the occurrence of shorts, but even so, the membranes were quite thin, on the order of 20  $\mu\text{m}$ . At low frequencies, the impedance spectroscopy suggests the possibility of a shorting or shuttle reaction that requires further investigation. Interestingly, the magnitude of the impedance agrees well with the earlier results of solvent-free melt formed composites that were subsequently treated with TEGDME vapor at room temperature. It appears that the role of TEGDME in both composites is to impede the crystallization of the PEO electrolyte. For further, an automated coating machine and a heated calendaring machine may be needed to ensure reproducible and high quality coatings, as hand spraying can sometimes lead to clumping when droplets dry before wetting the substrate.



Work also continued to quantify the solvent adsorption in melt processed composites. Thermal gravimetric analysis (TGA) was used to measure desorption of DMC and water from selected composites. The results indicate that the DMC vapor was indeed readily adsorbed by the composites, reaching at least 1 DMC molecule per Li ion in the composite. Surprisingly, the TGA results show that less water than DMC is adsorbed by the composite when available at similar vapor pressures and times.

## Patents/Publications/Presentations

### Presentation

- MRS meeting, Boston (December 2015): “A Composite Electrolyte for Solid State Lithium Batteries”; Nancy J. Dudney, Sergiy Kalnaus, Cara Herwig, and Frank Delnick.



## Task 7.4 – Overcoming Interfacial Impedance in Solid-State Batteries (Eric Wachsman, Liangbing Hu, and Yifei Mo, University of Maryland – College Park)

**Project Objective.** Develop a multifaceted and integrated (experimental and computational) approach to solve the key issue in solid-state, Li-ion batteries (SSLIBs), interfacial impedance, with a focus on garnet-based solid-state electrolytes (SSEs), the knowledge of which can be applied to other SSE chemistries. The focus is to develop methods to decrease the impedance across interfaces with the solid electrolyte, and ultimately demonstrate a high power/energy density battery employing the best of these methods.

**Project Impact.** Garnet electrolytes have shown great promise for safer and high-energy density batteries. The success of the proposed research can lead to dramatic progress on the development of SSLIBs based on garnet electrolytes. With regard to the fundamental science, the project methodology by combining computations and experiments can lead to an understanding of the thermodynamics, kinetics and structural stability, and evolution of SSLIBs with the garnet electrolytes. Due to the ceramic nature of garnet electrolyte, being brittle and hard, garnet electrolyte particles intrinsically lead to poor contacts among themselves or with electrode materials. A fundamental understanding at the nanoscale and through computations, especially with interface layers, can guide improvements to their design and eventually lead to the commercial use of such technologies.

**Approach.** SSLIB interfaces are typically planar, resulting in high impedance due to low specific surface area, and attempts to make 3D high surface area interfaces can also result in high impedance due to poor contact (for example, pores) at the electrode-electrolyte interface that hinder ion transport or degrade due to expansion/contraction with voltage cycling. This project will experimentally and computationally determine the interfacial structure-impedance relationship in SSLIBs to obtain fundamental insight into design parameters to overcome this issue. Furthermore, it will investigate interfacial modification (layers between SSE and electrode) to see if it can extend these structure-property relationships to higher performance.

**Collaborations.** This project is in collaboration with Dr. Venkataraman Thangadurai on garnet synthesis. It will collaborate with Dr. Leonid A. Bendersky (Leader, Materials for Energy Storage Program at NIST) and use neutron scattering to investigate the lithium profile across the bilayer interface with different charge-discharge rates. The project is in collaboration with Dr. Kang Xu in ARL with preparation of PFPE electrolyte.

### Milestones

1. Identify compositions of gel electrolyte to achieve  $100 \Omega \cdot \text{cm}^2$ . (Milestone 1 – Complete)
2. Determination of interfacial impedance in layered and 3D controlled solid state structures. (Milestone 2 – In progress)

## Progress Report

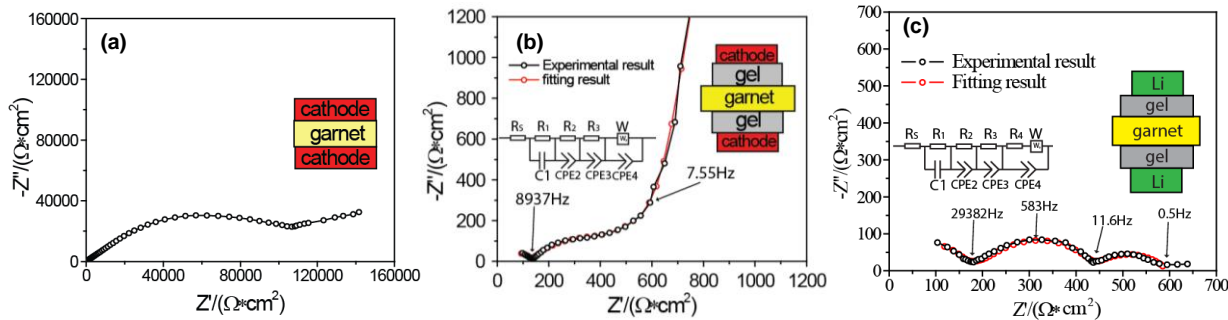


Figure 59. (a) Electrochemical impedance spectroscopy (EIS) plot of cathode/garnet/cathode half cell without gel electrolyte. (b) EIS of cathode/gel/garnet/gel/cathode half cell. (c) EIS of Li/gel/garnet/gel/Li half cell.

**Identify compositions of gel electrolyte to achieve  $100 \Omega \cdot \text{cm}^2$ .** Gel interface cells were fabricated and interfacial impedance determined by EIS. Figure 59a indicates that the total resistance of cathode/garnet/cathode half cell without electrolyte interfacial layer is  $\sim 10^6 \text{ Ohm} \cdot \text{cm}^2$  due to poor contact between the garnet electrolyte and  $\text{LiFePO}_4$  cathode. Gel electrolyte as an interlayer effectively solves this problem. Figure 59b is the EIS of cathode/gel/garnet/gel/cathode half-cell. The high-frequency arc is garnet interface, and low frequency is interfacial impedance. The interfacial resistance is about  $350 \text{ Ohm} \cdot \text{cm}^2$  for cathode/gel/garnet interface, much lower than that without the interlayer. Similar tests were done to lithium/gel/garnet/gel/lithium system. Figure 59c is the EIS plot of Li/gel/garnet/gel/Li. The interfacial impedance is  $\sim 250 \text{ Ohm} \cdot \text{cm}^2$  compared to that of the Li-garnet interface without the gel which is  $2 \times 10^5 \text{ Ohm} \cdot \text{cm}^2$ .

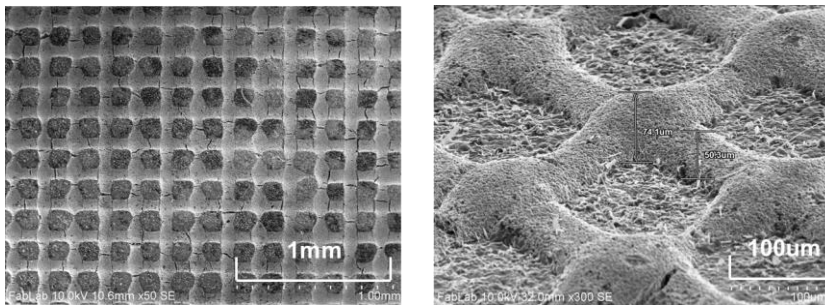


Figure 60. 3D surface modification of garnet extends the surface area.

### 3D printed garnet structure.

Fabrication of controlled garnet interface structures was accomplished by 3D printing. Garnet structures were printed directly on polished garnet disk surfaces using nScript 3D-printer followed by thermal treatment to burn out organics and form strong bond between layers. Figure 60 shows the printed microstructure on smooth garnet surface that provides greater contact surface area for subsequent cathode deposition.

## Patents/Publications/Presentations

### Presentations

- Materials Research Society, Boston (29 November – 4 December 2015): “All-Solid-State Li-Ion Batteries for Transformational Energy Storage”; Eric Wachsman.
- Materials Research Society, Boston (2015): “Stability of the Lithium Solid Electrolyte Materials and the Role of Interphases in All-Solid-State Li-Ion Batteries: Insights from First Principles Calculations”; Yizhou Zhu, Xingfeng He, and Yifei Mo.

### Publications

- Zhu, Yizhou, and Xingfeng He and Yifei Mo\*. “First Principles Study on Electrochemical and Chemical Stability of the Solid Electrolyte-Electrode Interfaces in All-Solid-State Li-Ion Batteries.” *Journal of Materials Chemistry A*. In press.
- Zhu, Yizhou, and Xingfeng He and Yifei Mo\*. “Origin of Outstanding Stability in the Lithium Solid Electrolyte Materials: Insights from Thermodynamic Analyses Based on First-Principles Calculations.” *ACS Applied Materials & Interfaces* 7 (2015): 23685–23693.

## Task 7.5 – Nanoscale Interfacial Engineering for Stable Lithium Metal Anodes (Yi Cui, Stanford University)

**Project Objective.** This study aims to render lithium metal anode with high capacity and reliability by developing chemically and mechanically stable interfacial layers between lithium metal and electrolytes, which is essential to couple with sulfur cathode for high-energy, lithium-sulfur batteries. With the nanoscale interfacial engineering approach, various kinds of advanced thin films will be introduced to overcome issues related to dendritic growth, reactive surface, and virtually “infinite” volume expansion of lithium metal anode.

**Project Impact.** Cycling life and stability of lithium metal anode will be dramatically increased. The success of this project, together with breakthroughs of sulfur cathode, will significantly increase the specific capacity of lithium batteries and decrease cost as well, therefore stimulating the popularity of EVs.

**Out-Year Goals.** Along with suppressing dendrite growth, the cycle life, CE, and current density of lithium metal anode will be greatly improved (No dendrite growth for current density up to  $3.0 \text{ mA/cm}^2$ , with CE > 99.5%) by choosing the appropriate interfacial nanomaterial along with rational electrode material design.

### Milestones

1. Demonstrate the improved cycling performance and effective dendrite suppression using nanoporous Li metal electrode with largely increased electrode active surface area. (12/31/2015 – Complete)
2. Achieve minimum relative volume change during electrochemical cycling via host-Li composite electrode design. (12/31/2015 – Complete)

## Progress Report

In addition to the well known problem of lithium metal anode such as dendrite formation and low cycling efficiency, virtually infinite volume change also prevents practical use of Li metal. Previously, this project developed a thermal infusion method to afford Li-coated polyimide (PI) nanoporous electrode. A thin layer of zinc oxide was applied at the interface between polymer and Li, whose “lithiophilicity” was essential for Li infusion.

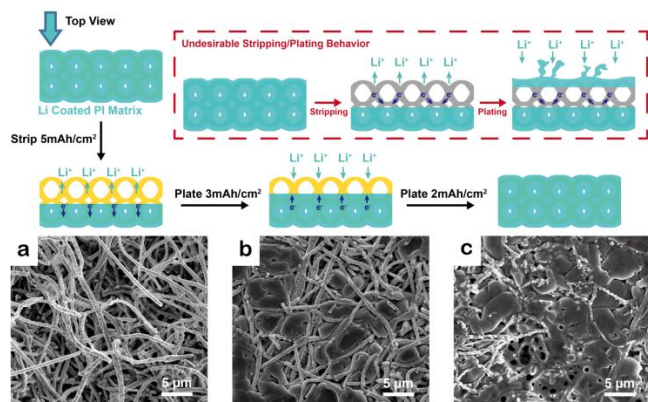


**Figure 61.** Scanning electron microscopy images and schematics showing the well-confined stripping/plating behavior of the Li-coated polyimide matrix. (a) Exposed top fibers after stripping away 5 mAh cm<sup>-2</sup> Li. (b) Exposed top fibers partially filled with Li when plating 3 mAh cm<sup>-2</sup> Li back. (c) Completely filled matrix after plating an additional 2 mAh cm<sup>-2</sup> Li back. The top-right schematic illustrates the alternative undesirable Li stripping/plating where after stripping, Li nucleates on the top surface, leading to volume change and dendrites shooting out of the matrix.

be efficiently transported to the electrolyte-facing top surface, undesirable stripping/plating behavior might occur after recurrent cycles. Direct Li nucleation on the top surface might be easier due to high availability of both electrons and Li ions, which provides favorable sites for dendrite growth while leaving interior voids empty.

To test the CE, hereby, the obtained nanoporous Li (~10 mAh/cm<sup>2</sup>) electrode was paired with lithium titanate (LTO, ~3 mAh/cm<sup>2</sup>) cathode to study its performance in a full cell configuration (Figure 62). The slightly oversized nanoporous Li-LTO exhibited outstanding cycling stability of more than 100 cycles compared to bare Li foil (50 μm, ~10 mAh/cm<sup>2</sup>) or electrodeposited Li, confirming the improved CE of the Li-coated PI nanoporous electrode.

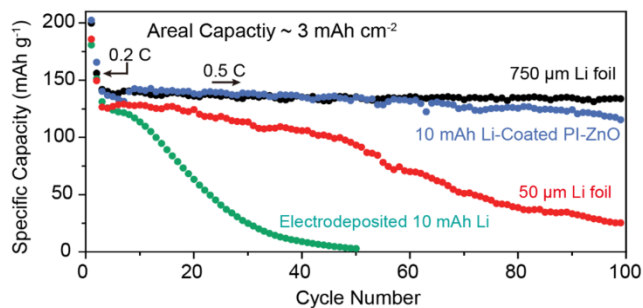


**Figure 62.** Discharge capacity of various Li metal anode-LTO cathode full cells for the first 100 galvanostatic cycles in EC/DEC with 1 vol % vinylene carbonate. Rate was set at 0.2 C for the first 2 cycles and 0.5 C for later cycles (1 C = 170 mA g<sup>-1</sup>).

### Patents/Publications/Presentations

Publication. Liu, Y., et al. “Lithium Coated Polymeric Matrix as Minimum Volume Change and Dendrite Free Lithium Metal Anode.” **In press**.



## Task 7.6 – Lithium Dendrite Suppression for Lithium-Ion Batteries (Wu Xu and Ji-Guang Zhang, Pacific Northwest National Laboratory)

**Project Objective.** The project objective is to enable lithium metal to be used as an effective anode in rechargeable Li-metal batteries for long cycle life at a reasonably high current density. The investigation will focus on the effects of various lithium salts, additives and carbonate-based electrolyte formulations on Li anode morphology, Li CE, and battery performances in terms of long-term cycling stability at room temperature and elevated temperatures and at various current density conditions, rate capability, and low-temperature discharge behavior. The surface layers on Li anode and cathode will be systematically analyzed. The properties of solvates of cation-solvent molecules will also be calculated to help explain the obtained battery performances.

**Project Impact.** Li metal is an ideal anode material for rechargeable batteries. Unfortunately, uncontrollable dendritic Li growth and limited CE during Li deposition/stripping inherent in these batteries have prevented their practical applications. This work will explore the new electrolyte additives that can lead to dendrite-free Li deposition with high CE. The success of this work will increase energy density of Li and Li-ion batteries and accelerate market acceptance of electrical vehicles (EV), especially for plug-in hybrid electrical vehicles (PHEV) required by the EV Everywhere Grand Challenge proposed by the DOE/EERE.

**Out-Year Goals.** The long-term goal of the work is to enable Li and Li-ion batteries with >120 Wh/kg (for PHEVs), 1000 deep-discharge cycles, a 10-year calendar life, improved abuse tolerance, and less than 20% capacity fade over a 10-year period.

**Collaborations.** This project engages in collaboration with the following:

- Bryant Polzin (ANL) – NCA, NMC and graphite electrodes
- Vincent Battaglia (LBNL) – LFP electrode
- Chongmin Wang (PNNL) – Characterization by TEM/SEM

### Milestones

1. Develop mixed salts electrolytes to protect Al substrate and Li metal anode, and to maintain Li CE over 98%. (12/31/2015 – Complete)
2. Demonstrate over 500 cycles for Li|LFP cells with high LFP loading and at high current density cycling. (3/31/2016 – Ongoing)
3. Demonstrate over 200 cycles for 4-V Li-metal batteries with high cathode loading and at high current density cycling. (6/30/2016 – Ongoing)
4. Achieve over 500 cycles for 4-V Li-metal batteries with high cathode loading and at high current density cycling. (9/30/2016 – Ongoing)

## Progress Report

This quarter, the effect of a LiTFSI-LiBOB dual-salt electrolyte with EC-EMC (ethyl methyl carbonate) solvent mixture on the cycling stability of Li||NCA coin cells at fast charging was investigated with a comparison to the control electrolyte based on 1.0 M LiPF<sub>6</sub>/EC-EMC. The anodic polarization tests at 60°C for one week indicate that both LiTFSI-LiBOB and LiPF<sub>6</sub> electrolytes are compatible with Al foil (the substrate for the cathode) at 4.3 V and 4.4 V. At 4.5 V, both electrolytes exhibit slight corrosion to Al, but the LiTFSI-LiBOB electrolyte shows much better stability (Figure 63a) than the LiPF<sub>6</sub> control electrolyte (Figure 63b). This LiTFSI-LiBOB electrolyte also enables the Li||NCA cells to exhibit good cycling stability during fast charging (at a relatively high current density of 1.5 mA/cm<sup>2</sup>) with a cycling efficiency of about 98%, while the cells with the LiPF<sub>6</sub> control electrolyte failed quickly at the same cycling condition (Figure 64). The analyses on the cycled Li anodes indicate that the LiTFSI-LiBOB dual-salt electrolyte had good film-formation ability on Li metal surface and the interface layer enriched with boron and sulfur species is highly conductive.

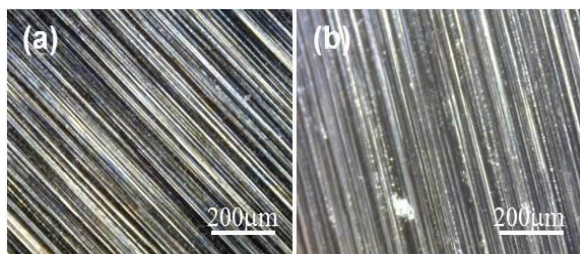


Figure 63. Optical images of Al foils after anodic polarization test at 4.5 V and 60°C for one week in the electrolytes of (a) LiTFSI-LiBOB and (b) LiPF<sub>6</sub> with EC-EMC solvent mixture.

The effect of discharging current density on the cycling performance of Li metal cells was studied as well. Similar to the charge current density, the discharge rate also greatly affects the cycling stability of Li metal batteries (Figure 65). For Li||NMC cells with an areal capacity of 2.0 mAh/cm<sup>2</sup>, discharge rates at and higher than 1C result in stable cycling for at least 150 cycles, while the discharge at less than 1C rate leads to fast capacity fading (Figure 65a). The evolution of charge/discharge voltage profiles at C/10 (Figure 65b) and 1C (Figure 65c) discharge rates corroborates the above finding. When the charge/discharge current density was switched back to C/10 after 150 cycles at C/3 charge and various discharge rates (Figure 65d), the cells cycled at and above 1C discharge rate could go back to the initial values, demonstrating good stability; however, the cells previously discharged at low rates could not, indicating capacity degradation is irreversible. More investigations are under way.

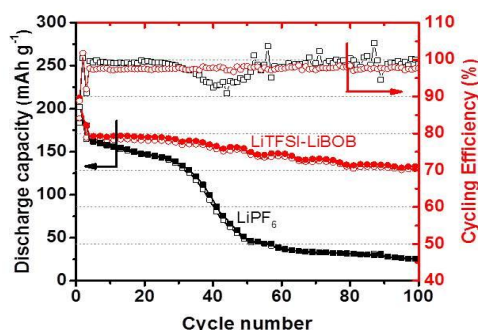


Figure 64. RT cycling performance of Li||NCA cells using LiTFSI-LiBOB and LiPF<sub>6</sub> electrolytes in the voltage range of 3.0 V and 4.3 V. The cells were cycled at 1C (that is, 1.5 mA/cm<sup>2</sup>) after two formation cycles at C/10 rate.

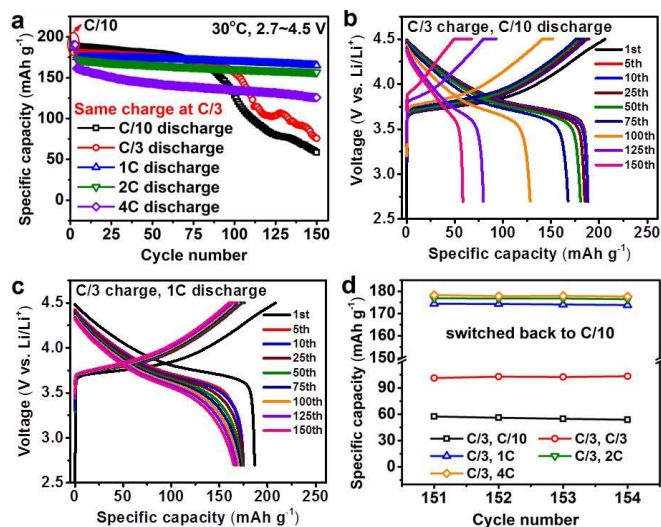


Figure 65. (a) Cycling stability of Li||NMC cells using LiPF<sub>6</sub> electrolyte at different discharge rates. (b-c) Evolution of charge/discharge voltage profiles at C/10 (b) and 1C (c) discharge. (d) Discharge capacities at C/10 after 150 cycles from (a). For all cells, the formation cycles were conducted at C/10 rate, and all other charge processes were performed at C/3 rate.

## Patents/Publications/Presentations

### Presentation

- 228<sup>th</sup> ECS Meeting, Phoenix (11–15 October 2015): “Behind the Stability of Graphite Anode in PC-Containing Electrolytes with a New Additive CsPF<sub>6</sub>”; H. Xiang, D. Mei, P. Yan, P. Bhattacharya, S. D. Burton, A. V. Cresce, R. Cao, M. H. Engelhard, M. E. Bowden, Z. Zhu, B. J. Polzin, C. Wang, K. Xu, J.-G. Zhang, and W. Xu.

### Publication

- Zheng, J., and P. Yan, R. Cao, H. Xiang, M. H. Engelhard, B. J. Polzin, C. Wang, J.-G., Zhang,\* and W. Xu.\* “Effects of Propylene Carbonate Content in CsPF<sub>6</sub>-Containing Electrolytes on the Enhanced Performances of Graphite Electrode for Lithium-Ion Batteries.” *ACS Appl. Mater. Interfaces*. Under review.

## TASK 8 – LITHIUM SULFUR BATTERIES

### Summary and Highlights

Advances in Li-ion technology have been stymied by challenges involved in developing high reversible capacity cathodes and stable anodes. Hence, there is a critical need for development of alternate battery technologies with superior energy densities and cycling capabilities. In this regard, lithium-sulfur batteries have been identified as the next flagship technology, holding much promise due to the attractive theoretical specific energy densities of 2,567 Wh/kg. In addition, realization of the high theoretical specific capacity of 1,675 mAh/g corresponding to formation of  $\text{Li}_2\text{S}$  using earth-abundant sulfur renders the system highly promising compared to other available cathode systems. Thus, the research focus has shifted to developing Li-S batteries. This system, however, suffers from major drawbacks, as elucidated below.

- Limited inherent electronic conductivity of sulfur and sulfur compound based cathodes.
- Volumetric expansion and contraction of both the sulfur cathode and lithium anode.
- Soluble polysulfide formation/dissolution and sluggish kinetics of subsequent conversion of polysulfides to  $\text{Li}_2\text{S}$  resulting in poor cycling life.
- Particle fracture and delamination as a result of the repeated volumetric expansion and contraction.
- Irreversible loss of lithium at the sulfur cathode, resulting in poor CE.
- High diffusivity of polysulfides in the electrolyte, resulting in plating at the anode and consequent loss of driving force (that is, drop in cell voltage).

These major issues cause sulfur loss from the cathode, leading to mechanical disintegration. Additionally, surface passivation of anode and cathode systems results in a decrease in the overall specific capacity and CE upon cycling. As a result, the battery becomes inactive within the first few charge-discharge cycles. Achievement of stable high capacity in Li-S batteries requires execution of fundamental studies to understand the degradation mechanisms in conjunction with engineered solutions. The BMR Task 8 addresses both aspects with execution of esoteric, fundamental *in situ* XAS and *in situ* electron paramagnetic resonance (EPR) studies juxtaposed with applied research comprising use of suitable additives, coatings, and exploration of composite morphologies. Both ANL and LBNL use X-ray based techniques to study phase evolution and loss of CE in  $\text{Se}_8$  during lithiation/delithiation, while understanding polysulfide formation in sulfur and polysulfides (PSL) in oligomeric polyethylene oxide (PEO) solvent, respectively. Work from PNNL, University of Pittsburgh (U Pitts), and Stanford University demonstrates high areal capacity electrodes in excess of 2 mAh/cm<sup>2</sup>. Following loading studies reported in the first quarter, PNNL has performed *in situ* EPR to study reaction pathways mediated by sulfur radical formation. Coating/encapsulation approaches adopted by U Pitts and Stanford comprise flexible sulfur wire (FSW) electrodes coated with Li-ion conductors, and  $\text{TiS}_2$  encapsulation of  $\text{Li}_2\text{S}$  in the latter, both ensuring polysulfide retention at sulfur cathodes. BNL work has focused on benchmarking of pouch cell testing by optimization of the voltage window and study of additives such as LiI and  $\text{LiNO}_3$ . *Ab initio* studies at Stanford and U Pitts involving calculation of binding energies and reaction pathways, respectively, augment the experimental results. *Ab initio* molecular dynamics (AIMD) simulations performed at TAMU reveal multiple details regarding electrolyte decomposition reactions and the role of soluble polysulfides (PS) on such reactions. Using KMC simulations, electrode morphology evolution and mesostructured transport interaction studies were also executed. Each of these projects has a collaborative team of experts with the required skill set needed to address the EV Everywhere Grand Challenge of 350 Wh/kg and 750 Wh/l, and cycle life of at least 1000 cycles.

The highlights from this quarter are as follows:

- Use of  $\text{TiS}_2$  as a substitute for conductive carbon in Li-S cells was demonstrated to yield improved high power cycling performance with both higher capacity and better capacity retention. (Gan, Takeuchi-BNL)
- Fluorinated co-solvent 1,3-dioxolane/1,1,2,2-tetrafluoroethyl-2,2,3,3-tetrafluoropropyl ether (DOL/TTE) showed (Amine-ANL) substantially higher CE than the commonly used solvent mixture 1,3-dioxolane/dimethyl ether (DOL/DME).

## Task 8.1 – New Lamination and Doping Concepts for Enhanced Li – S Battery Performance (Prashant N. Kumta, University of Pittsburgh)

**Project Objective.** To successfully demonstrate generation of novel sulfur cathodes for Li-S batteries meeting the targeted gravimetric energy densities  $\geq 350$  Wh/kg and  $\geq 750$  Wh/l with a cost target \$125/kWh and cycle life of at least 1000 cycles for meeting the EV Everywhere blueprint. The proposed approach will yield sulfur cathodes with specific capacity  $\geq 1400$  mAh/g, at  $\geq 2.2$  V, generating  $\sim 460$  Wh/kg energy density higher than the target. Full cells meeting the required deliverables will also be made.

**Project Impact.** Identification of new laminated Sulfur cathode based systems displaying higher gravimetric and volumetric energy densities than conventional lithium ion batteries will likely result in new commercial battery systems that are more robust, capable of delivering better energy and power densities, and more lightweight than current Li-ion battery packs. Strategies and configurations based on new lithium-ion conductor (LIC)-coated sulfur cathodes will also lead to more compact battery designs for the same energy and power density specifications as current Li-ion systems. Commercialization of these new S cathode based Li-ion battery packs will represent, fundamentally, a major hallmark contribution of the DOE VTO and the battery community.

**Out-Year Goals.** This is a multi-year project comprising of three major phases to be successfully completed in three years. Phase 1 (Year 1): Synthesis, Characterization and Scale up of suitable LIC matrix materials and multilayer composite sulfur cathodes. This phase is completed. Phase 2 (Year 2): Development of LIC coated sulfur nanoparticles, scale up of high-capacity engineered LIC coated multilayer composite electrodes and doping strategies for improving electronic conductivity of sulfur. Phase 3 (Year 3): Advanced high energy density, high rate, extremely cyclable cell development.

**Collaborations.** The project collaborates with the following members with the corresponding expertise:

- Dr. Spandan Maiti (U Pitts): for mechanical stability and multi-scale modeling
- Dr. A. Manivannan (NETL): for XPS for surface characterization
- Dr. D. Krishnan Achary (U Pitts): for solid-state magic angle spinning nuclear magnetic resonance (MAS-NMR) characterization

### Milestones

1. Develop novel LIC membrane systems using *ab initio* methods displaying impermeability to sulfur diffusion. (December 2014 – Complete)
2. Demonstrate capabilities for generation of novel sulfur 1D, 2D and 3D morphologies exhibiting superior stability and capacity. (June 2015 – Complete)
3. Identification and synthesis of LIC materials for use as coatings for sulfur cathodes. (June 2015 – Complete)
4. Identification of suitable dopants and dopant compositions to improve electronic conductivity of sulfur. (October 2015 – Complete)
5. Demonstrate synthesis of doped LIC membrane with improved Li-ion conductivity. (December 2015 – Complete)
6. Identify and develop effective coating methods to form a uniform lamina of LIC membrane over sulfur hetero-structures. (March 2016 – Ongoing)
7. Synthesis of VACNT and LIC coated nanosulfur based composite materials. (March 2016 – Ongoing)



## Progress Report

Phase 1 concluded with the successful identification of effective LIC membrane and the ability of LIC to shield the polysulfide species from dissolving into the electrolyte. Gel-based polymer electrolytes (GPE), flexible polymer-sulfur hybrids, and nanoporous complex framework materials (CFM) combined with novel LIC coating strategies improved cycling with scope for further improvement. The aim of Phase-2 studies is to

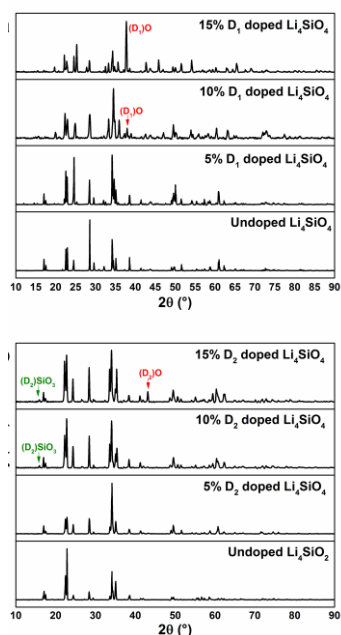


Figure 66. X-ray diffraction spectrum of  $\text{Li}_4\text{SiO}_4$  doped with (a) dopant  $\text{D}_1$  and (b) dopant  $\text{D}_2$ .

synthesize LIC materials identified in Phase 1, develop effective coating strategies of these materials, and to generate hetero structured composites of Sulfur with CNT. In FY15, DFT studies showed an improvement in ionic conductivity upon the introduction of vacancies in the lattice. Solid state high-temperature processing route from suitable precursors was employed to generate doped nanoparticles of LIC. Different precursor ratios were used to tailor the atomic% of lithium vacancies in the LIC and tested for ionic conductivity. Figure 66 shows the evolution of XRD spectra of LIC upon doping with two dopants  $\text{D}_1$  and  $\text{D}_2$ . Creation of vacancies in the LIC crystal structure by doping with  $\text{D}_1$  resulted in increase in conductivity from  $1.75 \times 10^{-12} \text{ S/cm}$  to  $1.41 \times 10^{-9} \text{ S/cm}$ , as shown by EIS analysis. Figure 67 shows the improvement in ionic conductivity of LIC upon doping  $\text{D}_1$  and  $\text{D}_2$ , as shown by EIS. Under another first-quarter subtask, nanostructured polymer-sulfur electrode system with higher sulfur content were synthesized using a combination of solution coating and vulcanization. These electrodes not only consisted of nanofibers but also displayed considerable flexibility for generation of bendable electrodes. The CFM networks from Phase 1 demonstrates stable cycling performance of  $\sim 650 \text{ mAh/g}$  for over 300 cycles with  $< 0.02\%$  fade rate. A comprehensive study utilizing sputter deposition technique to form uniform ultrathin coatings of LIC onto sulfur heterostructures has been initiated to meet second-quarter deliverables.

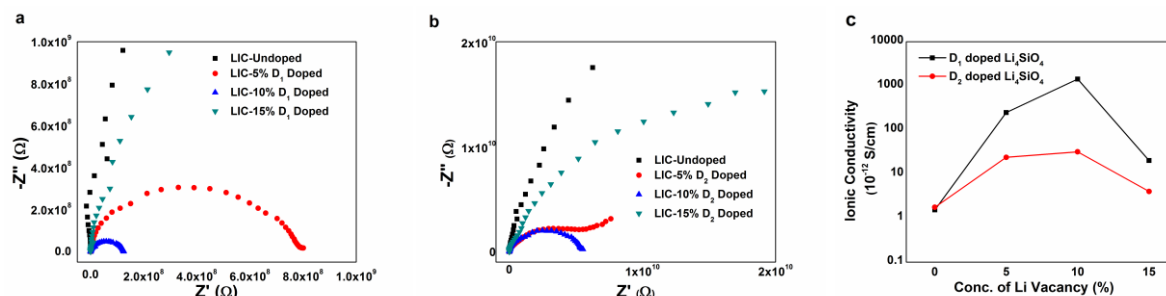


Figure 67. Electrochemical impedance spectroscopy plots of lithium-ion conductor for different doping concentration of (a) dopant  $\text{D}_1$  and (b) dopant  $\text{D}_2$ . (c) Ionic conductivity versus concentration of Li vacancies for dopants  $\text{D}_1$  and  $\text{D}_2$ .

## Patents/Publications/Presentations

Publication. Jampani, P. H., and B. Gattu, P. M. Shanthi, S. S. Damle, Z. Basson, R. Bandi, M. K. Datta, S. K. Park, and P. N. Kumta. "Flexible Sulfur Wires (Flex-SWs) – A Versatile Platform for Lithium-Sulfur Batteries." *J. Materials Chemistry A* (2016). In press.

## Task 8.2 – Simulations and X-ray Spectroscopy of Li-S Chemistry (Nitash Balsara, Lawrence Berkeley National Laboratory)

**Project Objective.** Lithium-sulfur cells are attractive targets for energy storage applications as their theoretical specific energy of 2600 Wh/kg is much greater than the theoretical specific energy of current lithium-ion batteries. Unfortunately, the cycle-life of lithium-sulfur cells is limited due to migration of species generated at the sulfur cathode. These species, collectively known as polysulfides, can transform spontaneously, depending on the environment, and it has thus proven difficult to determine the nature of redox reactions that occur at the sulfur electrode. The project objective is to use X-ray spectroscopy to track species formation and consumption during charge-discharge reactions in a lithium-sulfur cell. Molecular simulations will be used to obtain X-ray spectroscopy signatures of different polysulfide species, and to determine reaction pathways and diffusion in the sulfur cathode. The long-term objective is to use mechanistic information to build high specific energy lithium-sulfur cells.

**Project Impact.** Enabling rechargeable lithium-sulfur cells has the potential to change the landscape of rechargeable batteries for large-scale applications beyond personal electronics due to: (1) high specific energy, (2) simplicity and low cost of cathode (the most expensive component of current lithium-ion batteries), and (3) earth abundance of sulfur. The proposed diagnostic approach also has significant potential impact as it represents a new path for determining the species that form during charge-discharge reactions in a battery electrode.

**Out-Year Goals.** The out-year goals are as follows:

- Year 1: Simulations of sulfur and polysulfides (PSL) in oligomeric PEO solvent. Prediction of X-ray spectroscopy signatures of PSL/PEO mixtures. Measurement of X-ray spectroscopy signatures of PSL/PEO mixtures.
- Year 2: Use comparisons between theory and experiment to refine simulation parameters. Determine speciation in PSL/PEO mixtures without resorting to adhoc assumptions.
- Year 3: Build an all-solid lithium-sulfur cell that enables measurement of X-ray spectra *in situ*. Conduct simulations of reduction of sulfur cathode.
- Year 4: Use comparisons between theory and experiment to determine the mechanism of sulfur reduction and  $\text{Li}_2\text{S}$  oxidation in all-solid lithium-sulfur cell. Use this information to build lithium-sulfur cells with improved life-time.

**Collaborations.** This project collaborates with Tsu-Chien Weng, Dimosthenis Sokaras, and Dennis Nordlund at SSRL, SLAC National Accelerator Laboratory in Stanford, California.

### Milestones

1. Establish disproportionation thermodynamics in solvents with high and low electron pair donor (EPD) numbers using theoretical calculations. (12/15/15 – Complete)
2. Extend theoretical calculations of XAS to dimethylformamide, a model solvent for high electron pair donor number solvents that stabilize radical polysulfide anions. (2/15/16 – On schedule)
3. Perform *in situ* XAS tests of Li-S charge/discharge. (5/20/16 – On schedule)
4. Vary charge/discharge rate for *in situ* XAS testing; compare reaction pathways. (8/23/16 – On schedule)

## Progress Report

Recent literature surrounding Li-S chemistry has focused on the presence of radical polysulfide anions and the effects that these species may have on the charge and discharge processes. Work published by the Balsara/Prendergast team has shown that radical species simplify the reaction pathway; additionally, Nazar et al. have shown that radical species may be redox mediators. Thus, the aim of material development for Li-S batteries may soon point toward developing materials that facilitate radical formation. The question of what systems favor radical species is then an important one. Qualitatively, it is well known that radical species are favored in solvents with high EPD numbers like dimethylformamide (DMF). However, a quantitative and thermodynamic examination of the energetics of radical solvation in high EPD solvents versus low EPD solvents has not been carried out. Thus, the energy of formation of radical species in DMF (high EPD) and an ether-based solvent, diglyme (DGM) (low EPD), were calculated. As Figure 68 shows, the Gibbs free energy of formation for polysulfide radical anions in DMF is less than that in DGM, but within an order magnitude.

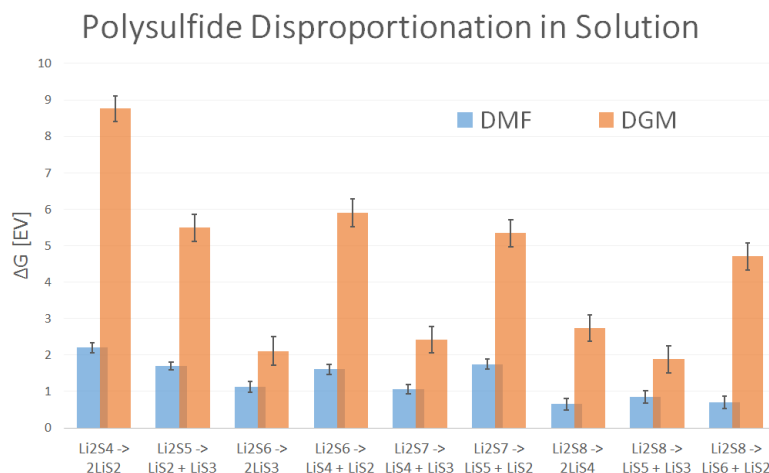


Figure 68. Energy of formation for radical polysulfide anions in dimethylformamide (DMF) and diglyme (DGM).

In addition to previously shown *in situ* XAS data for a discharging Li-S cell, also obtained is *in situ* XAS of a cell that was discharged and stopped mid-discharge at 2.25 V. After stopping, OCV was measured and spectra were obtained periodically for four hours (Figure 69). Thus, the data represent the disproportionation reactions that occur in the battery cathode. These data, as well as the previously shown *in situ* data, are under detailed analysis.

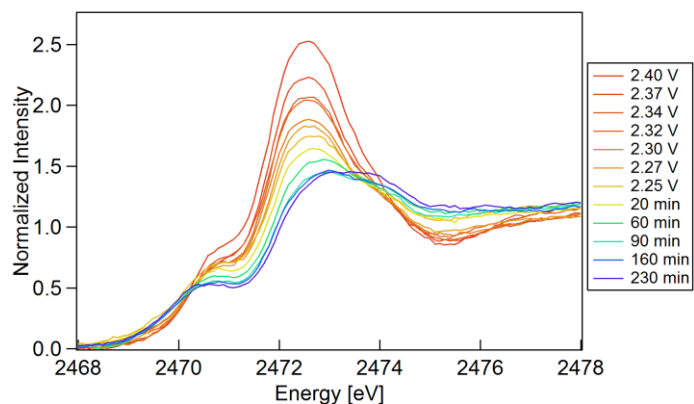


Figure 69. *In situ* X-ray absorption spectroscopy of an Li-S cell stopped mid-discharge at 2.25 V. Spectra taken thereafter represent the subsequent disproportionation process.

### Task 8.3 – Novel Chemistry: Lithium Selenium and Selenium Sulfur Couple (Khalil Amine, Argonne National Laboratory)

**Project Objective.** The project objective is to develop a novel  $S_xSe_y$  cathode material for rechargeable lithium batteries with high energy density and long life, as well as low cost and high safety.

**Project Impact.** Development of a new battery chemistry is promising to support the goal of PHEV and EV applications.

**Approach.** The dissolution of lithium polysulfides in nonaqueous electrolytes has been the major contribution to the low energy efficiency and short life of Li/S batteries. In addition, the insulating characteristics of both end members during charge/discharge (S and  $Li_2S$ ) limit their rate capacity. To overcome this problem, S or  $Li_2S$  are generally impregnated in a carbon conducting matrix for better electronic conductivity. However this makes it difficult to increase the loading density of practical electrodes. It is proposed here to solve the above barriers using the following approaches: (1) partially replace S with Se and (2) nano-confine the  $S_xSe_y$  in a nanoporous conductive matrix.

**Out-Year Goals.** When this new cathode is optimized, the following result can be achieved:

- A cell with nominal voltage of 2 V and energy density of 600 Wh/kg.
- A battery capable of operating for 500 cycles with low capacity fade.

**Collaborations.** This project engages in collaboration with the following:

- Prof. Chunsheng Wang of University of Maryland
- Dr. Yang Ren and Dr. Chengjun Sun of APS at ANL

### Milestones

The following are the milestones for each quarter during FY16:

1. Investigate the phase diagram of  $S_xSe_y$  system. (Q1 – Complete)
2. Encapsulating  $Se_2S_5$  in nanoporous carbon. (Q1 – Ongoing)
3. Investigating the impact of fluorinated solvents. (Initiation in Q2)
4. Stabilizing materials with a higher S content for a higher energy density. (Initiation in Q3)
5. Investigating the impact of the pore structure of carbon matrix. (Initiation in Q4)

## Progress Report

The S-Se phase diagram was previously explored using differential scanning microcalorimetry (DSC), Raman spectroscopy and high-energy X-ray diffraction (HEXRD). It was found that the alloying process between S and Se can result in an amorphous region, primarily resulting from the interaction between S and Se at the atomic level. This series of materials was further investigated using pair distribution function (PDF) measurements, carried out at sector 12-ID-B of the APS. Figure 70 shows the PDF profiles within the radial distance between 1.5 Å and 3.0 Å. The intensity of the PDF peak depicts the probability of finding a pair of atoms in the material with a specific radial distance. Figure 70 shows that that S-S bond length is about 2.067 Å, while the Se-Se length is about 2.368 Å. In the high S-content region (bottom part), the S-S length remains constant, and its intensity decreases with the addition of Se. However, in the high Se-content region (top part), the Se-Se distance decreases with the addition of S to Se.

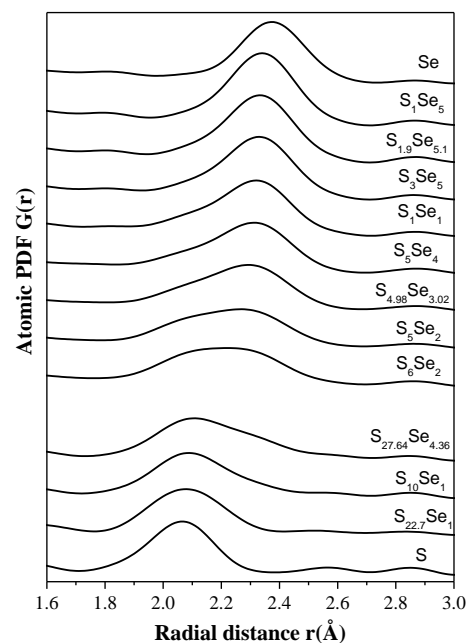


Figure 70. PDF profiles of  $S_xSe_y$  showing the dependence of the bond length on the composition of the materials.

Last quarter, it was reported that the addition of fluoroether 1,1,2,2-tetrafluoroethyl-2,2,3,3-tetrafluoropropyl ether (TTE) as a co-solvent improved the reversible specific capacity, as well as the capacity retention during continuous charge/discharge cycling of the  $S_5Se_2/Li$  cell. Figure 71 compares the electrochemical performance of  $S_5Se_2/Li$  cells using different electrolytes. Please note that DOL stand for 1,3-dioxolane and DME stands for dimethyl ether. Figure 71 clearly shows that both cells had similar charge capacity during the electrochemical test. However, a severe gap between the charge capacity and discharge capacity was observed for the cell using the non-fluorinated solvent (DOL/DME). This gap is primarily caused by the dissolution of lithium polysulfides or lithium polyselenide, which significantly reduces the CE. On the other hand, the cell using a fluorinated co-solvent (DOL/TTE) showed substantially higher CE and a good capacity retention. The impact of the solvent on the electrochemical performance of  $S_xSe_y/Li$  cells will be systematically investigated in the coming quarters.

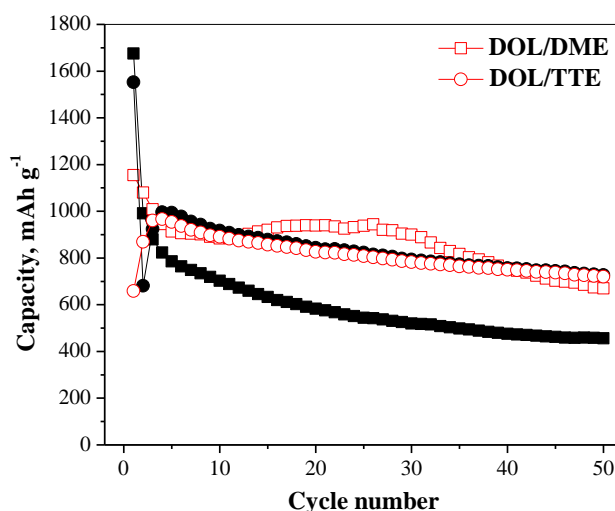


Figure 71. Charge/discharge capacity of  $S_5Se_2/Li$  cells using different electrolytes, showing that the fluorinated ether significantly suppresses the shuttle mechanism and has a high Coulombic efficiency. Note that open symbols are for charge capacities, and solid symbols are for discharge capacity.

## Patents/Publications/Presentations

Presentation. Fall Meeting of Material Research Society, Boston (November 2015): “Rechargeable Batteries Using  $S_xSe_y$  Cathodes”; Z. H. Chen and K. Amine. Invited.

## Task 8.4 – Multi-Functional Cathode Additives (MFCA) for Li-S Battery Technology (Hong Gan, Brookhaven National Laboratory; and Co-PI Esther Takeuchi, Brookhaven National Laboratory and Stony Brook University)

**Project Objective.** Develop a low-cost battery technology for PEV application utilizing Li-S electrochemical system by incorporating multifunctional cathode additives (MFCA), consistent with the long-term goals of the DOE EV Everywhere Grand Challenge.

**Project Impact.** The Li-S battery system has gained significant interest due to its low material cost potential (35% cathode cost reduction over Li-ion) and its attractive 2.8x (volumetric) to 6.4x (gravimetric) higher theoretical energy density compared to conventional Li-ion benchmark systems. Commercialization of this technology requires overcoming several technical challenges. This effort will focus on improving the cathode energy density, power capability, and cycling stability by introducing MFCA. The primary deliverable is to identify and characterize the best MFCA for Li-S cell technology development.

**Approach.** Transition metal sulfides are evaluated as cathode additives in sulfur cathode due to their high electronic conductivity and chemical compatibility to the sulfur cell system. Electrochemically active additives are also selected for this investigation to further improve energy density of the sulfur cell system. In the first year, the team has established the individual baseline sulfur and transition metal sulfide coin cell performances, and demonstrated the strong interactions between sulfur and various MFCA within the hybrid electrode.  $\text{TiS}_2$  and  $\text{FeS}_2$  were selected as the leading candidates for additional optimization studies with synthetic method developed. During the second year, leading candidates for the cathode optimization studies will be further narrowed down. More attention will be directed into electrode optimization and cell system optimization for improved electrode integrity, energy density and electrochemical charge/discharge cycling performance. Examples for these effort are electrode components (binder, carbon) and electrode formulation optimization, and electrolyte optimization, etc.

**Out-Year Goals.** This is a multi-year project comprised of two major phases to be successfully completed in three years. Phase 1 includes cathode and MFCA proof of concept investigations to be mostly completed during year 1 investigations. Phase 2 will include cell component interaction studies and full cell optimization. The work scope for year 2 will focus on the leading MFCA candidate selection, followed by hybrid electrode processing, material and formulation studies for optimized energy density, and cell electrochemical performance testing. The mechanistic studies of MFCA and sulfur interaction will continue throughout the year to advance fundamental understanding of the system.

**Collaborations.** This project collaborates with Dong Su at BNL and with Amy Marschilok and Kenneth Takeuchi at SBU.

### Milestones

1. Synthesized MFCA evaluation and selection. (Q1 – Ongoing)
2. MFCA particle size effect study and best candidate selection. (Q2 – Ongoing)
3. Cathode process and material optimization. (Q3 – On schedule)
4. Cathode formulation optimization. (Q4 – On schedule)



## Progress Report

**Synthesized FeS<sub>2</sub> evaluation.** The effect of synthesized FeS<sub>2</sub> was evaluated in sulfur hybrid electrodes this quarter. To access the electrochemical performance of FeS<sub>2</sub>, discharge to ~1 V in the first cycle is needed. A large internal cell resistance developed as the cells were cycled from 2.6 V to 1.0 V due to the reduction of LiNO<sub>3</sub> at a voltage below 1.6 V. Removing LiNO<sub>3</sub> from the electrolyte led to a severe shuttling effect during cell charging, preventing cell cycling. Therefore, evaluation of the S:FeS<sub>2</sub> hybrid cells with synthesized FeS<sub>2</sub> was performed with cycling between 2.6 V and 1.8 V at a 1C rate in the presence of LiNO<sub>3</sub>. Although the presence of FeS<sub>2</sub> exhibited no detrimental effect, notably, synthesized FeS<sub>2</sub> was necessary, yet no significant improvement in cycling performance was seen (Figure 72).

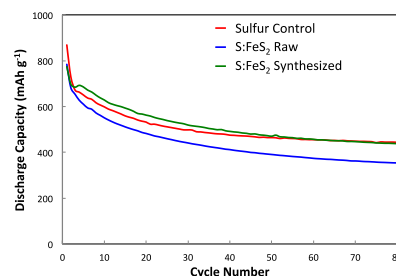


Figure 72. Synthesized FeS<sub>2</sub> in hybrid cathode.

**TiS<sub>2</sub> particle size effect.** TiS<sub>2</sub> was demonstrated to have a beneficial effect on sulfur cell cycling. The particle size effect of TiS<sub>2</sub> was studied this quarter. The raw TiS<sub>2</sub> material with BET surface area of 3.7 m<sup>2</sup>/g was milled to produce a sample with BET surface area of 9.4 m<sup>2</sup>/g with reduced particle size. By substituting part of the carbon in the control electrode (S:C:PVDF = 50:42:8) with either raw or milled TiS<sub>2</sub>, hybrid electrodes (S:TiS<sub>2</sub>:C:PVDF = 50:17:25:8) were prepared. Electrodes with the milled TiS<sub>2</sub> exhibited more uniform Ti distribution than the raw TiS<sub>2</sub> sample, as evidenced by EDS mapping (Figure 73). The cycling performance of the hybrid electrodes using TiS<sub>2</sub> additive and control sulfur electrodes under 2C rate discharge is shown in Figure 74. Clearly, both cells with electrodes containing the TiS<sub>2</sub> additive exhibited higher discharge capacities and lower capacity fade than the control cells over 300 cycles, which is consistent with the observation from the previous proof of concept study. In addition, the hybrid electrodes with the milled TiS<sub>2</sub> resulted in better overall cycling capacity retention than the cells with raw TiS<sub>2</sub> additive. The data demonstrate that smaller particle size and more uniform distribution of TiS<sub>2</sub> within the sulfur electrode is beneficial for sulfur cell cycle life under a 2C rate discharge.

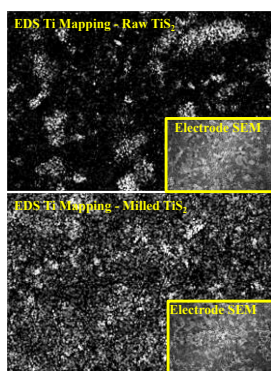


Figure 73. Ti Mapping by EDS.

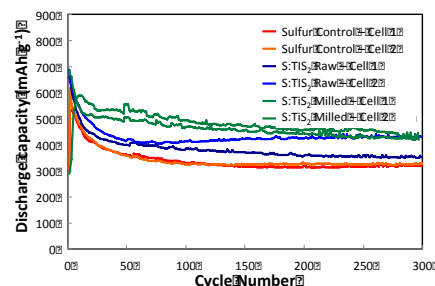


Figure 74. TiS<sub>2</sub> particle size effect on S:TiS<sub>2</sub> hybrid electrode cell cycling at 2C discharge rate.

**High-power TiS<sub>2</sub> cell demonstration.** The TiS<sub>2</sub> electrode high-power capability was also examined. Cells with cathode formulation of TiS<sub>2</sub>:Carbon:PVDF ratio 85:0:15 were compared with control cells with ratio of 70:15:15. Figure 75 shows the cycling capability of these cells at various cycling rates between 3.0 V to 1.5 V. For cells without carbon, >40% of the theoretical capacity was delivered at 10C rate, indicating the conducting nature of the TiS<sub>2</sub>. These results corroborate the above finding that TiS<sub>2</sub> can be used as a conductive additive to replace part of the carbon in sulfur electrode and yield improved high-power cycling performance with both higher capacity and better capacity retention.

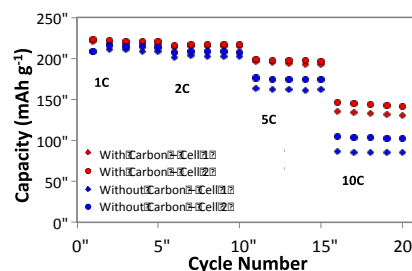


Figure 75. High-power TiS<sub>2</sub> cell without carbon.

## Patents/Publications/Presentations

### Publication

- Sun, Ke, and Dong Su, Qing Zhang, David C. Bock, Amy C. Marschilok, Kenneth J. Takeuchi, Esther S. Takeuchi, and Hong Gan. “Interaction of CuS and Sulfur in Li-S Battery System.” *J. Electrochem. Soc.* 162, no. 14 (2015): A2834–A2839.

### Presentations

- American Institute of Chemical Engineers (AIChE) Annual Meeting (8–13 November 2015): “The Effects of Carbon Type and Cathode Loading on Li-S Battery Performance”; Helen Liu, Ke Sun, and Hong Gan. Poster.
- Long Island Forum for Technology (LIFT), Farmingdale State College Renewable Energy and Sustainability Center (4 December 2015): “Li-S Battery – Sulfur Utilization and Cell Design”; Hong Gan, Ke Sun, and Helen Liu.

## Task 8.5 – Development of High-Energy Lithium-Sulfur Batteries (Jie Xiao and Jun Liu, Pacific Northwest National Laboratory)

**Project Objective.** The project objective is to develop high-energy, low-cost lithium sulfur (Li-S) batteries with long lifespan. All proposed work will employ thick sulfur cathode ( $\geq 2$  mAh/cm<sup>2</sup> of sulfur) at a relevant scale for practical applications. The diffusion process of soluble polysulfide out of thick cathode will be revisited to investigate cell failure mechanism at different cycling. Alternative anode will be explored to address the lithium anode issue. The fundamental reaction mechanism of polysulfide under the electrical field will be explored by applying advanced characterization techniques to accelerate development of Li-S battery technology.

**Project Impact.** The theoretical specific energy of Li-S batteries is ~2300 Wh/kg, which is almost three times higher than that of state-of-the-art Li-ion batteries. The major challenge for Li-S batteries is polysulfide shuttle reactions, which initiate a series of chain reactions that significantly shorten battery life. The proposed work will design novel approaches to enable Li-S battery technology and accelerate market acceptance of long-range EVs required by the EV Everywhere Grand Challenge.

**Out-Year Goals.** This project has the following out-year goals:

- Fabricate Li-S pouch cells with thick electrodes to understand sulfur chemistry/electrochemistry in the environments similar to the real application.
- Leverage the Li-metal protection project funded by the DOE and PNNL advanced characterization facilities to accelerate development of Li-S battery technology.
- Develop Li-S batteries with a specific energy of 400 Wh/kg at cell level, 1000 deep-discharge cycles, improved abuse tolerance, and less than 20% capacity fade over a 10-year period to accelerate commercialization of electrical vehicles.

**Collaborations.** This project engages in collaboration with the following:

- Dr. Xiao-Qing Yang (LBNL) – *In situ* characterization
- Dr. Bryant Polzin (ANL) – Electrode fabrication
- Dr. Xingcheng Xiao (GM) – Materials testing
- Dr. Jim De Yoreo (PNNL) – *In situ* characterization

### Milestones

1. SEI study on graphite surface in the new EC-free electrolyte. (12/31/2015 – Complete)
2. Demonstrate prototype Li-ion sulfur cells with > 95% CE (no additive) and > 80% capacity retention for 100 cycles. (3/31/2016 – In progress)
3. Identify effective approaches to facilitate electrolyte penetration within thick sulfur cathode ( $\geq 4$  mg/cm<sup>2</sup>). (6/30/2016 – In progress)
4. Complete pouch cell assembly and testing by using optimized electrode and electrolyte. (9/30/2016 – In progress)

## Progress Report

Previous reports indicated that long-term cycling stability of Li-S batteries strongly depended on the stability of Li metal anode. To decouple the sulfur cathode from sophisticated side reactions initiating on Li anode side, a new prototype of “Li-ion sulfur” battery was developed by using intercalation compound, graphite as the anode, which was stable in the 5M LiTFSI-DOL electrolyte in the absence of EC additive (M refers to mol salt/liter solvent). The finding of this new series of ether-based electrolyte enabled the stable cycling of graphite in sulfur batteries, which provided a unique platform to further understand the fundamental reaction mechanism in the sulfur cathode side.

This quarter, interfacial reactions on graphite in the 5M LiTFSI-DOL were carefully explored. An *in situ* AFM was used to study a freshly cleaved Highly Oriented Pyrolytic Graphite (HOPG) electrode immersed in this electrolyte with/without an electric field. In the absence of the field, highly ordered surface structures covering the surface of the HOPG were clearly observed (Figure 76a). The application of the polarization (electric field) to the HOPG electrode (working electrode) led to profound changes at the electrode surface. Immediately upon polarization of the electrode to 1.0 V (vs.  $\text{Li}^+/\text{Li}$ ) from the open circuit potential (OCP) at 2.85 V, the HOPG surface transformed from the ordered structure (Figure 76a) into a compact surface coating (Figure 76b), denoting the fast response of the surface structuring to an electric field. Shortly thereafter, a second, non-uniform coating of crystal-like aggregates began to grow above the compact coating. Polarization to more negative potentials and for longer periods of time resulted in the continuous growth of this second coating (Figure 76c-e). Upon removal of the field, that is, at OCP, the height of the second layer coating decreased and almost completely disappeared after a 20 min rest (Figure 76f-h). The formation of these coatings at low potential was largely reversible, indicating that their identities differed markedly from that of a traditional insoluble SEI layer. Notably, a significant restructuring of the surface was evident at 1.0 V (Figure 76b), a potential at which there was a negligible current (from CV data, not shown here), confirming that solvent/anion reduction reactions were not the origin of the transformation. Instead, a completely new SEI formation and function mechanism has been discovered, in which the electrolyte components reversibly formed a protective surface coating on a graphite electrode during the  $\text{Li}^+$  intercalation/de-intercalation upon changing the potential (Figure 76j).

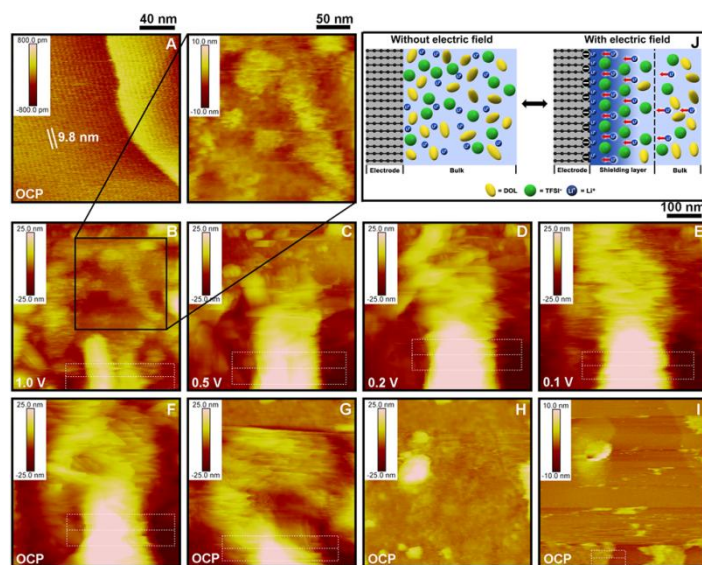


**Figure 76.** AFM topographic images of an HOPG electrode immersed in 5M LiTFSI-DOL electrolyte with and without electrode polarization. (a) Before polarization (at open circuit potential). Polarized at: (b) 1.0 V, (c) 0.5 V, (d) 0.2 V, (e) 0.1 V. Time after removal of polarization: (f) 10.4 min, (g) 17.2 min, (h) 20.5 min. Time after addition of free DOL in (h): (i) 24.2 min. (j) Schematic diagram of electrode-concentrated electrolyte interface with and without electrode polarization.

## Patents/Publications/Presentations

Publication. Lu, D., and J. Tao, P. Yan, W. A. Henderson, Q. Li, Y. Shao, G. L. Graff, B. Polzin, C. Wang, J. Zhang, J.D. Yoreo, J. Liu, and J. Xiao. “Reversible Shielding of Electrodes.” *Nature Materials*. Under review.

## Task 8.6 – Nanostructured Design of Sulfur Cathodes for High Energy Lithium-Sulfur Batteries (Yi Cui, Stanford University)

**Project Objective.** The charge capacity limitations of conventional transition metal oxide cathodes are overcome by designing optimized nano-architected sulfur cathodes.

This study aims to enable sulfur cathodes with high capacity and long cycle life by developing sulfur cathodes from the perspective of nanostructured materials design, which will be used to combine with lithium metal anodes to generate high-energy lithium-sulfur batteries. Novel sulfur nanostructures as well as multifunctional coatings will be designed and fabricated to overcome issues related to volume expansion, polysulfide dissolution, and the insulating nature of sulfur.

**Project Impact.** The capacity and the cycling stability of sulfur cathode will be dramatically increased. This project's success will make lithium-sulfur batteries to power electric vehicles and decrease the high cost of batteries.

**Out-Year Goals.** The cycle life, capacity retention, and capacity loading of sulfur cathodes will be greatly improved (200 cycles with 80% capacity retention,  $>0.3 \text{ mAh/cm}^2$  capacity loading) by optimizing material design, synthesis and electrode assembly.

**Collaborations.** This project engages in collaboration with the following:

- BMR program principal investigators
- SLAC: *In situ* X-ray, Dr. Michael Toney
- Stanford: Prof. Nix, mechanics; Prof. Bao, materials

### Milestones

1. Demonstrate synthesis to generate monodisperse sulfur nanoparticles with/without hollow space. (October 2013 – Complete)
2. Develop surface coating with one type of polymers and one type of inorganic materials. (January 2014 – Complete)
3. Develop surface coating with several types of polymers; Understand amphiphilic interaction of sulfur and sulfide species. (April 2014 – Complete)
4. Demonstrate sulfur cathodes with 200 cycles with 80% capacity retention and  $0.3 \text{ mAh/cm}^2$  capacity loading. (July 2014 – Complete)
5. Demonstrate  $\text{Li}_2\text{S}$  cathodes capped by layered metal disulfides. (December 2014 – Complete)
6. Identify the interaction mechanism between sulfur species and different types of sulfides/oxides/metals, and find the optimal material to improve the capacity and cycling of sulfur cathode. (July 2015 – On track)
7. Demonstrate the balance of surface adsorption and diffusion of  $\text{Li}_2\text{S}_x$  species on nonconductive metal oxides. (December 15 – Complete)



## Progress Report

Last quarter, the electrochemical performance of sulfur cathodes incorporated with non-conductive oxides, including  $\text{Al}_2\text{O}_3/\text{C}$ ,  $\text{CeO}_2/\text{C}$ ,  $\text{La}_2\text{O}_3/\text{C}$ ,  $\text{MgO}/\text{C}$ ,  $\text{CaO}/\text{C}$  composites was evaluated. The cathodes based on  $\text{MgO}/\text{C}$ ,  $\text{CeO}_2/\text{C}$ ,  $\text{La}_2\text{O}_3/\text{C}$  show better cycling performance and higher capacities than that of  $\text{Al}_2\text{O}_3/\text{C}$  and  $\text{CaO}/\text{C}$ . Adsorption experiments and DFT calculation reveal that the polysulphide capture on the metal oxides is monolayered chemisorption. In this report, the DFT results indicate that the better surface diffusion leads to higher deposition efficiency of sulphur species on electrodes.

The diffusion of lithium on the surface of various metal oxides has been investigated by DFT calculation (Figure 77). Because the most favorable binding site of sulphides is two Li bonding with metal oxide, the calculated Li ion diffusion can also indicate the diffusivity of sulphides on the surface of the oxide. On  $\text{MgO}(100)$ ,  $\text{CaO}(100)$ , and  $\text{La}_2\text{O}_3(001)$  surfaces, the diffusions of Li in different dimensional can be realized on three equivalent adsorption sites (Figure 77). Among the three kinds of surfaces, the diffusion barrier of Li on  $\text{CaO}(100)$  is largest. The space group of  $\text{MgO}$  is the same with  $\text{CaO}$ ; however, the diffusion barrier of Li on  $\text{MgO}(100)$  is about 0.45 eV lower than that on  $\text{CaO}(100)$ . The suitable adsorption energies of lithium sulphur species and small diffusion barriers of Li on  $\text{MgO}$  will lead to the formation of abundant lithium sulphide particles on  $\text{MgO}/\text{C}$  surfaces, which are responsible for the best cycling performance of  $\text{MgO}/\text{C}$  cathodes. On  $\text{CeO}_2(111)$  surfaces, the large diffusion barrier is 0.66 eV, which is similar with that on  $\text{La}_2\text{O}_3(001)$  surfaces. This may explain why  $\text{CeO}_2/\text{C}$  and  $\text{La}_2\text{O}_3/\text{C}$  cathodes show similar cycling performance. Among the five kinds of metal oxides surfaces, the largest diffusion barrier (1.22 eV) of Li is found to be on  $\text{Al}_2\text{O}_3(110)$ , which is about three times of that on  $\text{MgO}(100)$ . It is seen that lithium sulphide species can strongly adsorb; however, it is difficult to diffuse on  $\text{Al}_2\text{O}_3$ . Although  $\text{Al}_2\text{O}_3$  has the best  $\text{Li}_2\text{S}_8$  adsorption performance, the slow diffusion of  $\text{Li}_2\text{S}_x$  indicated that  $\text{Al}_2\text{O}_3$  may not be a good additive for sulphur cathode. The results indicate that an optimized balance between lithium polysulphides adsorption and surface diffusion is favorable for the lithium sulphide species deposition on the surface of oxide/carbon matrix, keeping materials active during the cycling and ensuring final good cycling performance of batteries.

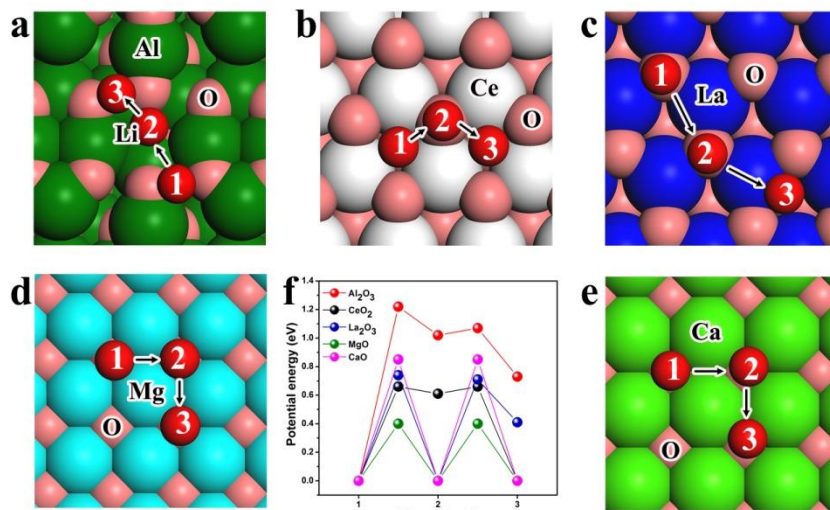


Figure 77. Lithium diffusion mechanism on the surface of various metal oxides. (a-e) Minimum energy path for lithium ion diffusion on  $\text{Al}_2\text{O}_3(110)$ ,  $\text{CeO}_2(111)$ ,  $\text{La}_2\text{O}_3(001)$ ,  $\text{MgO}(100)$  and  $\text{CaO}(100)$  surfaces, respectively. (f) Potential energy profiles for  $\text{Li}^+$  diffusion along different adsorption sites on the oxide surface.



## Task 8.7 – Addressing Internal “Shuttle” Effect: Electrolyte Design and Cathode Morphology Evolution in Li-S Batteries (Perla Balbuena, Texas A&M University)

**Project Objective.** The project objective is to overcome the lithium-metal anode deterioration issues through advanced Li-anode protection/stabilization strategies including (i) *in situ* chemical formation of a protective passivation layer and (ii) alleviation of the “aggressiveness” of the environment at the anode by minimizing the polysulfide shuttle with advanced cathode structure design.

**Project Impact.** Through formulation of alternative electrolyte chemistries as well as design, fabrication, and test of improved cathode architectures, it is expected that this project will deliver Li/S cells operating for 500 cycles at efficiency greater than 80%.

**Approach.** A mesoscale model including different realizations of electrode mesoporous structures generated based on a stochastic reconstruction method will allow virtual screening of the cathode microstructural features and the corresponding effects on electronic/ionic conductivity and morphological evolution. Interfacial reactions at the anode due to the presence of polysulfide species will be characterized with *ab initio* methods. For the cathode interfacial reactions, data and detailed structural and energetic information obtained from atomistic-level studies will be used in a mesoscopic-level analysis. A novel sonochemical fabrication method is expected to generate controlled cathode mesoporous structures that will be tested along with new electrolyte formulations based on the knowledge gained from the mesoscale and atomistic modeling efforts.

**Out-Year Goals.** By determining reasons for successes or failures of specific electrolyte chemistries, and assessing relative effects of composite cathode microstructure and internal shuttle chemistry versus that of electrolyte chemistry on cell performance, expected results are : (1) develop an improved understanding of the Li/S chemistry and ways to control it; (2) develop electrolyte formulations able to stabilize the Li anode; (3) develop new composite cathode microstructures with enhanced cathode performance; and (4) develop a Li/S cell operating for 500 cycles at an efficiency > 80%.

**Collaborations.** This is a collaborative work combining first-principles modeling (Perla Balbuena, TAMU), mesoscopic level modelling (Partha Mukherjee, TAMU), and synthesis, fabrication, and test of Li/S materials and cells (Vilas Pol, Purdue University).

### Milestones

1. Complete coin cell testing of various C/S electrodes. (December 2015 – Complete)
2. Using electrochemical and transport modeling gain an understanding of the mesoscopic interfacial reactions. (March 2016)
3. Complete evaluation of deposition-induced stress and mechanical interplay. (June 2016)
4. Determination of SEI nucleation and growth at the PS/Li anode interface . *Go/No-Go*: Determine reasons for electrolyte failure or success. (September 2016)

## Progress Report

**Experimental advances to control polysulfide dissolution at the C/S cathode.** Low dopant values of various metals, metal oxides, and metal composites synthesized via a solid-state thermal decomposition technique were tested with varying degrees of success to polysulfide suppression. Chemical barriers of metal or metal oxide composition were deposited onto the surface of lithium-sulfur battery cathodes using a specific ALD technique via pulse-layering exposures, which allows deposition of a metal or metal oxide layer coating onto the surface of a lithium-sulfur cathode electrode without disruption or sublimation of the sulfur content of the electrode at  $\sim 80^\circ\text{C}$ . The coatings studied include aluminum oxide, and fluorinated aluminum-tungsten composites (Figure 78). It is concluded that the coating thickness plays a pivotal role upon the effectiveness of an underlying polysulfide retention mechanism. Additional experiments are underway to understand and optimize the aforementioned coatings and new formulations.

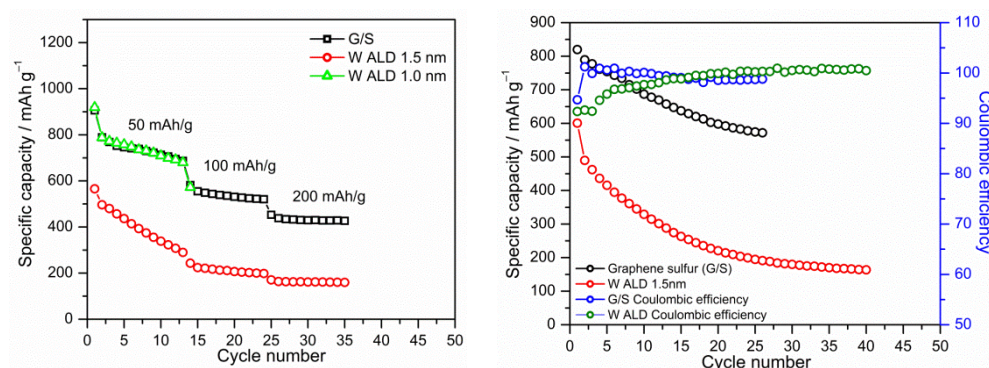


**Figure 78. Performance of cathode-coated materials with graphene-sulfur and Al-W coatings. Left: Effect of Al-W thickness in comparison with graphene-sulfur. Right: Comparative performance of the 1.5 nm Al-W 1.5 nm coating with graphene-S system at 50 mAh/g.**

**Multiscale modeling on cathode.** Silicene as cathode host to immobilize polysulfides was evaluated by a mesoscale simulation strategy involving atomistic and coarse-grained molecular models. Results show that the binding forces between  $\text{Li}_2\text{S}_x$  ( $x = 1, 2, 4$ ) molecules and silicene are much stronger than those between  $\text{Li}_2\text{S}_x$  and carbon-based materials. Electronic structure analysis shows that  $\text{Li}_2\text{S}_x$  interacts with silicene via strong chemical bonds.  $\text{Li}_2\text{S}$  (111)/silicene interfacial structures are thermodynamically stable, and the interaction is dominated by Li-Si chemical bonds. Hence, the silicene-based cathode framework has the ability to trap polysulfides and mitigate the “shuttle effect.” Results also show that the silicene substrate can facilitate dissociation and electrochemical reduction of long-chain polysulfides to short-chain polysulfides. Precipitation of  $\text{Li}_2\text{S}$  on the cathode surface investigated by a coarse-grained model reveals that  $\text{Li}_2\text{S}$  coverage grows faster on silicene than on graphene, suggesting that the silicone-based cathode may have better surface passivation. A paper based on this work has been submitted. In addition, nanopores of graphene,  $\text{MoS}_2$  and Mo-doped graphene, and  $\text{MnO}_2$  and  $\text{Fe}_2\text{O}_3$  were analyzed. Adsorption energies of the polysulfide to the surfaces and detailed Li and S interactions with the substrate were characterized via charge and geometric analyses. Both the Mo-containing materials and the oxides adsorb polysulfides much more strongly than graphene nanopores do. However, some of these surfaces are excessively reactive. A balance between affinity for S and moderate surface reactivity appears as a promising design guideline for these materials.

**Multiscale modeling on Li anode.** The precipitation of  $\text{Li}_2\text{S}$  on the Li metal surface, which is caused by the shuttle effect, adversely impacts the performance of Li-S batteries. DFT analysis demonstrates that the  $\text{Li}_2\text{S}$  film is strongly bonded to the Li substrate via Li-S bonds, and the decomposition of the precipitated film is difficult. *Ab initio* molecular dynamics simulations follow the time evolution of the reactions leading to the  $\text{Li}_2\text{S}$  film formation and the dependence of the film structure on the nature of the exposed surface. A paper based on this study has been submitted to ACS Applied Materials & Interfaces.

## Patents/Publications/Presentations

### Presentation

- BMR Meeting, LBNL, Berkeley, California (22 January 2015): “Addressing Internal ‘Shuttle’ Effect: Electrolyte Design and Cathode Morphology Evolution in Li-S Batteries (DE-EE-0006832)”;

P. B. Balbuena.

### Publications

- Liu, Z., and D. Hubble, P. B. Balbuena, and P. P. Mukherjee. “Adsorption of Insoluble Polysulfides  $\text{Li}_2\text{S}_x$  ( $x = 1, 2$ ) on  $\text{Li}_2\text{S}$  Surfaces.” *Phys. Chem. Chem. Phys.* 17 (2015): 9032–9039.
- Camacho-Forero, Luis E., and Taylor W. Smith, Samuel Bertolini, and Perla B. Balbuena. “Reactivity at the Lithium-Metal Anode Surface of Lithium-Sulfur Batteries.” *J. Phys. Chem. C* 119, no. 48 (2015): 26828–26839.
- Tsai, C. S.J., and A. D. Dysart, J. H. Beltz, and V. G. Pol. “Identification and Mitigation of Generated Solid By-Products during Advanced Electrode Materials Processing.” *Environmental Science and Technology* (2016). In press.
- Dysart, Arthur A., and Juan C. Burgos, Aashutosh Mistry, Chien-Fan Chen, Zhixiao Liu, Perla B. Balbuena, Partha P. Mukherjee, and Vilas G. Pol. “Towards Next Generation Lithium-Sulfur Batteries: Non-Conventional Carbon Compartments/Sulfur Electrodes and Multi-Scale Analysis.” *J. Electrochem. Soc.* Under review.
- Liu, Zhixiao, and Samuel Bertolini, Partha Mukherjee, and Perla B. Balbuena. “ $\text{Li}_2\text{S}$  Film Formation on Lithium Anode Surface of Li-S batteries.” Submitted (December 2015).
- Kamphaus, Ethan, and Perla B. Balbuena. “Long-Chain Polysulfide Retention at the Cathode of Li-S Batteries.” Submitted (December 2015).
- Liu, Zhixiao, and Perla B. Balbuena and Partha P. Mukherjee. “Evaluating Silicene as a Potential Cathode Host to Immobilize Polysulfides in Lithium-Sulfur Batteries.” Submitted (December 2015).

## Task 8.8 – Mechanistic Investigation for the Rechargeable Li S Batteries (Deyang Qu, University of Wisconsin - Milwaukee; Xiao-Qing Yang, BNL)

**Project Objective.** The primary objectives are to conduct focused fundamental research on the mechanism for Li-S batteries, investigate the kinetics of the sulfur redox reaction, develop electrolyte and additives to increase the solubility of  $\text{Li}_2\text{S}$ , and optimize the sulfur electrode design. In this objective, special attention will be paid to the investigation of highly soluble polysulfide species including both ions and radicals, and the potential chemical equilibrium among them. Through such investigation, the detail pathway for polysulfide shuttle will be better understood, and alleviation of the obstacle will be explored.

**Project Impact.** Rechargeable Li-S battery is a potential candidate to meet the demand of high energy density for next generation rechargeable Li battery. Through the fundamental mechanistic investigation, the mechanism of Li-S batteries can be better understood, which will lead to the material design and battery engineering to materialize the potential of Li-S chemistry. Li-S batteries could enable competitive market entry of EVs by reducing the cost and extending the driving distance per charge.

**One-Year Goals.** Complete development of an analytical method for the quantitative and qualitative determination of all polysulfide ions in non-aqueous electrolytes and the initial design of an *in situ* electrochemical study for the sulfur reduction reaction.

**Collaborations.** The PI is the Johnson Control Endowed Chair Professor; the UWM and BNL team has close collaboration with Johnson Controls' scientists and engineers. The collaboration enables the team to validate the outcomes of fundamental research in pilot-scale cells. This team has been closely working with top scientists on new material synthesis at ANL, LBNL, and PNNL, with U.S. industrial collaborators at General Motor, Duracell, and Johnson Control; as well as international collaborators in Japan and South Korea. These collaborations will be strengthened and expanded to give this project a vision on both today's state-of-the-art technology and tomorrow's technology in development, with feedback from the material designer and synthesizers upstream as well as from the industrial end users downstream.

### Milestones

1. Complete literature review and feasibility study of the methods for polysulfide determination. (December 2015 – Complete)
2. Complete development of the essay to determine all polysulfide ions. (March 2016 – In progress)
3. Complete design qualification for an *in situ* electrochemical HPLC-MS cell for Li-S investigation. (June 2016 – In progress)
4. Complete identification of polysulfide ions formed from elemental sulfur. (September 2016 – In progress)

## Progress Report

This quarter, an extensive literature search was done for the quantitative and qualitative analysis of the dissolved elemental sulfur and polysulfides, as well as the studies of the mechanism of the sulfur redox reaction. It was concluded that even with decades of genuine effort, there still is a lack of a reliable analytical method to qualitatively separate and analyze the polysulfide ions of various lengths, which hinders the comprehensive understand of the reaction mechanism.

The main issue for the instrumental analysis of polysulfides is that it is almost impossible to prepare polysulfide anions with a precisely defined chain length in solution for reference measurements, since disproportionation and redox reactions result in distribution of polysulfide anions with various chain lengths. Due to the differing chain length and molar mass of different polysulfide species, the powerful and widely used analytical method, chromatography in tandem with mass spectroscopy (MS), could potentially be used to analyze the polysulfide species, because no reference of pure polysulfides are needed for the quantitative and qualitative measurement. HPLC-MS was reported once as means to identify polysulfides in Li-S cells [Diao Y., and K. Xie, S. H. Xiong, X. B. Hong, *J. Electrochem. Soc.* 159 (2012): A421–A425]. Unfortunately, the data interpretation in the publication was proven wrong. It was further proven by the PI that polysulfide ions cannot be separated by HPLC due to lack of retention mechanism. Further work is clearly needed to develop a feasible assay for analysis of polysulfide ions produced during operation of a Li-S battery.

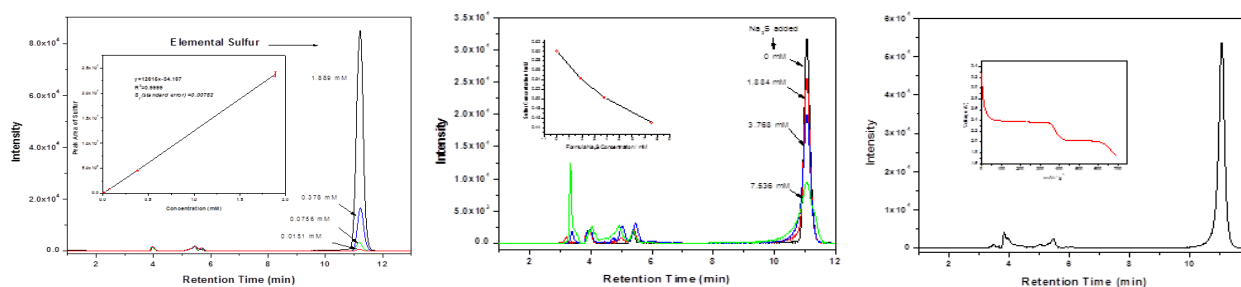


**Figure 79.** (left) The calibration curve and chromatograms of different elemental sulfur standards. (middle) The chromatograms of different simulated electrolytes and blank S/DME solution. The inset shows the change of S concentration with the amount of Na<sub>2</sub>S added. (right) The chromatogram of electrolyte from discharged Li-S battery and the discharged profile of Li-S battery.

The solubility of S in 12 different pure solvents and in 22 different electrolytes was determined. It was found that the solubility of elemental sulfur is dependent on the Lewis basicity, the polarity of solvents, and the salt concentration in the electrolytes. In addition, the S content in the electrolyte recovered from a discharged Li-S battery was successfully determined by the proposed HPLC/UV method. Thus, the feasibility of the method to the online analysis for a Li-S battery is demonstrated.

**Table 1.** Solubility of elemental S in pure solvents and in corresponding electrolytes with different LiTFSi concentrations obtained through HPLC/UV method.

Solvent	Solubility mM, pure solvent	Solubility (mM), 0.1M electrolyte	Solubility (mM), in 1.0M electrolyte
AN	0.610	0.596	0.390
PY	48.046	28.005	15.909
DMF	5.944	5.895	2.603
PC	1.318	1.255	0.633
GBL	3.888	3.366	1.606
DGME	10.259	9.511	3.875
DME	9.957	8.963	3.994
DMSO	3.936	3.845	1.933
BMPTFSi	0.349	0.245	0.216

## Patents/Publications/Presentations

### Publication

- Zheng, Dong, and Xuran Zhang, Jiankun Wang, Deyu Qu, Xiaoqing Yang, and **Deyang Qu**. “Reduction Mechanism of Sulfur in Lithium-Sulfur Battery: From Elemental Sulfur to Polysulfide.” *J. of Power Sources* 301(2016): 312–316.

### Presentation

- University of Washington, Department of Material Engineering, Seattle (2 November 2015): “Rechargeable Lithium Sulfur Batteries – the Mechanism of Sulfur Redox Reaction.” Invited.



## Task 8.9 – Statically and Dynamically Stable Lithium Sulfur Batteries (Arumugam Manthiram, U Texas – Austin)

**Project Objective.** The project objective is to develop statically and dynamically stable lithium-sulfur batteries by integrating polysulfide-filter-coated separators with a protected lithium-metal anode through additives or a modified  $\text{Li}_2\text{S}$  cathode with little or no charge barrier during first charge.

The project includes demonstration of electrochemically stable cells with sulfur capacities of  $> 1,000 \text{ mA h g}^{-1}$  and cycle life in excess of 500 cycles (dynamic stability) along with positive storage properties (static stability) at  $> 70 \text{ wt\%}$  sulfur content and  $\sim 5 \text{ mg cm}^{-2}$  loading that will make the Li-S technology superior to the present-day Li-ion technology in terms of cost and cell performance.

**Project Impact.** The combination of polysulfide-filter-coated separator, lithium-metal-protection additives, and  $\text{Li}_2\text{S}$  cathode modifications offers a viable approach to overcome the persistent problems of Li-S batteries. This project is systematically integrating the basic science understanding gained in its laboratory of these three aspects to develop the Li-S technology as the next-generation power source for EVs. The project targets demonstrating cells with sulfur capacities of over  $1,000 \text{ mA h g}^{-1}$  and cycle life in excess of 500 cycles along with good storage properties at high sulfur content and loading that will make the Li-S technology superior to the present-day Li-ion technology in terms of cost and cell performance.

**Out-Year Goals.** The overall goal is to develop statically and dynamically stable Li-S batteries with custom cathode and stabilized anode active materials. In addition to developing a high-performance battery system, a fundamental understanding of the structure-configuration-performance relationships will be established.

Specifically, optimization of the electrochemical and engineering parameters of polysulfide-filter-coated separators aims at comprehensively investigating different coating materials and their corresponding coating techniques for realizing various high-performance custom separators. The developed polysulfide-filter-coated separators can be coupled with pure sulfur cathodes and allow pure sulfur cathodes to attain high sulfur loading and content. Multifunctional polysulfide-filter-coated separators, high-loading sulfur cathodes, stabilized-Li-metal anodes, activated- $\text{Li}_2\text{S}$  cathodes, and novel approaches on the cell design and optimization are anticipated to provide an in-depth understanding of the full-cell battery chemistry and to realize statically and dynamically stable Li-S batteries for EVs.

**Collaborations.** This project collaborates with ORNL.

### Milestones

1. Database of coating materials and polysulfide-filter coatings established. (December 2015 – Complete)
2. Database of fabrication parameters and S-filter-coated separators established. (March 16 – Ongoing)
3. Low-capacity fade rate and self-discharge testing completed. (June 2016)
4. *Go/No-Go*: Lightweight design and electrochemical stability demonstrated. (September 2016 – Ongoing)

## Progress Report

This quarter, the physical/chemical characteristics of the coating materials were investigated for creating a materials chemistry database. Four major carbon materials categorized by their different morphologies were selected: (i) spherical carbons, (ii) carbon nanofibers (CNFs), (iii) graphene, and (iv) carbon nanotubes (CNTs). Figure 80 and Table 2 summarize the materials chemistry and the suggested coating methods for various carbon materials. Focus will be on the microporosity that majorly influences the polysulfide-trapping capability of the polysulfide-filter coatings.

**Table 2. Materials Chemistry Database.**

Coating material / coating methods	Carbon sample	Surface area [ $\text{m}^2 \text{g}^{-1}$ ]	Pore volume [ $\text{cm}^3 \text{g}^{-1}$ ]	Avg. pore size [nm]	Microporosity	
					Pore volume [ $\text{cm}^3 \text{g}^{-1}$ ]	Surface area [ $\text{m}^2 \text{g}^{-1}$ ]
(i): T, B	Acetylene Black	82	0.29	14	0	0
(i): T, B	Super P carbon	89	0.44	19	0	0
(i): T, B	Carbon Black (Lampblack)	30	0.22	29	0	0
(i): T, B	Carbon Black (Vulcan)	298	1.03	14	85	0.04
(i): T, B	Activated Charcoal	1002	0.7	3	754	0.40
(i): T, B	Activated Carbon	732	0.53	3	627	0.33
(ii): T, V	CNF	26	0.09	14	0	0
(iii): T, B, V	graphene	109	0.53			
(iv): B, V	CNT	279	2.48	36	0	0
Coating materials: (i) spherical carbons, (ii) carbon nanofibers (CNF), (iii) graphene, and (iv) carbon nanotubes (CNT)						
Coating methods: tape-casting (T), binder-supporting (B), or vacuum-filtration process (V)						

In category (i), six spherical carbons with different microstructures and porosities have been investigated. The Super P carbon and Acetylene Black with a low porosity represent the nonporous carbons. The Activated Charcoal and Activated Carbon exhibiting high surface area and abundant micropores are distinguished as the porous carbons. Both nonporous and porous spherical carbons are able to be uniformly coated onto a Celgard membrane by tape-casting and binder-supporting methods. The preliminary cell performance proves that the spherical carbon-coated separators work well in Li-S cells. In category (ii), a nonporous CNF as the standard sample was targeted in the control cells for studying the effect of porosity/microstructure toward cell performance. The CNFs were smoothly coated onto the Celgard membrane by a vacuum-filtration method, which is an easy method for adjusting the thickness of polysulfide-filter coatings. Figure 81 shows the cell performance of the cell employing the standard CNF-coated separator. The CNF coating provides a conductive thin film in between the cathode and the separator so that the pure sulfur cathode with a high sulfur loading of  $2.7 \text{ mg cm}^{-2}$  and high sulfur content of 70 wt% shows a peak discharge capacity of  $1200+ \text{ mAh g}^{-1}$ , attaining the targeted capacity of  $1000 \text{ mAh g}^{-1}$ . The CNF coating also functions as the polysulfide filter for suppressing the severe polysulfide migration. To study the conductivity and porosity of the coating layer towards cell performance, the nonporous standard samples in category (ii) - (iv) were activated for generating micro/meso porosity.

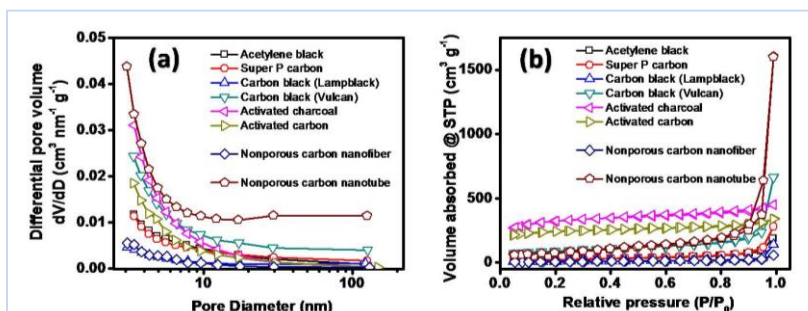


**Figure 80. Physical/chemical characteristics of various carbon materials: (a) pore-size distributions and (b) isotherms.**

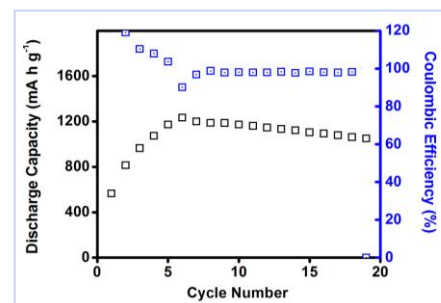


**Figure 81. Cell performance of the cell employing the CNF-coated separator.**

## Patents/Publications/Presentations

### Presentations

- International Symposium on Clusters and Nanomaterials, Richmond, Virginia (26 – 29 October 2015): “Nanomaterials for Electrical Energy Storage”; A. Manthiram. Invited.
- 2015 International Conference on Innovative Electrochemical Energy Materials and Technologies (EEMT2015), Nanning, China (8 – 11 November 2015): “Electrical Energy Storage: Next Generation Battery Chemistries”; A. Manthiram. Invited plenary talk.
- 2015 Fall Meeting of the Materials Research Society, Symposium X: Frontiers of Materials Research, Boston (29 November – 4 December 2015): “Electrical Energy Storage: Materials Challenges and Prospects”; A. Manthiram. Invited.

## TASK 9 – LI-AIR BATTERIES

### Summary and Highlights

High-density energy storage systems are critical for EVs required by the EV Everywhere Grand Challenge. Conventional Li-ion batteries still cannot fully satisfy the ever-increasing needs because of their limited energy density, high cost, and safety concerns. As an alternative, the rechargeable Li-O<sub>2</sub> battery has the potential to be used for long-range EVs. The practical energy density of a Li-O<sub>2</sub> battery is expected to be ~ 800 Wh kg<sup>-1</sup>. The advantages of Li-O<sub>2</sub> batteries come from their open structure; that is, they can absorb the active cathode material (oxygen) from the surrounding environment instead of carrying it within the batteries. However, the open structure of Li-O<sub>2</sub> batteries also leads to several disadvantages. The energy density of Li-O<sub>2</sub> batteries will be much lower if oxygen has to be provided by an onboard container. Although significant progress has been made in recent years on the fundamental properties of Li-O<sub>2</sub> batteries, the research in this field is still in an early stage, and many barriers must be overcome before practical applications. The main barriers include:

- Instability of electrolytes. Superoxide species generated during discharge or O<sub>2</sub> reduction process is highly reactive with electrolyte and other components in the battery. Electrolyte decomposition during charge or O<sub>2</sub> evolution process is also significant due to high over-potentials.
- Instability of air electrode (dominated by carbonaceous materials) and other battery components (such as separators and binders) during charge/discharge processes in an oxygen-rich environment.
- Limited cyclability of the battery associated with instability of the electrolyte and other components of the batteries.
- Low energy efficiency associated with large over-potential and poor cyclability of Li-O<sub>2</sub> batteries.
- Low power rate capability due to electrode blocking by the reaction products.
- Absence of a low-cost, high-efficiency oxygen supply system (such as oxygen selective membrane).

The main goal of the PNNL Task is to provide a better understanding on the fundamental reaction mechanisms of Li-O<sub>2</sub> batteries and identify the required components (especially electrolytes and electrodes) for stable operation of Li-O<sub>2</sub> batteries. The PNNL researchers will investigate stable electrolytes and oxygen evolution reaction (OER) catalysts to reduce the charging overvoltage of Li-O<sub>2</sub> batteries and improve their cycling stability. New electrolytes will be combined with stable air electrodes to ensure their stability during Li-O<sub>2</sub> reaction. Considering the difficulties in maintaining the stability of conventional liquid electrolyte, the Liox team will explore the use of a nonvolatile, inorganic molten salt comprising nitrate anions and operating Li-O<sub>2</sub> cells at elevated temperature (> 80°C). It is expected that these Li-O<sub>2</sub> cells will have a long cycle life, low over potential, and improved robustness under ambient air compared to current Li-air batteries. At ANL, new cathode materials and electrolytes for lithium-air batteries will be developed for Li-O<sub>2</sub> batteries with long cycle life, high capacity, and high efficiency. The state-of-the-art characterization techniques and computational methodologies will be used to understand the charge and discharge chemistries. University of Massachusetts/BNL team will investigate the root causes of the major obstacles of the air cathode in the Li-air batteries. Special attention will be paid to optimizing high surface carbon material used in the gas diffusion electrode, catalysts, electrolyte, and additives stable in Li-air system and with capability to dissolve Li oxide and peroxide. Success of this project will establish a solid foundation for further development of Li-O<sub>2</sub> batteries toward practical applications for long-range EVs. The fundamental understanding and breakthrough in Li-O<sub>2</sub> batteries may also provide insight on improving the performance of Li-S batteries and other energy storage systems based on chemical conversion processes.

## Task 9.1 – Rechargeable Lithium-Air Batteries (Ji-Guang Zhang and Wu Xu, PNNL)

**Project Objective.** The project objective is to develop stable electrolyte and air electrode to reduce the charging overvoltage and improve the cycling stability of rechargeable lithium-oxygen (Li-O<sub>2</sub>) batteries. New air electrode will be synthesized to improve the capacity and cycling stability of Li-O<sub>2</sub> batteries. New electrolytes will be investigated to ensure their stability during Li-O<sub>2</sub> reaction.

**Project Impact.** Li-air batteries have a theoretical specific energy that is more than five times that of state-of-the-art Li-ion batteries and are potential candidates for use in next-generation, long-range EVs. Unfortunately, the poor cycling stability and low CE of Li-air batteries have prevented practical application to date. This work will explore a new electrolyte and electrode that could lead to long cyclability and high CE in Li-air batteries that can be used in the next generation EVs required by the EV Everywhere Grand Challenge.

**Out-Year Goals.** The long-term goal of the proposed work is to enable rechargeable Li-air batteries with a specific energy of 800 Wh/kg at cell level, 1000 deep-discharge cycles, improved abuse tolerance, and less than 20% capacity fade over a 10-year period to accelerate commercialization of long-range EVs.

**Collaborations.** This project engages in collaboration with the following:

- Chunmei Ben (NREL) – Metal oxide coated glassy carbon electrode
- Chongmin Wang (PNNL) – Characterization of cycled air electrodes by TEM/SEM

### Milestones

1. Synthesize and characterize the modified solvent and the transition metal oxide catalyst coated carbon material (12/31/2015 – Complete)
2. Identify a modified carbon air electrode which is stable in a Li-O<sub>2</sub> battery by using conventional glyme solvent (6/30/2016 – Ongoing)
3. Demonstrate stable operation of Li-O<sub>2</sub> battery by employing the new electrolyte and modified air electrode (9/30/2016 – Ongoing)



## Progress Report

This quarter, the binder-free air electrode based on nanowire (NW) nickel cobalt oxide ( $\text{NiCo}_2\text{O}_4$ , NCO) catalyst on carbon fabric (CF) composite has been investigated systematically. The morphology and crystal structure of the NCO/CF composite are shown in Figure 82. When the binder-free NCO/CF electrode was assembled into a half cell versus Li anode and pre-lithiated to a certain voltage in an argon atmosphere, the nanowired NCO was transformed to nanosized (about 2 nm) Ni and Co particles well dispersed in  $\text{Li}_2\text{O}$  moiety (Figure 83), according to the conversion reaction of  $\text{NiCo}_2\text{O}_4 + 8\text{Li}^+ + 8\text{e}^- \rightarrow \text{Ni} + 2\text{Co} + 4\text{Li}_2\text{O}$ .

When the prelithiated NCO (PLNCO) electrode was assembled into the  $\text{Li-O}_2$  cells with 1 M LiTf-tetraglyme electrolyte and run the discharge/charge cycling between 2.0~4.5 V, nanosized Ni and Co particles acted as the catalysts for oxygen reduction during the first discharge process. During the first charge process, the nanosized Ni and Co would be oxidized to NiO and CoO nanoparticles by chemical reactions via oxidation and/or electrochemical reactions via  $\text{Ni} + \text{Li}_2\text{O} \rightarrow \text{NiO} + 2\text{Li}^+ + 2\text{e}^-$  and  $\text{Co} + \text{Li}_2\text{O} \rightarrow \text{CoO} + 2\text{Li}^+ + 2\text{e}^-$ . Since the reversible reactions of NiO (or CoO) to Ni (or Co) with  $\text{Li}_2\text{O}$  occur at a voltage of about 1.2 V, below the discharge voltage (2.0 V) set for the cycling protocol, the NiO and CoO nanoparticles were the catalysts starting from the second discharge/charge cycle. That is one reason why the capacity of the first cycle is so much higher than the second cycle.

The prelithiations of NCO were performed at several cutoff voltages. The optimal prelithiation cutoff voltage was found to be 0.5 V, which allows the  $\text{Li-O}_2$  cells with the prelithiated NCO/CF electrode to show stable cycling at a capacity above  $1200 \text{ mAh g}^{-1}$  for 120 cycles and  $1000 \text{ mAh g}^{-1}$  for 140 cycles. At higher prelithiation cutoff voltages, the lithiation of NCO was limited; but at lower prelithiation cutoff voltages, the NCO nanowires experienced irreversible damage and the electrode surface was covered with thick discharge products. In both of these cases, the capacity of  $\text{Li-O}_2$  batteries using these electrodes was largely reduced.

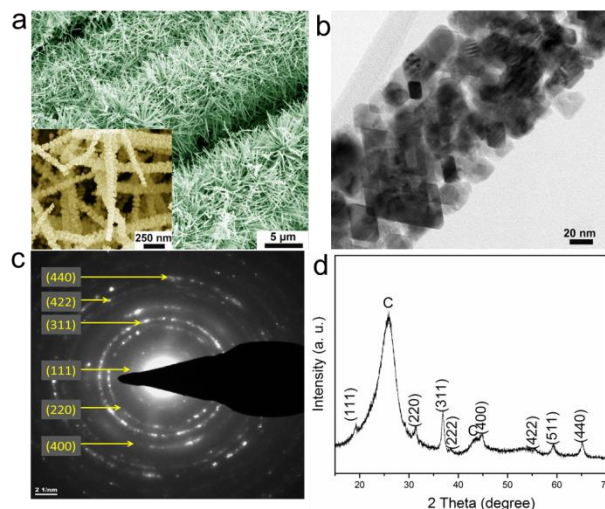


**Figure 82. Morphology and crystal structure characterizations of NCO/carbon fabric (CF).** (a) Scanning electron microscopy image of NCO nanowires (NW) grown on carbon fabric, where the inset is high-resolution image of NCO NWs. (b) Transmission electron microscopy image of single NCO NW. (c) Selected area electron diffraction pattern of NCO from its single NW. (d) X-ray diffraction pattern of the resulting NCO/CF composite.

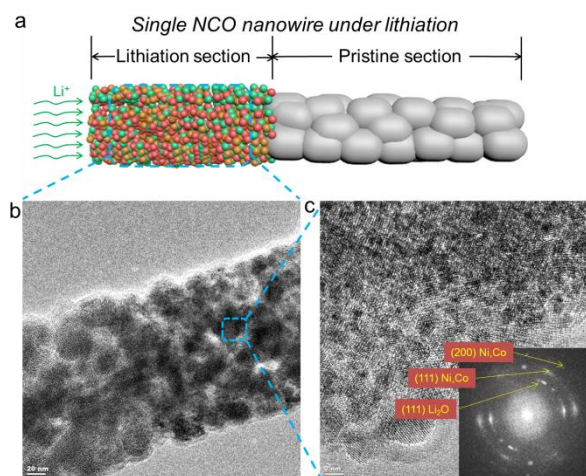


**Figure 83. Characterization of lithiated NCO nanowire (NW).** (a) Schematic illustration of NCO NW under lithiation. (b) Transmission electron microscopy and (c) high-resolution transmission electron microscopy images of selected lithiation area of NCO NW. Inset: Selected area electron diffraction pattern of lithiated NCO.



## Patents/Publications/Presentations

### Publication

- Liu, B., and W. Xu,\* P. Yan, X. Sun, M. E. Bowden, J. Read, J. Qian, D. Mei, C.-M. Wang, J.-G. Zhang\*. “Enhanced Cycling Stability of Rechargeable Li-O<sub>2</sub> Batteries Using High Concentration Electrolytes.” *Adv. Funct. Mater.* (2015). doi: 10.1002/adfm.201503697.

### Presentations

- MRS Fall Meeting and Exhibit, Boston (29 November – 4 December 2015): “Enhanced Cycling Stability of Rechargeable Li-O<sub>2</sub> Batteries Using High Concentration Electrolytes”; B. Liu, and W. Xu, P. Yan, X. Sun, M. E. Bowden, J. Read, J. Qian, D. Mei, C.-M. Wang, J.-G. Zhang.
- MRS Fall Meeting and Exhibit, Boston (29 November – 4 December 2015): “Micro-Scarecrow’s Party at the Harvest-Moment”; Bin Liu and J.-G. Zhang. First place winner in “Science as Art” competition.

## Task 9.2 – Efficient Rechargeable Li/O<sub>2</sub> Batteries Utilizing Stable Inorganic Molten Salt Electrolytes (Vincent Giordani, Liox)

**Project Objective.** The project objective is to develop high specific energy, rechargeable Li-air batteries having lower overpotential and improved robustness under ambient air compared to current Li-air batteries. The technical approach involves replacing traditional organic and aqueous electrolytes with a nonvolatile, inorganic molten salt comprising nitrate anions and operating the cell at elevated temperature (> 80°C). The research methodology includes powerful *in situ* spectroscopic techniques coupled to electrochemical measurements (for example, electrochemical MS) designed to provide quantitative information about the nature of chemical and electrochemical reactions occurring in the air electrode.

**Project Impact.** If successful, this project will solve particularly intractable problems relating to air electrode efficiency, stability, and tolerance to the ambient environment. Furthermore, these solutions may translate into reduced complexity in the design of a Li-air stack and system, which in turn may improve prospects for use of Li-air batteries in EVs. Additionally, the project will provide materials and technical concepts relevant for development of other medium temperature molten salt Li battery systems of high specific energy, which may also have attractive features for EVs.

**Out-Year Goals.** The long-term goal of this project is to develop Li-air batteries comprising inorganic molten salt electrolytes and protected Li anodes that demonstrate high (> 500 Wh/kg) specific energy and efficient cyclability in ambient air. By the end of the project, it is anticipated that problems hindering use of both the Li anode and air electrode will be overcome due to materials advances and strategies enabled within the intermediate (> 80°C) operating temperature range of the system under development.

**Collaborations.** This project engages in collaboration with the following:

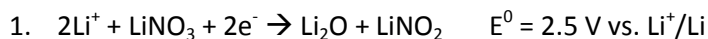
- Bryan McCloskey (LBNL): Analysis of air electrode and electrolyte
- Julia Greer (Caltech): Design of air electrode materials and structures

### Milestones

1. Quantify  $e^-/\text{O}_2$  and OER/ORR (oxygen reduction reaction) ratio for metals and metal alloys in half cells under pure O<sub>2</sub>. (12/31/15 – Complete)
2. Determine the kinetics and mechanisms of electrochemical nitrate reduction in the presence of O<sub>2</sub>, H<sub>2</sub>O, and CO<sub>2</sub>. (3/31/16 – Ongoing)
3. Synthesize electronically conductive ceramics and cermets. (March 2016 – Ongoing)
4. Quantify  $e^-/\text{O}_2$  and OER/ORR ratio for electronically conductive ceramics and cermets in half cells under pure O<sub>2</sub>. (6/30/16 – Ongoing)
5. Demonstrate  $e^-/\text{O}_2=2$  and OER/ORR ratio=1, +/- 5% and correcting for the effect of Li<sub>2</sub>O<sub>2</sub> crossover. (6/30/16 – Ongoing)
6. Demonstrate Li<sub>2</sub>O yield=1,  $e^-/\text{O}_2=4$  and OER/ORR ratio=1, +/- 5%. (9/30/16 – Ongoing)
7. Demonstrate discharge specific power and power density  $\geq 800$  W/kg and  $\geq 1600$  W/L, respectively, based on air electrode mass and volume. (9/30/16 – Ongoing)
8. Demonstrate solid electrolytes that are stable to molten nitrate electrolytes over a temperature range of 100°C to 150°C for 6 months or greater. (9/30/16 – Ongoing)

## Progress Report

The  $e^-/O_2$  and OER/ORR ratio for nanoporous Au has been reported in the last report ( $e^-/O_2$  discharge=3.8,  $e^-/O_2$  charge=5.7, OER/ORR=0.77). In accordance with the current quarter milestone,  $e^-/O_2$  and OER/ORR ratios on assorted metals and metal alloys have been measured, including Ni, Fe, Co and Pt nanoparticles (See Figure 84a voltage profiles). All nanopowders (~10-20 m<sup>2</sup>/g BET surface area, 10-60 nm average particle size) were dry pressed (~20 mg) on a 10 mm OD stainless steel mesh without any binder, inside an Ar glovebox. Cells were cycled under pure O<sub>2</sub> at 250  $\mu$ A constant current (12.5 mA/g<sub>cathode</sub>) at 150°C using a Li anode and a LiNO<sub>3</sub>-KNO<sub>3</sub> melt. As Figure 84a indicates, only a small amount of charge is passed before the cell polarizes to the potential for nitrate reduction according to the following reaction:



Once each cell polarizes to below this potential, nitrate reduction becomes the dominant reaction over O<sub>2</sub> reduction. Consequently, the  $e^-/O_2$  and OER/ORR measurements are based on discharges constrained to a lower voltage limit of 2.6 V. Figure 84b shows the first cycle with *in situ* pressure analysis for an exemplary Li/O<sub>2</sub> cell using a Ni cathode. It is found that  $e^-/O_2$  discharge=2.2,  $e^-/O_2$  charge=8.0, OER/ORR=0.28. The high  $e^-/O_2$  charge ratio indicates parasitic processes which the project hypothesizes to involve oxidation of the Ni surface. Moreover, low discharge capacity within this voltage range at the reported current densities was consistently observed, which may be due to the very low physical solubility of O<sub>2</sub> in the nitrate melt.

New approaches will be developed to address the twin challenges of low O<sub>2</sub> solubility and the high cathodic limit for the nitrate electrolyte, which are the subject of a paper in preparation and patent applications. Specifically, the following approaches will be used: (1) testing electrolyte additives that enhance the chemical absorption of O<sub>2</sub> into the molten salt, and (2) demonstrating catalysts that enable reversible nitrate reduction according to reaction 1. The latter concept actually provides the basis for a high-capacity rechargeable battery that does not require O<sub>2</sub> exchange with the environment. More will be described relating to these approaches following publication. In addition, solid electrolytes will be screened for lithium protection with molten nitrate catholytes.

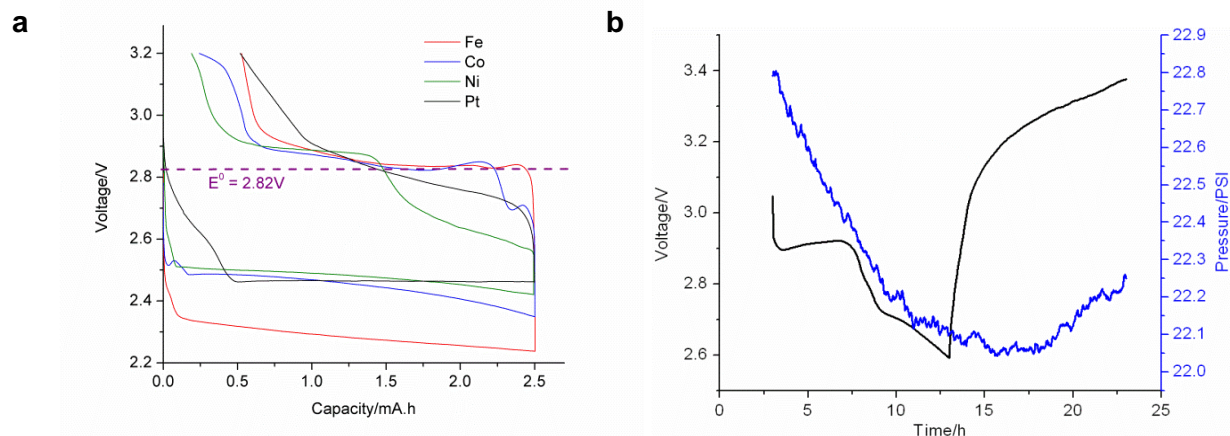


Figure 84. (a) Voltage-capacity profile for molten nitrate Li/O<sub>2</sub> cells using different nanopowder cathodes.  $E^0$ : thermodynamic potential for  $2Li + O_{2(g)} \rightleftharpoons Li_2O_2$  cell reaction. (b) *In situ* pressure analysis for the cell containing the Ni cathode cycled at 100  $\mu$ A constant current (5 mA/g).

## Patents/Publications/Presentations

Publication. Giordani, Vincent, and Dylan Tozier, Hongjin Tan, Colin Burke, Betar Gallant, Jasim Uddin, Julia Greer, Bryan McCloskey, Gregory Chase, and Dan Addison. "A Molten Salt Lithium-Oxygen Battery." *JACS*. Submitted..

## Task 9.3 – Li-Air Batteries (Khalil Amine, ANL)

**Project Objective.** This project will develop new cathode materials and electrolytes for lithium-air batteries for long cycle life, high capacity, and high efficiency. The goal is to obtain critical insight that will provide information on the charge and discharge processes in lithium-air batteries to enable new advances to be made in their performance. This will be done using state-of-the-art characterization techniques combined with state-of-the-art computational methodologies to understand and design new materials and electrolytes for lithium-air batteries.

**Project Impact.** The instability of current non-aqueous electrolytes and degradation of cathode materials limits the performance of lithium air batteries. The project impact will be to develop new electrolytes and cathode materials that are stable and can increase cycle life and improve efficiency of lithium-air batteries

**Approach.** The project is using a joint theoretical/experimental approach for design and discovery of new cathode and electrolyte materials that act synergistically to reduce charge overpotentials and increase cycle life. Synthesis methods, in combination with design principles developed from computations, are used to make new cathode architectures. Computational studies are used to help understand decomposition mechanisms of electrolytes and how to design electrolytes with improved stability. The new cathodes and electrolytes are tested in Li-O<sub>2</sub> cells. Characterization along with theory is used to understand the performance of the materials used in the cell and make improved materials.

**Out-Year Goals.** The out-year goals are to find catalysts that promote discharge product morphologies that reduce charge potentials and find electrolytes for long cycle life through testing and design.

**Collaborations.** This project engages in collaboration with Professor Amin Salehi (University of Illinois-Chicago), Professor Yang-Kook Sun (Hanyang University), Professor Yiying Wu (Ohio State University), and Dr. Dengyun Zhai (China).

### Milestones

1. Development of new cathode materials based on Pd nanoparticles and ZnO coated carbon that can improve efficiency of Li-O<sub>2</sub> batteries through control of morphology and oxygen evolution catalysis. (12/31/15 – Complete)
2. Investigations of mixed K/Li salts and salt concentration on the performance of Li-O<sub>2</sub> batteries with goal of increasing cycle life. (3/31/16 – Ongoing)
3. Computational studies of electrolyte stability with respect to superoxide species and salt concentrations for understanding and guiding experiment. (6/30/16 – Ongoing)
4. Investigation of use of electrolytes to control the lithium superoxide content of discharge products of Li-O<sub>2</sub> batteries to help improve efficiency and cycling. (9/30/16 – Ongoing)

## Progress Report

Uniformly dispersed Pd nanoparticles on ZnO-passivated porous carbon were synthesized via an ALD technique. The Pd and ZnO ALD process was carried out in a commercial benchtop ALD reactor. Graphitized carbon black with an average particle size of 330 nm and a surface area of  $70 \text{ m}^2 \text{ g}^{-1}$  was used as the substrate. The ZnO was used to passivate carbon defect sites on the carbon surface to prevent electrolyte decomposing during cycling. Various numbers of ALD cycles of ZnO deposition was used in the synthesis. This was used to assess the dependence of the battery performance on the thickness of the passivation layer on the carbon. TEM was used to characterize the Pd/ZnO/C cathode materials as shown in Figure 85. It showed discrete crystalline Pd nanoparticles decorating the surface of the ZnO-passivated porous carbon support, in which the size of the nanoparticles ranged from 3–6 nm, depending on the number of Pd ALD cycles performed. XAS at the Pd K-edge revealed that the carbon-supported Pd existed in a mixed phase of metallic palladium and palladium oxide. The TEM images also showed a uniform dispersion of the Pd nanoparticles over the carbon substrate. It should also be pointed out that the porous structure of carbon is well preserved during the process of synthesizing Pd nanoparticles on the ZnO-passivated carbon samples by ALD. A well preserved porous structure with the appropriate pore size is needed for good electrochemical performance, since it is considered one of the factors having significant impact on cell capacity and cycle life in Li-O<sub>2</sub> cells.

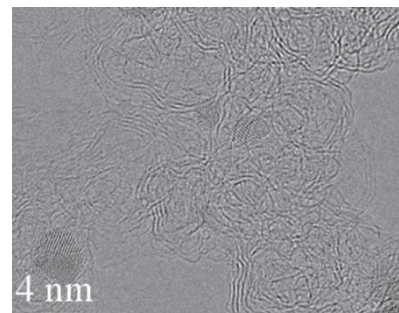


Figure 85. Scanning electron microscopy image of 3c-Pd/2c-ZnO/C sample; c refers to number of ALD cycles.

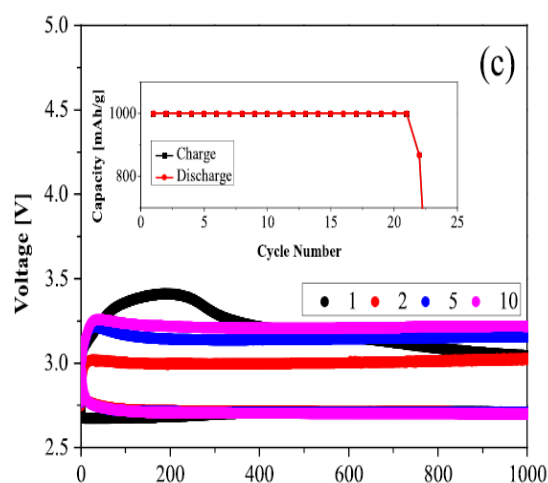


Figure 86. Voltage profile for 13c-Pd/2c-ZnO/C sample; c refers to number of ALD cycles.

The Pd/ZnO/C cathode material was tested in a rechargeable Li-O<sub>2</sub> battery, and it showed a highly active catalytic effect toward the electrochemical reaction—in particular, the OER. The electrochemical performance of these cathode architectures was evaluated in a Swagelok-type cell under one atm O<sub>2</sub> atmosphere with a MACCOR cyclor. The cell consisted of a Li-foil anode, an as-prepared Pd/ZnO/C cathode and a TEGDME-LiCF<sub>3</sub>SO<sub>3</sub>. As shown in Figure 86, the performance of the Li-O<sub>2</sub> cell is significantly improved when Pd nanoparticles on ZnO-passivated carbon are used as the electrocatalyst. The Pd-based cathode not only contributes to a higher capacity by providing more active sites for the ORR reaction, but also leads to a different morphology of the discharge products. The results also showed that the ALD Pd/ZnO tandem bilayer on carbon is an effective cathode architecture for significantly decreasing the charge potential of Li-O<sub>2</sub> batteries, which leads to a high round-trip efficiency of the cell. Finally, it should also be pointed out that the cells with a Pd/ZnO/C-based cathode started to fade with relatively short discharge/charge cycles, even under the capacity-controlled mode. The reason for this is the accumulation of LiOH on the lithium anode due to the oxygen-cross-over. A large number of microscopic ‘tunnels’ exist within the LiOH layer, which provides a pathway for sustained ion transport by enabling the connection of lithium with the electrolyte. This results in the complete degradation of the Li anode by the corrosion of the oxygen

## Patents/Publications/Presentations

### Publication

- Luo, X., and M. Piernavieja-Hermida, J. Lu, T. Wu, J. Wen, Y. Ren, D. Miller, Z. Zak Fang, Y. Lei, and K. Amine. *Nanotechnology* 26 (2015): 164003.

### Presentations

- PacifiChem, Honolulu, Hawaii (15 – 20 December 2015): “Computational Studies of Catalytic Materials for Li-O<sub>2</sub> Batteries”; L. A. Curtiss.
- ECS Meeting, Phoenix (11 – 15 October 2015): “Computational Insight and Design of Cathodes Materials and Electrolytes for Li-O<sub>2</sub> Batteries”; L. A. Curtiss.
- International Symposium on Clusters and Nanomaterials (ISCAN), Richmond, Virginia (26 – 29 October 2015): “Subnanometer Metal Clusters as Catalysts in Li-O<sub>2</sub> Batteries”; L. A. Curtiss.



## TASK 10 – NA-ION BATTERIES

### Summary and Highlights

To meet the challenges of powering the PHEV, the next generation of rechargeable battery systems with higher energy and power density, lower cost, better safety characteristics, and longer calendar and cycle life (beyond lithium-ion batteries, which represent today's state-of-the-art technology) must be developed. Recently, Na-ion battery systems have attracted increasing attention due to the more abundant and less expensive nature of the Na resource. The issue is not insufficient lithium on a global scale, but what fraction can be used in an economically effective manner. Most untapped lithium reserves occur in remote or politically sensitive areas. Scale-up will require a long lead time, involve heavy capital investment in mining, and may require the extraction and processing of lower quality resources, which could drive extraction costs higher. Currently, high costs remain a critical barrier to the widespread scale-up of battery energy storage. Recent computational studies on voltage, stability, and diffusion barriers of Na-ion and Li-ion materials indicate that Na-ion systems can be competitive with Li-ion systems.

The primary barriers and limitations of current state-of-the-art of Na-ion systems are as follows:

- Building a sodium battery requires redesigning battery technology to accommodate the chemical reactivity and larger size of sodium ions.
- Lithium batteries pack more energy than sodium batteries per unit mass. Therefore, for sodium batteries to reach energy densities similar to lithium batteries, the positive electrodes in the sodium battery need to hold more ions.
- Since Na-ion batteries are an emerging technology, new materials to enable Na electrochemistry and the discovery of new redox couples along with the diagnostic studies of these new materials and redox couples are quite important.
- In sodium electrochemical systems, the greatest technical hurdles to overcome are the lack of high-performance electrode and electrolyte materials that are easy to synthesize, safe, and non-toxic, with long calendar and cycling life and low cost.
- Furthermore, fundamental scientific questions need to be elucidated, including (1) the difference in transport and kinetic behaviors between Na and Li in analogous electrodes; (2) Na insertion/extraction mechanism; (3) SEI layer on the electrodes from different electrolyte systems; and (4) charge transfer in the electrolyte–electrode interface and Na<sup>+</sup> ion transport through the SEI layer.

This task will use the synchrotron based *in situ* X-ray techniques and other diagnostic tools to evaluate new materials and redox couples, to explore fundamental understanding of the mechanisms governing the performance of these materials and provide guidance for new material developments. This task will also be focused on developing advanced diagnostic characterization techniques to investigate these issues, providing solutions and guidance for the problems. The synchrotron based *in situ* X-ray techniques (X-ray diffraction and hard and soft X-ray absorption) will be combined with other imaging and spectroscopic tools such as HRTEM, MS, and TXM.

## Task 10.1 – Exploratory Studies of Novel Sodium-Ion Battery Systems (Xiao-Qing Yang and Xiqian Yu, Brookhaven National Laboratory)

**Project Objective.** The primary project objective is to develop new advanced *in situ* material characterization techniques and to apply these techniques to explore the potentials, challenges, and feasibility of new rechargeable battery systems beyond the lithium-ion batteries (LIBs), namely the sodium-ion battery systems for PHEVs. To meet the challenges of powering the PHEV, new rechargeable battery systems with high energy and power density, low cost, good abuse tolerance, and long calendar and cycle life must be developed. This project will use the synchrotron based *in situ* X-ray diagnostic tools developed at BNL to evaluate the new materials and redox couples, exploring the fundamental understanding of the mechanisms governing the performance of these materials.

**Project Impact.** The Multi Year Program Plan (MYPP) of the VTO describes the goals for battery: “Specifically, lower-cost, abuse-tolerant batteries with higher energy density, higher power, better low-temperature operation, and longer lifetimes are needed for the development of the next-generation of HEVs, PHEVs, and EVs.” If this project succeeds, the knowledge gained from diagnostic studies and collaborations with U.S. industries and international research institutions will help U.S. industries develop new materials and processes for a new generation of rechargeable battery systems beyond lithium-ion batteries, such as Na-ion battery systems in their efforts to reach these VTO goals.

**Approach.** This project will use the synchrotron based *in situ* X-ray diagnostic tools developed at BNL to evaluate the new materials and redox couples to enable a fundamental understanding of the mechanisms governing the performance of these materials and to provide guidance for new material and new technology development regarding Na-ion battery systems.

**Out-Year Goals.** Complete the *in situ* X-ray diffraction and absorption studies of tunnel structured  $\text{Na}_{0.66}[\text{Mn}_{0.66}\text{Ti}_{0.34}]\text{O}_2$  with high capacity and  $\text{Na}(\text{NiCoFeTi})_{1/4}\text{O}_2$  with high rate and long cycle life capability as cathode materials for Na-ion batteries during charge-discharge cycling.

**Collaborations.** The BNL team has been working closely with top scientists on new material synthesis at ANL, LBNL, and PNNL, with U.S. industrial collaborators at General Motors, Duracell, and Johnson Control, and with international collaborators.

### Milestones

1. Complete the synchrotron-based *in situ* XRD studies of tunnel structured  $\text{Na}_{0.44}[\text{Mn}_{0.44}\text{Ti}_{0.56}]\text{O}_2$  as cathode material for Na-ion batteries during charge-discharge cycling. (December 2015 – Complete)
2. Complete *in situ* XRD of the  $\text{Na}_{0.66}[\text{Mn}_{0.66}\text{Ti}_{0.34}]\text{O}_2$  high-capacity cathode material for Na-ion half-cell during discharge/charge cycling in a voltage range between 1.5 V and 3.9 V. (March 2016 – In Progress)
3. Complete the synchrotron based XANES studies of  $\text{Na}(\text{NiCoFeTi})_{1/4}\text{O}_2$  at Ni, Co, Fe, and Ti K-edge as cathode material for Na-ion batteries during charge-discharge cycling. (June 2016 – In Progress)
4. Complete the synchrotron based *in situ* XRD studies of  $\text{Na}(\text{NiCoFeTi})_{1/4}\text{O}_2$  as cathode material for Na-ion batteries during charge-discharge cycling (December 2016 – In Progress)

## Progress Report

The first milestones for FY16 are complete. BNL has been focused on studies of a new cathode material for sodium-ion batteries. The capacity retention of  $\text{Na}_{0.44}[\text{Mn}_{0.44}\text{Ti}_{0.56}]\text{O}_2$  is higher than 96% after 1100 cycles, indicating the very high structural stability during Na insertion and extraction. To understand the structural changes in  $\text{Na}_{0.44}[\text{Mn}_{0.44}\text{Ti}_{0.56}]\text{O}_2$  during Na insertion and extraction, *in situ* XRD experiment was performed, and the results are presented in Figure 87a. Most of the XRD reflections [for example, (040), (130), (140)] reveal continuous peak shift during Na insertion/extraction. There is no evidence of a new phase formation upon Na insertion/extraction into/from  $\text{Na}_{0.44}[\text{Mn}_{0.44}\text{Ti}_{0.56}]\text{O}_2$  in a wide Na content range. The main crystal structure was maintained during the entire charge/discharge process without any obvious structure transformation. This is further supported by *ex situ* STEM results. All of the XRD patterns recorded during the *in situ* investigations have been refined, and the evolutions of the lattice parameters are plotted in Figure 87b.

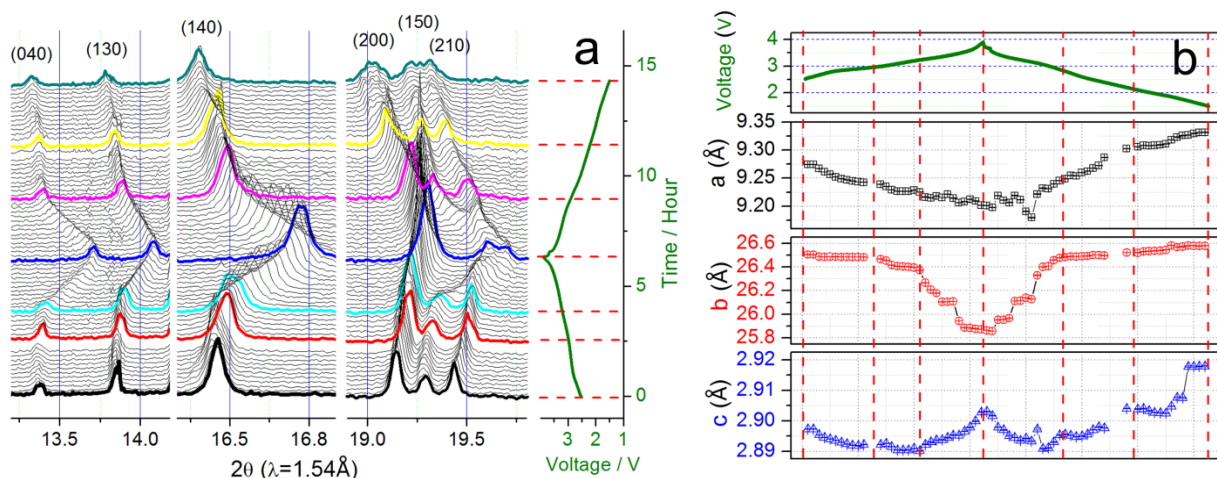


Figure 87. Structure evolution upon Na extraction/insertion. (a) *In situ* X-ray diffraction patterns collected during the first discharge/charge of the  $\text{Na}/\text{Na}_{0.44}[\text{Mn}_{0.44}\text{Ti}_{0.56}]\text{O}_2$  cell under a current rate of C/10 at a voltage range between 1.5 V and 3.9 V. (b) Evolutions of the lattice parameters during charge/discharge process.

## Patents/Publications/Presentations

### Publications

- Wang, Y., and L. Mu, J. Liu, Z. Yang, X. Yu\*, L. Gu, Y.-S. Hu\*, H. Li, X.-Q. Yang, L. Chen, and X. Huang. "A High-Capacity Positive Electrode Material with Tunnel-Type Structure for Aqueous Sodium-Ion Batteries." *Adv. Energy Mater.* 5 (2015): 1501005.
- Yue, Ji-Li, and Yong-Ning Zhou,\* Xiqian Yu, Seong-Min Bak, Xiao-Qing Yang\*, and Zheng-Wen Fu\*. "O3-type Layered Transition Metal Oxide  $\text{Na}(\text{NiCoFeTi})_{1/4}\text{O}_2$  as a High Rate and Long Cycle Life Cathode Material for Sodium Ion Batteries." *Journal of Materials Chemistry A* (October 2015).

### Presentation

- 228<sup>th</sup> ECS Meeting, Phoenix (12 October 2015): "Thermal Stability Studies in Charged Layered Sodium Transition Metal Oxide Cathode Materials for Na-Ion Batteries"; Seongmin Bak and Yongning Zhou, Enyuan Hu, Xiqian Yu, and Xiao-Qing Yang.